Molecular characterization of human regulatory and conventional T cells

Dissertation zur Erlangung des Doktorgrades der Naturwissenschaften (Dr. rer. nat.) der Fakultät für Biologie und vorklinische Medizin der Universität Regensburg

vorgelegt von

Christian Schmidl

aus Tauberfeld

im Jahr 2012

Das Promotionsgesuch wurde eingereicht am: 9. Oktober 2012

Die Arbeit wurde angeleitet von: Prof. Dr. Michael Rehli

Unterschrift:

_____

(Christian Schmidl)

Table of contents

1 Summary

Complex multicellular organisms give rise to a wide range of cell types and tissues, even though all the cells share the same DNA sequence. Key to this diversity is differential gene expression in the different types of cells. Gene expression is orchestrated by regulatory DNA sequences, which can be bound by transcription factors mediating the activation or repression of a target gene. These processes interplay with epigenetic mechanisms including DNA methylation and histone modifications that shape the chromatin structure and control its accessibility for transcription factors and other accessory proteins. Here, regulatory and conventional T cells (Treg and Tconv, respectively) were utilized as a model system to get basic insights in differential gene expression and how it is affected by epigenetic mechanisms. Treg can suppress the activation, proliferation and function of a wide range of immune cells and are thus indispensable for immune homeostasis and tolerance to self-antigens. Tconv develop into different T helper (Th) cells that boost specialized immune reactions. Both Treg as well as Tconv are closely related CD4+ T cells and, due to their variable abilities a suitable model to study differential gene expression.

An adaption of our methyl-CpG-immunoprecipitation method allowed us to systematically investigate DNA methylation in T cells, which resulted in the identification of more than 130 differentially methylated regions (DMRs) between Treg and Tconv. The DMRs were located in the vicinity of immunologically important genes including *FOXP3*, *CTLA4*, *IL2RA* and *CD40LG*. Most DMRs had a low CpG content, showed no conservation and did not overlap with a gene promoter. In addition, it was demonstrated that many DMRs were associated with "active" histone modifications and showed enhancer activity in reporter assays. These results were among the first to describe widespread differences in DNA methylation at non-promoter regions and to connect them to enhancer function.

CD4+CD25+ Treg represent a heterogeneous population and consist of CD45RA+ naïve Treg as well as CD45RA- memory Treg. Upon *in vitro* expansion CD45RA- memory Treg downregulate the expression of the Treg lineage-determining transcription factor FOXP3. Hence, we improved technologies to obtain DNA and RNA from intracellular FOXP3-stained and sorted human Treg to analyze stability, plasticity and heterogeneity of Treg subpopulations. Gene expression analyses demonstrated that *in vitro* expanded CD45RA-FOXP3- Treg differentiated into a proinflammatory Th2-like phenotype and expressed the Th2-associated transcription factor GATA3 as well as the cytokines IL-4, IL-5 and IL-13. Blockade of the Th2-inducing IL-4 signaling pathway did not abrogate the observed Th2 differentiation, arguing for a yet unknown, alternative pathway. In addition, *in vitro* expanded CD45RA- Treg expressed the Th17-determining transcription factor RORC and IL-17A, with the most significant increase in FOXP3+

cells. In line with these observations, CpGs at the *RORC* locus were most prominently demethylated in *in vitro* expanded CD45RA-FOXP3+ cells similar to the methylation status of *in vitro* generated Th17 cells. In contrast, CD45RA+ naïve Treg showed a stable phenotype without converting into proinflammatory Th2 or Th17-like cells even after prolonged *in vitro* expansion, and therefore represent the most promising population for clinical applications.

In the context of the FANTOM5 project, modern sequencing methods identified the exact location of transcription start sites (TSS) in primary and *in vitro* expanded naïve and memory Treg and Tconv. Several thousand non-annotated TSS were discovered, and some were validated as alternative promoters of known genes including the well-studied Treg-specific *FOXP3* and *CTLA4* genes. In addition, genome-wide histone modification profiling generated the most comprehensive atlas of cell type-specific enhancers in Treg and Tconv subpopulations. *De novo* motif analysis of enhancer elements identified transcription factors that were potentially involved in cell type-specific gene regulation. Continuative experiments could demonstrate a participation of the transcription factors STAT5 as well as FOXP3 and ETS1 as well as RUNX1 in Treg- or Tconv-specific enhancer architecture, respectively.

Taken together, the molecular characterization of Treg and Tconv subpopulations described in this thesis provided insights into basic principles of gene regulation and demonstrates the impact of DNA methylation, histone modifications and transcription factor binding on cell type-specific gene expression. Moreover, technical refinements of standard methodologies allowed the concrete analysis of the stability, heterogeneity as well as plasticity of T cell subsets. The integrated analysis of genome-wide datasets helped to define key regulators that shape gene expression programs of T cell subpopulations and will be of use to improve the therapeutic potential of Treg for clinical applications.

2 Introduction

One of the most fascinating aspects of complex multicellular development is the ability of a single genome to give rise to a wide panel of different cell types and tissues, all with unique phenotypes and abilities. How can these differences in development and function be achieved when all these cell types share, with minor exceptions, the same DNA sequence? The answer to this question is differential gene expression. In each distinct cell type only a fraction of all genes encoded in the DNA sequence –that is to say the genes needed for its phenotype and function– are transcribed. The decision to what extent a gene is transcribed is controlled by so-called regulatory modules, which are DNA-elements that can integrate environmental and inherited cues to establish cell type-specific gene expression programs. The current understanding classifies regulatory modules into promoters, enhancers, silencers and boundary elements. These DNA sequences can bind transcription factors (TFs) that activate or repress the binding and activity of the basal transcription machinery to influence transcription of a target gene and hence ultimately shape the cellular phenotype. These processes interplay with epigenetic mechanisms, namely DNA methylation, histone modifications and non-coding RNAs that shape the chromatin structure and control its accessibility for TFs and other accessory proteins.

The main focus of this thesis lies on regulatory and conventional T cells (Treg and Tconv). As explained below, the former are a specialized immune cell population that is crucial for immune tolerance and homeostasis. Further, the administration of Treg is explored as a curative treatment for immunological and transplantation-related diseases. Treg and Tconv are both closely related hematopoietic cells emerging from the same progenitor. Nevertheless, both cell types have different development potential, phenotype and function ascribed to their specialized gene expression programs, which renders comparative analysis of Treg and Tconv cells a suitable model to study genetic and epigenetic mechanisms of differential gene expression. With regards to their crucial role in maintaining a stable immune system and with respect to their clinical application, the analysis of gene regulation in Treg compared to Tconv will not only give insights into basic mechanisms of differential gene expression; it will also be essential to understand Treg development and function and thereby help to improve their effective and save clinical application. Thus, in the first part of the introduction basic concepts of gene regulation are described while the specific characterization on gene regulation of regulatory t cells is introduced in the second part.

2.1 Epigenetics

2.1.1 DNA methylation

Proposed in 1975 by Holliday and Pugh, the longest known epigenetic modification is the attachment of a methyl group (CH_3) to the 5' carbon atom of the base cytosine (C) (Holliday and Pugh 1975). In mammals, 5'-methyl cytosine (5mC) is mainly associated with guanine (G) in CG dinucleotides (CpGs) although recent findings confirm early reports describing non-CpG methylation in embryonic stem cells (Salomon and Kaye 1970; Grafstrom et al. 1985; Ramsahoye et al. 2000; Lister et al. 2009). DNA methylation is considered to mediate stable gene silencing at promoters and is essential for embryonic development (Li et al. 1992; Okano et al. 1999), genomic imprinting (Li et al. 1993), centromeric stability (Moarefi and Chédin 2011), splicing (Shukla et al. 2011), X chromosome inactivation in mammals (Lee 2011) and silencing of potential harmful DNA elements such as endogenous retroviruses and transposons (Bird 2002). Aberrant DNA methylation has been associated with abnormal developmental processes including cancer (Plass and Soloway 2002). In mammals three known enzymes, DNA methyltransferase 1, 3A and 3B (DNMT1, 3A and 3B) catalyze the transfer of CH_3 from S-adenosylmethionine (SAM) to cytosine (Wigler et al. 1981; Okano et al. 1999). DNMT1 is the "maintenance" methyltransferase that adds methyl groups to the newly synthesized and therefore hemimethylated DNA-strand after replication, providing the basis for inheriting methylation patterns over cell divisions and therefore rendering DNA methylation the only "real" epigenetic mark (Wigler et al. 1981). Dnmt3A and Dnmt3B catalyze *de novo* methylation but might also be involved in maintaining methylation patterns (Okano et al. 1999; Jones and Liang 2009). DNA methylation is essential for normal development, as murine knockout mice for all three DNMTs die *in utero* or shortly after birth, and mutations in *DNMT3B* are associated with the ICF syndrome (immunodeficiency, centromeric instability and facial anomalies) in humans (Xu et al. 1999). CpG dinucleotides show a bimodal distribution throughout the genome: Most CpGs in mammals are methylated, distributed randomly and appear rarer than statistically expected, possibly caused by hydrolytic deamination of 5mC to thymine, resulting in a C to T transition and a decrease of CpGs over time in evolution (Jones 2012). However, there are also regions with higher CpG density, so called CpG islands (CGIs) that are often associated with promoter regions and are preferentially unmethylated (Suzuki and Bird 2008). Basically, DNA methylation can influence gene expression by (i) steric hindrance of protein binding to DNA due to the exposure of the methyl group into the DNA-helix grooves (Tate 1993) and (ii) by attracting gene-regulatory proteins recognizing 5mC (methyl-CpG binding proteins, MBPs) (Robertson 2000). The proteins MBD1, 2 and 4 as well as MeCP2 can bind methylated DNA with their methyl-CpG binding domain (MBD) while the protein Kaiso does so with its zinc-finger

domain (Prokhortchouk et al. 2001; Klose and Bird 2006). The MBPs come in complexes with repressor molecules that alter gene expression by the modification of the chromatin conformation, as explained later (Jones et al. 1998; Nan et al. 1998; Ng et al. 1999; Zhang et al. 1999). Subject of controversy is the mechanism of active DNA demethylation (Ooi and Bestor 2008). Passive demethylation after DNA replication can be logically explained by TFs occupying DNA and thereupon blocking DNMT-mediated remethylation of the hemimethylated DNA strand. However, DNA demethylation was observed in differentiation models in the absence of cell division and thereby DNA replication (Klug et al. 2010), arguing for active demethylation processes. The role of activation-induced cytidine deaminases (AID), thymine DNA glycosidases (TDG), alpha growth arrest and DNA-damage-inducible (GADD45a) and ten-eleven translocation (TET) dioxygenases in active demethylation processes are currently under investigation (Ooi and Bestor 2008; Jones 2012). TET proteins can process 5mC to 5-formylcytosine and 5-carboxylcytosine that are readily excised by TDG as a possible mechanism of active demethylation (Ito et al. 2010; He et al. 2011; Ito et al. 2011). However, the mechanisms of active demethylation need further investigations, preferentially in non-artificial systems to exclude aberrant methylation phenomena described for cell lines and *in vitro* differentiation systems (Paz et al. 2003; Meissner et al. 2008).

2.1.2 Chromatin

DNA is packed into chromatin, which consists of DNA, histone proteins and non-histone proteins (Bell et al. 2011). The basic subunit of chromatin is the nucleosome core particle, comprised of ~145 base pairs (bp) of DNA wrapped around an octamer consisting of two copies each of histones H2A, H2B, H3 and H4 in a 1.65 left-handed, superhelical turn (Kornberg and Thomas 1974; Kornberg 1977; Luger et al. 1997). The nucleosomes are arranged like “beads on a string”, and metazoan chromatin contains the linker histone H1 that helps to condense the “string” into a tighter packed, higher order structure whose organization is still incompletely understood (Felsenfeld and Groudine 2003). The packing of DNA into chromatin is repressive to transcription per se as it potentially blocks the accessibility of DNA elements for transcription factors and the transcription machinery (Lorch et al. 1987). Therefore, the chromatin accessibility of regulatory elements such as promoters and enhancers is actively formed. Classically, regions of compacted chromatin are termed heterochromatin, whereas accessible chromatin is called euchromatin (Bell et al. 2011). As a part of chromatin modifying processes, ATP-dependent remodeling complexes are capable of positioning or removing nucleosomes on the DNA (Clapier and Cairns 2009) to expose regulatory sequences to their target proteins. In addition, post-translational modifications (PTMs) of histones regulate chromatin accessibility: Amino acids on the N-terminal histone tails can be acetylated, phosphorylated, β-N-

acetylglucosaminated, ADP-ribosylated, deaminated, ubiquitinated and sumoylated (Bannister and Kouzarides 2011).

Methylation and acetylation are the best-studied histone PTMs. Histone acetylation is mediated by the opposing action of histone acetyl transferases (HAT) and histone deacetylases (HDAC). Acetylation of histones is supposed to decrease the interaction of positively charged lysine residues of histone tails with the negatively charged DNA sugar-phosphate backbone to promote an accessible chromatin conformation (Sterner and Berger 2000). More important, gene-regulatory proteins with a bromodomain can recognize and bind acetylated histones. To name just a few, remodeling complexes such as SWI/SNF (Hassan et al. 2002), coactivators (Dhalluin et al. 1999), as well as the general TF TFIID (Jacobson et al. 2000) have a bromodomain and can be recruited by acetylated histones to promote transcription. Histone methylation is mainly observed at arginine and lysine residues of histone tails and controlled by histone methyl transferases (HMT) or recently discovered histone demethylases (Shi et al. 2004). As an example, Histone 3 Lysine 4 methylation (H3K4me) is associated with "active" chromatin in eukaryotes (Bernstein et al. 2005; Barski et al. 2007). The modification is established by SET domain containing HMTs that are recruited to the target histones by other histone modifications such as ubiquitinated H2B, the active form of RNA Polymerase II (PolII) or specific TFs (Shilatifard 2008). The established H3K4me can be "read" by other factors with a chromodomain such as some chromatin remodeling complexes (Santos-Rosa et al. 2003; Wysocka et al. 2006), HATs (Vermeulen et al. 2010) and TFIID (Vermeulen et al. 2007) to promote transcription. Interestingly, the latter binding is synergistically enhanced by H3K14 acetylation. In contrast, H3K9 di- and trimethylation is catalyzed by the HMT Suv39H1 and is recognized by heterochromatin protein 1 (HP1) that helps to stably compact chromatin (Bannister et al. 2001; Peters et al. 2001; Beisel and Paro 2011). Suv39H1 interacts with HP1, providing a possible "feed forward" mechanism of H3K9 methylation and HP1 binding to sustain chromatin compaction once it was initiated (Schotta et al. 2002). Classes of histone modifying enzymes that are supposed to set and interpret histone modifications to maintain a certain chromatin state as described for HP1-Suv39H1 are the trithorax group (TrxG) and polycomb group (PcG) proteins (Ringrose 2007). TrxG include HMTs to set H3K4 methylation as already described and stabilize chromatin states favoring transcription. Contrary, PcG proteins come in large complexes and establish and maintain a chromatin environment repressive for transcription. The polycomb repression complex 2 (PRC2) methylates H3K27 and creates a platform for polycomb repressive complex 1 (PRC1) that establishes a compacted chromatin environment repressing transcription (Ringrose 2007).

Interestingly, PcG-mediated silencing is interconnected to DNA methylation. PRC2 directly controls DNA methylation by interacting with DNMTs (Viré et al. 2006). Further, promoters with

H3K27me are more frequently *de novo* methylated than other promoters and undergo aberrant DNA methylation in human cancers, suggesting that the PcG-repressed state is established during development and may predispose genes to *de novo* methylation in early developmental processes (Schlesinger et al. 2007; Mohn et al. 2008). Moreover, the interplay of DNA methylation and chromatin structure is illustrated by the associations of the aforementioned MBPs with chromatin-modifying enzymes. MeCP2 for example is associated with the Sin3A/HDAC corepressor complex (Jones et al. 1998; Nan et al. 1998). In addition, the MeCP1 complex is associated with HDACs and can bind methylated DNA via MBD2 (Ng et al. 1999). Moreover, MBD1 can also bind methylated DNA and act as a repressor (Fujita et al. 2000). In contrast to these processes that prohibit chromatin access for transcription, the recently identified protein Cfp1 is recruited to unmethylated CpG islands and interacts with a H3K4 methyltransferase to create a chromatin environment that favors transcription (Lee et al. 2007; Thomson et al. 2010).

2.1.3 Non-coding RNAs

Due to their active participation in shaping the chromatin environment, short (<200 nucleotides) and long (>200 nucleotides) non-coding RNAs are classified as "epigenetic" regulators as well. First described in 1961 (Lyon 1961), the phenomenon of X chromosome inactivation in mammals (XCI) is a prime example of RNA-mediated regulation of gene expression. In females, one of the two X chromosomes is inactivated during embryogenesis, a process controlled by antagonistic roles of two non-coding RNAs, Xist and Tsix (Lee 2011): Sustained expression of Tsix prevents expression of Xist and XCI, but when XCI is initiated Tsix expression is lost at one X chromosome. This allows transcription of the lncRNA Xist, and Polycomb repressive complex 2 is recruited to a PRC2-binding motif in the lncRNA and effectively tethered to the locus via PolII. The RNA–PRC2 complex is loaded onto chromatin co-transcriptionally through TFs such as YY1, promoting H3K27me3 and heterochromatin formation in *cis* (Lee 2011). In fission yeast, transcription of repeat regions within heterochromatin domains triggers the RNA interference machinery, generating small 21 nucleotide long RNAs (siRNAs). The siRNAs associate with Argonaute protein (Ago1) and guide the Ago1-containing RNA-induced initiation of the transcriptional gene-silencing complex (RITS complex) to homologous sequences of nascent chromatin-associated transcripts for heterochromatin formation (Bühler et al. 2006). Recently it was demonstrated that small RNA species (piRNAs) act in *trans* to silence transposable elements in mammals by mediating indirect heterochromatin formation and DNA methylation at target loci (Aravin et al. 2008). These examples illustrate the connection between histone modifications, non-coding RNAs, DNA methylation and chromatin accessibility to prepare and sustain the genetic environment for

gene activation or repression. These findings are summarized in **Figure 1**. Still, some basic concepts of epigenetics are incompletely understood. It is not clear, if and how chromatin modifications can be passed on over cell divisions, as there is no such simple mechanism as a "maintenance" enzyme as in DNA methylation. Moreover, there is no clear agreement if the establishment of DNA methylation patterns is a cause or a consequence of gene silencing or activation as mechanistic studies are scarce and need further investigations. The idea of heritable changes in gene expression without changes in the DNA sequence was widely hoped to explain gene expression patterns in developmental processes and diseases. The efforts that were made to understand epigenetic mechanisms are illustrated by the roughly 25000 PubMed citations for the term "epigenetic" (until August 2012).

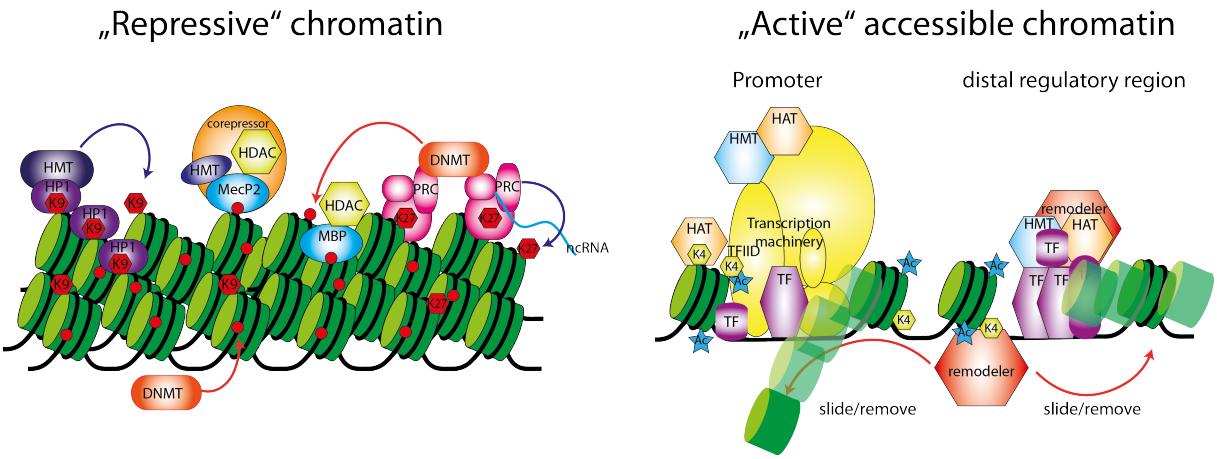

Figure 1
Epigenetic mechanisms and gene regulation. General properties of repressive and active chromatin environments; DNA (black lines) is wrapped around nucleosomes (green cylinders); red circles: methylated CpG dinucleotide; small red and yellow hexagons: histone methylation at H3K9, H3K27 or H3K4; blue star: histone acetylation; other objects: transcription factors and histone- as well as DNA-modifying enzymes as described in the introduction. (Adapted from Laird 2005)

2.1.4 *Cis*-regulatory modules

2.1.4.1 Transcription factors

Sequence-specific transcription factors comprise at least a DNA binding domain for recognizing and binding specific sites in the genome and a transactivation domain to recruit coactivators and other accessory proteins such as DNA and histone modifying proteins that ultimately help to facilitate transcription (MacQuarrie et al. 2011). Transcription factors are activated through signaling events triggered by environmental cues and can establish logic networks to drive

complex programs of gene expression as seminal work of Nüsslein-Volhard and colleagues demonstrated in drosophila (St Johnston and Nusslein-Volhard 1992). In humans, a manually curated list of 1391 DNA-binding TFs was recently published showing that many TFs were expressed in a tissue-specific manner but remain largely uncharacterized regarding their function and mechanism of action (Vaquerizas et al. 2009).

2.1.4.2 Promoters

Promoters of genes are genomic loci that overlap with the transcription start site (TSS) from which messenger RNA (mRNA) transcription is initiated at a rate determined by the complete integrated regulatory input for this gene (Lenhard et al. 2012). PolII catalyzes transcription of protein-coding genes and some small RNA species in eukaryotes. Therefore, components of the basal transcription machinery are recruited to the "core promoter", the region in close vicinity to the TSS, with the help of general and cell type-specific TFs recognizing DNA sequence motifs (transcription factor binding sites TFBS) at the core promoter or distal *cis*-regulatory regions such as enhancers (Maston et al. 2006). Due to their difference in dynamic expression range - from constant expression ("house keeping genes") to cell type and developmental state-specific expression- attempts were made to classify promoters based on their expression dynamics and nucleotide composition. Recent advances in TSS detection and gene expression analysis such as RNA-seq (Ozsolak and Milos 2011) and cap analysis of gene expression (CAGE, (Kanamori-Katayama et al. 2011)) allow fine mapping of TSS and gene expression analysis throughout the genome. Integrated analysis suggests three main classes of promoters: "adult" (type I), "ubiquitous" (type II) and "developmentally regulated" (type III) (Lenhard et al. 2012). Type I promoters show tissue-specific expression in differentiated cell types from a focused TSS, have mostly a low CG and CpG content and are enriched for a TATA-box, a sequence motif recognized by the TATA-box binding protein which is a component of the basal transcription machinery. Type II promoters are ubiquitously expressed ("house-keeping") from broadly dispersed TSS, are TATA-box depleted and overlap with CpG islands at their TSS (Deaton and Bird 2011; Lenhard et al. 2012). Type III promoters share molecular characteristics with type II promoters but are developmentally regulated (Lenhard et al. 2012). In contrast to prokaryotic organisms, in eukaryotes the promoter alone is not sufficient to regulate gene and often produces only low levels of mRNA on its own (Wittkopp and Kalay 2012). On that account, enhancers, insulators and boundary elements control the "fine tuning" of gene expression in complex organisms.

2.1.4.3 Enhancers and silencers

Enhancers were described as non-coding regulatory DNA sequences that can enhance the expression of a target gene in a distance- and orientation-independent manner (Banerji et al.

1981). Distal non-coding sequences are often necessary for the activation and/or correct lineage-specific expression of a gene as promoters alone often fail to establish accurate expression patterns. For example, studies in transgenic mice showed that the transfer of small fragments surrounding the human *CD14* gene locus (24-33kb) only establish correct CD14 expression in liver whereas a much larger region of 80 kb is needed to express CD14 in a monocyte-specific fashion (Pan et al. 2000). Another well-studied example is the locus encoding the T helper cell type 1 (Th1)-specific cytokine interferon gamma (*Ifng*). An 8.6 kb transgene of the human *IFNG* locus was sufficient for constitutive IFN-γ production, but only a 191 kb transgene established restricted *IFNG* expression in Th1 cells (Soutto et al. 2002). Enhancers are thought to bind combinations of transcription factors that create physical interactions via the mediator complex and cohesin with the target gene promoter and help to recruit the general transcription machinery (Kornberg 2005; Kagey et al. 2010). The enhancer and target promoter can be distant from each other (up to a million base pairs away) or even on another chromosome (Spilianakis and Flavell 2004; Lomvardas et al. 2006; Amano et al. 2009). These observations were made possible by labeling distant gene loci with fluorescent probes (fluorescence in situ hybridization, FISH (Ong and Corces 2011)) or by the chromosome conformation capture technique introduced by Dekker and colleagues 2002 (Dekker et al. 2002), a technique that uses formaldehyde crosslinking to capture physical interactions between chromosome arms. Silencers function by recruiting TFs repressing transcription, block DNA binding of activators or hinder the assembly of the transcription machinery (Maston et al. 2006), but are less well characterized than enhancers.

2.1.4.4 Boundary elements

Boundary elements were also described to potentially act as repressive elements by blocking the interaction of a distal enhancer with its target promoter as intensively studied at the *IGF2*/*H19* locus where the presence of the CCCTC binding protein (CTCF) blocks the interaction of an enhancer with the *IGF2* gene on the maternal allele (Bell and Felsenfeld 2000). CTCF, so far the only identified "boundary" element in humans, was also described to isolate "active" and "repressive" chromatin environments and is involved in many developmental processes such as stem cell differentiation, neural development, cytokine expression and immunoglobulin chain recombination by mediating long-range interactions of chromatin elements (Herold et al. 2012). A positive function in gene regulation by the boundary element CTCF is also supported by a recent study highlighting the role of CTCF in mediating enhancer-promoter interactions and chromatin organization (Handoko et al. 2011). An overview of *cis*-regulatory modules is shown in **Figure 2**.

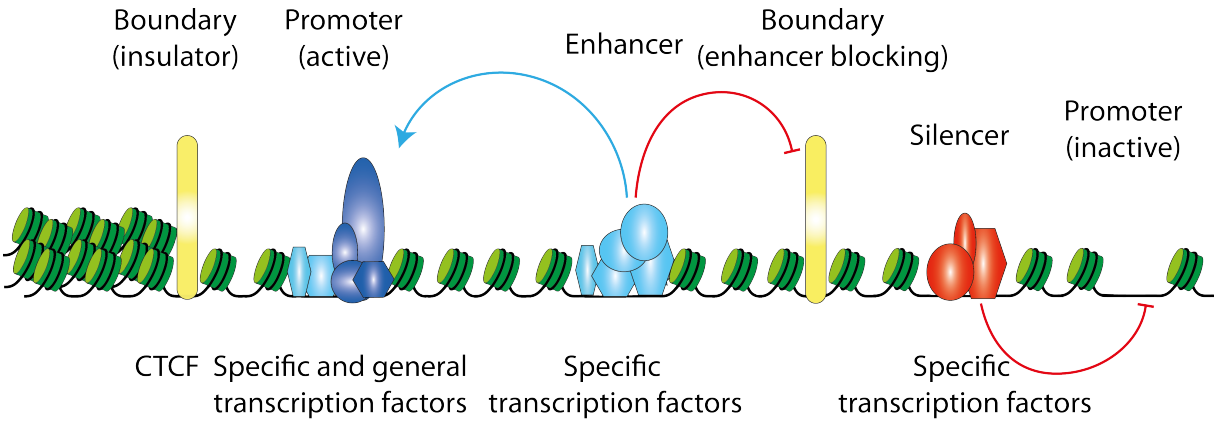

Figure 2
***Cis*-regulatory modules in the genome.** (Adapted from Heintzman and Ren 2009)

2.1.5 Epigenetics at *cis*-regulatory modules and the impact on gene regulation

During the making of this thesis, progress in high throughput and next generation sequencing technologies now permits the examination of global epigenetic and functional properties of *cis*-regulatory modules.

In terms of DNA methylation analysis, previous studies concentrated on CGIs in cancer as aberrant DNA methylation is often observed upon malignant transformation (Plass and Soloway 2002). CpG islands at promoters are normally unmethylated independent of their expression status (Weber et al. 2007; Mohn et al. 2008). However, some CGIs become *de novo* methylated in a cell type-specific manner, resulting in long-term repression of the associated gene (Weber et al. 2007; Farthing et al. 2008; Meissner et al. 2008; Mohn et al. 2008). Long-term repression of CGI-associated genes is described for imprinted genes (genes that show parent-of-origin expression), for CGI-associated genes of the inactivated X-chromosome and for some tissue-specific genes (Jones 2012). Gene repression by CGI methylation is still rare and may not be the prevalent mechanism of gene silencing (Mohn et al. 2008; Jones 2012). Moreover, for instance, at the inactive X chromosome, DNA methylation comes late during the inactivation and silencing process (Lee 2011). Yet, it seems to provide an additional "layer" of gene repression to ensure long-term silencing. Interestingly, regions of intermediate CpG content are more commonly *de novo* methylated and repressed, whereas low CpG promoters tend to be methylated regardless of their expression state (Weber et al. 2007; Ball et al. 2009). In contrast, DNA methylation of gene bodies was positively correlated to gene expression (Ball et al. 2009; Lister et al. 2009). However, far less is known about DNA methylation at non-promoter regions. Regions of intermediate or low CpG content came into focus with the development of sensitive locus-wide or genome-wide DNA methylation analysis (Schilling and Rehli 2007; Meissner et al. 2008; Klug et al. 2010; Stadler et al. 2011). Interestingly, DNA methylation is more dynamic at CpG poor

regions (Meissner et al. 2008; Stadler et al. 2011), and differential DNA methylation was observed at cell type-specific enhancers that were bound by lineage specific TFs (Sérandour et al. 2011; Stadler et al. 2011; Wiench et al. 2011). Indeed, on a genome-wide scale TF-bound regions are associated with local hypomethylation (Lister et al. 2009). Cell type-specific DNA methylation patterns seem to be established by both *cis* and *trans* acting factors: At CGIs for example, combinatorial binding of TFs protected them from aberrant *de novo* methylation (Gebhard et al. 2010). In a different experimental setting, core promoters introduced into a new locus in the mouse genome were able to recapitulate autonomously their original DNA methylation state (Lienert et al. 2011). Mutation of TF binding sequences in the respective promoters inhibited this process, which suggests DNA methylation control in *cis.* In mice, several differentially methylated regions were identified that were controlled in *cis* by the underlying DNA sequence, but also *trans*-acting elements orchestrated DNA methylation patterns in different DMRs (Schilling et al. 2009).

Considering the association of gene-regulatory elements with the disposal of certain histone modifications, chromatin accessibility and nucleosome remodeling, genome-wide approaches were used to systematically isolate regulatory elements based on their biochemical markers. Chromatin immunopreciptiation, deoxyribonuclease/micrococcal nuclease digestion and comparable techniques coupled to next generation sequencing (ChIP-seq, DNase-seq, MNase-seq) allow the genome-wide mapping of TF, histone modifications and "open" chromatin regions sensitive to DNase digestion (Bell et al. 2011; Zhou et al. 2011). Among other modifications, promoters of active genes in metazoans are associated with H3K4me3 and H3K27ac, with intermediate levels of H3K4me2 and low levels/absence of H3K4me1 (Barski et al. 2007; Guenther et al. 2007; Heintzman et al. 2007; Mikkelsen et al. 2007; Wang et al. 2008b; Bell et al. 2011). Inactive type I promoters (without a CpG island spanning the TSS) lack these active histone modifications whereas type II and type III CpG Island promoters always show detectable H3K4 trimethylation (Barski et al. 2007; Guenther et al. 2007; Wang et al. 2008b; Bell et al. 2011; Deaton and Bird 2011). Interestingly, genes important for development share the active H3K4me3 and the repressive H3K27me3 polycomb modification, probably "poising" genes for their fast activation or silencing, dependent on the fate of the cell (Bernstein et al. 2006). Moreover, active promoters are DNase hypersensitive due to a nucleosome-free region (NFR) directly upstream of the TSS, show binding of the active form of PolII and are frequently associated with histone variants H3.3 and H2A.Z (Jin et al. 2009; Bell et al. 2011).

Most of these findings can be transferred to enhancer regions (Ong and Corces 2011). Compelling evidence from genome wide studies identified the enrichment of H3K4me1/me2 and additionally H3K27ac at "poised" and "active" enhancers, respectively (Heintzman et al. 2007; Heintzman et al. 2009; Creyghton et al. 2010; Rada-Iglesias et al. 2011). Poised enhancers were

shown to acquire an active state during development when the linked gene was needed to be expressed (Rada-Iglesias et al. 2011). Enhancers are further characterized by DNase hypersensitivity, NFR, binding of a coactivator such as p300 (a HAT) (Visel et al. 2009) (Blow et al. 2010), and H3.3 deposition. In contrast to promoters, enhancers were first described to show low levels of H3K4me3 and no transcriptional activity (Heintzman et al. 2007). However, some enhancers produce transcripts (enhancer RNAs or eRNAs) and were bound by PolII (Kim et al. 2010; Melgar et al. 2011). Another report attributed H3K4me3 at some enhancers as well, making it difficult to definitely separate enhancers and promoters (Pekowska et al. 2011). Still, enhancer and promoter prediction by chromatin patterns and TF occupancy is more effective than approaches that rely on conservation or accumulation of sequence motifs for TFs (Hardison and Taylor 2012a). Interestingly, when comparing the diversity of promoter and enhancer signatures between cell types, enhancers show a more cell type-specific distribution and variety than promoters, highlighting their role in tissue-specific gene expression (Heintzman et al. 2009; Ernst et al. 2011). Global histone profiling further classified DNA elements associated with different function, e.g.. H3K36me3- and H4K20me1-marked regions are linked with transcriptional elongation and H3K27me3 is preferentially associated with PCG-repressed regions (Barski et al. 2007; Mikkelsen et al. 2007).

The question arises how cell type specificity of regulatory elements is created and interpreted by transcription factors. Namely, the sole expression of a TF does not result in its binding to its recognition sequence in the genome: As an example, there are ~ 2 million binding sites of the TF PU.1 located in the human genome, but only ~ 80.000 of these sites are effectively bound in PU.1-expressing macrophages or monocytes (Pham et al. 2012). In contrast to shared binding sites, cell type-specific PU.1 binding in each cell type was associated with the co-binding of lineage-specific TFs, suggesting the combinatorial action of general and specific transcription factors to establish cell type-specific enhancers (Heinz et al. 2010; Pham et al. 2012). Moreover, these regions were marked by nucleosome repositioning and accumulation of H3K4me1 to "prepare" chromatin for signal-dependent gene activation (Ghisletti et al. 2010; Heinz et al. 2010). In MCF7 and LNCaP cells FoxA1 is recruited to different sites distinguished by specific H3K4 dimethylation (Lupien et al. 2008). At these specific enhancers, FoxA1 remodels chromatin to mediate MCF7 or LNCaP specific gene expression programs in collaboration either with estrogen receptor alpha or androgen receptor TFs. These observations lead to a model of "pioneer" TFs that can easily access and prepare chromatin for the binding of other transcription factors that act in combination to drive cell type-specific expression programs (Lupien et al. 2008; Heinz et al. 2010; Zaret and Carroll 2011). Constitutive binding sites, on the other hand, do not seem to rely on co-binding with other TFs, partially explained by a stronger TF consensus site as demonstrated for FoxA2 binding in liver (Tuteja et al. 2008). However, potential co-

binding and consensus site quality do not explain all of the observed binding behavior of TFs suggesting additional determinants. Nevertheless, it was demonstrated for several cell types that enhancers are defined by combinations of key regulators (Lupien et al. 2008; Heinz et al. 2010; Lin et al. 2010b; Mikkelsen et al. 2010). This allows the computational analysis of regulatory elements to isolate overrepresented binding sites and hence the identification of key TFs by the sole knowledge of histone modifications in a certain cell type (Pham et al. 2012). Currently, many laboratories and big international consortia such as the ENCODE (ENCODE-consortium 2011) gather epigenomes of many different cells with the hope to understand gene regulation in development, disease and cellular states.

2.2 T helper cells

The mammalian immune system comprises several specialized cell types to protect the host from exogenous pathogens such as fungi, viruses, bacteria and parasites (Delves and Roitt 2000). Cells from the innate immune system are regarded as a "first line of defense" against pathogens as they can recognize conserved and widely distributed features of pathogens with special receptors (pattern recognition receptors) to mount initial immune responses (Janeway and Medzhitov 2002; Underhill and Ozinsky 2002). Besides killing microbes and cytokine production to boost inflammation, innate immune responses include the incorporation and digestion of pathogens by professional phagocytes such as monocytes, macrophages as well as dendritic cells. The phagocytes then present parts of the digested microbes to cells of the adaptive immune system that can recognize the presented molecules ("antigens") with their diverse T and B cell receptors (Delves and Roitt 2000; Guermonprez et al. 2002; Jutras and Desjardins 2005). Somatic recombination and random events create a theoretical diversity of up to 10^{18} different antigen receptors that enable cells of the adaptive immune system to recognize virtually every antigen presented (Davis and Bjorkman 1988). If a cell recognizes a presented antigen with its matching receptor, it proliferates to increase cell numbers with the same receptor ("clonal expansion") to effectively detect and fight the corresponding pathogen (Delves and Roitt 2000). The adaptive immune system comprises B and T lymphocytes that develop in the bone marrow or in the thymus, respectively (Delves and Roitt 2000). T lymphocytes expressing the CD4 coreceptor emerge as naïve CD4 cells and give rise to different T helper (Th) cell subsets in dependence of signals from the innate immune system and other environmental cues. Th1 cells produce the cytokine interferon gamma (Ifn-γ) and mediate host defense against intracellular pathogens while Th2 cells produce Interleukin (Il)-4, Il-5 and Il-13 and effectively resolve helminthic infections (Mosmann et al. 1986; Heinzel et al. 1989; Romagnani 1994). Recently, Th cells producing Il-17A (Th17 cells) were described to contribute to defense against extracellular pathogens and fungi (Infante-Duarte et al. 2000; Ye et al. 2001; Ouyang et al. 2008).

With Th subsets arising from the same progenitor cell, they are ideal to study TF networks and epigenetic mechanisms that govern and stabilize their differential gene expression programs.

Th1 development is favored by the signal transducer and activator of transcription (Stat)1 and Stat4 that are activated by innate immune cell-derived Ifn-γ and Il-27 or Il-12, respectively (Schoenborn and Wilson 2007). Stat1 activation induces Tbx21 (also called T-bet), a key Th1 TF that induces among others Runx3. In cooperation with Tbx21 and Stat4, Runx3 binds to the *Ifng* promoter to sustain its expression in a positive feedback loop while binding to a silencing element in the *Il-4* gene to suppress its transcription and hence abrogate Th2 differentiation (Djuretic et al. 2007a). In addition, Tbx21 interferes with the Th2 transcription factor Gata3 to prevent it from binding to target genes (Hwang et al. 2005). Gata3 is sufficient and necessary for Th2 development (Zheng and Flavell 1997). Gata3 is expressed upon Il-4 induced Stat6 activation and T cell receptor (TCR) signaling-derived TFs (Ansel et al. 2006) or by Notch signaling (Amsen et al. 2007). Gata3 induces Maf, and in cooperation with Stat6 these three TFs upregulate transcription of the Th2 cytokines Il-4, Il-5 and Il-13, again creating a positive feedback loop to stabilize Th2 differentiation (Ansel et al. 2006). Gata3 also hinders Th1 differentiation by preventing Runx3 to activate Th1-essential genes (Yagi et al. 2010). In mice, Th17 development is initiated by transforming growth factor beta (Tgf-ß) that induces the Th17 determining TF retinoic acid receptor related orphan receptor-gamma t (Rorc or Rorγt) or the regulatory T cell (Treg) determining TF Foxp3 (Chen et al. 2003; Ivanov et al. 2006; Manel et al. 2008). In combination with Il-6, Stat3 abrogates Treg development and supports Th17 differentiation and production of Il-21 (Zhou et al. 2007; Zhou et al. 2008a). Il-21 and Stat3 activation stabilize the Th17 phenotype via a positive feedback loop and also upregulate the Il-23 receptor to support Stat3 activation via antigen presenting cell (APC)- derived Il-23 (Zhou et al. 2007). Tgf-ß-independent Th17 generation was also reported recently (Ghoreschi et al. 2010). In humans, requirements for Th17 cell development are still under discussion (Annunziato et al. 2007; Evans et al. 2007; Manel et al. 2008; Volpe et al. 2008; Annunziato and Romagnani 2011).

2.2.1 Epigenetics in Th development

As illustrated in the previous paragraph, TF networks are (i) able to sustain phenotypes in feedback loops and (ii) can prohibit differentiation to other phenotypes by direct interference with other TFs or by binding to regulatory regions such as the *Il-4* silencer. However, many studies suggested that DNA methylation, chromatin remodeling complexes and chromatin modifications influence Th development and function: at the Th1-signature gene *Ifng*, many *cis*-regulatory elements were described that showed Th1-specific demethylation, TF binding and "active" chromatin modifications (Hatton et al. 2006; Jones and Chen 2006; Schoenborn et al.

2007a). Some putative enhancers interacted with the *Ifng* promoter in a cell type-specific manner (Hadjur et al. 2009). The establishment of cell type-specific epigenetic patterns is mediated by lineage-specific TFs. As an example, Stat4 was reported to recruit the remodeling complexes Swi-SNF to the *Ifng* promoter, which is essential for nucleosome remodeling and *Infg* expression (Zhang and Boothby 2006). Similarly, Tbx21 was described to be associated with a H3K27 demethylase to remove this repressive chromatin mark at its target genes to promote Th1 development (Miller et al. 2008). With respect to Th2 development, regulatory elements at the *Il-4* locus acquire active histone marks and become demethylated in Th2 cells but not in Th1 cells (Avni et al. 2002; Lee et al. 2002). Gata3 is in parts responsible for chromatin remodeling and DNA demethylation at the Th2 cytokine genes (Lee et al. 2000; Yamashita et al. 2004) to create an open chromatin environment and was described to counteract DNA methylation-mediated gene silencing by interference with Mbd2 and Dnmt1 binding (Hutchins et al. 2002; Makar et al. 2003; Makar and Wilson 2004). In line with these observations, ablation of Mbd2, Dnmt1 or general inhibition of DNA methylation with 5-azacytidine lead to de-repression of cytokine genes normally silenced in Th1 or Th2 cells (Ballas 1984; Hutchins et al. 2002; Makar et al. 2003). In addition, acquired Th2-state seems to be maintained by Mll, a TrxG protein that stabilizes open chromatin conformation at the Th2 cytokine locus to sustain the expression of Th2 related genes (Onodera et al. 2010). These examples illustrate the participation of epigenetic mechanisms in T helper cell specification.

2.2.2 Regulatory T cells

When T cells generate T cell receptors to recognize antigen they often produce by chance TCRs that are reactive to self-antigens. This would cause immune responses against the own body and is therefore restricted by anergy or deletion of self-reactive cells (negative selection) during T cell development in the thymus (Delves and Roitt 2000). However, some self-reactive T cells escape negative selection and have to be controlled in the periphery, a task that is in part accomplished by another Th subset, so-called regulatory T cells (Sakaguchi et al. 2006).

2.2.2.1 Phenotypic characterization

The notion that thymus-derived T cells contain a population responsible for peripheral tolerance emerged from experiments where neonatal thymectomy in mice at day 2-4 after birth resulted in autoimmune diseases that were prevented by inoculation of the mice with thymocytes or spleen cells from non-thymectomized mice (Nishizuka and Sakakura 1969; Sakaguchi et al. 1982). Further work identified CD25 (IL-2 receptor alpha chain) as a surface marker for these so-called “regulatory T cells” (Treg) (Sakaguchi et al. 1995), although CD25 was also expressed on non-regulatory conventional CD4+ T cells (Tconv) upon stimulation (Wing et al. 2005; Allan

et al. 2007) disqualifying CD25 as an exclusive Treg marker. A major breakthrough in Treg research was the discovery of the transcription factor Foxp3 that was soon recognized as the "master regulator" of the Treg lineage (Fontenot et al. 2003; Hori et al. 2003; Zheng and Rudensky 2007). Foxp3 is crucial for Treg development and function as mutations in *Foxp3* cause lethal autoimmune disease in humans (immune dysregulation, polyendocrinopathy, enteropathy, X-linked syndrome; IPEX) and mice (*scurfy* phenotype) (Bennett et al. 2001; Brunkow et al. 2001). Since Foxp3 is a nuclear protein it cannot be used to sort living cells for functional analysis by fluorescence-activated cell sorting (FACS). Therefore Treg have to be sorted by surrogate markers for functional analysis, e.g. by high expression of the surface proteins CD4 and CD25, and by low expression of the Interleukin-7 receptor (CD127) (Liu et al. 2006).

2.2.2.2 Development

CD4+CD25+FOXP3+ Treg differentiate in the thymus (and are thus called "natural" Treg) and contain a high frequency of T cell receptor specificities reacting to self-antigen (Jordan et al. 2001; Sakaguchi 2005). During thymic development, an intermediate avidity for self-antigens seems to predispose for the development of Treg, while a low reactivity of TCR to self-antigens (self-reactivity) promotes the development of conventional T cells (positive selection) and high self-reactivity causes deletion of potentially harmful T cells (negative selection) (Delves and Roitt 2000; Maloy and Powrie 2001). In addition to TCR signals, the co-stimulation via CD28 and CD40 by antigen-presenting cells (APCs) enhances Treg development (Lohr et al. 2004; Lio et al. 2010). The self-antigens in the thymus are presented via major histocompatibility (MHC) class II complexes by APCs including dendritic cells (DCs) and cortical- and medullary thymic epithelial cells (cTEC and mTEC, respectively) (Hsieh et al. 2012). This releases a population of Treg into the periphery with TCR repertoires recognizing self-antigens presented in the thymus. The observation that Treg are induced by self-antigens normally only produced in special peripheral tissues raises the question how the thymus can present these antigens (Seddon and Mason 1999). One possibility is the capturing of peripheral antigens by migrating APCs or the ability of mTEC to express low levels of self-antigens regulated by autoimmune regulator (AIRE) (Mathis and Benoist 2009; Kyewski and Peterson 2010; Hsieh et al. 2012). In addition to TCR signaling and co-stimulatory signals, cytokines are required for Treg development and survival. Due to high expression of the Il-2 receptor alpha subunit, Il-2 was suspected to be essential for Treg generation. Indeed, genetic ablation of CD25 resulted in reduced Treg numbers, and deletion of the common gamma chain of the Il-2 receptor as well as combined deletion of interleukins signaling through it (Il-2, Il-7 and Il-15) led to a complete loss of the Treg compartment (Fontenot et al. 2005a; Burchill et al. 2007; Vang et al. 2008). In addition to thymus derived Treg,

induced Treg (iTreg) are generated in the periphery by Tgf-ß (Chen et al. 2003) and retinoic acid (Sun et al. 2007; Nolting et al. 2009). Induced Treg seem particular important for homeostasis and tolerance at mucosal sites or in the gut (Sun et al. 2007; Barnes and Powrie 2009; Josefowicz et al. 2012).

2.2.2.3 Mechanisms of suppression

Treg themselves lack many properties ascribed to conventional effector cells: Treg do not proliferate upon sole TCR stimulation but need additional Il-2 and CD28 co-stimulation to overcome anergy (Thornton et al. 2004). Moreover, they do not produce proinflammatory cytokines and survival factors such as Il-2 that potentially boost effector T cell functions: On the molecular level cytokine production is in part controlled by Foxp3 itself as it was shown to interact with the transcription factors NFAT and NFkB to hinder transcriptional activation of Il-2, Il-4 and Ifn-γ (Bettelli et al. 2005; Wu et al. 2006). Most importantly, they can suppress the activation, proliferation and effector function of a wide range of immune cells such as T cells, B cells, mast cells, natural killer cells and APCs including macrophages and dendritic cells (DCs) (Vignali et al. 2008; Shevach 2009). Various contact-dependent and -independent mechanisms were proposed: human Treg express granzyme A while mouse Treg express granzyme B (Grossman et al. 2004; Gondek et al. 2005), both molecules that can kill target cells by cytolysis. Moreover, Treg can induce apoptosis in T cells by galectin-1 (Lgals1) (Garín et al. 2007). Regulatory T cells constitutively express the cytotoxic T-lymphocyte-associated protein 4 (Ctla4), a molecule that downregulates co-stimulatory molecules on APCs and hence attenuates effector T cell activation by APCs (Read et al. 2000; Wing et al. 2008). It was also described that Treg can upregulate lymphocyte-activation antigen 3 (Lag3) that ligates to major histocompatibility (MHC) class II molecules on DCs to inhibit their maturation and thereby their immune-stimulatory function (Liang et al. 2008). Recent discoveries propose “metabolic” disruption as another possibility to inhibit T cell function: The ectoenzymes ectonucleoside triphosphate diphosphohydrolase 1 (Entpd1) and ecto-5'-nucleotidase (Nt5e) expressed in Treg generate immune-suppressive extracellular adenosine (Deaglio et al. 2007). In addition there is a discussion about the possibility that Treg deprive the microenvironment of the essential survival cytokine Il-2 by binding it with their highly expressed Interleukin-2 receptor (Fontenot et al. 2005a; Pandiyan et al. 2007). Treg also secrete cytokines with immunosuppressive function, namely Il-10, Tgf-ß and Il-35, but the importance for Il-10 and Tgf-ß was questioned by differing observations in *in vitro* and *in vivo* studies (Vignali et al. 2008).

An exciting current research topic is how Treg control different types of immune reactions. Apparently Treg can express transcription factors crucial for Th1, Th2, Th17 and follicular T helper differentiation (T-box 21, interferon regulatory factor 4 [Irf4], Stat3 and B cell

leukemia/lymphoma [Bcl6], respectively) to activate transcriptional programs in Treg to enable their correct homing to the site of inflammation to suppress corresponding T helper responses (Chaudhry et al. 2009; Koch et al. 2009; Zheng et al. 2009; Linterman et al. 2011). Further research is needed to determine factors driving these specialized Treg and how they influence the corresponding Tconv at different sites of inflammation.

2.2.2.4 Gene regulation at the FOXP3 *locus and beyond*

The signals from TCR engagement, co-stimulation and cytokines in Treg development and function are all integrated to drive a Treg-specific gene expression program. As stable expression of FOXP3 is essential for Treg, the *FOXP3* locus has been studied extensively with respect to transcription factor binding and epigenetic modifications (Huehn et al. 2009). *FOXP3* is encoded at the X-chromosome and consists of 11 exons. Besides the promoter, 3 intragenic conserved non-coding sequences (CNS1, CNS2 and CNS3) were described to be important for correct orchestration of FOXP3 expression:

Initial TCR engagement in the thymus results in the binding of c-Rel, a NFkB-family TF, to CNS3 (Long et al. 2009; Zheng et al. 2010) and the promoter (Ruan et al. 2009), which is regarded as a crucial pioneer signal for Foxp3 expression in the thymus. Genetic ablation of CNS3 resulted in reduced Treg numbers due to lower probability of Foxp3 expression (Zheng et al. 2010). TCR engagement also increased nuclear factor of activated T cells (NFAT) and activator protein 1 (AP1)-dependent activation of the FOXP3 promoter in humans (Mantel et al. 2006). In mice it was shown that cyclic-AMP-responsive-element (CREB) and activating transcription factor (ATF) bound to a CpG-rich intronic conserved sequence (CNS2) after TCR-ligation and increased Foxp3 expression (Kim and Leonard 2007). Interestingly, this binding was controlled by DNA methylation in this experimental setting, and reduction of DNA methylation by 5-deazacytidine or by knocking out DNA methyltransferase 1 (*Dnmt1*) increased FoxP3 expression in Treg (Kim and Leonard 2007). In line with this, reduction of DNA methylation by 5-aza-2'-deoxycytidine increased FOXP3 expression also in human natural killer (NK) cells *in vitro* as reported by Zorn and colleagues (Zorn et al. 2006). CNS2 was termed the Treg-specific demethylated region (TSDR) and is the best-studied enhancer in Treg (Huehn et al. 2009). Notably the TSDR is completely demethylated in stable Treg and completely methylated in Tconv (Floess et al. 2007; Polansky et al. 2008). TGF-ß induced Foxp3 expression in Tconv was only transient and resulted in an incomplete demethylation of the TSDR, observations also published in the human system (Baron et al. 2007). Even in the absence of FOXP3-inducing TGF-ß, FOXP3 expression was increased after inhibition of DNA methylation by 5-acacytidine in human Treg (Zorn et al. 2006). The methylation status of the TSDR is regarded as such a sensitive molecular marker that it is used to quantify Treg in blood samples (Wieczorek et al. 2009; de Vries et al. 2011).

In addition to TCR signaling-dependent TFs, other transcription factors were described to bind the TSDR, partially in a methylation dependent manner as described for ETS-1 (Polansky et al. 2010). Runt-related transcription factors (Runx) with their associated TF regulatory core-binding factor beta (Cbfb) were shown to maintain Foxp3 expression in Treg via a feed forward loop (Bruno et al. 2009; Rudra et al. 2009) and are critical for the regulation of Foxp3 downstream genes. Interestingly, Foxp3 and Cbfb bind to the TSDR in a DNA methylation dependent manner *in vitro* (Zheng et al. 2010), providing further support for a role of DNA methylation in Foxp3 expression. These data suggest a role for the TSDR, once demethylated and accessible for diverse TFs, as a "memory" module to sustain Foxp3 expression over time, which is supported by the observation that genetic ablation of the TSDR led to progressive loss of Foxp3 expression in Treg (Zheng et al. 2010). Recent publications ad the Foxo proteins Foxo1 and Foxo3a as well as Gata3 to the panel of TFs binding to the TSDR and/or promoter to control Foxp3 transcription (Harada et al. 2010; Kerdiles et al. 2010; Ouyang et al. 2010; Wang et al. 2011). However, the role of Gata3 is controversial as Gata3 can inhibit Foxp3 expression in Th2-polarized cells by binding to the *Foxp3* promoter and on the other hand is important for Treg development and function by acting in concert with Foxp3 to activate Foxp3 expression (Mantel et al. 2007; Wang et al. 2011).

Cytokine signaling also tightly controls the development and function of Treg. Il-2 activates signal transducer and activator of transcription 5 (Stat5), a TF that was shown to bind the TSDR in mice (Yao et al. 2007). STAT5 activation increased the frequency of Treg in peripheral blood in cancer patients *in vivo* and is needed for the *in vitro* expansion of regulatory T cells (Hoffmann et al. 2004; Hoffmann et al. 2006a; Zorn et al. 2006). A mediator of peripheral induction of Foxp3 expression is TGF-ß. Activation of downstream signaling cascades recruits SMAD proteins to CNS1 that cooperate with TCR stimulation-activated NFAT to induce Foxp3 expression (Tone et al. 2008). In line with these observations, genetic deletion of CNS1 limits TGF-ß induction of Treg in the periphery (Zheng et al. 2010).

Taken together, these data confirmed a role for many TFs (derived from different input signals) for stable Foxp3 expression as summarized in **Figure 3**. Knock out models of the corresponding TFs or regulatory CNS sequences at the *Foxp3* locus resulted in drastically reduced Treg numbers or non-functional cells (Yao et al. 2007; Kerdiles et al. 2010; Ouyang et al. 2010; Zheng et al. 2010; Wang et al. 2011). However, global views of key gene loci, their target genes and underlying epigenetic mechanisms in gene regulation are essential to understand basic principles in cell stability and identity. This is of great interest to evaluate the potential application of drugs targeting transcription factor signaling or altering the epigenetic status of cells. First attempts to the global characterizations of Treg were made by analyzing Foxp3 targets in mice and humans by next generation sequencing or ChIP-on-chip experiments (Zheng

et al. 2007; Sadlon et al. 2010; Birzele et al. 2011), revealing new Foxp3 target genes and that Foxp3 is not only a repressor but can also positively influence gene expression. Genome wide maps of H3K4me3 and H3K27ac in different mouse CD4+ Th cell populations (Th1, Th2, Treg and Th17 cells) gave insights into histone patterns around lineage defining genes and explained some observed heritable gene expression programs in fully polarized cells (Wei et al. 2009). Interestingly, these experiments revealed that Treg have no repressing chromatin modification at the Th2 cytokine locus encoding Il-4, while they have both, repressive and active histone modification patterns at the lineage-specific TFs Rorc, Tbx21 and Gata3. Thus, they perhaps activate Il-4 and Gata3 expression and this may explain the observed Il-4 driven Th2 differentiation of Foxp3-losing cells (Wan and Flavell 2007). "Poised" chromatin modifications at the aforementioned TFs could promote their expression in specialized Treg subsets to drive specific suppressor programs as discussed before. In humans, Tian and colleagues identified cell type-specific enhancers by comparative analysis of H3K4me1 ChIP-seq in Treg and activated Tconv (Tian et al. 2011). They demonstrated that H3K4me3 signatures representing promoters were very similar in Treg and Tconv, while broad differences in H3K4me1 marked putative enhancer regions were detected. Nevertheless, comparative enhancer studies of Treg subpopulations and the identification of involved TFs shaping epigenetic patterns are still elusive, but would be important to understand gene regulation in Treg populations on a molecular level. Furthermore, several groups recently observed mechanisms involving non-coding RNAs to participate in Treg development (Chong et al. 2008; Zhou et al. 2008b) and function (Zhou et al. 2008b; Lu et al. 2010b; Beyer et al. 2011).

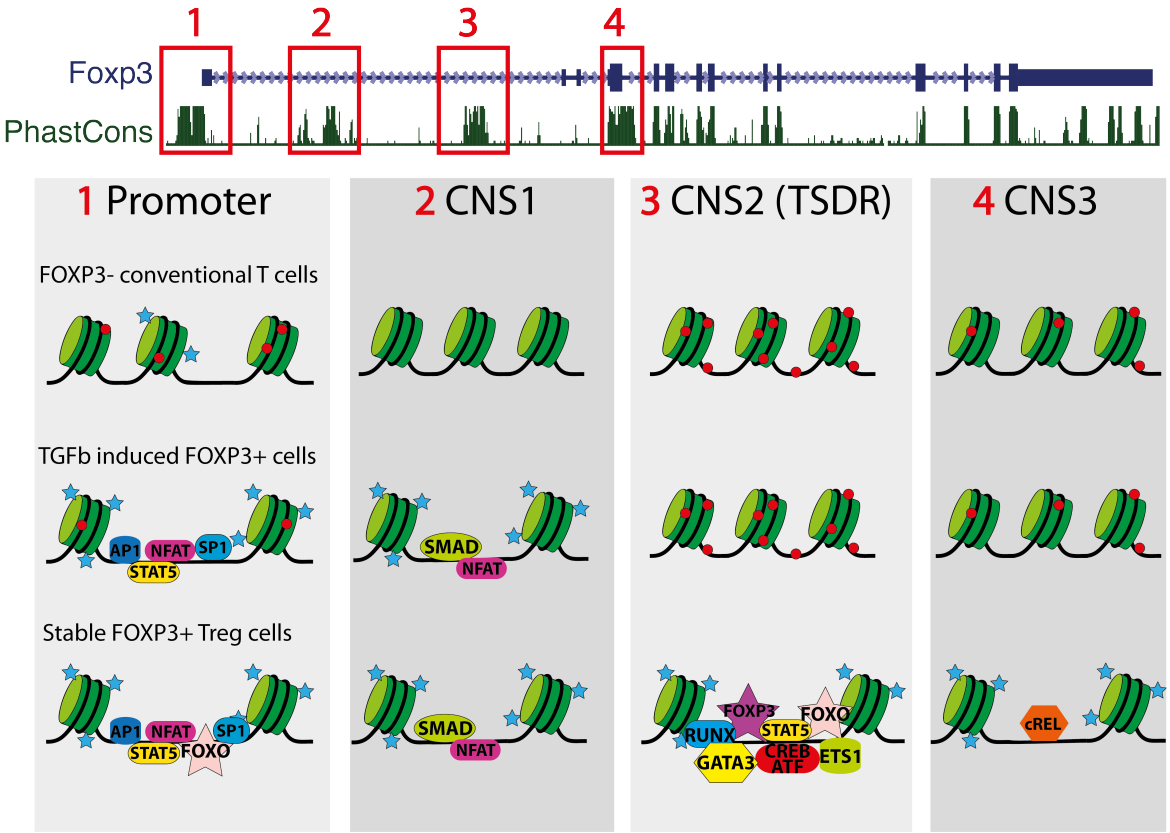

Figure 3
Gene regulation at the *Foxp3* locus. Chromatin structure, DNA methylation and transcription factor binding at the *Foxp3 cis*-regulatory elements (promoter as well as CNS1-3) in conventional T cells, Tgfß-induced Foxp3+ cells as well as stable Foxp3+ Treg cells; DNA (black lines) is wrapped around nucleosomes (green cylinders); red circles: methylated CpG dinucleotide; small red and yellow hexagons: histone methylation at H3K9, H3K27 or H3K4; blue star: histone acetylation; other objects: transcription factors as described in the introduction. (Adapted from Huehn et al. 2009)

2.2.2.5 Stability and heterogeneity

It has long been accepted that thymus-derived CD4+CD25+FOXP3+ Treg represent a stable lineage (Fontenot et al. 2003; Hori et al. 2003; Fontenot et al. 2005b; Sakaguchi 2005; Ziegler 2006). However, recent advances in genomic fate mapping, where permanent expression of fluorescence proteins label cells that once expressed Foxp3, identified populations of "exFoxp3" cells that lost Foxp3 expression and exhibited a memory or effector phenotype (Komatsu et al. 2009; Zhou et al. 2009c). Thus, these findings challenge the view of Treg as a stable lineage. Moreover, it was shown that Foxp3+ cells can convert into pathogenic Foxp3- Th cells after adoptive transfer (Duarte et al. 2009) or in proinflammatory milieus (Xu et al. 2007; Yang et al. 2008a). In contrast, a recent study suggests that the observed plasticity of Foxp3+ cells is restricted to a small population of conventional T cells promiscuously expressing Foxp3 and not

a feature of natural regulatory T cells, suggesting that thymus-derived Treg represent a stable lineage (Miyao et al. 2012).

Seminal work in the human system of Hoffmann and colleagues demonstrated that CD4+CD25+ Treg comprise a "naïve" and memory population discriminated by the expression of CD45RA (Hoffmann et al. 2006b). Naïve Treg stably expressed FOXP3 even after *in vitro* expansion while expansion of memory Treg resulted in loss of FOXP3 expression and secretion of proinflammatory cytokines (Hoffmann et al. 2006b). Based on this it was shown that human memory Treg contain a subpopulation of cytokine-secreting FOXP3lo cells with limited suppressive capabilities but the potential to differentiate into Th17 cells (Miyara et al. 2009). In line with this, a population of FOXP3+ cells was described that expressed RORC and produced the proinflammatory cytokine IL-17 (Ayyoub et al. 2009; Voo et al. 2009). Gene expression profiling of different *ex vivo* Treg subsets also revealed the heterogeneity of Treg populations in different organs, as demonstrated for adipose tissue-derived Treg (Feuerer et al. 2010; Cipolletta et al. 2012). Furthermore, heterogeneity of cells solely characterized by expression of FOXP3 can also emerge from the ability of human Tconv to upregulate FOXP3 upon activation without acquiring a Treg phenotype and function (Gavin et al. 2006). Molecular characterization of key cytokine- and TF loci in Treg/Foxp3+ subpopulations could help to delineate their identity and pathogenic potential.

2.2.2.6 Treg in transplantation

When hematopoietic cells or solid organs are transplanted between genetically different individuals, donor T cells in the transplant recognize the host tissue as foreign, which can mount immune reactions that are harmful for the host. As Treg are suppressive, they are promising agents to prevent such unwanted immune reactions, a hypothesis that was already tested successfully in mouse models (Hoffmann et al. 2002b; Edinger and Hoffmann 2011b) and first clinical studies (Edinger Matthias, unpublished observations; (Brunstein et al. 2011b; Di Ianni et al. 2011a). Interestingly, co-transplantation of Treg in hematopoietic stem cell transplantation (e.g. to cure leukemia) did not impair the beneficial graft-versus-leukemia effect, a process in which transplanted Tconv help to eradicate residual host leukemic cells (Edinger et al. 2003). To obtain sufficient numbers for the repetitive application of regulatory T cells in transplantation, the cells can be expanded up to 40000-fold by repeated TCR stimulations in the presence of high-dose IL-2 (Hoffmann et al. 2004). Furthermore, efficient enrichment methods for the isolation of CD4+CD25+ Treg under good manufacturing practice (GMP) conditions have already been established (Hoffmann et al. 2006a).

2.3 Objectives

With the goal to apply Treg in clinical trials, the lack of understanding in Treg gene regulation, mechanisms of suppression, cellular development as well as the observations about their heterogeneity, plasticity and behavior in expansion systems demand their thorough molecular characterization. This thesis focuses on basic principles of gene regulation in Treg and Tconv to understand the interaction of transcription factor networks with regulatory elements and their impact on gene expression. Moreover, molecular methods are applied to analyze distribution, differences and dynamics of epigenetic features in regulatory and conventional T cell subpopulations and their connected gene expression programs. Furthermore, the question of stability and heterogeneity of Treg subpopulations is addressed to improve potential clinical application of Treg.

3 Chapters identical to manuscripts

3.1 Lineage-specific DNA methylation in T cells correlates with histone methylation and enhancer activity

Published in: Genome Research. 2009 Jul;19(7):1165-74. Epub 2009 Jun 3

PMID: 19494038

Christian Schmidl performed experiments, analyzed data and wrote parts of the manuscript

Lineage-specific DNA methylation in T cells correlates with histone methylation and enhancer activity

Christian Schmidl, Maja Klug, Tina J. Boeld, Reinhard Andreesen, Petra Hoffmann, Matthias Edinger, Michael Rehli#

Department of Hematology, University Hospital Regensburg, 93042 Regensburg, Germany

Corresponding Author:
PD Dr. Michael Rehli
Department of Hematology
University Hospital Regensburg
D-93042 Regensburg
Germany
Tel: 49 941 - 944 - 5587
Fax: 49 941 - 944 - 5593
email: Michael.Rehli@klinik.uni-regensburg.de

Running Titel: Lineage-specific DNA methylation in T cells
Keywords: DNA methylation, Gene regulation, Hematopoiesis

Abstract

DNA methylation participates in establishing and maintaining chromatin structures and regulates gene transcription during mammalian development and cellular differentiation. With few exceptions, research thus far focused on gene promoters, and little is known about the extent, functional relevance and regulation of cell type-specific DNA methylation at promoter-distal sites. Here, we present a comprehensive analysis of differential DNA methylation in human conventional $CD4^+$ T cells (Tconv) and $CD4^+CD25^+$ regulatory T cells (Treg), cell types whose differentiation and function are known to be controlled by epigenetic mechanisms. Using a novel approach that is based on the separation of a genome into methylated and unmethylated fractions, we examined the extent of lineage-specific DNA methylation across whole gene loci. More than one hundred differentially methylated regions (DMR) were identified that are mainly present in cell type-specific genes (e.g. *FOXP3*, *IL2RA*, *CTLA4*, *CD40LG* and *IFNG*), and show differential patterns of histone H3 lysine 4 methylation. Interestingly, the majority of DMR was located at promoter-distal sites and many of these areas harbor DNA methylation-dependent enhancer activity in reporter gene assays. Thus, our study provides a comprehensive, locus-wide analysis of lineage-specific methylation patterns in Treg and Tconv cells, links cell type-specific DNA methylation with histone methylation and regulatory function and identifies a number of cell-type specific, CpG methylation-sensitive enhancers in immunologically relevant genes.

All microarray data have been submitted and are available from the NCBI/GEO repository (accession number GSE14281). The manuscript is accompanied by six supplemental tables and seven figures as well as twelve UCSC Genome Browser track files.

Introduction

A cell's identity and its developmental potential are governed by epigenetic mechanisms which control chromatin structure and accessibility of regulatory DNA sequences. Methylation of cytosine residues in genomic DNA is an important epigenetic mark that is essential for normal embryonic development in mammals (Okano et al. 1999) , imprinting (Li et al. 1993), X-inactivation (Goto and Monk 1998) and silencing of potential hazardous genetic elements like transposons (Walsh et al. 1998). In general, DNA methylation is linked to gene silencing, but its capacity to repress gene transcription depends on the surrounding sequence context and in particular on the local density of CpGs (Weber et al. 2007). The repressor function of CpG methylation is best studied for CpG-dense promoter regions (the so called CpG islands) that are frequently silenced in cancer as a consequence of disease-associated aberrant CpG methylation (Plass and Soloway 2002; Herman and Baylin 2003). Its influence on gene expression in normal physiological settings is less well understood. The great majority of CpG islands is protected from CpG methylation in normal cells, probably due to the presence and function of general transcription factors like specific protein (Sp) 1 and 3 (Brandeis et al. 1994). There is substantial evidence that less CpG-dense promoter regions are more frequently targeted by DNA methylation and that gene expression and CpG methylation status often correlate (Schilling and Rehli 2007; Weber et al. 2007). Traditionally, the tissue- or cell type-specific DNA methylation studies focused on proximal promoter regions. However, a number of recent observations suggest that only a limited number of promoters display cell type-specific CpG methylation, suggesting that DNA methylation might have a minor role in controlling cell type- or lineage-specific gene regulation (Meissner et al. 2008; Mohn et al. 2008).

With few exceptions, promoter-distal sequences have received little attention so far, and we know little about the global distribution and dynamics of DNA methylation during normal developmental processes, particularly in lineage-specification and differentiation processes in the adult organisms. To gain a better understanding of their biological role, CpG methylation patterns have to be studied globally in well defined model systems like embryonic stem cells or the hematopoietic system. The latter is of particular interest for epigenetic studies as progenitor cells as well as various differentiated cell lineages can be isolated and purified for a comparative analysis of homogenous cell subpopulations. With the development and therapeutical use of 'epigenetic drugs' like DNA methyltransferase- or histone deacetylase inhibitors, it is of growing importance to understand the underlying regulatory mechanisms and potential effects on the normal hematopoietic cell system.

Natural $CD4^+CD25^+$ regulatory T (Treg) cells play a fundamental role in maintaining immunological self tolerance and immune homeostasis (Vignali et al. 2008) . They develop in the thymus as an independent $CD4^+$ T cell lineage and represent a prime example for epigenetic regulation. It was shown that the functional program of Treg cells is at least partially controlled by miRNA pathways (Chong et al. 2008; Liston et al. 2008; Zhou et al. 2008b) and the continuous expression of the lineage-directing transcription factor FOXP3 is dependent on its DNA methylation status at a methylation sensitive, Treg cell-specific enhancer (Floess et al. 2007; Kim and Leonard 2007; Polansky et al. 2008).

Apart from this particular region at the *FOXP3* locus, we know little about the regulatory role of DNA methylation during Treg lineage commitment, differentiation and cell type-specific gene regulation. Here we describe a comprehensive comparative analysis of DNA methylation patterns at selected gene loci in human $CD4^+CD25^-$ conventional T cells (Tconv) and Treg cells. In line with recent observations in other cell systems (Meissner et al. 2008; Song et al. 2009), we found that the majority of differentially methylated regions (DMR) are located at promoter-distal sites. Many of these areas were found to harbor DNA methylation-dependent enhancer activity in reporter gene assays and cell type-specific demethylation was found to correlate with increased methylation at histone H3 lysine 4 (H3K4).

Thus, we identified a number of cell type-specific, CpG methylation-sensitive enhancers at immunologically relevant genes in Treg and Tconv cells. In a more general point of view, our data suggest that the restriction of cell type-specific enhancers is a key function of DNA methylation in adult progenitor cells and that differentiation and lineage commitment are associated with specific methylation or demethylation events in such enhancer regions.

Results

Identification of differentially methylated regions (DMR) in Treg and Tconv cells using Methyl-CpG Immunoprecipitation (MCIp)

The recent development of fractionation techniques that enrich for methylated DNA fragments now permits the examination of CpG methylation on global platforms such as oligonucleotide tiling arrays or next generation sequencers. Current technologies are particularly well suited to address CpG methylation in CpG-dense regions, whereas it remains difficult to systematically analyze regions of lower CpG content that comprise the majority of mammalian genomes.

We previously developed technologies for the fractionation of genomic DNA fragments depending on their CpG density (methyl-CpG immunoprecipitation, MCIp (Gebhard et al. 2006; Schilling and Rehli 2007), and adapted this approach to identify regions that are differentially methylated in two closely related T cell populations, namely Treg and Tconv cells. Due to the low frequency of Treg cells in peripheral blood we FACS-purified CD45RA$^+$ naïve CD4$^+$CD25^{high} T cells and expanded those cells *in vitro* (see "Material & Methods"). We previously showed that these cells homogeneously maintain all phenotypic, functional and epigenetic Treg cell characteristics even after extensive in vitro proliferation (Hoffmann et al. 2006b; Baron et al. 2007). We separated gDNA from both, expanded Treg and Tconv cells (Treg^{exp} and Tconv^{exp}) into unmethylated (CpG) and methylated pools (mCpG) using MCIp and compared cell type-specific differences in DNA methylation by co-hybridization of the two umethylated or the two methylated DNA subpopulations of Treg and Tconv cells, respectively, to locus-wide tiling arrays. As enriched DNA-fragments from a cell type in the methylated fraction should be depleted in the unmethylated fraction, the signal intensities in CpG pool and mCpG pool hybridizations should complement each other ("Mirror-Image" approach, see **Figure 1A**) and thereby allow the identification of differentially methylated regions (DMR). Because we expected to find lineage-specific methylation differences with greater probability in regions associated with differential transcriptional activity, we limited our analysis to gene loci that showed cell type-specific gene expression in Treg versus Tconv cells (both, *in vitro* expanded or freshly isolated) plus several control regions that were equally expressed in both cell types. Gene loci were selected based on own and previously published expression studies (Pfoertner et al. 2006; Hill et al. 2007) to mainly include those genes that are differentially expressed in freshly isolated (unstimulated) cells but also in *ex vivo* cultured and expanded T cell subsets that underwent several cycles of polyclonal TCR activation (Hoffmann et al. 2006b). The microarray used in this study covered 12 megabases of the human genome and contained 69 regions (with a

median size of 100 kb) and 128 proximal promoter regions and 181 genes, including a number of well known and functionally relevant genes like *CD40LG*, *IFNG*, *FOXP3*, *IL2R*, *CTLA4*, etc. (the complete list of selected regions is given in **Supplemental Table S1**).

A representative scatter plot of comparative microarray hybridizations from unmethylated (CpG) and methylated pools (mCpG) is shown in **Figure 1B**, where microarray probes showing the expected complementary behavior are colored in red (hypomethylated in Treg) and blue (hypomethylated in Tconv). In total, we identified 132 regions with lineage-specific CpG methylation that were associated with 53 genes (A complete list of DMR is given in **Supplemental Table S2)**. The majority of DMR (89%) were of low CpG content (LCRs) and all residual sites are of intermediate CpG content using the classification described by Weber et al. (2007)(Weber et al. 2007). Only seven out of 132 DMR overlapped with known proximal gene promoters, 64% of all DMR were located within gene bodies, whereas 36% were located in intergenic areas. As shown in **Supplemental Figure S1**, DMR status and differential mRNA expression status were significantly correlated regardless of the relative DMR position (intergenic/intragenic). Next, we searched for known sequence motifs enriched in T cell subset-specific DMR. Consensus sites enriched in DMR as compared to the whole genome included cAMP-responsive ATF/CREB-sites (in DMR hypomethylated in Tconv cells) or STAT5-motifs (in DMR hypomethylated specifically in Treg cells). Lists of the top ranking motifs are provided in **Supplemental Table S3**.

To validate and quantify methylation differences, a representative set of DMR was selected for MALDI-TOF MS analysis (for information on amplicons and MALDI-TOF MS results for all samples see **Supplemental Tables S4 and S5**). Mass spectrometry yields quantitative methylation data of short stretches of subsequent CpGs in high-throughput and consequently allows validation of large sample sets. An example of microarray and corresponding MS results is shown in **Figure 1C**. *LRRC32*, encoding the Treg cell-specific surface molecule GARP that mediates suppressive function and *FOXP3* induction (upon ectopic expression in naïve Tconv cells), contained a region in intron 1 that showed a hybridization pattern indicative of Treg cell-specific hypomethylation (**Figure 1C**, left bottom panel): microarray signal ratios of Treg-Tconv comparisons were high in the unmethylated (CpG) and low in the methylated pools (mCpG), resulting in a significant hypomethylation score. Mass spectrometry of bisulfite-treated DNA demonstrated that the center region was indeed completely methylated in Tconv cells and only weakly methylated in Treg cells, regardless whether cells were freshly isolated or expanded (**Figure 1C**, right bottom panel). In total, 26 out of 31 selected DMR were confirmed by MS.

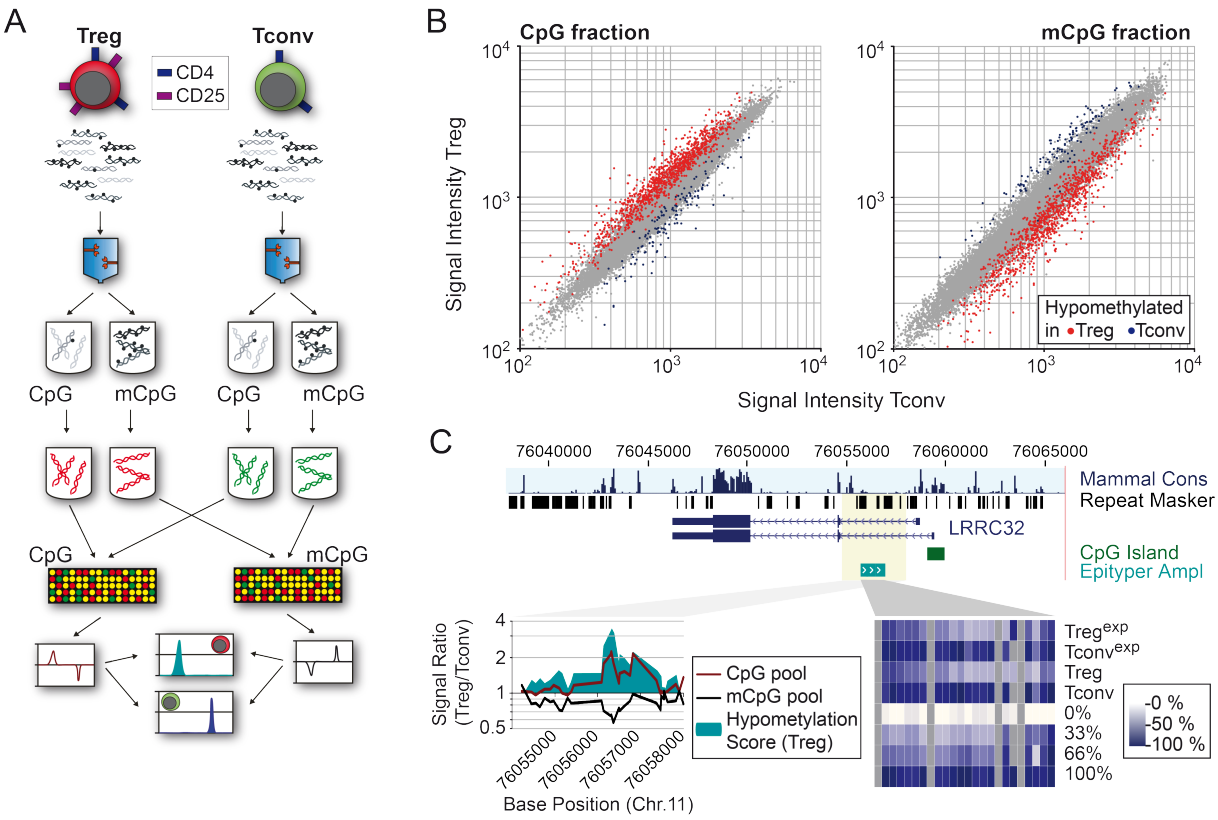

Figure 1:

Locus-wide identification of DMR using the MCIp 'mirror image' approach. (A) Schematic outline of the MCIp fragmentation and hybridization strategy. The fragmented genomes of Tconv and Treg cells are separated into unmethylated (CpG) and methylated (mCpG) pools. Each pool is directly labeled using fluorescent dyes and each pool of one cell type is compared to the corresponding pool of the other cell type on a locus-wide microarray. Microarray images are compared to identify regions that show a reciprocal hybridization behavior. (B) Representative scatter plots of CpG- and mCpG-pool hybridizations are shown. Probes with reciprocal signal intensity ratios indicate the presence of DMR and are marked in red (Treg cells) or blue (Tconv cells). (C) Exemplary validation of microarray results using mass spectrometry. The intron 1 region of *LRRC32* is enriched in the unmethylated (CpG, red line) and depleted in the methylated (mCpG, black line) pools of Treg cells. A large hypomethylation score (defined as the difference product of Log_{10} signal intensity ratios of both hybridizations) indicates differential methylation (left bottom panel). The same region was analyzed by MALDI-TOF MS (Epityper) and results are shown as a heatmap (the scale ranges from pale yellow (no methylation) to dark blue (100% methylation).

Methylation levels at DMR in other hematopoietic cell types

To investigate whether the identified DMR were specific for T cell populations, we also obtained mass spectrometry data for other major blood cell types including $CD8^+$ T cells, $CD19^+$ B cells, $CD56^+$ NK cells, $CD14^+$ monocytes and $CD34^+$ hematopoietic progenitor cells as well as the Jurkat T cell line. $CD34^+$ cells represent a mixture of mainly committed myeloid, but also common hematopoietic progenitor cells. As shown in **Supplemental Figure S2**, the majority of CpG dinucleotides located in DMR are methylated in $CD34^+$ hematopoietic progenitor cells, suggesting that CpGs in T cell-specific DMR are demethylated during progenitor cell differentiation. It is also noteworthy that the observed CpG methylation differences were detected both in freshly isolated T cells subsets as well as in T cells that were cultured and expanded *in vitro*. Since the latter involved a polyclonal TCR-stimulation for both conventional and regulatory T cell subsets it is likely that the observed differences are characteristic for each lineage and are not affected by T cell activation.

MS-derived hematopoietic methylation profiles are shown in detail for *CTLA4* (**Figure 2**), *IL2RA* (**Figure 3**) and *FOXP3*, *CD40LG, IFNG* and *LRRC32* (**Supplemental Figures S3-S6**). When compared with other blood cell types, only few regions were T cell type-specific, including two upstream regions of *CTLA* (s. **Figure 2**), a region in intron1 of *IL2RA* (s. **Figure 3**), intron 1 of *FOXP3* and intron 1 of the neighboring *PPP1R3F* (see **Supplemental Figure S3**), intron 4 of CD40LG (see **Supplemental Figure S4**), and the downstream DMR of *LRRC32* (see **Supplemental Figure S6**).

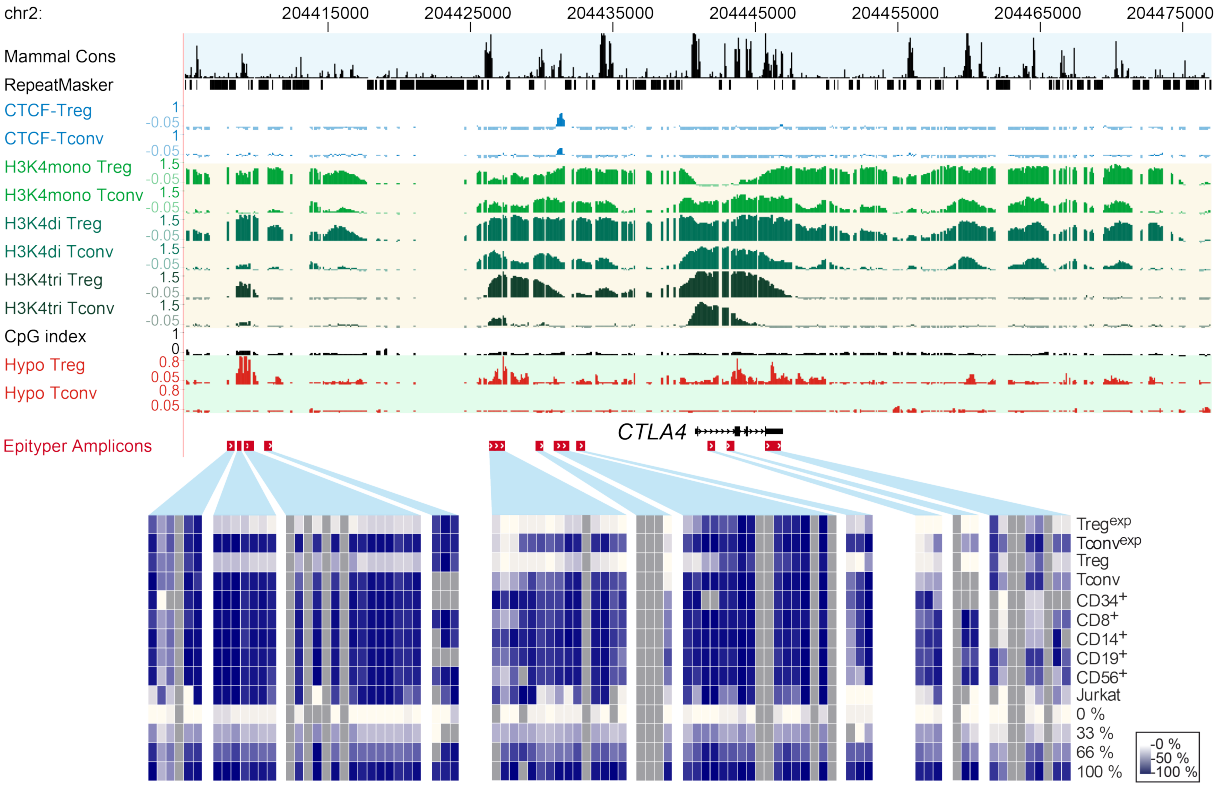

Figure 2:

Chromatin modification and CTCF binding patterns across the *CTLA4* gene locus. Shown are the following tracks (from top to bottom): mammalian Consensus (Cons), repetitive regions as identified by the RepeatMasker program (both in black), ChIP-on-Chip tracks for CTCF (in blue), monomethylated (pale green), dimethylated (green) and trimethylated (darkgreen) lysine 4 of histone H3, the CpG index (indicating the methylation density 300 bp up- or downstream of each microarray probe) as well as hypomethylation scores (in red) for both cell types. Several amplicons were designed for MALDI-TOF MS analysis of bisulfite treated DNA as indicated below the tracks. Methylation levels of individual CpGs in the indicated cell types are shown color-coded as described in the **Figure 1** legend.

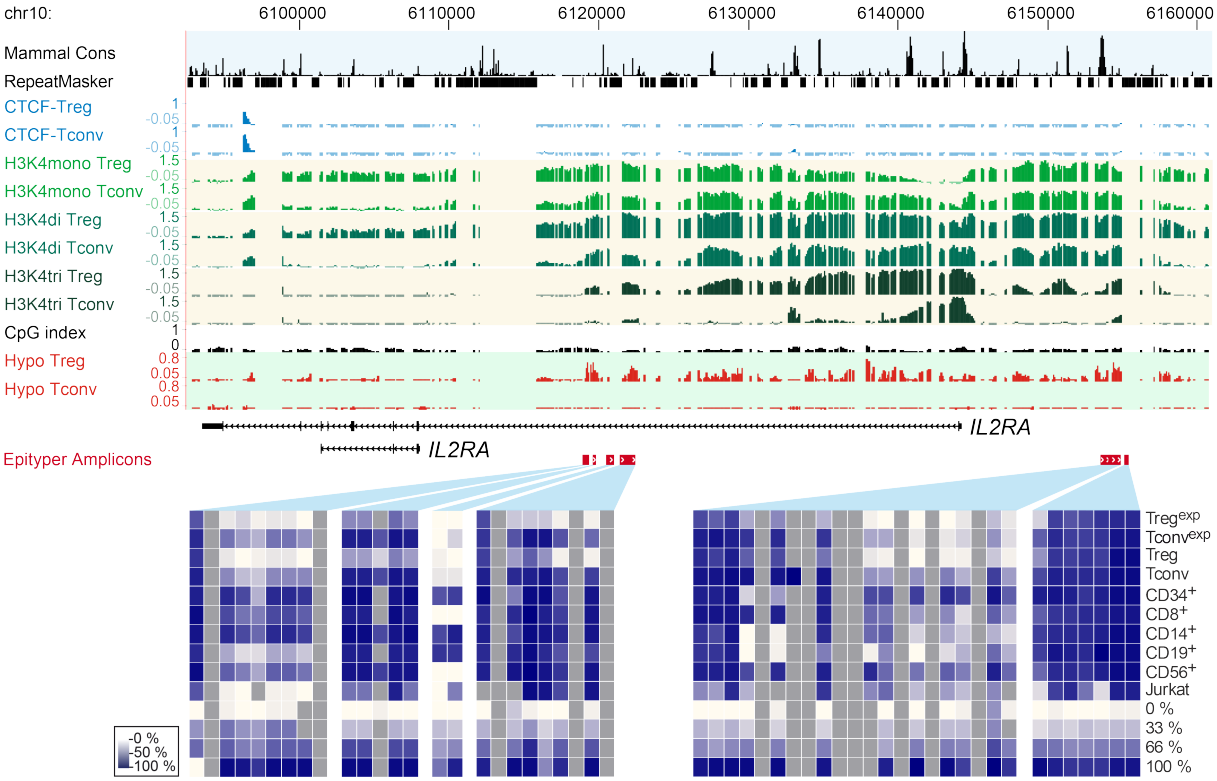

Figure 3:

Chromatin modification and CTCF binding patterns across the *IL2RA* gene locus. Tracks and heat maps are shown as described in the legend of **Figure 2**.

Correlation between DNA methylation, chromatin boundaries and histone methylation.

The majority of detected DMR were located at promoter-distal sites. To characterize potential functions of these regions, we next examined binding sites of the insulator protein CTCF. Binding of CTCF at imprinted loci restricts or directs enhancer-promotor interactions, and this binding is often regulated by DNA methylation (Bell and Felsenfeld 2000). We mapped CTCF binding sites using ChIP-on-Chip on our locus-wide tiling array. The binding pattern of CTCF was almost identical to the published data set for $CD4^+$ T cells (Barski et al. 2007) and showed little variation between Treg and Tconv cells. In addition, we found no overlap between DMR and CTCF binding (data not shown), suggesting that the regulation of CTCF controlled chromatin boundaries is not a major function of DMR at the non-imprinted loci investigated in this study.

To address the question whether DMR at promoter-distal sites harbor regulatory functions, we examined the association of methylation patterns with other chromatin modifications known to control enhancer elements. Mono- and dimethylation of histone H3 lysin 4 (H3K4) were previously shown to mark enhancer regions (Heintzman et al. 2007), whereas H3K4 trimethylation generally associates with transcription start sites (Barski et al. 2007). Using the ChIP-on-Chip approach we mapped these three histone marks in expanded Treg and Tconv cells. In general, we observed the expected continuous pattern of H3K4 methylation: Mono- and di-methylation were often found together and showed a similar distribution if no tri-methylation was present. If tri-methylation is detected, mono-methylation tends to decrease (relative to di-methylation). Mono-methylation without di-methylation or tri-methylation without di-methylation we rarely detected. Examples of selected gene loci are presented in **Figure 2** and **3**, as well as in **Supplemental Figures S3-S6** (the complete set of microarray data is provided as UCSC Genome browser track files in the **Supplemental Material**).

Since the three possible methylation states of H3K4 are not independent from each other they cannot be correlated with differential CpG methylation independently. However, if DMR correlated with H3K4 methylation, one would expect to observe a co-enrichment of cell type-specific hypomethylation and H3K4 methylation in isolates from the same cell type. The diagrams in **Figure 4** show that this is indeed the case. Di- and trimethylated H3K4 clearly correlated with the differential methylation status at sites where H3K4 methylation was observed. Due to the interdependence of H3K4 methylation states and the frequent appearance of di- and trimethylation states, monomethylated H3K4 did not correlate with the differential methylation status. We also classified DMR regions according to their relative H3K4 methylation status. Pie charts in **Figure 4D** illustrate the distribution of H3K4 methylation patterns at cell type specific DMR. Regions with activating regulatory function are most likely in those classes

where hypomethylation in one cell type correlates with an increased level of H3K4 methylation in the same cell type. The distribution of H3K4 methylation patterns at cell type-specific DMR depending on their relative position (intergenic/intragenic) are shown in **Supplemental Figure S7**. In line with previous observed distribution of global patterns (Barski et al. 2007; Heintzman et al. 2007), trimethylation of H3K4 was more strongly associated with intragenic DMR.

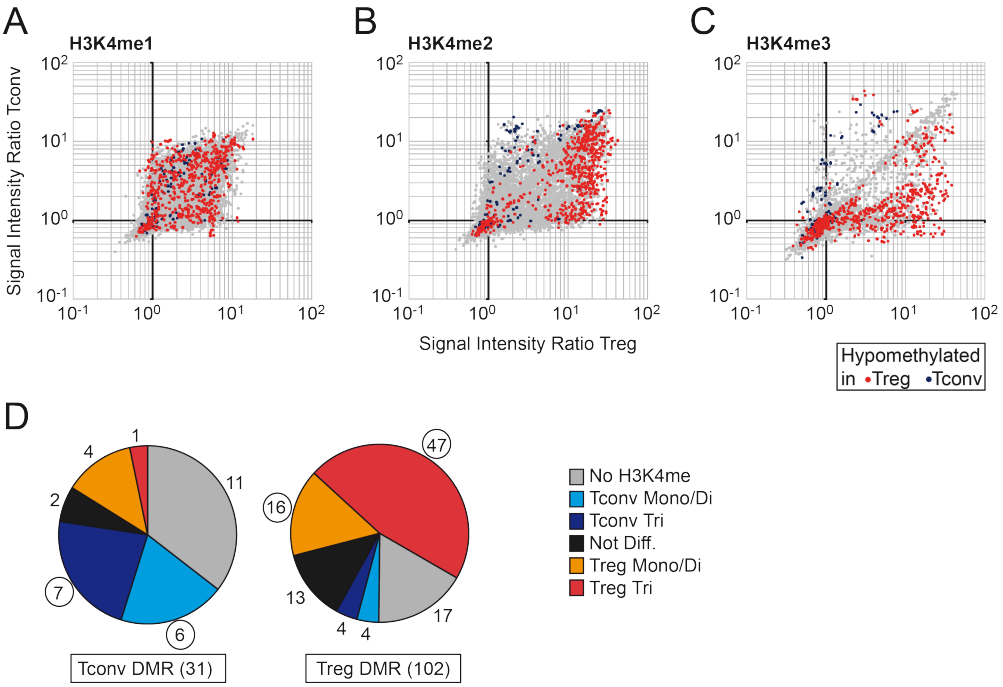

Figure 4:

Correlation of DNA demethylation and H3K4 methylation status. (A-C) Probe signal ratios of Tconv and Treg cells are plotted against each other for ChIP-on-Chip experiments of monomethylated (A), dimethylated (B) and trimethylated (C) lysine 4 of histone H3. Probes that appear along the diagonal indicate similar H3K4 methylation levels, whereas probes above or below the diagonal indicate higher methylation levels in Tconv or Treg cells, respectively. Probes in DMR are colored (unmethylated in Tconv: blue; unmethylated in Treg: red), all other probes are in gray. (D) The two pie charts illustrate the relationship of associated H3K4 methylation and DMR hypomethylated in Tconv (left chart) or Treg (right chart). The H3K4 methylation status was classified as follows: DMR with increased H3K4 tri-methylation in Treg or Tconv cells (Treg Tri or Tconv Tri, respectively), DMR with increased H3K4 mono-, or di-, but no tri-methylation in Treg or Tconv cells (Treg or Tconv Mono/Di respectively), DMR with H3K4 methylation present but not difference between T cell subsets (Not diff.) and DMR with no detectable H3K4 methylation (No H3K4me). The numbers of DMR in each sub-class are shown next to each piece of pie. Sub-classes where hypomethylation in one cell type correlates with an increased level of H3K4 methylation in the same cell type are marked by a circled number.

Enhancer activity of T cell-specific DMR

As methylated H3K4 has previously been associated with enhancer activity (Heintzman et al. 2007) and co-segregated with DMR in our experiments, we next asked whether DMR associate with enhancer activity. Properties of generic enhancers include their ability to increase transcriptional activity in a heterologous context, which can be studied using traditional reporter gene assays. We recently developed a reporter vector that completely lacks CpG dinucleotides (Klug and Rehli 2006) and utilized this system to test for heterologous enhancer activity of 24 selected DMR. We preferentially selected DMR that were associated with genes that also showed differential gene expression and H3K4 methylation (general properties of the selected DMR are listed in **Supplemental Table S7**). Transient transfections were performed in untreated, PMA/ionomycin-, or PHA-treated Jurkat T cells using unmethylated (CpG) or in vitro *SssI* methylated (mCpG) reporter plasmids. As shown in **Figure 5**, twelve out of 24 DMR significantly enhanced the activity of the basal (CpG-free) EF1 promoter. Importantly, all regions lost enhancer activity when methylated, suggesting that their activity is critically dependent on their CpG methylation status. Functionality in the enhancer assay did not correlate with DMR positioning (intergenic/intragenic), conservation status, the presence of DNaseI hypersensitive sites in CD4+ T cells (Boyle et al. 2008) or H3K4 methylation status (for details see **Supplemental Table S7**). However, the majority of regions that did not show enhancer activity in Jurkat cells corresponded to Treg cell-specific DMR, including e.g. both upstream *CTLA4* regions, and an upstream region of *ZNFN1A2*. In line with this, DMR that did show enhancer activity in Jurkat cells were enriched for Tconv cell-associated consensus binding sites (cAMP-responsive ATF/CREB-sites and ELK1-sites; for a list of the top ranking motifs see **Supplemental Table S8)**. Since Jurkat T cells represent a leukemic counterpart of conventional T cells, it is possible that they lack Treg cell-specific transcription factors that are necessary for enhancer functions of these regions. However, some Treg cell-specific DMR did function even in Jurkat cells, suggesting that the relevant transcription factors required for enhancer activity at these sites were available.

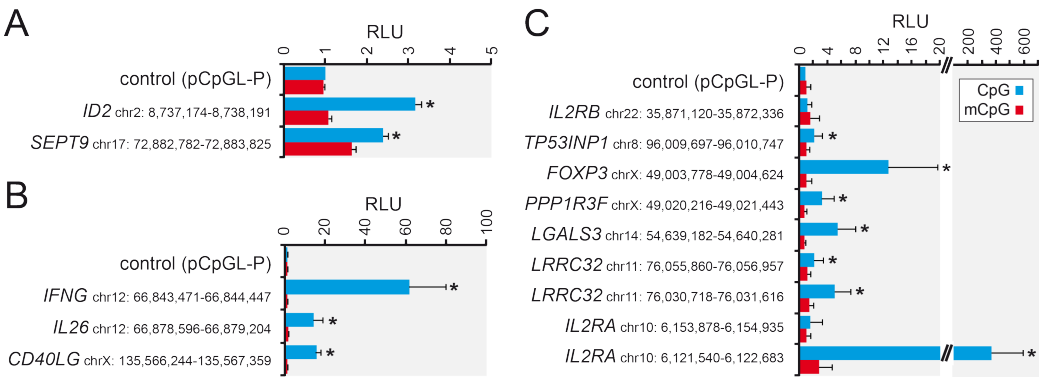

Figure 5:

CpG methylation-dependent enhancer activity of selected DMR. Several DMR were cloned upstream of a basic EF1-promoter into the CpG-free luciferase vector pCpGL-P. The indicated plasmids were *in vitro Sss*I-methylated (mCpG) or unmethylated (CpG) and transiently transfected into Jurkat T cells that were left untreated (A), stimulated with PMA and ionomycin (B) or PHA (C) after transfection. Luciferase activity was normalized against the activity of a co-transfected *Renilla* construct and mean values +/- SD are shown relative to the unmethylated pCpGL-P. An asterisks indicates a significant difference between methylated and unmethylated plasmids ($P < 0.05$ paired Student's t-test).

Discussion

In this study we utilized a combination of DNA methylation-dependent genome fractionation using methyl-CpG immunoprecipitation (MCIp) and quantitative methylation analysis on a mass spectrometry platform (Sequenom MassARRAY system) to identify differentially methylated regions (DMR) in two closely related T cell subtypes (Treg and Tconv cells). We identified more than one hundred DMR in 69 selected geneloci that were primarily located at promoter-distal regions, correlated with differential H3K4 methylation patterns and were mostly methylated in $CD34^+$ hematopoietic progenitor cells. Many of the DMR show properties of methylation-sensitive enhancers, suggesting that DNA methylation plays a role in establishing and maintaining cell type-specific gene regulation by restricting lineage-specific enhancers.

Previous studies largely focused on gene promoter regions and, although there is ample evidence for cell type-specific DNA methylation at proximal promoters, it appears to regulate only a small proportion of genes and thus seems to play only a minor role for lineage-specific gene regulation. For example, in an ES cell model of neuronal differentiation, DNA methylation was shown to play a minor role in regulating gene promoters upon terminal differentiation whereas it appeared to restrict promoters of pluripotency genes in lineage-committed progenitor cells (Mohn et al. 2008).

In this study, only a small proportion (approximately 5%) of all Treg or Tconv cell-specific DMR were located at proximal promoters, indicating that at least in this particular model system, differences in DNA methylation occur mainly at promoter-distal sites and were thus largely neglected in previous studies. Our findings in $CD4^+$ T cells are in line with a recent study in ES cells which also identified promoter-distal regions as the main sites of dynamic changes in DNA methylation upon differentiation (Meissner et al. 2008) and with a study on tissue-specific CpG island methylation which demonstrated that methylation of CpG islands in normal tissues preferentially occurs at promoter-distal sites (Illingworth et al. 2008). Most DMR that we identified were of low CpG content (LCR), suggesting that promoter-distal elements may differ from promoter-proximal sites, where cell type-specific changes more frequently occur in intermediate CpG content regions (Mohn et al. 2008). Interestingly, DMR were significantly enriched for transcription factor binding motifs that were previously shown to play a role in each T cell subset. DMR hypomethylated in Tconv cells were enriched for ATF/CREB consensus sites which are known to mediate mitogenic and CD28-dependent signals (Hsueh et al. 1997). Regions specifically demethylated in Treg cells were enriched for STAT5 consensus sites. Treg cell survival critically depends on the presence of IL-2. The transcription factor STAT5 is activated through the IL-2 receptor (Hou et al. 1995), has an essential role in CD25+CD4+ regulatory T cell homeostasis (Antov et al. 2003) and is known to regulate the lineage-specific

transcription factor FOXP3 through an intronic, methylation sensitive enhancer (Zorn et al. 2006). The significant enrichment of consensus sites does not necessarily imply a biological significance. Further experiments are needed to show that these motifs are actually bound by transcription factors *in vivo*. However, the fact that enriched consensus motifs belong to transcription factors with known importance in each lineage may point to a functional role of lineage-specific DMR.

The majority of DMR in both T cell subsets were methylated in $CD34^+$ hematopoietic progenitor cells and often also methylated in other mature hematopoietic lineages. $CD34^+$ cells comprise a relatively heterogeneous mixture of committed and uncommitted progenitor cells. However, the percentage of uncommitted as well as T cell lineage-committed precursors is likely to be small. Since we were unable to obtain sufficient numbers of primary human T cell progenitors, it is unclear whether individual methylation patterns are created by methylation of previously unmethylated CpG residues or by demethylation of previously methylated sites. Because CpG methylation is often found in $CD34^+$ progenitors and mature cells of both myeloid and lymphoid lineages, it is likely that, in many cases, methylation marks are removed during lineage commitment of either T cell subtype.

Previous studies suggested that mono-, dimethylation or trimethylation at lysine 4 of histone H3 (H3K4) at promoter-distal sites is often associated with enhancer function (Barski et al. 2007; Heintzman et al. 2007; Wang et al. 2008b). In line with the findings of a recent study (Meissner et al. 2008), we observed an enrichment of H3K4 methylation (both di- and trimethylation) at many DMR in the T cell type that was hypomethylated, which suggested a regulatory function for these regions. DMR will be most likely associated with an active regulatory function when hypomethylation in one cell type correlates with an increased level of H3K4 methylation in the same cell type. However, since some gene regulatory events during the differentiation of conventional and regulatory T cells may only be of transient nature, it is possible that DMR displaying no H3K4 methylation in our analysis have lost this dynamic histone mark but retained the more stable CpG methylation pattern. Converse patterns (hypomethylation in one cell type correlates with an increased level of H3K4 methylation in the other cell type) are rarely observed but validated in at least one case: the DMR located upstream of *ID2* (chr2:8735102-8735444) shows hypomethylation in Treg cells but an increased H3K4 methylation in Tconv cells. The biological significance of the converse patterns is unclear; however, it is possible that silencing elements may also be subject to regulation by DNA methylation.

Three of the identified DMR were previously described as functional enhancer elements. Both upstream regions at the *IFNG*/*IL26* locus were defined as conserved, activation-induced enhancers in conventional murine $CD4^+$ T cells (Schoenborn et al. 2007b). In Treg cells, a

functionally important intronic enhancer of the *FOXP3* gene was shown to be methylation-sensitive (Baron et al. 2007; Floess et al. 2007; Kim and Leonard 2007). Therefore, we now asked whether other DMR might also demonstrate enhancer properties and whether methylation would restrict enhancer activity. Half of the twenty-four tested DMR significantly enhanced the activity of a heterologous promoter in transient reporter gene assays performed in a T cell leukemia line (Jurkat). Most strikingly, all regions lost enhancer activity upon CpG methylation. Even some Treg-specific DMR showed enhancer activity in the Jurkat cells, suggesting that these cells per se express the required factors for enhancer function and that CpG methylation may be critical to restrict the lineage-specific enhancer function of these DMR in Tconv cells.

In some cases, DMR (e.g. both DMR upstream of *CTLA4*) co-located with trimethylated H3K4 that were not associated with detectable transcription (no associated ESTs or CAGE tags published in human or mouse, data not shown). Trimethylated H3K4 is usually associated with promoters and its occurrence at enhancers is debated. Whereas Heintzmann et al. (2007) (Heintzman et al. 2007) preferentially found H3K4 monomethylation (and little or no H3K4 trimethylation) at p300 associated enhancers, Barski et al (2007) (Barski et al. 2007) identified all three methylation states at functional enhancers. It is therefore unclear whether the promoter-distal, H3K4 trimethylated sites identified in this study associate with so far uncharacterized functional transcription units, or whether they act as (transcribed) enhancer regions like e.g. the upstream enhancer of the myeloid- and B cell specific *SPI1* gene (Hoogenkamp et al. 2007). Since Treg cells represent only a minor fraction of $CD4^+$ T cells, their transcriptome is likely under-represented in public cDNA sequence databases. Therefore, further studies aiming at understanding cell type-specific gene regulation in T cell subtypes will require a more comprehensive definition of transcription units, especially in Treg cells.

A recent comprehensive study of the regulatory potential of mammalian conserved non-coding sequences suggests that only a small proportion of these regions can be expected to exhibit classical *cis*-regulatory activity in standard experimental assays (Attanasio et al. 2008). In our hands, only a minority of the identified DMR were conserved during evolution. For example, the intronic DMR of *IL2RA* was not conserved across species but acted as the strongest enhancer in heterologous reporter assays. Our data suggest that conservation-centred approaches to identify enhancer elements may miss out on a large number of important regulatory sites.

In addition to the basic findings on cell type-specific DNA methylation described above, our study identifies a number of putative regulatory elements in genes that are highly important for T cell function. For example, we found a methylation-sensitive enhancer in intron 4 of *CD40LG* in Tconv cells. The encoded cell surface receptor plays an important role in regulating B cell

function through its interaction with CD40 on B cells and dendritic cells (vanKooten and Banchereau 1997). The majority of interesting regions, however, were associated with genes important for Treg cell biology. It was previously shown that sustained expression of the lineage-determining transcription factor FOXP3 is dependent on its DNA methylation status at a methylation-sensitive, Treg cell-specific enhancer in intron I (Baron et al. 2007; Floess et al. 2007; Kim and Leonard 2007). Our locus-wide analysis identifies an extensively demethylated area at this locus that extends into the neighboring protein phosphatase 1, regulatory (inhibitor) subunit 3F (*PPP1R3F*) gene, where we identified an additional methylation-dependent enhancer. Two DMR with enhancer function were identified at the *LRRC32* locus encoding a recently described surface molecule (also called GARP) that seems to contribute to the suppressive function of Treg cells (Wang et al. 2008a). A novel and potent enhancer was found at the *IL2RA* gene that encodes the alpha chain of the IL-2 receptor (CD25). This methylation-sensitive enhancer region was specifically demethylated in both freshly isolated Treg cells as well as in Treg cells that were cultured and expanded *in vitro*. Since cultured and expanded conventional T cells express high levels of CD25 as a consequence of TCR activation, this region may contribute to regulating constitutive (rather than activation-induced) CD25 expression in Treg cells.

Additional DMR were found upstream of *ZNFN1A2*, encoding a regulator of lymphocyte development (Dovat et al. 2005), **a**nd *CTLA4,* encoding a molecule that is constitutively expressed on Treg cells and that suppresses immune responses by affecting the activating potency of antigen-presenting cells (Wing et al. 2008)**.** Although both upstream *CTLA4* regions and the upstream region of *ZNFN1A2* showed no enhancer activity in transient transfection assays, the exclusive DNA demethylation and the increased H3K4 methylation in Treg cells indicate a functional importance of these regions. Their activation may actually require Treg-specific *trans*-acting factors that are not present in Jurkat cells used for the reporter gene studies. The further characterization of the identified DMR, including the identification of DNA-binding factors mediating the observed enhancer activities, will likely reveal important insights into cell type-specific gene regulation in T cells.

In conclusion, the observed distribution of DMR at promoter-distal regions, their association with functional chromatin marks and, most strikingly, their methylation-sensitive enhancer activity suggest a role for DNA methylation in controlling lineage-specific gene expression mainly by restricting promoter-distal regulatory elements. This basic principle is likely not confined to the two closely related T cell populations but may generally apply to somatic cell lineages in adult organisms.

Methods

Cell purification and culture

MNC were isolated from leukapheresis products of healthy volunteers (after their informed consent and in accordance with protocols approved by the local authorities) by density gradient centrifugation over Ficoll/Hypaque (Biochrom AG, Berlin, Germany). $CD4^+$ cells were enriched using magnetically labeled human CD4 MicroBeads (Miltenyi Biotec, Bergisch Gladbach, Germany) and the Midi-MACS system (Miltenyi Biotec). The $CD4^+$ fraction was stained with CD4-FITC (SK3), CD25-PE (2A3) and CD3-APC (UCHT1) and separated into $CD3^+CD4^+CD25^-$ conventional T cells and $CD3^+CD4^+CD25^{high}$ regulatory T cells on a FACS-Aria high-speed cell sorter (BD Biosciences, Heidelberg, Germany). The $CD4^-$ fraction was stained with CD19-FITC (4G7), CD56-PE (B159), CD3-PerCP (SK7) and CD8-APC (SK1) and sorted into $CD19^+CD3^-$ B cells, $CD56^+CD3^-$ NK cells and $CD3^+CD8^+$ T cells. Monocytes were enriched from MNC using counter-current elutriation in a J6M-E Beckman centrifuge (Beckman, Munich, Germany) with a large chamber and a JE-5 rotor at 1100g at a flow rate of 110 ml/min in Hanks' balanced salt solution as described previously. Enriched cell fractions were stained with CD14-PE (M P9) and CD3-APC (UCHT1), and $CD14^+CD3^-$ monocytes were further purified by FACS. All antibodies used were from BD Biosciences. All staining was performed in PBS / 2% FCS. Dead cells were excluded by staining with propidium iodide. All cell populations showed a purity of > 95 % upon re-analysis.

T cell populations for expansion cultures were isolated as described in detail before (Hoffmann et al. 2006b). In brief, PBMC were stained with anti-CD25-PE and $CD25^+$ cells were enriched by the use of anti-PE magnetic beads and the Midi-MACS system (Miltenyi Biotec). $CD4^+CD25^-$ Tconv cells were FACS-purified from the CD25-depleted cell fraction after staining with anti-CD4-FITC, $CD4^+CD25^{high}CD45RA^+$ Treg cells were sorted from the CD25-enriched population after staining with anti-CD4-FITC and anti-CD45RA-APC. Reanalysis after sorting showed a purity of > 98 %.

FACS–purified Tconv and Treg cell populations were polyclonally expanded in vitro for 11-14 d as previously described (Hoffmann et al. 2004). Briefly, cells were stimulated with anti-CD3 (OKT3; kind gift from Janssen-Cilag, Neuss, Germany) and anti-CD28 (CD28.2; BD Biosciences) antibodies presented by CD32-expressing L 929 cells in the presence of high-dose recombinant human IL-2 (rhIL-2, 300 U/mL; Proleukin, Chiron, Amsterdam, the Netherlands). To exclude any contamination by feeder cells, all cultured populations were stained with CD4-FITC and PI and FACS-sorted immediately prior to DNA isolation.

Jurkat cells (humane T cell leukemia) were grown in 90 % 1640 RPMI (PAN Biotech GmbH) plus 10 % foetal bovine serum (FBS) supplemented with 2 mM L-Glutamine (Biochrome), MEM non-essential amino acids (Gibco), sodium pyruvate (Gibco), MEM vitamines (Gibco), 50 U/ml penicillin/streptomycin (Gibco), and 50 nM 2-mercaptoethanol (Gibco) in a humified incubator at 37°C and 5 % CO_2.

RNA and DNA preparation

Total cellular RNA of the different cell types was isolated using the RNeasy Kit (Qiagen). RNA concentration was measured with a ND-1000 Spectrophotometer (NanoDrop, Thermo Fisher Scientific) and quality was controlled on agarose gels or using the Bioanalyzer (Agilent, Boeblingen, Germany). Genomic DNA was prepared using the Qiagen Blood & Cell Culture DNA Kit or the Qiagen DNeasy Blood & Tissue Kit when working with smaller cell numbers. DNA concentration was determined with the NanoDrop spectrophotometer and quality was assessed by agarose gel electrophoresis.

T cell transcriptome analysis

RNA preparations from cultures of Treg and Tconv cells from four independent donors, as well as RNA preparations of freshly sorted Treg and Tconv cells from three independent donors were analyzed using Whole Human Genome Oligo Microarrays (Agilent). Labeling and hybridization were performed using the Agilent Gene Expression system according to the manufacturer's instructions. In brief, 200 ng to 1000 ng of high-quality RNA were amplified and Cyanine 3-CTP labeled with the One Color Low RNA Input Linear Amplification Kit (Agilent). Labeling efficiency was controlled using the NanoDrop spectrophotometer, and 1.65 µg labeled cRNA were fragmented and hybridized on the Whole Human Genome Expression Array (4x44K, Agilent). Images were scanned immediately after washing using a DNA microarray scanner (Agilent), processed using Feature Extraction Software 9.5.1 (Agilent) and further analyzed using GeneSpring GX software. Microarray data have been submitted and are available from the NCBI/GEO repository (accession number GSE14281). Median normalized expression ratios for genes associated with DMR are given in **Supplemental Table S2**. A detailed description of the T cell transcriptome analysis will be published elsewhere.

Methyl-CpG immunoprecipitation (MCIp)

The recombinant MBD-Fc protein was produced as previously described (Gebhard et al. 2006). Methyl-CpG immunoprecipitation was performed as described with slight modifications (Schilling and Rehli 2007). In brief, genomic DNA was sonicated to a mean fragment size of 350-400 bp. Four µg of each sample were incubated with 200 µl Protein A-Sepharose 4 Fast Flow beads (GE Healthcare) coated with 80 µg purified MBD-Fc protein in 2 ml Ultrafree-MC centrifugal filter devices (Amicon/Millipore) for 3 h at 4°C in buffer containing 300 mM NaCl. Beads were centrifuged to recover unbound DNA fragments (300 mM fraction) and subsequently washed with buffers containing increasing NaCl concentrations (350, 400, 450 and 1000 mM). All fractions were desalted using the MinElute PCR purification kit (Qiagen). The distribution of CpG methylation densities of individual MCIp fractions was controlled by qPCR using primers covering the imprinted *SNRPN* and a genomic region lacking CpGs (empty6.2). Fractions containing unmethylated DNA (300-400 mM) or methylated DNA (≥450 mM) were pooled before subsequent labeling.

Chromatin Immunoprecipitation (ChIP)

ChIP analysis of expanded and sorted Treg and Tconv cells was performed essentially as described (Metivier et al. 2003). Precipitation of pre-cleared chromatin from $2x10^6$ cells was done overnight at 4 °C using 2 µg anti-histone H3 lysine 4 monomethyl (Abcam), anti-histone H3 lysine 4 dimethyl (Upstate), anti-histone H3 lysine 4 trimethyl (Upstate), anti-CTCF (a gift from V. Lobanenkow) and anti-rabbit IgG (Upstate). After reversion of crosslinks, enriched DNA fragments were recovered using the Qiaquick PCR-purification kit (Qiagen). The quality of each ChIP was controlled at known target sites by qPCR. For ChIP-on-Chip analysis, all samples as well as an aliquot of equally treated input DNA were amplified by LM-PCR for subsequent labeling.

Ligation mediated PCR (LM-PCR)

ChIP and input DNA were blunted and phosphorylated for 30 minutes at 20 °C in 50 µl reactions containing 10x T4 DNA ligase buffer, 2 µl dNTP mix (10 mM each), 3 U T4 DNA polymerase, 10 U T4 polynucleotide kinase and 1 U Klenow DNA polymerase. Purification using the Qiaquick PCR purification kit (Qiagen) was followed by the addition of Adenine to 3'-ends using Klenow fragment (3' to 5' exo minus), and dATP (1 mM) for 30 minutes at 37 °C. After clean-up using the MinElute kit (Qiagen), DNA fragments were ligated to linker DNA (60 µM pre-annealed JW102s

5'-GCG GTG ACC CGG GAG ATC TGA ATT CT-3' and JW103 5'-GAA TTC AGA TC-3') with 4 µl DNA Quick-Ligase (NEB) in a 30 µl reaction for 15 minutes at RT. Samples were cleaned-up (Qiaquick PCR purification kit (Qiagen)) and amplified using Phusion Polymerase and JW102s oligonucleotide for 15 cycles. The product of the first amplification was diluted 1/20 with ddH2O and 5 µl of the dilution were used for a second round of amplification (15 cycles) using Phusion Polymerase HOT START and JW102s oligonucleotide. The amplified ChIP and input material was purified using Qiaquick PCR purification kit (Qiagen).

Design, handling and analysis of locus-wide microarrays

Fifty-one highly regulated genes and 18 control genes were selected based on mRNA expression profiles of freshly sorted and expanded T cell subsets. Custom tiling arrays were designed for the 69 selected loci using the eArray webtool (earray.chem.agilent.com/earray/). Fluorescently labeled DNA for microarray hybridization of DNA pools from MCIp or LM-PCR amplified ChIP samples (1µg of amplified DNA) were generated by direct labeling with Alexa Fluor 555–aha–dCTP and Alexa Fluor 647–aha–dCTP using the BioPrime Plus Array CGH Genomic Labeling System (Invitrogen). Hybridization and washing was performed as recommended by the manufacturer (Agilent). Images were scanned immediately using a DNA microarray scanner (Agilent) and processed using Feature Extraction Software 9.5.1 (Agilent) and a standard CGH protocol. Processed signal intensities were further normalized using GC-dependent regression and imported into Microsoft Office Excel 2007 for further analysis. Probes with abnormal hybridization behavior (extremely low (2507 probes) or high (5149 probes) signal intensities in both channels) were excluded. The results from two (CTCF) or three (H3K4 methylation marks) independent ChIP-on-Chip experiments were averaged and converted into UCSC Genome Browser tracks (genome.ucsc.edu/) for visualization. To detect differentially methylated regions (DMR) Log_{10} ratios of individual probes from both comparative genome pool hybridizations were subtracted to obtain hypomethylation scores which were either positive (indicating hypomethylation in Treg cells) or negative (indicating hypomethylation in Tconv cells). Hypomethylation scores of two independent experiments were averaged and regions were counted as hypomethylated if the average hypomethylation score of three consecutive probes was above a threshold of 0.2333 (at least above the 97th percentile of all scores). Averaged results from both independent experiments were also converted into UCSC Genome Browser tracks (genome.ucsc.edu/) and all track files are provided in the **Supplemental Material**. ChIP- and MCIP-on-Chip microarray data have been submitted and are available from the NCBI/GEO repository (accession number GSE14281). Overlaps of the identified DMR with conserved sequence elements predicted by the phastCons program based on a whole-genome alignment of

vertebrates and with DNaseI Hypersensitive Sites (DHS) in CD4+ T-cells (Boyle et al. 2008) were determined using the Table Browser at the UCSC Genome Browser web site (genome.ucsc.edu/). DMR were classified into three categories according to their CpG content using the promoter definitions proposed by Weber et al. (2005) (Weber et al. 2007): HCRs (high-CpG regions) contain a CpG ratio above 0.75 and GC content above 55% within a 500 bp DMR-centered region; LCRs (low-CpG regions) do not contain a 500-bp area with a CpG ratio above 0.48; and ICRs (intermediate CpG regions) are neither HCRs nor LCRs. Enriched transcription factor consensus motifs in DMR (500 bp regions) were identified using the RegionMiner tool (www.genomatix.de).

Mass spectrometry analysis of bisulfite-converted DNA

We chose a set of genomic regions based on the MCIp microarray results and designed 95 amplicons for bisulfite conversion. Genomic sequences were extracted from the UCSC genome browser (www.genome.ucsc.edu/). PCR primers were designed using the Epidesigner web tool (www.epidesigner.com/). For each reverse primer, an additional T7 promoter tag for *in vivo* transcription was added, as well as a 10-mer tag on the forward primer to adjust for melting temperature differences. All primers were purchased from Sigma-Aldrich (Munich, Germany) (for sequences see **Supplemental Table S4**). Sodium bisulfite conversion was performed using EZ DNA methylation kit (Zymo Research, California, USA) using 1 µg of genomic DNA and an alternative conversion protocol. Amplification of target regions was followed by SAP treatment, reverse transcription and subsequent RNA base-specific cleavage (MassCLEAVE, Sequenom, San Diego, CA) as previously described (Ehrich et al. 2005). Cleavage products were loaded onto silicon chips (spectroCHIP, Sequenom, San Diego, CA) and analysed by MALDI-TOF mass spectrometry (MassARRAY Compact MALDI-TOF, Sequenom, San Diego, CA). Methylation was quantified from mass spectra using the Epityper software v1.0 (Sequenom, San Diego, CA).

Reporter assays

DMR regions (ranging from 800 -1200 bp) were PCR-amplified from human genomic DNA and cloned directly into the CpG-free pCpGL-CMV/EF1 vector (Klug and Rehli 2006) by ligation or using the In-Fusion cloning system (Clontech, Saint-Germain-en-Laye, France) replacing the CMV enhancer with the DMR regions. Primer sequences are given in **Supplemental Table S6**. All inserts were verified by sequencing. Luciferase reporter constructs were either mock-treated or methylated *in vitro* with *Sss*I methylase for 4 hours at 37°C and purified with the Plasmid Quick Pure Kit (Macherey-Nagel, Dueren, Germany). One million Jurkat cells were transfected using

DEAE-dextran and 1.0 µg of each reporter plasmid, and 0.15 µg Renilla control vector as described. After transfection, cells were either left untreated, stimulated with 20 ng/ml PMA and 1 µM Ionomycin or with PHA (1µg/ml) alone. Triplicate transfections were harvested after 24h. Cell lysates were assayed for firefly and Renilla luciferase activities using the Dual-Luciferase Reporter Assay System (Promega) on a Lumat LB9501 (Berthold, Bad Wildbach, Germany). Firefly luciferase activity of individual transfections was normalized against Renilla luciferase activity.

Acknowledgments

We thank Ruediger Eder for excellent cell sorting, Lucia Schwarzfischer and Dagmar Glatz for technical assistance and V. Lobanenkow for providing the anti-CTCF antibodies.

Funding

This work is funded by a grant from the Deutsche Forschungsgemeinschaft to MR and PH.

Competing interests

None

Abbreviations

ChIP, chromatin immunoprecipitation; DMR, differentially methylated region; ICR, intermediate CpG content region; LCR, low CpG content region; MALDI-TOF, Matrix Assisted Laser Desorption Ionization Time-of-flight; MCIp, methyl-CpG immunoprecipitation; MS, mass spectrometry; qPCR, quantitative PCR; Tconv cell, conventional T cell; Treg cell, regulatory T cell;

Figures and text from chapter 3.1 are taken from Christian Schmidl, Maja Klug, Tina J. Boeld, Reinhard Andreesen, Petra Hoffmann, Matthias Edinger, Michael Rehli, “Lineage-specific DNA methylation in T cells correlates with histone methylation and enhancer activity” Genome Research. 2009 Jul;19(7):1165-74. Epub 2009 Jun 3.

Supplementary Information

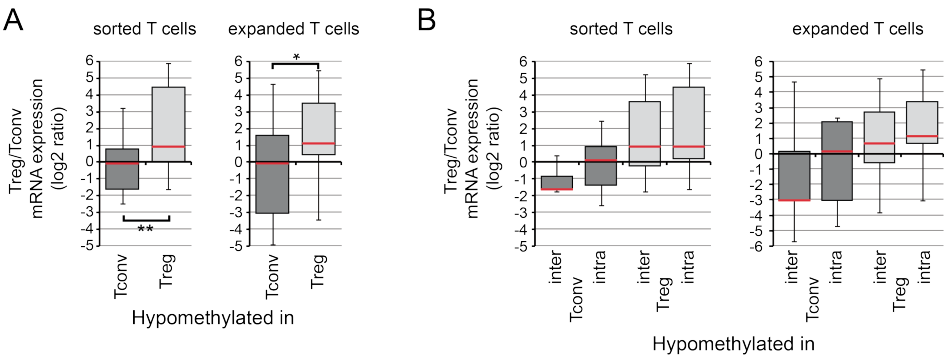

Supplemental Figure S1: Comparison of methylation states in T cells and mRNA expression data of associated genes. (A) The box plots show the distribution of of mRNA expression ratios (freshly sorted T cells, left panel; *in vitro* expanded T cells, right panel) conditional on the methylation status of the associated DMR. The red lines denote medians, boxes the interquartile ranges, and whiskers the 5th and 95th percentiles. Pair wise comparisons of mRNA expression ratios associated with DMR hypermethylated in Tconv or Treg cells are significant (** P<0.001, * P<0.01 ,Mann–Whitney U test, two-sided). (B) Box plots are shown as in (A) with DMR divided into the two major position classes: intergenic and intragenic. Differences between inter- and intragenic pairs of the same cell type and the same DMR status were not significant (P>0.05, Mann–Whitney U test, two-sided).

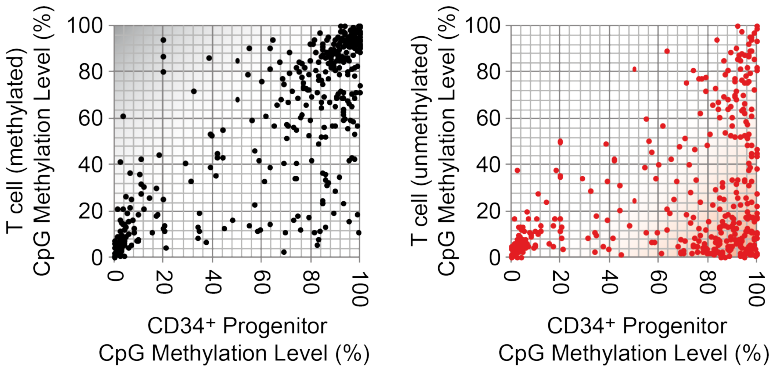

Supplemental Figure S2: Comparison of methylation states in T cells and CD34+ progenitor cells. The methylation states of individual CpG residues obtained by MALDI-TOF MS were compared between CD34+ progenitor cells and the highest (left diagram) or the lowest T cell methylation value (right diagram). Differentially methylated CpG residues that acquire methylation (compared to the progenitor cell) should be found in the upper left corner of the left diagram, whereas CpG residues that are demethylated (compared to the progenitor cell) should be found in the lower right corner of the right diagram.

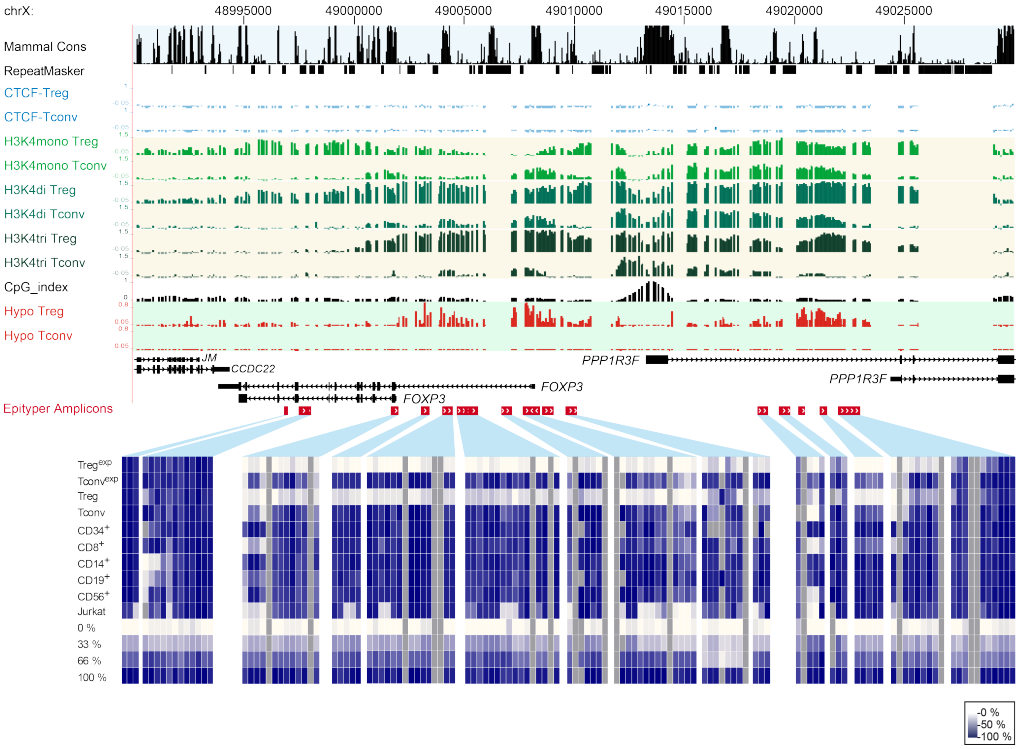

Supplemental Figure S3: Chromatin modification and CTCF binding patterns across the *FOXP3* gene locus. Tracks and heat maps are shown as described in the legend of Figure 2.

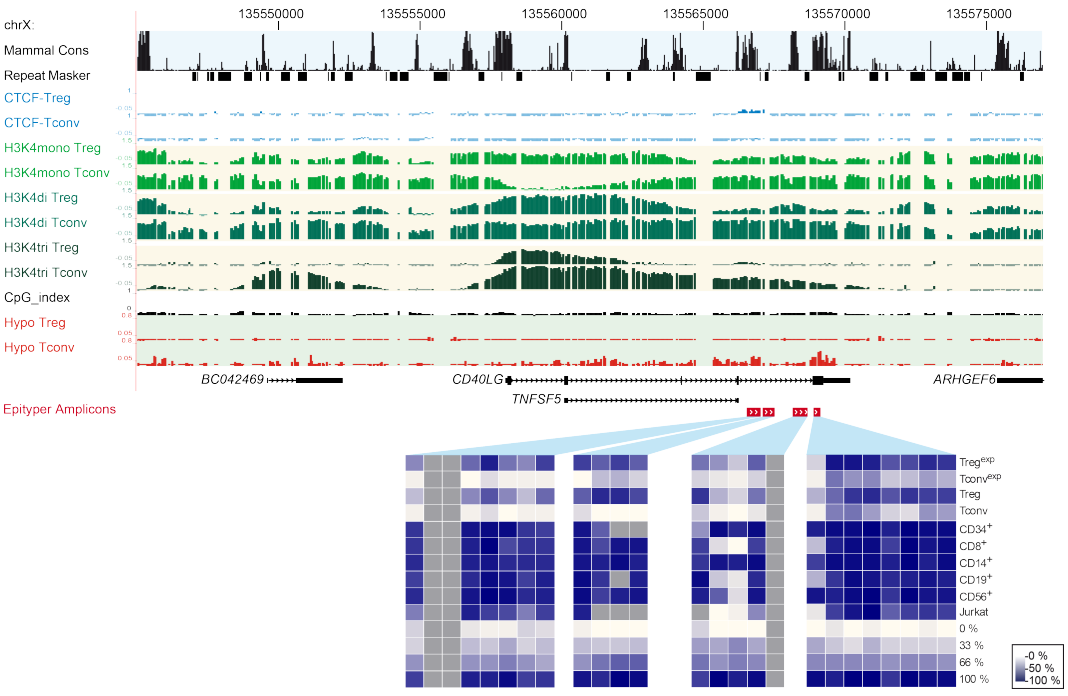

Supplemental Figure S4: Chromatin modification and CTCF binding patterns across the *CD40LG* gene locus. Tracks and heat maps are shown as described in the legend of Figure 2.

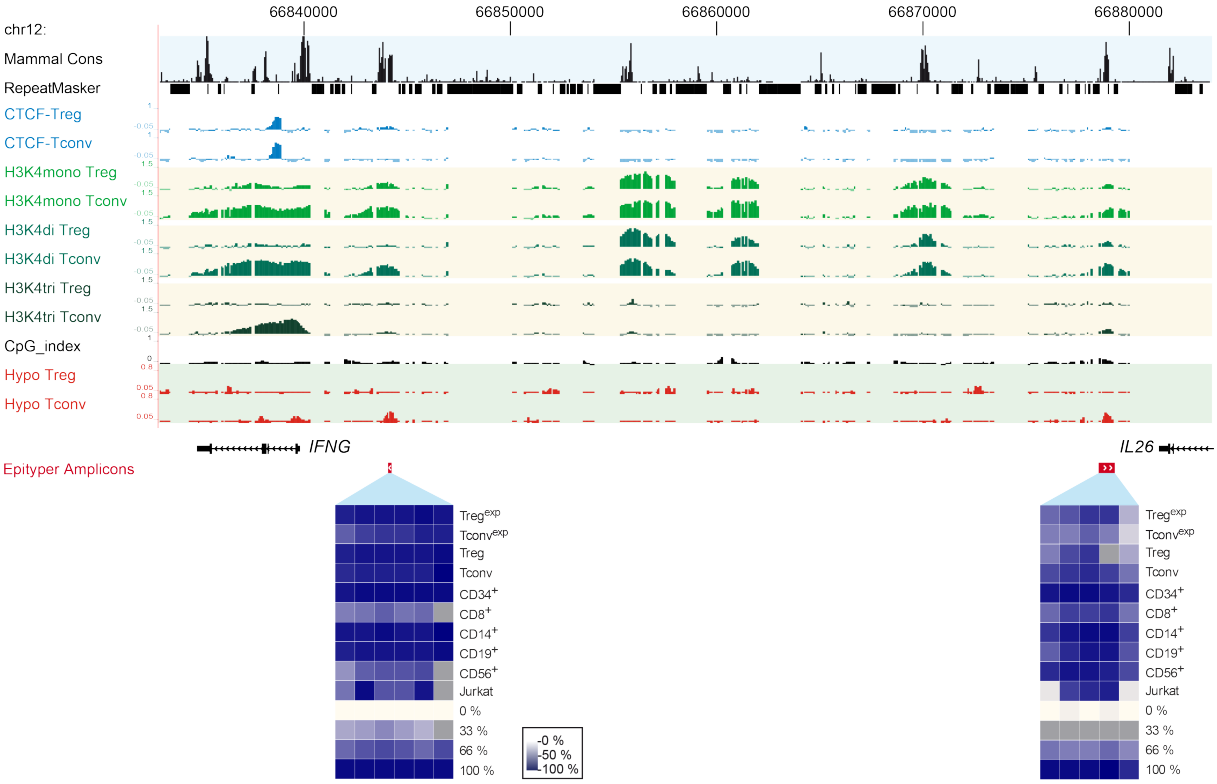

Supplemental Figure S5: Chromatin modification and CTCF binding patterns across the *IFNG* gene locus. Tracks and heat maps are shown as described in the legend of Figure 2.

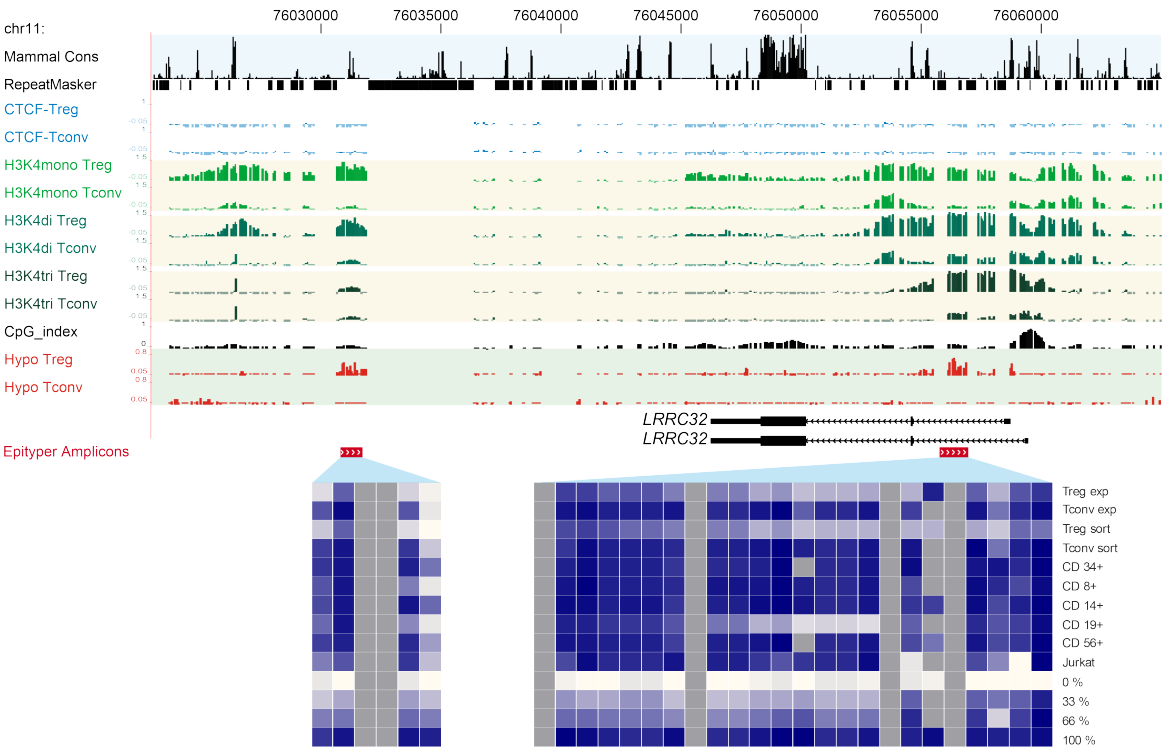

Supplemental Figure S6: Chromatin modification and CTCF binding patterns across the *LRRC32* gene locus. Tracks and heat maps are shown as described in the legend of Figure 2.

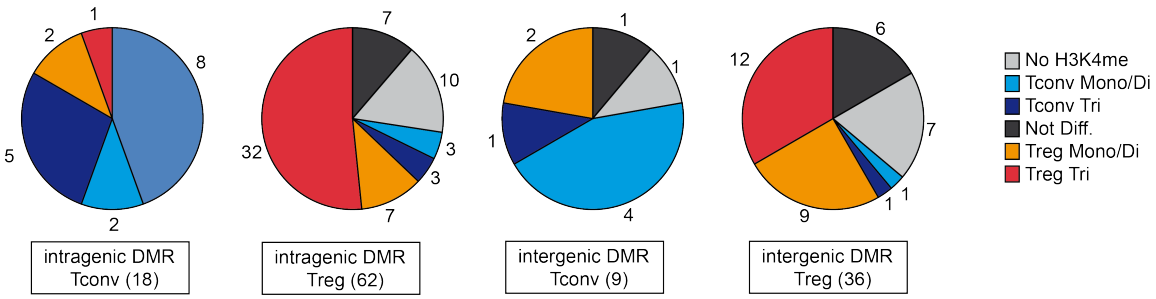

Supplemental Figure S7: Distribution of H3K4 methylation patterns at cell type-specific DMR depending on their relative position (intergenic/intragenic).

Supplemental Table S1

Genomic regions selected for Treg/Tconv cell DMR screening

Gene Symbol	Location (Mar. 06 (hg18) Assembly)	Region Size
ADC	chr1:33,280,000-33,380,000	100000
ANK3	chr10:61,350,000-62,200,000	850000
ANXA1	chr9:74,900,000-75,030,000	130000
CD40LG	chrX:135,520,000-135,580,000	60000
CHD7	chr8:61,700,000-62,000,000	300000
CYSLTR1	chrX:77,300,000-77,600,000	300000
GZMA	chr5:54,320,000-54,450,000	130000
HOP	chr4:57,170,000-57,300,000	130000
ID2	chr2:8,680,000-8,770,000	90000
IFNG	chr12:66,780,000-66,880,000	100000
IL18RAP	chr2:102,380,000-102,450,000	70000
MGC33556	chr1:44,900,000-44,980,000	80000
NELL2	chr12:43,130,000-43,680,000	550000
TARP/CD3G	chr7:38,230,000-38,340,000	110000
IL4	chr5:132,000,000-132,060,000	60000
ADAMTS4	chr1:159,400,000-159,460,000	60000
ARG1	chr6:131,860,000-132,000,000	140000
DYX1C1	chr15:53,430,000-53,610,000	180000
FCRL3	chr1:155,840,000-155,960,000	120000

FOXP3	chrX:48,970,000-49,030,000	60000
IL1R2/IL1R1	chr2:101,870,000-102,175,000	305000
LRRC32	chr11:76,000,000-76,150,000	150000
RTKN2	chr10:63,580,000-63,780,000	200000
F5/SELP	chr1:167,730,000-167,900,000	170000
CAMTA1/TNFRSF9/UTS2	chr1:7,600,000-7,940,000	340000
WDFY4	chr10:49,620,000-49,900,000	280000
WNT10A	chr2:219,443,000-219,490,000	47000
IKZF2	chr2:213,500,000-213,850,000	350000
NOG	chr17:51,970,000-52,070,000	100000
IL7R	chr5:35,850,000-35,940,000	90000
PTPRC	chr1:196,800,000-197,020,000	220000
TP53INP1	chr8:96,000,000-96,045,000	45000
IL6R	chr1:152,590,000-152,720,000	130000
AMOTL2	chr3:135,500,000-135,630,000	130000
PKD2	chr4:89,120,000-89,230,000	110000
LGALS3	chr14:54,605,000-54,685,000	80000
LCAM3	chr9:132,800,000-132,980,000	180000
PERP	chr6:138,420,000-138,520,000	100000
S100Z	chr5:76,165,000-76,270,000	105000
CTLA4	chr2:204,390,000-204,490,000	100000
IL2RA	chr10:6,060,000-6,170,000	110000
IL2RB	chr22:35,835,000-35,905,000	70000

ENTPD1	chr10:97,440,000-97,670,000	230000
NT5E	chr6:86,170,000-86,270,000	100000
PDE4D	chr5:58,250,000-59,850,000	1600000
ZEB1	chr10:31,600,000-31,900,000	300000
FCER1G	chr1:159,445,000-159,460,000	15000
TRAT1	chr3:109,990,000-110,090,000	100000
FAIM3	chr1:205,128,000-205,168,000	40000
MAP3K5	chr6:136,915,000-137,180,000	265000
GJB6	chr13:19,665,000-19,765,000	100000

Supplemental Table S1 (continued)

Genomic regions selected for Treg/Tconv cell DMR screening

Gene Symbol	Location (Mar. 06 (hg18) Assembly)	Region Size
ACTB*	chr7:5,520,000-5,570,000	50000
B2M	chr15:42,760,000-42,810,000	50000
LTB	chr6:31,636,000-31,686,000	50000
SEPT9	chr17:72,740,000-73,040,000	300000
HPRT1	chrX:133,390,000-133,490,000	100000
UBC	chr12:123,950,000-123,980,000	30000
KLF2	chr19:16,265,000-16,325,000	60000
CD2	chr1:117,070,000-117,130,000	60000
SPI1	chr11:47,330,000-47,380,000	50000

TLR4	chr9:119,460,000-119,550,000	90000
TFEC	chr7:115,350,000-115,500,000	150000
CD14	chr5:139,980,000-140,000,000	20000
CD19	chr16:28,840,000-28,870,000	30000
NCAM1	chr11:112,300,000-112,660,000	360000
GATA1	chrX:48,515,000-48,547,000	32000
GATA4	chr8:11,500,000-11,660,000	160000
CSF1R	chr5:149,400,000-149,490,000	90000
HOXA9	chr7:27,080,000-27,220,000	140000

* Control loci are boxed in green.

Supplemental Table S2
Location and properties of DMR detected by MCIp

Gene Symbol and Gene ID	Log2 ratio freshly sorted Treg/Tconv[a]	Log2 ratio expanded Treg/Tconv	Probe ID	Chr. Location	Distance from TSS	Relative Position to Gene Transcript[b]	Hypomethylated T cell type	Epityper validation of MCIp results	CpG content class[c]	Overlap with PhastCons[d]	Overlap with DHS in CD4+ T cells[e]	H3K4 Methylation[f] Status
VAMP3 9341	0.01	0.33	A_24_P370887	chr1:7694083-7694556	-59600	intra	Treg		LCR			Treg Mono/Di
				chr1:7696779-7696912	-57074	intra	Tconv		LCR			no H3K4me
				chr1:7742983-7743147	-10855	intra	Tconv		LCR			no H3K4me
PER3 8863	0.12	-0.06	A_24_P291231	chr1:7763681-7763839	-3209	intra	Tconv		LCR			Tconv Mono/Di
				chr1:7780936-7781346[a]	14172	intra	Tconv		LCR	yes		no H3K4me
UTS2 10911	**4.66**	**5.61**	A_23_P63343	chr1:7836042-7836108	-393	5-proximal	Tconv		LCR			no H3K4me
TNFRSF9 3604	**3.58**	**4.06**	A_23_P51936	chr1:7921606-7922186	1574	intra	Treg		LCR			Treg Tri
				chr1:7923689-7923832	-291	5-proximal	Treg	yes	LCR			Treg Tri
				chr1:7931900-7932340	-8650	inter	Treg		ICR	yes	DHS	Treg Mono/Di
KIF2C 11004	0.52	**-3.02**	A_23_P34788	chr1:44978856-44978930	772	intra	Treg		LCR		DHS	Tconv Tri
PTPRC 5788	-0.27	0.46	A_23_P125451	chr1:196900673-196900751	25919	intra	Treg		LCR		DHS	Treg Tri
				chr1:196941013-196941144	66286	intra	Treg		LCR		DHS	Not diff.
FAIM3 9214	-0.44	**3.39**	A_23_P138125	chr1:205146071-205146415	15666	intra	Treg		LCR		DHS	Not diff.
				chr1:205159845-205160036	1968	intra	Treg		LCR		DHS	Treg Tri
				chr1:205160872-205161211	867	intra	Treg		LCR		DHS	Treg Tri
				chr1:205164864-205165172	-3109	inter	Treg		LCR		DHS	Treg Mono/Di
ID2 3398	**-2.41**	**-6.67**	A_32_P69368	chr2:8726198-8726662	-13206	inter	Treg		LCR			no H3K4me
				chr2:8735102-8735444	-4363	inter	Treg	yes	LCR	yes	DHS	Tconv Mono/Di
				chr2:8740559-8740969	1128	intra	Treg	no	ICR	yes	DHS	Tconv Tri
IL1R2 7850	**3.69**	**4.67**	A_23_P79398	chr2:101984548-101985058	2913	intra	Treg		LCR			Treg Mono/Di
				chr2:102045612-102046101	63967	inter	Treg		LCR			Not diff.
CTLA4 1493	**2.36**	**1.96**	A_23_P102481	chr2:204408646-204409889	-31484	inter	Treg	yes	LCR	yes		Treg Tri
				chr2:204426657-204428059	-13394	inter	Treg	yes	LCR	yes	DHS	Treg Tri
				chr2:204443336-204444178	3005	intra	Treg	yes	LCR	yes	DHS	Treg Tri
				chr2:204446111-204447000	5804	intra	Treg	yes	LCR	yes	DHS	Treg Tri
				chr2:204460103-204460326	19463	inter	Treg		LCR			Treg Mono/Di
IKZF2 22807	**4.49**	**3.84**	A_32_P114284	chr2:213658721-213658870	64554	intra	Treg		LCR	yes		Treg Mono/Di
				chr2:213680605-213681119	42488	intra	Treg		ICR	yes		Treg Tri
				chr2:213688110-213688358	35116	intra	Treg		LCR			Treg Mono/Di
				chr2:213697294-213697468	25969	intra	Treg	yes	LCR			Treg Tri
				chr2:213706776-213707454	16235	intra	Treg		LCR			Treg Tri
				chr2:213722578-213724345	-112	5-proximal	Treg	no	LCR	yes	DHS	Treg Tri
				chr2:213725364-213725750	-2207	inter	Treg		ICR	yes		Treg Tri
				chr2:213726946-213727686	-3966	inter	Treg	yes	LCR		DHS	Treg Tri
				chr2:213730460-213730581	-7171	inter	Treg		LCR			Treg Mono/Di
				chr2:213733406-213733693	-10200	inter	Treg		LCR			no H3K4me
SPAG16 79582	0.04	-0.21	A_23_P67785	chr2:213803183-213803316	-54169	inter	Treg		ICR			Treg Mono/Di
				chr2:213809847-213810325	-47333	inter	Treg	yes	LCR	yes		Treg Tri

Supplemental Table S2 (continued)
Location and properties of DMR detected by MCIp

Gene Symbol and Gene ID	Log2 ratio freshly sorted Treg/Tconv	Log2 ratio expanded Treg/Tconv	Probe ID	Chr. Location	Distance from TSS	Relative Position to Gene Transcript[b]	Hypomethylated T cell type	Epityper validation of MCIp results	CpG content class[c]	Overlap with PhastCons[d]	Overlap with DHS in CD4+ T cells[e]	H3K4 Methylation[f] Status
				chr2:213813204-213813362	-44136	inter	Treg		LCR	no	no	Treg Tri
				chr2:213814671-213814814	-42676	inter	Treg		LCR	no	no	Treg Tri
HOPX 84525	-0.83	**-3.75**	A_23_P254507	chr4:57215993-57216190	26128	intra	Tconv		ICR	no	DHS	Tconv Tri
				chr4:57242355-57242622	-269	5-proximal	Tconv		LCR	yes	DHS	ND
PKD2 5311	0.11	**1.79**	A_24_P106112	chr4:89148733-89149406	1160	intra	Treg		LCR	yes	DHS	Treg Tri
RAB3C 115827	0.91	**1.49**	A_23_P44794	chr5:58263564-58263732	348985	inter	Treg		LCR	no	no	no H3K4me
				chr5:58265981-58266738	351697	inter	Treg		LCR	yes	DHS	ND
				chr5:58369473-58369731	454939	intra	Treg		LCR	yes	DHS	Tconv Tri
				chr5:58371799-58371934	457204	intra	Tconv		LCR	no	DHS	Tconv Tri
				chr5:58374023-58374163	459430	intra	Treg		LCR	yes	DHS	Tconv Mono/Di
F2RL1 2150	0.61	**1.72**	A_23_P58835	chr5:76165074-76165598	14707	intra	Tconv		LCR	yes	DHS	no H3K4me
MAP7 9053	-0.40	-0.81	A_24_P98021	chr6:136915800-136915872	-2583	inter	Treg		LCR	no	no	no H3K4me
MAP3K5 4217	**1.31**	**2.40**	A_23_P134125	chr6:137124814-137124977	30453	intra	Treg		LCR	no	DHS	Treg Tri
				chr6:137139643-137139811	15622	intra	Tconv		LCR	no	no	Treg Mono/Di
				chr6:137156228-137156491	-1011	inter	Treg		LCR	no	DHS	ND
PERP 64065	**1.96**	**2.35**	A_23_P214950	chr6:138458928-138459115	11227	intra	Tconv		LCR	no	no	no H3K4me
				chr6:138468457-138468554	1743	intra	Tconv		LCR	no	no	Treg Tri
HOXA1 3198	0.91	**1.04**	A_23_P145752	chr7:27103645-27103925	-1645	intra	Treg		LCR	yes	no	ND
HOXA3 3200	0.91	**1.49**	A_23_P501538	chr7:27146342-27146410	-26	5-proximal	Tconv		ICR	yes	no	no H3K4me
HOXA10 3206	0.91	**2.17**	A_23_P253368	chr7:27184543-27184956	1449	intra	Tconv		LCR	yes	no	no H3K4me
HOXA13 3209	0.91	**1.88**	A_23_P31306	chr7:27208821-27209379	-2850	intra	Treg		LCR	no	no	no H3K4me
HOXA13 3209	0.91	**1.88**	A_23_P31306	chr7:27212390-27212560	-6225	inter	Treg		ICR	yes	no	no H3K4me
GATA4 2626	0.79	**1.13**	A_24_P932785	chr8:11580580-11581129	-18270	intra	Treg		LCR	yes	no	no H3K4me
				chr8:11583722-11583857	-15335	intra	Treg	no	LCR	no	no	no H3K4me
				chr8:11601942-11602190	2941	intra	Treg		LCR	no	no	no H3K4me
				chr8:11607397-11607483	8315	intra	Treg		LCR	no	no	no H3K4me
				chr8:11639562-11639728	40520	intra	Treg		LCR	no	no	no H3K4me
CHD7 55636	**-1.62**	**-3.04**	A_24_P58381	chr8:61727910-61728135	-25892	inter	Treg		LCR	no	DHS	ND
				chr8:61756004-61756256	2215	intra	Tconv		ICR	no	DHS	Tconv Tri
				chr8:61759841-61760294	6153	intra	Treg		LCR	no	DHS	Tconv Mono/Di
				chr8:61761414-61761574	7579	intra	Treg		LCR	no	no	ND
				chr8:61776071-61776160	22201	intra	Tconv		LCR	no	DHS	Tconv Mono/Di
				chr8:61942900-61943092	189081	inter	Tconv		LCR	no	DHS	Tconv Mono/Di
				chr8:61973666-61973792	219814	inter	Tconv		LCR	no	no	no H3K4me
				chr8:61979393-61979852	225708	inter	Tconv		LCR	no	no	Tconv Mono/Di
				chr8:61982195-61982630	228498	inter	Treg		ICR	no	no	ND
				chr8:61984364-61984705	230620	inter	Treg		LCR	yes	DHS	Tconv Tri
				chr8:61985582-61985644	231698	inter	Tconv		ICR	yes	DHS	Tconv Tri

Supplemental Table S2 (continued)
Location and properties of DMR detected by MCIp

Gene Symbol and Gene ID	Log2 ratio freshly sorted Treg/Tconv	Log2 ratio expanded Treg/Tconv	Probe ID	Chr. Location	Distance from TSS	Relative Position to Gene Transcrips[b]	Hypomethylated T cell type	Epityper validation of MCIp results	CpG content class[c]	Overlap with PhastCons[d]	Overlap with DHS in CD4+ T cells[e]	H3K4 Methylation[f] Status
				chr8:61987949-61988359	234239	inter	Tconv		LCR	yes	DHS	Tconv Mono/Di
TP53INP1 94241	0.93	**1.01**	A_23_P168882	chr8:96009841-96010902	-2996	intra	Treg	yes	LCR	yes	DHS	Treg Tri
				chr8:96028605-96029654	1630	intra	Treg		LCR	yes	DHS	Treg Tri
				chr8:96042041-96042225	-11373	intra	Treg		LCR	yes	DHS	ND
IL15RA 3601	0.70	0.54	A_23_P138680	chr10:6086021-6086185	-26153	inter	Tconv		LCR	no	no	Treg Mono/Di
IL2RA 3559	**5.87**	0.67	A_23_P127288	chr10:6119192-6119913	24725	intra	Treg	yes	LCR	no	DHS	Treg Tri
				chr10:6121979-6122460	22058	intra	Treg	yes	LCR	no	no	Treg Tri
				chr10:6128278-6128419	15929	intra	Treg		LCR	no	DHS	Treg Tri
				chr10:6129214-6129562	14890	intra	Treg		LCR	no	DHS	Treg Tri
				chr10:6134052-6134250	10127	intra	Treg		LCR	no	DHS	Treg Tri
				chr10:6136503-6137025	7514	intra	Treg		LCR	no	no	Treg Tri
				chr10:6137878-6138428	6125	intra	Treg		LCR	no	no	Treg Tri
				chr10:6139024-6140346	4593	intra	Treg		LCR	yes	no	Treg Tri
				chr10:6141939-6142194	2211	intra	Treg		LCR	no	no	Treg Tri
				chr10:6153181-6153487	-9056	inter	Treg	yes	LCR	no	no	Treg Tri
				chr10:6154347-6154892	-10342	inter	Treg	yes	LCR	no	DHS	Treg Tri
RBM17 84991	-0.14	-0.54	A_23_P423315	chr10:6164740-6165011	-6148	inter	Treg		LCR	no	no	Treg Tri
				chr10:6168811-6168881	-2178	inter	Treg		LCR	no	DHS	Treg Tri
ZEB1 6935	-0.01	-0.60	A_23_P202013	chr10:31650245-31650763	2357	intra	Treg		ICR	yes	DHS	ND
LRRC18 474354	0.13	-0.29	A_23_P35494	chr10:49833171-49833344	-40975	intra	Tconv		LCR	yes	no	no H3K4me
ANK3 288	**-3.25**	**-3.52**	A_23_P301530	chr10:61910645-61910927	-91151	intra	Tconv		LCR	no	no	no H3K4me
RTKN2 219790	**4.39**	**5.47**	A_24_P13041	chr10:63631396-63631747	66762	intra	Treg		LCR	yes	no	Treg Mono/Di
				chr10:63669692-63669980	28498	intra	Treg		LCR	no	DHS	Treg Tri
ENTPD1 953				chr10:97638620-97638752	132774	intra	Treg		LCR	no	no	no H3K4me
FANK1 92565	**6.32**	**5.84**	A_23_P115785	chr10:127661157-127661287	86070	intra	Treg		LCR	no	no	Treg Mono/Di
				chr10:127674302-127675105	99552	intra	Treg		LCR	no	no	Treg Tri
LRRC32 2615	**4.96**	**5.47**	A_24_P389916	chr11:76018362-76018714	40900	inter	Treg		LCR	yes	no	Treg Mono/Di
				chr11:76030870-76031550	28228	inter	Treg	yes	LCR	yes	no	Treg Tri
				chr11:76056081-76056862	2966	intra	Treg	yes	LCR	no	no	Treg Tri
				chr11:76058705-76058782	694	intra	Treg		LCR	yes	no	Treg Tri
NCAM1 4684	0.91	**1.26**	A_23_P1740	chr11:112345302-112345374	7987	intra	Treg		LCR	no	no	Tconv Mono/Di
				chr11:112350888-112350995	13591	intra	Treg		LCR	yes	no	no H3K4me
				chr11:112443435-112443585	106159	intra	Treg		LCR	yes	no	no H3K4me
TTC12 54970	-0.45	**1.08**	A_23_P24535	chr11:112638456-112638589	-51992	intra	Treg		LCR	yes	no	Treg Mono/Di
NELL2 4753	**-4.64**	**-6.42**	A_23_P10025	chr12:43288526-43288688	267807	intra	Treg		LCR	no	no	no H3K4me
IFNG 3458	**-1.90**	**-6.25**	A_23_P151294	chr12:66844066-66844304	-4395	inter	Tconv	yes	LCR	yes	no	Tconv Mono/Di
IL26 55801	-0.06	**-5.23**	A_23_P128503	chr12:66878821-66878935	26959	inter	Tconv	yes	ICR	yes	DHS	ND

Supplemental Table S2 (continued)
Location and properties of DMR detected by MCIp

Gene Symbol and Gene ID	Log2 ratio freshly sorted Treg/Tconv	Log2 ratio expanded Treg/Tconv	Probe ID	Chr. Location	Distance from TSS	Relative Position to Gene Transcrips[b]	Hypomethylated T cell type	Epityper validation of MCIp results	CpG content class[c]	Overlap with PhastCons[d]	Overlap with DHS in CD4+ T cells[e]	H3K4 Methylation[f] Status
GJB2 2706	0.91	**-3.44**	A_23_P204947	chr13:19666918-19667157	-1961	inter	Treg		LCR	no	DHS	Treg Mono/Di
				chr13:19669218-19669677	-4371	inter	Treg	no	LCR	yes	DHS	Treg Mono/Di
GJB6 10804	**1.79**	**2.18**	A_23_P2745	chr13:19764311-19764922	-99540	inter	Treg		ICR	no	no	no H3K4me
MAPK1IP1L 93487	0.03	0.23	A_24_P107674	chr14:54608917-54609194	20941	inter	Treg		LCR	no	DHS	ND
LGALS3 3958	**3.85**	**2.31**	A_23_P128919	chr14:54670099-54670231	4435	intra	Tconv		LCR	no	no	Treg Mono/Di
NOG 9241	**-1.08**	**5.52**	A_23_P341938	chr17:52024396-52024835	-1443	inter	Tconv	no	LCR	no	DHS	Treg Mono/Di
SEPT9 10801	-0.78	0.66	A_24_P147910	chr17:72787432-72787562	-1626	inter	Treg		LCR	no	no	no H3K4me
				chr17:72882994-72883638	-442	5-proximal	Tconv	yes	LCR	yes	no	Tconv Tri
				chr17:72914128-72914221	1422	intra	Treg		LCR	no	DHS	Treg Tri
EPS15L1 10365	-0.74	-0.74	A_23_P38941	chr19:16323001-16323171	-3971	inter	Treg		LCR	no	DHS	Treg Mono/Di
IL2RB 3560	**1.63**	0.62	A_24_P203000	chr22:35871285-35872166	4176	intra	Treg	yes	LCR	no	no	Treg Tri
				chr22:35893803-35894363	-18181	intra	Treg	yes	LCR	no	no	Treg Tri
CACNA1F 778	-0.27	-0.09	A_23_P148327	chrX:48975534-48975593	1180	intra	Treg		LCR	no	no	ND
FOXP3 7575	**3.68**	**4.60**	A_23_P159709	chrX:49002019-49005207	4581	intra	Treg	yes	LCR	yes	no	Treg Tri
				chrX:49007147-49009512	-136	5-proximal	Treg	yes	ICR	yes	no	Treg Tri
PPP1R3F 89801	0.21	**1.59**	A_24_P177604	chrX:49020095-49022146	7093	intra	Treg	yes	LCR	yes	DHS	Treg Tri
				chrX:49022670-49023240	8927	intra	Treg	yes	LCR	no	no	Treg Tri
CD40LG 959	**-2.48**	**-4.70**	A_23_P62220	chrX:135561484-135561563	3517	intra	Tconv		LCR	no	DHS	Tconv Tri
				chrX:135566710-135566897	8797	intra	Tconv	yes	LCR	yes	no	Tconv Tri

[a] Coloring indicates larger than 2 fold differences between gene expression levels as determined by microarray analysis. Genes with higher expression in Treg cells are marked in red, those with higher expression in Tconv cells in blue.
[b] DMR were classified either as intergenic (inter) or intragenic (intra) based on their position relative to known genes.
[c] DMR were classified according to their CpG content using the promoter definitions proposed by Weber et al. (2005) as described in the Methods section.
[d] Overlap of the identified DMR with conserved sequence elements predicted by the phastCons program based on a whole-genome alignment of vertebrates was done using the Table Browser at the UCSC Genome Browser web site (genome.ucsc.edu/).
[e] Overlap of the identified DMR with DNaseI hypersensitive sites (DHS) in CD4+ T-cells (Boyle et al, 2008) was determined using the Table Browser at the UCSC Genome Browser web site (genome.ucsc.edu/)
[f] Histone H3 lysine 4 methylation at DMR regions was classified as follows: Treg or Tconv Tri, increased H3K4 trimethylation in Treg or Tconv cells, respectively; Treg or Tconv Mono/Di, increased H3K4 mono-, or di-, but no trimethylation in Treg or Tconv cells, respectively; ND, H3K4 methylation present but not different between T cell subsets.

Supplemental Table S3

Sequence motifs associated with DMR

DMR class	TF Matrices	Number of Sequences[a]	Number of Matches[b]	Expected (genome)[c]	Std.dev.	representation (genome)[d]	Z-Score (genome)[e]
DMR hypomethylated in Tconv cells (n=31)	V$ATF.01	10	11	2.35	1.53	4.68	5.32
	V$CREB.02	9	11	2.42	1.55	4.55	5.2
	V$CTCF.03	6	13	3.7	1.92	3.51	4.57
	V$AHRARNT.03	9	9	2.27	1.51	3.96	4.13
	V$ELK1.02	8	10	2.98	1.73	3.36	3.78
	V$ATF6.02	8	9	2.52	1.59	3.57	3.77
	V$AP1.03	8	14	5.21	2.28	2.69	3.63
	V$NUDR.01	8	8	2.32	1.52	3.45	3.4
	V$ATF.02	9	13	5.21	2.28	2.5	3.2
	V$CTCF.04	4	9	3.03	1.74	2.97	3.14
	V$ZF5.01	3	7	2.08	1.44	3.37	3.07
	V$XBP1.01	6	9	3.16	1.78	2.85	3
DMR hypomethylated in Treg cells (n=101)	V$NRF1.01	4	21	4.96	2.23	4.23	6.98
	V$ZF5.01	9	24	6.77	2.6	3.55	6.43
	V$VMYB.05	32	35	15.56	3.94	2.25	4.8
	V$STAT5.01	30	66	36.75	6.06	1.8	4.75
	V$VMYB.03	30	33	15.51	3.94	2.13	4.31
	V$HMX2.01	28	55	30.92	5.56	1.78	4.24
	V$ZNF219.01	17	36	18.47	4.3	1.95	3.96
	V$KKLF.01	25	38	20.2	4.49	1.88	3.85

V$VMYB.04	32	38	20.78	4.56	1.83	3.67
V$MZF1.03	36	42	23.92	4.89	1.76	3.6
V$STAT.01	47	75	49.27	7.02	1.52	3.6
V$MZF1.01	37	43	24.7	4.97	1.74	3.58
V$NFKAPPAB65.01	28	36	20.05	4.48	1.8	3.45
V$MAZR.01	18	31	16.84	4.1	1.84	3.33
V$OLF1.01	20	27	14.14	3.76	1.91	3.29
V$VMYB.02	26	30	16.36	4.04	1.83	3.25
V$MZF1.02	43	52	32.93	5.74	1.58	3.24
V$HIVEP1.01	22	32	17.93	4.23	1.78	3.21
V$FLI.01	27	27	14.47	3.8	1.87	3.16
V$ELK1.02	19	20	9.7	3.11	2.06	3.15
V$HMX2.02	30	68	46.41	6.81	1.47	3.1
V$E2F.01	36	45	28.51	5.34	1.58	3

[a] Number of input sequences with at least one match.

[b] Number of matches in all sequences.

[c] Expected match numbers in an equally sized sample of the genomic background and the standard deviation.

[d] Overrepresentation against genomic background: Fold factor of match numbers in regions compared to an equally sized sample of the background (i.e. found versus expected).

[e] Z-score of overrepresentation against genomic background: The distance from the population mean in units of the population standard deviation. Shown are only highly significant motifs (Z score >3; a Z-score above 2 can be considered statistically significant).

Supplemental Table S4
Oligonucleotides for bisulfite amplicon generation

Amplicon	Chromosomal Location (hg18)	Sense	Antisense	Dir.
Epi00197_TNFRSF9.1	chr1:7932138-7932511	aggaagagagGGGTGTAGGTGATAATTGTGATTAAA	cagtaatacgactcactatagggagaaggctCTTCCATTATAATAAAAACACAAAAAAACA	+
Epi00003_IL2RA.1	chr10:6118877-6119370	aggaagagagTTGTAGATTGGGATTTGTTAGGGTA	cagtaatacgactcactatagggagaaggctCTAAATTCACCCAAAAAACAAAAAA	+
Epi00004_IL2RA.2	chr10:6119558-6119803	aggaagagagAGAGTTTGGGTTATTGGGTAAAGAG	cagtaatacgactcactatagggagaaggctCCACAAAAATTTCCTCTAAAAATCA	+
Epi00005_IL2RA.3	chr10:6120520-6121011	aggaagagagATAGTTTAAGGTGGTGGGATAGGAG	cagtaatacgactcactatagggagaaggctCAATCCAACATTCTATAACTACAAAATTA	+
Epi00203_IL2RA.1	chr10:6121399-6121972	aggaagagagTTTTTTTTATGATGGATAGGATAGATAGA	cagtaatacgactcactatagggagaaggctTTTTACACATTCTCTACCAAAATAACC	+
Epi00006_IL2RA.4	chr10:6122010-6122464	aggaagagagTTATAGGTAGAATGTTTTGTTGAAGTATGA	cagtaatacgactcactatagggagaaggctTAAACAAACAACAACCATCAAAAAT	+
Epi00017_IL2RA.15	chr10:6153564-6153844	aggaagagagGTAGTTTTTGGGGGTAATATTGAGG	cagtaatacgactcactatagggagaaggctAAACAAAAAATTCATCCAATACCAA	+
Epi00018_IL2RA.16	chr10:6153808-6154224	aggaagagagATATTGGTTTGATTGGTATTGGATG	cagtaatacgactcactatagggagaaggctAAAAATCCTACCACCTCAACCTACT	+
Epi00019_IL2RA.17	chr10:6154058-6154547	aggaagagagTATTTTGGGAAGTTAAGGTAGGAGG	cagtaatacgactcactatagggagaaggctTTCATTACCCAAAAAATCCCTACTT	+
Epi00020_IL2RA.18	chr10:6154524-6154923	aggaagagagAGTAGGGATTTTTTGGGTAATGAAG	cagtaatacgactcactatagggagaaggctAAAAAAACTAAAAATTCATCCCACAC	+
Epi00021_IL2RA.19	chr10:6155117-6155433	aggaagagagTTTTTTTTAGTTATTTTGGGTTTTG	cagtaatacgactcactatagggagaaggctAACTCACACTTATAATCCCAACACTTT	+
lrrc32_6534	chr11:76030804-76031729	aggaagagagTTTATAGTTGGTTGGGATGTAGATAATG	cagtaatacgactcactatagggagaaggctCACCAAAACTATCAACCTTCAAAAA	+
Epi00205_LRRC32.1	chr11:76055736-76056113	aggaagagagTTTTGAGTTTTAGTTTTTTTATTTGAGG	cagtaatacgactcactatagggagaaggctAAATACCTTTTCTCCTACAACATCC	+
Epi00206_LRRC32.2	chr11:76056033-76056454	aggaagagagTTTTAGGTTTTTTATAGTGGGTGTTTT	cagtaatacgactcactatagggagaaggctACTAACCAAACAAAACATACTCCCC	+
Epi00207_LRRC32.3	chr11:76056414-76056952	aggaagagagGGTTTTTTAGGTTATTGGGGAGTAT	cagtaatacgactcactatagggagaaggctCAAAAAAAACAATCAAAACCCACTA	+
Epi00026_IFNG.1	chr12:66844056-66844260	aggaagagagATGGTTAGAAGGTATAAAAGAAAAGGG	cagtaatacgactcactatagggagaaggctAAATCAATATTAAATCCATACCCCC	-
il26_6531	chr12:66878511-66879260	aggaagagagTTTGATTAGGGTTGAGGGAGAAG	cagtaatacgactcactatagggagaaggctCCCACAAATACCAATTTAAAAAAAA	+
Epi00208_GJB2.1	chr13:19668983-19669485	aggaagagagTGTTAAAAAGTATATTTTGGTTAGAAATGA	cagtaatacgactcactatagggagaaggctTAAAACCACAAACTCCATATCCAAT	+
Epi00209_GJB2.2	chr13:19669465-19670046	aggaagagagGATATGGAGTTTGTGGTTTTAGAATTT	cagtaatacgactcactatagggagaaggctCAACACCATTTCACATAAAATAACAA	+
Epi00210_GJB2.3	chr13:19669565-19670072	aggaagagagGAAAGAAGTTTTTTGTGTTTTTTGAT	cagtaatacgactcactatagggagaaggctAACCCTACTATCTCTCCTCTTAATAACAA	+
Epi00027_NOG.1	chr17:52016154-52016611	aggaagagagTTTTTTTTGGGTTAGGGTTTGAAAG	cagtaatacgactcactatagggagaaggctACTTAAACCTCTTTATCCCTTCCCT	+
Epi00030_NOG.4	chr17:52024346-52024855	aggaagagagTGGAAGATTGGTAAATATTTGAGTT	cagtaatacgactcactatagggagaaggctAAAATCTCCAAACCCCCAATATAA	+
Epi00211_SEPT9.1	chr17:72882880-72883313	aggaagagagTTAGGGGTTTTTTTTGTTTTAAATGT	cagtaatacgactcactatagggagaaggctCACCAAAATAATCTCAATAAACCCA	+
Epi00212_SEPT9.2	chr17:72883369-72883770	aggaagagagGGTTTTAATTTGTTGGTTTTTTGTG	cagtaatacgactcactatagggagaaggctTCCATACTAACTTCTCCCCCTACTAACTAA	+
Epi00241_ID2.1	chr2:8726166-8726763	aggaagagagTGGATGGATGTTTTAAAGTTTAGTTATT	cagtaatacgactcactatagggagaaggctAAACCACCATCATATTTAACAACATTA	+
Epi00047_ID2.1	chr2:8734408-8734815	aggaagagagTGTGTTTTTTGTTAGGGATTGTAAGT	cagtaatacgactcactatagggagaaggctCTTTCACAAAAAATTTTCCTATATCTT	+
Epi00048_ID2.2	chr2:8735298-8735692	aggaagagagATTTGGTTTTAGGGTAAGGGTTTTT	cagtaatacgactcactatagggagaaggctAAACCAAAAACTTCCAAATCAACTT	+
Epi00049_ID2.3	chr2:8735719-8736002	aggaagagagTATTAGAAAGGGGATTGGTTTGGTT	cagtaatacgactcactatagggagaaggctAACTTTAATCCTAAATTCCTAAAAATACC	+
Epi00050_ID2.4	chr2:8736649-8736919	aggaagagagGGAATGGATATAGTTGTGAGAATAAAA	cagtaatacgactcactatagggagaaggctCAACCTAACTCCAAAACTCACTCAC	+
Epi00051_ID2.5	chr2:8738550-8738834	aggaagagagAGTTTTGGAATTTTTTTAGGTGTTG	cagtaatacgactcactatagggagaaggctAAATACTTATTACAAACCATACCCAACC	+
Epi00052_ID2.6	chr2:8738655-8739088	aggaagagagGTTTTTTAAGGGTAGTGTATGTAAATG	cagtaatacgactcactatagggagaaggctAAAAAAACCACAATTCACTACAACC	+
Epi00053_ID2.7	chr2:8739870-8740348	aggaagagagTGTTATTTTAAGTTTAAGGAGTTGGTGT	cagtaatacgactcactatagggagaaggctTTTTTATAATCCACAAACCAACAAA	+
Epi00054_ID2.8	chr2:8740456-8740944	aggaagagagTGATAGTAAAGTATTGTGTGGTTGAA	cagtaatacgactcactatagggagaaggctAAAATCCCACATCACAAAATTAAAA	+
Epi00055_ID2.9	chr2:8741022-8741291	aggaagagagTTGTTGTTGGAGATTTAAATAGGAGA	cagtaatacgactcactatagggagaaggctCAAAAAATAAAAAAAATCATAAACACCTAC	+
Epi00246_ID2.6	chr2:8748975-8749253	aggaagagagGGTTGTTAATAAAGAAATGATTATTTGAA	cagtaatacgactcactatagggagaaggctTTAAACCAATTATCCAAAAATACCC	+
Epi00032_CTLA4.1	chr2:204407956-204408452	aggaagagagGTGTTTATGTGAGTTGAGGGATTAT	cagtaatacgactcactatagggagaaggctCAATCCAATTACAAACCATAAAAAATA	+
Epi00033_CTLA4.2	chr2:204408649-204408984	aggaagagagTGTTGTTGTTGGTTGTAAGTATTGTT	cagtaatacgactcactatagggagaaggctACCTACCCACTTACTCTAATTCTCA	+
Epi00213_CTLA4.1	chr2:204409089-204409645	aggaagagagTTTTTTGTTGTGATATTGTTTTAGG	cagtaatacgactcactatagggagaaggctATCCCTTCTAACCATTCAAATTTCT	+
Epi00034_CTLA4.3	chr2:204409465-204409854	aggaagagagGGTATTGGAGTTATTGAGTTGGTAGA	cagtaatacgactcactatagggagaaggctCCCCTACATACAAAAAAAACAACATA	+
Epi00214_CTLA4.2	chr2:204410553-204411141	aggaagagagTGAGTGAAAGAAGTTTATATGAAAAGGT	cagtaatacgactcactatagggagaaggctTCATTTCATAACATATAACAATCAATCAA	+
Epi00216_CTLA4.4	chr2:204426356-204426766	aggaagagagTTAAGTTTTAATTGGGTTAGGTTTG	cagtaatacgactcactatagggagaaggctTACCCAAACATCTAAAAAACATCAA	+

Oligonucleotides for bisulfite amplicon generation (continued)

Amplicon	Chromosomal Location (hg18)	Sense	Antisense	Dir.
Epi00217_CTLA4.5	chr2:204426643-204427110	aggaagagagTATGGAATTTTTTATGTGAGGTTTGTT	cagtaatacgactcactatagggagaaggctAACCAAAACAAAAACTCAATCCTCT	+
Epi00038_CTLA4.7	chr2:204427109-204427432	aggaagagagTTTTTTTGGTTGTTTTGTTTTGATT	cagtaatacgactcactatagggagaaggctAAAAAAAATTTCCTCCTTACCTACC	+
Epi00219_CTLA4.7	chr2:204429550-204430103	aggaagagagTTATGATTAAATTTAGTGTGATTAATTGGA	cagtaatacgactcactatagggagaaggctAAATAAAACTTTCCTAAAATTCCCAA	+
Epi00220_CTLA4.8	chr2:204430849-204431377	aggaagagagTTTTGTATGTGGTAAGAATTTTATGTGA	cagtaatacgactcactatagggagaaggctCCATCACCAACCAAAATCTAAAATA	+
Epi00221_CTLA4.9	chr2:204431356-204431929	aggaagagagTTTAGATTTTGGTTGGTGATGG	cagtaatacgactcactatagggagaaggctAAAATAAACCAAACACAAAAAAACAC	+
Epi00222_CTLA4.10	chr2:204432444-204433038	aggaagagagTTTAGGAGTTAGTGTTTGTTATAGATTGTG	cagtaatacgactcactatagggagaaggctCCCCACCTAAATAATACATTCAAAA	+
Epi00226_CTLA4.14	chr2:204441638-204442166	aggaagagagAAGGAAAAGGAAAGAAAGAAAGTTATTA	cagtaatacgactcactatagggagaaggctTTATAACCCACCCAAATAAACACTC	+
Epi00227_CTLA4.15	chr2:204443006-204443543	aggaagagagTGGGTGATAGAGGTTTAGGGTTAGT	cagtaatacgactcactatagggagaaggctAAAACCAAAAAAAACTCAATAAACTCA	+
Epi00233_CTLA4.21	chr2:204445693-204446278	aggaagagagTTTTATAATAGGGGTTTATGTGAAAATG	cagtaatacgactcactatagggagaaggctCCTTTAACATCACTAACTAAAACATAACCA	+
Epi00234_CTLA4.22	chr2:204446252-204446789	aggaagagagTTATGTTTTAGTTAGTGATGTTAAAGGTTG	cagtaatacgactcactatagggagaaggctTCTTCTATCCATAACATTAACCACATATT	+
Epi00236_IKZF2.2	chr2:213697351-213697584	aggaagagagTGAAATTGTTATTGTGTAGAAGGGG	cagtaatacgactcactatagggagaaggctCAAAAAAATTCATTACATAACATATCCA	+
Epi00040_ZNFN1A2.1	chr2:213723180-213723764	aggaagagagTTTTTTAATTTTTTAAAGAGGAGGTGA	cagtaatacgactcactatagggagaaggctTTACCAAAAACCAAAAACAATCCTA	+
Epi00041_ZNFN1A2.2	chr2:213723485-213723925	aggaagagagTTTTTAGGGATGGTTTAGTAGGAAAA	cagtaatacgactcactatagggagaaggctTCCAAATAAAAAATAATATCCAAATCC	+
Epi00239_IKZF2.5	chr2:213726239-213726736	aggaagagagAGAGAAATTATTTGGGTTTAGGTTTGTA	cagtaatacgactcactatagggagaaggctAACCAAAAACAAAAACTACATCAAC	+
Epi00045_ZNFA1N2.2	chr2:213727375-213727718	aggaagagagAGGGTTTTATTATGTTGGTTAGGGT	cagtaatacgactcactatagggagaaggctAACTAAAAAATCTATTTCCTCCCCA	+
Epi00046_ZNFN1A2.1	chr2:213809715-213810256	aggaagagagGGGAAGGTAGTATTATTTTTTGTTTTT	cagtaatacgactcactatagggagaaggctAATCTCTCCTAAATTCATTAAAATTCA	+
Epi00240_WNT10A.1	chr2:219476834-219477390	aggaagagagAGTTTTTTAAAGTGTTGGGATTATAGG	cagtaatacgactcactatagggagaaggctAAACCCAAATTAATACAAAAATCCA	+
Epi00248_IL2RB.2	chr22:35871983-35872251	aggaagagagTTTTTTATAGGGGATGTTTTTGGAT	cagtaatacgactcactatagggagaaggctCAAAAAAAACAAATAAAACCTACA	+
Epi00251_IL2RB.5	chr22:35893508-35893730	aggaagagagGTTTTATTGTTTTTGGTTGTTTGGT	cagtaatacgactcactatagggagaaggctAAACAAATCCTCCCACCTATACC	+
Epi00253_PDE4D.1	chr5:58457591-58458087	aggaagagagGGGGTTTTGATTTTGTGATATATAATTT	cagtaatacgactcactatagggagaaggctAATAACTAAAATACAACCTTCTCCTCTTTC	+
Epi00254_PDE4D.2	chr5:58458185-58458681	aggaagagagGGGTTGTTTTTTTAGTATTAGTTTATTTGA	cagtaatacgactcactatagggagaaggctATTTCAACTTTCACAAAACAACTCCA	+
Epi00067_TNF.1	chr6:31650965-31651237	aggaagagagTTTGGTTTTTAAAAGAAATGGAGGT	cagtaatacgactcactatagggagaaggctTCCTTAATAAAAAAACCCATAAACTCA	+
Epi00068_TNF.2	chr6:31651106-31651692	aggaagagagGGGTATTTTTGATGTTTGTGTGTTT	cagtaatacgactcactatagggagaaggctAACACTCACCTCTTCCCTCTAAAAA	+
Epi00069_TNF.3	chr6:31651639-31652152	aggaagagagTTTTGTTTGTTGTATTTTGGAGTGA	cagtaatacgactcactatagggagaaggctAAACATTCAACAACTCTTTCCCTAA	+
Epi00070_TNF.4	chr6:31651639-31651905	aggaagagagTTTTGTTTGTTGTATTTTGGAGTGA	cagtaatacgactcactatagggagaaggctAAACACCTTCCATATACCAAACATC	+
Epi00071_TNF.5	chr6:31652127-31652504	aggaagagagTTTAGGGAAAGAGTTGTTGAATGTT	cagtaatacgactcactatagggagaaggctAAAAAAAACTAAAACCCTTAAACTTCC	+
Epi00074_HOXA1.1	chr7:27095653-27096004	aggaagagagGGTTTAGAGTTAGAATTTTTTTTGGAA	cagtaatacgactcactatagggagaaggctTTACTAACCACCCACTCAATCAAAT	+
Epi00075_HOXA1.2	chr7:27096226-27096699	aggaagagagGAGATTAGGGATGTGGGTTTTATTTA	cagtaatacgactcactatagggagaaggctCTCTTCAAAAATCAAAATTCATATAATCA	+
Epi00077_GATA4.1	chr8:11583609-11584063	aggaagagagTATATTGAGGAGGTGGTTTTGTTTT	cagtaatacgactcactatagggagaaggctTTAACCCATAAAAAATTCCAAAAATC	+
Epi00259_TP53INP1.1	chr8:96010388-96010962	aggaagagagTAGAGGAAATTAGTTAGAGTGGATGGT	cagtaatacgactcactatagggagaaggctTCCACAAAATAAAAAATCCTCTATCAT	+
Epi00269_FOXP3.1	chrX:48996840-48997010	aggaagagagATTAAAGGATGTAAGAGGTTAAATGGT	cagtaatacgactcactatagggagaaggctAATAATTCCAAAAACACCTCCTTTC	+
Epi00270_FOXP3.2	chrX:48997485-48998052	aggaagagagGAGAGGTTGGTGATTTAGAGGTTTA	cagtaatacgactcactatagggagaaggctCCAAAAAAATTTAAATAACTTTCCCA	+
Epi00271_FOXP3.3	chrX:48997580-48997983	aggaagagagAGGTTGGAGTGTAGTGGTGTAATTT	cagtaatacgactcactatagggagaaggctATAATCCCAACATCAATAACCACAT	+
Epi00272_FOXP3.4	chrX:49001667-49002039	aggaagagagGTTTGTTTTATTTTGGGTTTAGGGT	cagtaatacgactcactatagggagaaggctATCCCAACCAATACCTACTTTAACC	+
Epi00081_FOXP3.1	chrX:49003029-49003414	aggaagagagGGGTTTTTTGTTGAGTTTTAGAATTT	cagtaatacgactcactatagggagaaggctCTAACAACCACCCCCAAAAAATAAC	+
Epi00082_FOXP3.2	chrX:49003993-49004485	aggaagagagATTTGTTTGGGGGTAGAGGATTTAG	cagtaatacgactcactatagggagaaggctACCCCAAAAATCCCAATATCTATAA	+
Epi00083_FOXP3.3	chrX:49004673-49005149	aggaagagagAGGGTTTTTTGTTTATTAGGTTTGG	cagtaatacgactcactatagggagaaggctAAAAAAAACCTAAACTACCATTCCC	+
Epi00088_FOXP3.8	chrX:49005022-49005472	aggaagagagTTTTTGTGTGTGTTTTTTTGTTTTT	cagtaatacgactcactatagggagaaggctAAACCTCACCTAACCCAACTCTTAT	+
Epi00084_FOXP3.4	chrX:49005180-49005620	aggaagagagGGTTTTTTAGTTGGGGAGAGAGTTAG	cagtaatacgactcactatagggagaaggctTTTCAAACAACATCAATTAAACCAA	+
Epi00277_FOXP3.9	chrX:49006709-49007185	aggaagagagTTTAGGGTTAGTTTAAGTAGAGGGAGT	cagtaatacgactcactatagggagaaggctAACCAAAATCCATATTCAAAAAACA	+
Epi00278_FOXP3.10	chrX:49007665-49008089	aggaagagagTAGAGAGATAGAGAAGGATGAGAGGTATT	cagtaatacgactcactatagggagaaggctTTCTATCAATCCACTTCACCAAAAT	+

Supplemental Table S6
Oligonucleotides for the amplification of DMR regions

Symbol	Chromosomal Location (hg18)	Sense primer	Antisense primer	Cloning
CTLA4	chr2:204408509-204409748	ATTAAAAGGAATTCCTGCAGTTTCTCAGTGCCTACAAGGTG	GCTCTTCTCCACTAGTTTGTCCAAATTCATCCCTACTCC	inFusion
	chr2:204426486-204427513	ATTAAAAGGAATTCCTGCAGAACCACGGTCTAGTTTCAACC	GCTCTTCTCCACTAGTTTTGAGAATTGAGGAGAAGGC	inFusion
FOXP3	chrX:49003778-49004624	ATTAAAAGGAATTCCTGCAGGCCAGAACAAACTAATACCGA	GCTCTTCTCCACTAGTCTACACATACTGAGACTTTGGG	inFusion
	chrX:49018113-49019122	ATTAAAAGGAATTCCTGCAGGAATGAAAGCAGACCATGTCC	GCTCTTCTCCACTAGTTTGATCCACTCGTTTCTCCTC	inFusion
	chrX:49020216-49021443	ATTAAAAGGAATTCCTGCAGTTGAGCCAATCCCAAGATCC	GCTCTTCTCCACTAGTTTTCACAGCCACCTTCAAACC	inFusion
IKZF2	chr2:213809332-213810300	ATTAAAAGGAATTCCTGCAGGACTCTATCAGATACTTTCAGTGTGG	GCTCTTCTCCACTAGTATTCTCATTCTGTTCAGTTCACCTC	inFusion
IL1R1	chr2:102045190-102046401	ATTAAAAGGAATTCCTGCAGATTCCTTTGTAACTTGGCTGAC	GCTCTTCTCCACTAGTGTGGATTCTGACTCTGGTGG	inFusion
IL2RA	chr10:6153878-6154935	ATTAAAAGGAATTCCTGCAGTAGAAATTCATCCCACACCCAC	GCTCTTCTCCACTAGTGCTGAGTAGGAGAGGAAGAC	inFusion
	chr10:6118859-6120070	ATTAAAAGGAATTCCTGCAGGCAGACTGGGATTTGTCAGG	GCTCTTCTCCACTAGTGGTTGGCCTAAATGATCTTTGAG	inFusion
	chr10:6121540-6122683	ATTAAAAGGAATTCCTGCAGGCAAAGAGTGGGTATCTATGG	GCTCTTCTCCACTAGTCAAAGATGCCATTAAGTCCTTGAG	inFusion
IL2RB	chr22:35871120-35872336	ATTAAAAGGAATTCCTGCAGTAGGAGCTCTGACCCAAACAC	GCTCTTCTCCACTAGTTTAGGCTTTGATTGCAACAGG	inFusion
	chr22:35893420-35894563	ATTAAAAGGAATTCCTGCAGGTCGCATGTTTCAGATGCAG	GCTCTTCTCCACTAGTCTTATGCAGTATCCAGGCCTC	inFusion
LGALS3	chr14:54608337-54609182	ATTAAAAGGAATTCCTGCAGGCAGTTACCAGTCATTGGAG	GCTCTTCTCCACTAGTCTATATTAGATGTGCATTGTTTGGG	inFusion
	chr14:54639182-54640281	ATTAAAAGGAATTCCTGCAGATACACCTTCCCTAAGCAATTCC	GCTCTTCTCCACTAGTATCTAAACCACTCATGCCCTG	inFusion
LRRC32	chr11:76055840-76056973	ATTAAAAGGAATTCCTGCAGGGCATGAACTCATTCCATCC	GCTCTTCTCCACTAGTTCTTTCAGGGAGAGCAGTCAG	inFusion
	chr11:76030698-76031632	ATTAAAAGGAATTCCTGCAGGGCTACACTATCAAGGGAAGG	GCTCTTCTCCACTAGTTTGAACTAGACTTTGATGCTCATGG	inFusion
TP53INP1	chr8:96009677-96010763	ATTAAAAGGAATTCCTGCAGAATCTCATGGCTGAACTTCTG	GCTCTTCTCCACTAGTTCTTTAACCACTCTGGCCTC	inFusion
CD40LG	chrX:135566244-135567359	GATGAATGCATGTACAGCACTCGACAGCATCAC	ATCCTACTAGTAGCATCTGAGCGGTAGCCAC	
CHD7	chr8:61987563-61988493	GATGAATGCATCCTGTTCTCACCTGCATCTGGG	ATCCTACTAGTGCAAGTGTCTCTTGGTCTCTGTC	
	chr8:61755811-61756623	GATGAATGCATAAATGTCTCCTACTTATCACCTAGAAAGGC	ATCCTACTAGTCCCTCTTCTGAACAGACAATGGAC	
ID2	chr2:8737174-8738191	GATGAATGCATTTAAGGTGATTTCATATTGGGCGTGCTG	ATCCTGCTAGCTTTGCATTTCAGAAAGCGGAAGGG	
IFNG	chr12:66843471-66844447	GATGAATGCATTCAATCGAAGTATTTGGCACTTGGT	ATCCTACTAGTCAGACTGGCAGTGAAACATCTGCT	
IL26	chr12:66878596-66879204	GATGAATGCATGTGCTTCCTGACTTTGATTCTCCA	ATCCTACTAGTCATCTGAACAATCCACAAGCCTCAC	
SEPT9	chr17:72882782-72883825	GATGAATGCATTGTGTTCCGTTGAGCCTCCTG	ATCCTACTAGTTCCTCTTGCAATCCAATTCCTACTCTCC	

Supplemental Table S7
Properties of DMR analyzed by enhancer reporter assays in Jurkat T cells

Closest Gene (Symbol)[a]	Chromosomal Location (hg18)	Hypomethylated T cell type	Overlap with PhastCons[b]	Overlap with DHS in CD4+ T cells[c]	Relative Position to Gene Transcripts[d]	CpG content class[e]	H3K4 Methylation Status[f]	Epityper validation of MCIp results	Reporter gene Active in Jurkat Cells
IFNG	chr12:66843471-66844447	Tconv	yes		**inter**	LCR	Tconv Mono/Di	yes	yes
IL26	chr12:66878596-66879204	Tconv	yes	DHS	**inter**	ICR	ND	yes	yes
SEPT9	chr17:72882782-72883825	Tconv	yes		intra	LCR	Tconv Tri	yes	yes
ID2	chr2:8737174-8738191	Tconv	yes	DHS	**inter**	LCR	Tconv Tri		yes
CHD7	chr8:61755811-61756623	Tconv		DHS	intra	ICR	Tconv Tri		
CHD7	chr8:61987563-61988493	Tconv	yes	DHS	**inter**	LCR	Tconv Mono/Di		
CD40LG	chrX:135566244-135567359	Tconv	yes		intra	LCR	Tconv Tri	yes	yes
IL2RA	chr10:6118859-6120070	Treg		DHS	intra	LCR	Treg Tri	yes	
IL2RA	chr10:6121540-6122683	Treg			intra	LCR	Treg Tri	yes	yes
IL2RA	chr10:6153878-6154935	Treg		DHS	**inter**	LCR	Treg Tri	yes	
LRRC32	chr11:76030698-76031632	Treg	yes		**inter**	LCR	Treg Tri	yes	yes
LRRC32	chr11:76055840-76056973	Treg			intra	LCR	Treg Tri	yes	yes
MAPK1IP1L	chr14:54608337-54609182	Treg		DHS	**inter**	LCR	ND		
LGALS3	chr14:54639182-54640281	Treg			**inter**	LCR	ND		yes
IL1R2	chr2:102045190-102046401	Treg			**inter**	LCR	ND		
CTLA4	chr2:204408509-204409748	Treg	yes		**inter**	LCR	Treg Tri	yes	
CTLA4	chr2:204426486-204427513	Treg	yes	DHS	**inter**	LCR	Treg Tri	yes	
SPAG16	chr2:213809332-213810300	Treg	yes		**inter**	LCR	Treg Tri	yes	
IL2RB	chr22:35871120-35872336	Treg			intra	LCR	Treg Tri	yes	
IL2RB	chr22:35893420-35894563	Treg			intra	LCR	Treg Tri	yes	
TP53INP1	chr8:96009677-96010763	Treg	yes	DHS	intra	LCR	Treg Tri	yes	yes
FOXP3	chrX:49003778-49004624	Treg	yes		intra	LCR	Treg Tri	yes	yes
PPP1R3F	chrX:49018113-49019122	Treg			intra	LCR	Treg Tri	yes	
PPP1R3F	chrX:49020216-49021443	Treg	yes	DHS	intra	LCR	Treg Tri	yes	yes

[a] For reporter gene assays, we preferentially selected differentially methylated regions (DMR) that were associated with genes that also showed differential gene expression. Shown are genes with the smallest distance between TSS and DMR. *MAPK1IP1L* and *SPAG16* were not differentially expressed in T cell subsets, however, the corresponding genes in the opposite direction (*LGALS* and *IKZF2*) were specifically expressed in Treg cells.

[b] Overlap of the identified DMR with conserved sequence elements predicted by the phastCons program based on a whole-genome alignment of vertebrates was done using the Table Browser at the UCSC Genome Browser web site (genome.ucsc.edu/).

[c] Overlap of the identified DMR with DNaseI hypersensitive sites (DHS) in CD4+ T-cells (Boyle et al, 2008) was determined using the Table Browser at the UCSC Genome Browser web site (genome.ucsc.edu/)

[d] DMR were classified either as intergenic (inter) or intragenic (intra) based on their position relative to known genes.

[e] DMR were classified according to their CpG content using the promoter definitions proposed by Weber et al. (2005) as described in the Methods section.

[f] Histon H3 lysin 4 methylation at DMR regions was classified as follows: Treg or Tconv Tri, increased H3K4 trimethylation in Treg or Tconv cells, respectively; Treg or Tconv Mono/Di, increased H3K4 mono-, or di-, but no trimethylation in Treg or Tconv cells, respectively; ND, H3K4 methylation present but not different between T cell subsets.

Supplemental Table S8
Sequence motifs associated with DMR showing enhancer activity

DMR class	TF Matrices	Number of Sequences[a]	Number of Matches[b]	Expected (genome)[c]	Std.dev.	Over representation (genome)[d]	Z-Score (genome)[e]
DMR showing no activity in the enhancer assay (n=12)	V$STAT5.01	8	26	9.22	3.03	2.82	5.36
	V$MYOD.01	7	10	2.59	1.61	3.86	4.29
	V$NFKAPPAB65.01	9	15	5.03	2.24	2.98	4.22
	V$HMX2.02	9	26	11.64	3.41	2.23	4.06
	V$MZF1.02	8	20	8.26	2.87	2.42	3.91
	V$STAT3.02	8	14	5.06	2.25	2.77	3.75
	V$HEN1.02	3	7	1.72	1.31	4.08	3.65
	V$GKLF.01	11	20	9.15	3.02	2.19	3.42
	V$E47.01	8	8	2.34	1.53	3.41	3.37
	V$ZID.01	5	8	2.38	1.54	3.36	3.31
	V$MARE.02	4	8	2.43	1.56	3.29	3.25
	V$NGN_NEUROD.01	7	11	4.24	2.06	2.59	3.04
	V$NFKAPPAB.01	5	9	3.15	1.77	2.86	3.02
DMR showing enhancer activity (n=12)	V$CREB2CJUN.01	2	4	0.28	0.53	14.06	6.03
	V$ATF.01	7	10	1.85	1.36	5.4	5.62
	V$ELK1.02	9	11	2.35	1.53	4.68	5.32
	V$CTCF.03	5	12	2.92	1.71	4.11	5.02
	V$HAND2_E12.01	4	11	2.71	1.65	4.06	4.73
	V$ATF6.02	7	9	1.99	1.41	4.53	4.62
	V$CTCF.04	5	10	2.39	1.55	4.18	4.59
	V$CREB1.01	5	7	1.31	1.15	5.32	4.52
	V$CREB.02	5	8	1.91	1.38	4.19	4.05
	V$GABPB1.01	7	10	2.86	1.69	3.5	3.93
	V$CETS1P54.01	9	13	4.42	2.1	2.94	3.85
	V$KLF6.01	7	10	3	1.73	3.34	3.76
	V$MZF1.03	6	15	5.79	2.41	2.59	3.62
	V$STAT5.01	7	20	8.9	2.98	2.25	3.56
	V$MZF1.01	6	15	5.98	2.45	2.51	3.48
	V$E4F.01	7	13	4.89	2.21	2.66	3.44
	V$HIF1.01	6	7	1.87	1.37	3.75	3.39
	V$ETS2.01	11	19	8.71	2.95	2.18	3.32
	V$RB_E2F1_DP1.01	4	8	2.42	1.55	3.31	3.27
	V$USF.04	6	11	3.99	2	2.76	3.26
	V$GKLF.01	11	19	8.83	2.97	2.15	3.25
	V$E2F.02	10	11	4.07	2.02	2.7	3.18
	V$ATF.02	9	11	4.11	2.03	2.68	3.16
	V$OLF1.02	7	10	3.64	1.91	2.75	3.07
	V$ROAZ.01	5	9	3.11	1.76	2.89	3.06

[a] Number of input sequences with at least one match.
[b] Number of matches in all sequences.
[c] Expected match numbers in an equally sized sample of the genomic background and the standard deviation.
[d] Overrepresentation against genomic background: Fold factor of match numbers in regions compared to an equally sized sample of the background (i.e. found versus expected).
[e] Z-score of overrepresentation against genomic background: The distance from the population mean in units of the population standard deviation. Shown are only highly significant motifs (Z score >3; a Z-score above 2 can be considered statistically significant).

3.2 Isolation of intact genomic DNA from FOXP3-sorted human regulatory T cells for epigenetic analyses

Published in: European Journal of Immunology. 2010 May;40(5):1510-2.

PMID: 20201041

Christian Schmidl performed mass spectrometry experiments, analyzed data and contributed to manuscript writing

Isolation of intact genomic DNA from FOXP3-sorted human regulatory T cells for epigenetic analyses

Leo Hansmann*, Christian Schmidl*, Tina J. Boeld*, Reinhard Andreesen, Petra Hoffmann, Michael Rehli+, Matthias Edinger+

Department of Hematology & Oncology, University Hospital Regensburg, 93042 Regensburg, Germany

* equal contribution; +co senior authors

Key words: epigenetics, immune regulation, methylation

Corresponding Authors:

Matthias Edinger, MD and Michael Rehli, PhD
Department of Hematology & Oncology
University Hospital Regensburg
Franz-Josef-Strauss-Allee 11
93053 Regensburg
Germany
phone: +49 (0)941-944 5580
FAX: +49 (0)941-944 5581
matthias.edinger@klinik.uni-regensburg.de
michael.rehli@klinik.uni-regensburg.de

Abstract

$CD4^+$ T cell subpopulations are defined through their lineage-specific expression of transcription factors. The expression of these master regulators in $CD4^+$ T cells is not solely controlled by their promotor activity, but also by epigenetic mechanisms. It has recently been shown that stable expression of the Treg lineage-directing transcription factor Foxp3 is dependent on its DNA methylation status at a methylation sensitive, Treg cell- specific enhancer, called Treg-specific demethylated region (TSDR). Thus far, the lack of methods for the isolation of intact genomic DNA after intracellular/intranuclear staining and FACS-sorting hampered downstream genetic and epigenetic analyses of these unique T cells subpopulations. Using Foxp3-specific FACS purification of human $CD4^+CD25^+$ T cells as an example, we now present a modified phenol-based DNA isolation protocol permitting further downstream applications, such as DNA methylation analyses.

Introduction

Several cell lineages and T cell-subpopulations are best defined by their expression of a specific transcription factor. Yet, purification of such cells for downstream genetic and epigenetic analyses still largely relies on the expression of surrogate markers, such as cell surface molecules, that often do not discriminate accurately enough to obtain pure populations. The $CD4^+$ T cell compartment represents a prime example of a cell lineage that is composed of various subpopulations and differentiation states, such as Th1, Th2, Th17 and natural (thymus-derived) regulatory T (Treg) cells. These T cell subpopulations can only be distinguished from each other by their cytokine secretion profile, their functional characteristics or, most reliably, their expression of lineage-defining transcription factors including T-bet (Szabo et al. 2000), GATA-3 (Zheng and Flavell 1997), RORγT (Ivanov et al. 2006) or FOXP3 (Fontenot et al. 2003), for Th1, Th2, Th17 and Treg cells, respectively. In transgenic mouse models, fluorescent reporter gene products permit the unequivocal identification and isolation of such subpopulations for downstream applications by fluorescence activated cell sorting (FACS) (Fontenot et al. 2005b). In humans, however, $CD4^+$ T cell subpopulations are indistinguishable by surrogate phenotypic markers and identified reliably only after intracellular staining with cytokine- or transcription factor-specific antibodies. Yet, formaldehyde fixation and permeabilization, required for the intranuclear staining of transcription factors, induce alterations (e.g. DNA-protein cross-links) that hamper the extraction of intact genomic DNA with commercially available isolation kits (e.g. silica membrane columns; data not shown). In addition, they introduce polymerase-"blocks" complicating genetic and epigenetic analyses. We now aimed to develop protocols for the isolation of intact genomic DNA from FACS-purified cells after formaldehyde fixation and intracellular staining.

Results and Discussion

It has previously been shown that stable expression of the Foxp3 gene in mice is regulated in parts by DNA methylation. Huehn and colleagues described a Treg-specific demethylated region (TSDR) within the Foxp3 locus that is completely methylated in conventional (Foxp3 negative) T cells and also in T cells transiently expressing Foxp3 after *in vitro* stimulation in the presence of TGF-β (so called "induced Treg cells") (Floess et al. 2007; Hoffmann et al. 2009). In addition, Leonhard and colleagues showed that this TSDR contains several transcription factor-binding sites, acts as enhancer and thereby stabilizes Foxp3 expression (Kim and Leonard 2007). Using high-expression of CD25 on $CD4^+$ T cells as a surrogate marker, we previously confirmed the specific demethylation in the TSDR also for human Treg cells (Baron et al. 2007; Hoffmann et al. 2009; Schmidl et al. 2009). To ultimately prove differential DNA methylation in FOXP3-expressing Treg cells, we now modified previously described methods for the extraction of DNA from fixed and paraffin embedded histological samples that so far only allowed the isolation of fragmented (200-400bp) DNA, that was unsuited for reliable epigenetic analyses (Jackson et al. 1990). For the isolation of intact genomic DNA from FOXP3-sorted Treg cells, we now isolated human $CD4^+$ T cells from MNCs and stained the cells for CD4, CD25 and intranuclear FOXP3 using standard protocols (s. Methods section). Afterwards, the cells were FACS-sorted into $CD4^+CD25^+FOXP3^+$, $CD4^+CD25^+FOXP3^-$ and $CD4^+CD25^-FOXP3^-$ subpopulations and re-analyzed by flow cytometry to confirm their purity (Fig. 1a). Intact genomic DNA from the FACS-sorted subpopulations was then isolated using a modified phenol-based DNA extraction protocol, first described in 1956 (Kirby 1956). The implemented modifications included the supplementation of sufficient RNAse and protease activity for the liberation of DNA and the provision of substantial kinetic and thermal energy, which was decisive to reverse fomaldehyde-induced conformational changes and non-covalent as well as covalent cross-links (Fowler et al. 2008). Incubation of the cells in an appropriate lysis buffer (see Methods) at 60°C on a temperature-controlled shaker for approximately 24h turned out to be the crucial step for the isolation of intact and pure genomic DNA. We obtained 12.7±2.4 µg high molecular DNA from $2x10^6$ cells (n = 9 independent isolations), which is well in line with standard extraction procedures from unfixed cells. The DNA was of high purity as revealed by UV spectrometry with a mean absorption ratio at A260/A280 of 1.93 and a mean absorption ratio at A260/A230 of 2.23 (Fig. 1b, for details on individual extractions see Supplementary Fig. 1 and Supplementary Tab. 1).

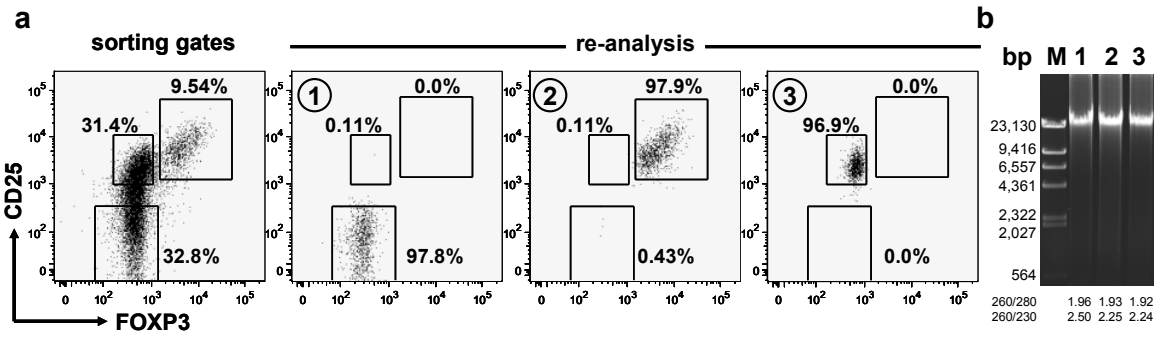

Figure 1:

DNA isolation from CD4⁺ T cells stained and FACS-sorted for differential expression of the transcription factor FOXP3 (a) Sort gates for the FACS purification and re-analysis of FOXP3-stained CD4⁺ T cells. One representative out of three independent experiments is shown. **(b)** Isolation of highly pure genomic DNA as indicated by fragment length and absorbance ratios (A260 nm/A280 nm, A260 nm/A230 nm) detected by UV spectrometry. Displayed is one representative out of three independent experiments. 1: $CD4^+CD25^-$ T cells; 2: $CD4^+CD25^+FOXP3^+$ Treg cells; 3: $CD4^+CD25^+FOXP3^-$ T cells; M: λ Hind III-marker; bp: basepairs.

Genomic DNA isolated by this method was perfectly suited for downstream applications, as exemplarily shown in a MALDI-TOF mass-spectrometry-based DNA methylation analysis of the human *FOXP3* gene. As shown in Figure 2 (and Supplementary Table 2), the DNA methylation status of the *FOXP3* locus was profoundly different in the three T cell subpopulations: As expected, $CD4^+CD25^+FOXP3^+$ cells showed complete demethylation over a large genomic interval, including the methylation sensitive, Treg cell specific enhancer TSDR (Floess et al. 2007; Kim and Leonard 2007). In contrast, $CD4^+CD25^+FOXP3^-$ T cells were demethylated only at the proximal promoter CpGs, whereas the majority of CpGs (including the TSDR) were methylated to the same extent as in $CD4^+CD25^-$ conventional T cells. The partial demethylation of the Foxp3 promoter in $CD4^+CD25^+FOXP3^-$ T cells indicates the proven ability of activated T cells to transiently express FOXP3 without demethylation of the TSDR region (Huehn et al. 2009).

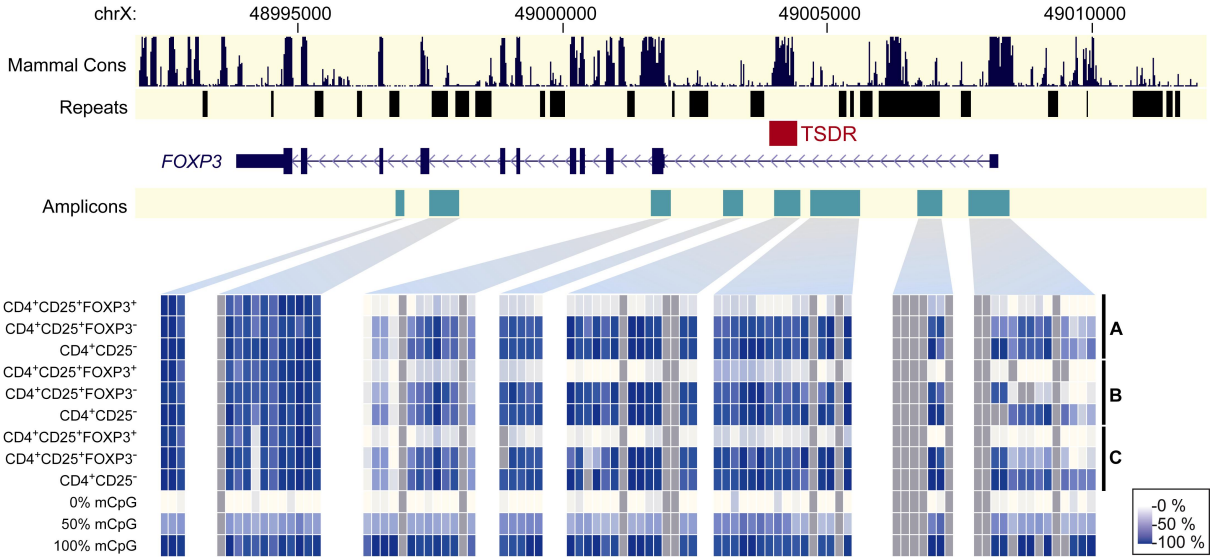

Figure 2:

Methylation analysis of the *FOXP3* locus. The DNA methylation status of the *FOXP3* locus was analyzed by MALDI-TOF MS. Results are shown as heatmap (the scale ranges from white (no methylation) to dark blue (100% methylation)); CpGs not detectable by MS are marked in gray. A, B and C mark isolates from three separate experiments. In $CD4^+CD25^+FOXP3^+$ T cells the DNA of the *FOXP3* locus is completely demethylated, while CpGs of $CD4^+CD25^-$ T cells are completely methylated. $CD4^+CD25^+FOXP3^-$ T cells resemble $CD4^+CD25^-$ T cells except for the *FOXP3* promoter region, which is partially demethylated.

Concluding Remarks

In summary, we present a new and reliable method for the isolation of high molecular DNA from FACS-sorted cells that are fixed, permeabilized and stained for intranuclear transcription factors. Genomic DNA from such cells is of high purity and suited for sensitive downstream applications such as MALDI-TOF MS based DNA methylation analysis, that includes bisulphite conversion and PCR amplification of the extracted DNA. As a proof of principle, we examined the methylation status of the TSDR in FACS-sorted human $FOXP3^+$ Treg cells, which was shown to have crucial enhancer activity and to be critically involved in the maintenance of natural Treg lineage stability (Baron et al. 2007; Floess et al. 2007; Kim and Leonard 2007; Polansky et al. 2008; Hoffmann et al. 2009; Huehn et al. 2009; Schmidl et al. 2009). Overall, this method offers new prospects for the analysis of molecularly defined cell populations, such as natural and induced Treg cells, and will also be valuable for a broad range of other cellular systems.

Materials and Methods

Isolation, FOXP3-staining and FACS-sorting of human CD4$^+$ T cells. Human PBMC were isolated by Ficoll (Biocoll; Biochrom AG, Berlin, Germany) density gradient centrifugation from leukapheresis products of healthy volunteers (after their informed consent and in accordance with protocols approved by the local authorities). CD4$^+$ cells were enriched with CD4 MicroBeads (Miltenyi Biotec, Bergisch Gladbach, Germany) using the Midi-MACS® system (Miltenyi Biotec). CD4-enriched cells were stained with anti-CD4-FITC and anti-CD25-APC (both BD Biosciences, NJ, USA) and anti-FOXP3-PE (eBioscience, San Diego, CA). For intracellular FOXP3 staining, the FOXP3 Staining Buffer Set (eBioscience) was used according to the manufacturer's instructions, with the following modifications: 1x10^8 CD4-enriched cells were resuspended in 20 ml fixation/permeabilization buffer for 30 min at 4°C; for intracellular staining, 1x10^8 cells were resuspended in 2 ml permeabilization buffer and 40 µl normal rat serum (eBioscience) were added. After incubation for 15 min at 4°C in the dark, 450 µl of anti-human FOXP3-PE antibody were added followed by incubation for another 30 min at 4°C in the dark. Finally, cells were resuspended in PBS and sorted into CD4$^+$CD25$^-$, CD4$^+$CD25$^+$FOXP3$^+$ and CD4$^+$CD25$^+$FOXP3$^-$ T cells using a FACS-Aria® high-speed cell sorter (BD Biosciences). Sorting gates were defined as shown in Figure 1a and sorted cell populations routinely showed >96% purity (range: 96%-98%) upon re-analysis. All buffers for staining and fixation were free of DNase-activity.

DNA isolation from FOXP3-sorted cells. The DNA extraction procedure is a modified phenol-based protocol (Kirby 1956). Up to 2.5 x 10^6 FACS-sorted cells were resuspended in 300 µl lysis-buffer containing 100 mM NaCl (C. Roth GmbH, Karlsruhe, Germany), 10 mM Tris HCl (Roth), 50 mM EDTA (Merck KGaA, Darmstadt, Germany), 0.5% SDS (Roth), 0.1 mg/ml proteinase K (Roche Diagnostics GmbH, Mannheim, Germany), 20 µg/ml RNase A (Qiagen GmbH, Hilden, Germany) and the pH was adjusted to 8.0 with NaOH (Roth). The lysate was incubated on a thermoshaker at 60°C for approximately 24 h. Then, 300 µl phenol were added and mixed rapidly. After centrifugation at 3.400 x *g* for 5 min at 4°C, the aqueous (upper) phase was transferred into a new tube and 900 µl of 95% ethanol (Mallinckrodt Baker, Deventer, The Netherlands), 0.12 M sodium acetate (Merck) were added. After vigorous mixing, DNA precipitated and became visible. After incubation for at least 20 min at -20°C, DNA was pelleted for 15 min at 13,700 x *g* at 4°C and washed with 600 µl 70% Ethanol for 5 min at RT. After centrifugation for 15 min at 13.700 x *g* at 4°C the supernatant was completely removed and DNA was dried for 10 min at RT

or at 60°C to remove residual ethanol. Finally, DNA was dissolved in 100 µl TE-buffer (Qiagen) for approximately 24 h on a shaker at 60°C and another 24 h at 4°C. DNA content and purity were measured using the NanoDrop 1000 spectrometer (NanoDrop Technologies, Wilmington, USA). Fragment length of the obtained DNA was determined by 0.5 % Agarose gel-electrophoresis and ethidium-bromide stained gels were scanned on a Typhoon 9200 (GE Healthcare, Piscataway, NJ) (Fig. 1b and Supplementary Fig. 1).

Mass spectrometry analysis of bisulfite-converted DNA. We previously designed a set of 11 partially overlapping amplicons covering regions of the human FOXP3 gene to detect differentially methylated regions (DMR) in $CD4^+CD25^+$ and $CD4^+CD25^-$ T cells (Schmidl et al. 2009). The same regions were analyzed in $CD4^+CD25^-$, $CD4^+CD25^+FOXP3^+$ and $CD4^+CD25^+FOXP3^-$ T cells and 0%, 50% and 100% methylated control templates were generated as previously described (Schmidl et al. 2009). Sodium bisulfite conversion was performed using the EZ DNA methylation kit (Zymo Research, Orange, CA) using 1 µg of genomic DNA and an alternative conversion protocol. The incubation parameters where changed as follows: 95°C for 30 sec, 50°C for 15 min (repeated for 20 cycles). PCR amplification of target regions was followed by SAP treatment, reverse transcription and subsequent RNA base-specific cleavage (MassCLEAVE, Sequenom, San Diego, CA) as previously described (Ehrich et al. 2005). Cleavage products were loaded onto spectroCHIPs (Sequenom) and analysed by MALDI-TOF mass spectrometry (MassARRAY Compact MALDI-TOF, Sequenom). Methylation ratios were determined from mass spectra using the Epityper software v1.0 (Sequenom).

Acknowledgements

We gratefully acknowledge R. Eder and J. Stahl for expert technical assistance and cell sorting.

This work was supported by grants from the Deutsche Forschungsgemeinschaft to M.E. (KFO146) and to M.R. & P.H. (Re1310/10) and the Wilhelm Sander Stiftung (ME). The José Carreras Foundation co-funded the cell sorting facility (M.E.).

Conflict of interest

The authors declare no conflict of interests.

Supplementary Information

Supporting Information to Hansmann et al.: Isolation of intact genomic DNA from FOXP3-sorted human regulatory T cells for epigenetic analyses

Copyright

Figures and Text from chapter 3.2 are taken from: Leo Hansmann, Christian Schmidl, Tina J. Boeld, Reinhard Andreesen, Petra Hoffmann, Michael Rehli, Matthias Edinger," Isolation of intact genomic DNA from FOXP3-sorted human regulatory T cells for epigenetic analyses". 2010. European Journal of Immunology 40(5): 1510-1512. (pre-peer reviewed version)

The final version of this article was published at:

http://onlinelibrary.wiley.com/doi/10.1002/eji.200940154/abstract

Copyright Wiley-VCH Verlag GmbH & Co. KGaA. Reproduced with permission.

Materials and Methods

Isolation, FOXP3-staining and FACS-sorting of human CD4+ T cells. Human PBMC were isolated by Ficoll (Biocoll; Biochrom AG, Berlin, Germany) density gradient centrifugation from leukapheresis products of healthy volunteers (after their informed consent and in accordance with protocols approved by the local authorities). CD4+ cells were enriched with CD4 MicroBeads (Miltenyi Biotec, Bergisch Gladbach, Germany) using the Midi-MACS® system (Miltenyi Biotec). CD4-enriched cells were stained with anti-CD4-FITC and anti- CD25-APC (both BD Biosciences, NJ, USA) and anti-FOXP3-PE (eBioscience, San Diego, CA). For intracellular FOXP3 staining, the FOXP3 Staining Buffer Set (eBioscience) was used according to the manufacturer's instructions, with the following modifications: 1x108 CD4-enriched cells were resuspended in 20 ml fixation/permeabilization buffer for 30 min at 4°C; for intracellular staining, 1x108 cells were resuspended in 2 ml permeabilization buffer and 40 µl normal rat serum (eBioscience) were added. After incubation for 15 min at 4°C in the dark, 450 µl anti-human FOXP3-PE antibody was added followed by incubation for another 30 min at 4°C in the dark. Finally, cells were resuspended in PBS and sorted into CD4+CD25-, CD4+CD25+FOXP3+ and CD4+CD25+FOXP3- T cells using a FACS-Aria® highspeed cell sorter (BD Biosciences). Sorting gates are shown in Figure 1A and sorted cell populations routinely showed >96% purity (range: 96%-98%) upon re-analysis. All buffers for staining and fixation were free of DNase-activity.

DNA isolation from FOXP3-sorted cells. The DNA extraction procedure is a modified phenol-based protocol (Kirby 1956). Up to 2.5 x 106 FACS-sorted cells were resuspended in 300 µl lysis-buffer containing 100 mM NaCl (C. Roth GmbH, Karlsruhe, Germany), 10 mM Tris HCl (Roth), 50 mM EDTA (Merck KGaA, Darmstadt, Germany), 0.5% SDS (Roth), 0.1 mg/ml proteinase K (Roche Diagnostics GmbH, Mannheim, Germany), 20 µg/ml RNase A (Qiagen GmbH, Hilden, Germany) and the pH was adjusted to 8.0 with NaOH (Roth). The lysate was incubated on a thermoshaker at 60°C for approximately 24 h. Then, 300 µl phenol were added and mixed rapidly. After centrifugation at 3.400 x g for 5 min at 4°C, the aqueous (upper) phase was transferred into a new tube and 900 µl of 95% ethanol (Mallinckrodt Baker, Deventer, The Netherlands), 0.12 M sodium acetate (Merck) were added. After vigorous mixing, DNA precipitated and became visible. After incubation for at least 20 min at -20°C, DNA was pelleted for 15 min at 13,700 x g at 4°C and washed with 600 µl 70% Ethanol for 5 min at RT. After centrifugation for 15 min at 13.700 x g at 4°C the supernatant was completely removed and DNA was dried for 10 min at RT

or at 60°C to remove residual ethanol. Finally, DNA was dissolved in 100 µl TE-buffer (Qiagen) for approximately 24 h on a shaker at 60°C and another 24 h at 4°C. DNA content and purity were measured using the NanoDrop 1000 spectrometer (NanoDrop Technologies, Wilmington, USA). Fragment length of the obtained DNA was determined by 0.5 % Agarose gel-electrophoresis and ethidiumbromide stained gels were scanned on a Typhoon 9200 (GE Healthcare, Piscataway, NJ) (Fig. 1B and Supplementary Fig. 1). Mass spectrometry analysis of bisulfite-converted DNA. We previously designed a set of 11 partially overlapping amplicons covering regions of the human FOXP3 gene to detect differentially methylated regions (DMR) in CD4+CD25+ and CD4+CD25- T cells (Schmidl et al. 2009). The same regions were analyzed in CD4+CD25-, CD4+CD25+FOXP3+ and CD4+CD25+FOXP3- T cells and 0%, 50% and 100% methylated control templates were generated as previously described (Schmidl et al. 2009). Sodium bisulfite conversion was performed using the EZ DNA methylation kit (Zymo Research, Orange, CA) using 1 µg of genomic DNA and an alternative conversion protocol. The incubation parameters where changed as follows: 95°C for 30 sec, 50°C for 15 min (repeated for 20 cycles). PCR amplification of target regions was followed by SAP treatment, reverse transcription and subsequent RNA base-specific cleavage (MassCLEAVE, Sequenom, San Diego, CA) as previously described (Ehrich et al. 2005). Cleavage products were loaded onto spectroCHIPs (Sequenom) and analysed by MALDI-TOF mass spectrometry (MassARRAY Compact MALDI-TOF, Sequenom). Methylation ratios were determined from mass spectra using the Epityper software v1.0 (Sequenom).

3.3 Epigenetic reprogramming of the *RORC* locus during *in vitro* expansion is a distinctive feature of human memory but not naïve Treg cells

Published in: European Journal of Immunology. 2011 May;41(5):1491-8.
doi: 10.1002/eji.201041067. Epub 2011 Apr 12.

PMID: 21469109

Christian Schmidl performed experiments, analyzed data and contributed to manuscript writing

Epigenetic reprogramming of the *RORC* locus during *in vitro* expansion is a distinctive feature of human memory but not naïve Treg cells

Christian Schmidl*, Leo Hansmann*, Reinhard Andreesen, Matthias Edinger, Petra Hoffmann+, Michael Rehli+

Department of Hematology & Oncology, University Hospital Regensburg, 93042 Regensburg, Germany

*these authors contributed equally to this work

+co senior authors

Keywords: Treg cell plasticity, RORc enhancer regions, DNA demethylation, Th17 cells

Corresponding Authors:
Prof. Dr. Michael Rehli
Department of Hematology & Oncology
University Hospital Regensburg
D-93042 Regensburg
Germany
Tel: 49 941 - 944 - 5587
Fax: 49 941 - 944 - 5593
email: Michael.Rehli@klinik.uni-regensburg.de

PD Dr. Petra Hoffmann
Department of Hematology & Oncology
University Hospital Regensburg
D-93042 Regensburg
Germany
Tel: 49 941 - 944 - 5514
Fax: 49 941 - 944 - 5502
email: Petra.Hoffmann@klinik.uni-regensburg.de

Abbreviations: DMR, differentially methylated region; RA+/RA- Treg, CD45RA-positive (naïve)/negative (memory) Treg; Tconv, conventional T cell; TSS, transcription start site

SUMMARY

The adoptive transfer of *in vitro* expanded regulatory T (Treg) cells is a promising treatment option for autoimmune as well as alloantigen-induced diseases. Yet, concerns about the phenotypic and functional stability of Treg cells upon *in vitro* culture command both, careful selection of the starting population and thorough characterization of the final cell product. Recently, a high degree of developmental plasticity has been described for murine Treg and Th17 cells. Similarly, IL-17-producing FOXP3$^+$ cells have been detected among the CD45RA$^-$ memory-type subpopulation of human Treg cells *ex vivo*. This prompted us to investigate the predisposition of human naïve and memory Treg cells to develop into Th17 cells during polyclonal *in vitro* expansion. Here, we show that stimulation-induced DNA demethylation of *RORC*, which encodes the lineage-defining transcription factor for Th17 cells, occurs selectively in CD45RA$^-$ memory-type Treg cells, irrespective of their FOXP3 expression level. In contrast, naïve CD45RA$^+$ Treg cells retain stable CpG methylation across the *RORC* locus even upon prolonged *ex vivo* expansion and in consequence show only a marginal tendency to express *RORC* and develop into IL-17-producing cells. These findings are highly relevant for the generation of therapeutic Treg cell products.

INTRODUCTION

Natural $CD4^+CD25^{high}FOXP3^+$ Treg cells play a central role in maintaining immune homeostasis and preventing destructive auto- or allo-immune responses, as demonstrated in several murine disease models (Asano et al. 1996; Salomon et al. 2000; Hoffmann et al. 2002a; Taylor et al. 2002; Edinger et al. 2003; Mottet et al. 2003). Due to their scarcity in peripheral blood, potential therapeutic Treg cell applications in humans will require their *ex vivo* expansion. Yet, the now well-documented heterogeneity and developmental plasticity of Treg cells *in vitro* and *in vivo* (Hoffmann et al. 2009; Miyara et al. 2009; Zhou et al. 2009b; Zhou et al. 2009c) raises concerns that *ex vivo* culture may alter the molecular and functional characteristics of the cells. We previously showed that FOXP3, the transcription factor determining Treg lineage commitment and required for their suppressive function, is progressively down-regulated upon *in vitro* expansion of memory-type $CD45RA^-$ Treg cells (RA- Treg), a process that correlates with increased DNA methylation at several regions within the *FOXP3* locus, reduced suppressive activity and increased expression of IL-2 and IFNg in these converting cells (Hoffmann et al. 2006b; Hoffmann et al. 2009). Interestingly, naïve $CD45RA^+$ Treg cells (RA+ Treg), despite the acquisition of a memory phenotype in many other aspects ((Hoffmann et al. 2006b; Hoffmann et al. 2009) and own unpublished data), retain stable FOXP3 expression and suppressive activity and show no tendency to up-regulate those proinflammatory cytokines, even after prolonged *in vitro* expansion. Several reports, however, have now demonstrated a particularly close relationship between Treg and Th17 cells in the murine system and a high degree of developmental plasticity, including the occurrence of $FOXP3^+$ T cells co-expressing IL-17 and/or the retinoic acid receptor-related orphan receptor gt (RORgt), the lineage-defining transcription factor for Th17 cells (Ivanov et al. 2006; Lochner et al. 2008; Yang et al. 2008b; Zhang et al. 2008; Tartar et al. 2010). Similarly, Voo et al. recently detected FOXP3/RORC double-positive cells in peripheral blood as well as in lymphoid organs of healthy human volunteers (Voo et al. 2009). Furthermore, the groups led by Sakaguchi and Valmori both showed that peripheral blood derived memory-type, but not naïve human $CD4^+CD25^{high}FOXP3^+$ T cells express high levels of RORC *ex vivo* and that a minor fraction of these cells indeed produce IL-17 after *in vitro* stimulation (Ayyoub et al. 2009; Miyara et al. 2009). In addition, *in vitro* conversion of human Treg cells, especially of those with memory phenotype, into IL-17-producing effector T cells has been reported, provided cells were kept under Th17-polarizing culture conditions (Deknuydt et al. 2009). Since the long predicted precursor–progeny relationship between $CD45RA^+$ naïve and $CD45RA^-$ memory Treg cells has now been confirmed *in vivo* (Miyara et al. 2009), we investigated the predisposition of human naïve and memory-type Treg cells to develop into

potentially pathogenic Th17 cells when stimulated under the non-polarizing culture conditions designed for clinical Treg cell products. We now show that under such conditions an epigenetic reprogramming of the *RORC* locus and emergence of IL-17 secreting cells occur selectively in memory-type, but not in naïve Treg cells. Interestingly, by further subdividing the memory Treg cell pool, we reveal that DNA demethylation of the *RORC* locus is even more pronounced in the subset with preserved FOXP3 expression as compared to those cells that have already down-regulated FOXP3 expression after repeated *in vitro* stimulation.

RESULTS AND DISCUSSION

DNA demethylation at the RORC *locus occurs in human memory but not in naïve Treg cells upon* in vitro *expansion*

Recently, the paradigm of stable lineage commitment of $CD4^+$ T cells had to be revised considerably. Differentiation of naïve, $Foxp3^-$ conventional T cells (Tconv) into $Foxp3^+$ Treg cells in the periphery is now well accepted (Chen et al. 2003; Klunker et al. 2009). Likewise, conversion of Treg cells into pro-inflammatory effector T cells that no longer express Foxp3 has been shown by us and others both in the murine and in the human system (Hoffmann et al. 2006b; Hoffmann et al. 2009; Zhou et al. 2009c). With the identification of $FOXP3^+$IL-17^+ T cells in the peripheral blood of healthy human subjects another level of complexity in this field has been unravelled (Ayyoub et al. 2009; Miyara et al. 2009). Whereas the physiological role of such cells is still under debate (Lochner et al. 2008; Yang et al. 2008b; Tartar et al. 2010), recent reports about the emergence of IL-17 producing cells in human Treg cultures (Koenen et al. 2008; Ayyoub et al. 2009; Beriou et al. 2009) have revived the question of phenotypic and functional stability of Treg cells during *in vitro* expansion and the safety of such cell products for clinical application. We therefore determined the predisposition of highly purified naïve and memory Treg cells to convert into $FOXP3^+$IL-17^+ T cells and consequently into potentially hazardous Th17 cells during *in vitro* expansion under the non-polarizing culture conditions intended for clinical trials.

The regulation of key developmental as well as functionally important genes is in part orchestrated by epigenetic mechanisms such as histone modification and DNA (CpG) methylation. The importance of such epigenetic regulation for stable expression or repression of *FOXP3* (and that of several other Treg signature genes) has recently been shown by us and others for murine as well as human Treg cells (Baron et al. 2007; Hoffmann et al. 2009; Huehn et al. 2009; Lal and Bromberg 2009; Lal et al. 2009; Schmidl et al. 2009). Since expression of the transcription factor RORC is central for the development of Th17 cells, we focused our investigation on cell-specific changes in the DNA methylation patterns at this gene locus.

We first isolated $CD45RA^+$ naïve and $CD45RA^-$ memory-type $CD4^+CD25^{high}$ T cells (RA+ and RA- Treg, respectively) by FACS from the peripheral blood of healthy volunteers (Fig. 1A), determined their DNA methylation status at several conserved non-coding regions across the *RORC* locus and compared it to that found in *in vitro* generated, FACS-purified Th17 cells (Fig. 1B). Clear differences between the DNA methylation patterns of Th17 cells and both Treg populations could be observed that were particularly noticeable in the proximal promoter

region (covered by amplicons R4/R5 in Fig. 1B and shown in more detail for the promoter region around the transcription start site (TSS; amplicon R5) in Fig. 1C). RA- Treg showed significantly less DNA methylation at the promoter region *ex vivo* as compared to RA+ Treg ($P < 0.001$; n =3-5; Student's *t*-test), which is in line with recent reports detecting *RORC* mRNA expression in freshly isolated human memory-type but not naïve Treg cells (Ayyoub et al. 2009). We then expanded both Treg populations (RA+ and RA- Treg) under non-polarizing culture conditions and, given the dissociation of RA- Treg into a FOXP3-maintaining and a FOXP3-downregulating subpopulation after two to three rounds of re-stimulation (Hoffmann et al. 2006b), we FACS-sorted the two populations and analyzed their DNA methylation status at the *RORC* locus individually. Isolation of intact genomic DNA from fixed and intracellularly stained cells was achieved with our recently described protocol (Hansmann et al. 2010). Direct comparison of freshly isolated and expanded cells revealed a further loss of CpG methylation in RA- Treg cells during expansion at several regions within the *RORC* locus, including the proximal promoter (Fig. 1B and 1C), which was most pronounced in the subpopulation that maintained FOXP3 expression during culture. In fact, this subpopulation of RA- Treg cells developed a CpG methylation pattern almost identical to that of Th17 cells (Fig. 1B). Since the cells were kept under non-polarizing conditions during *in vitr*o expansion, these changes might be due to triggering signals received already *in vivo* that primed RA- Treg cells for a stimulation-dependent epigenetic reprogramming. In support of this view, Lochner et al. (Lochner et al. 2008) as well as Tartar et al. (Tartar et al. 2010) reported on $Foxp3^{+}RORgt^{+}$ T cells in immunocompetent mice that showed the potential to develop into either $Foxp3^{+}RORgt^{-}$ Treg or $Foxp3^{-}RORgt^{+}IL\text{-}17^{+}$ Th17 cells in response to respective lineage-driving stimuli. *In vivo*, such developmentally flexible precursor cells might thus provide the basis for an efficient, yet regulated immune response. In contrast, *in vitro* expansion had no detectable impact on the methylation status of *RORC* in RA+ Treg cells, irrespective of the number of restimulation cycles or FOXP3 expression levels, suggesting that polyclonal TCR triggering and co-stimulation via CD28 *in vitro* is insufficient to induce DNA demethylation of the *RORC* locus and thus a Th17 developmental program in naïve Treg cells. In support of these results, *RORC* mRNA levels in freshly isolated (d0) as well as in *in vitro* expanded RA+ Treg were found to be almost 100-fold lower than in RA- Treg, even after prolonged *in vitro* culture (> 36d) (Fig. 1D). Similar differences were observed in freshly isolated and 14d expanded RA+ and RA- Tconv cells (Suppl. Fig. S2A). Interestingly, even when *in vitro* expanded RA+ Treg cells were cultured under Th17-polarizing conditions for an additional 6 days, their *RORC* locus remained methylated and neither *RORC* mRNA levels nor the number of IL-17-producing cells increased in such cultures (see Fig. 1B and Suppl. Fig. S2B and S2C). Importantly, this pronounced maintenance of DNA methylation in RA+ Treg cells during expansion was not due to a general inability to demethylate DNA, since the Tconv cell-specific differentially methylated region (DMR) at the

CD40LG locus (Schmidl et al. 2009) gradually lost DNA methylation in the few FOXP3$^-$ Treg cells that appeared during extensive *in vitro* culture (data not shown).

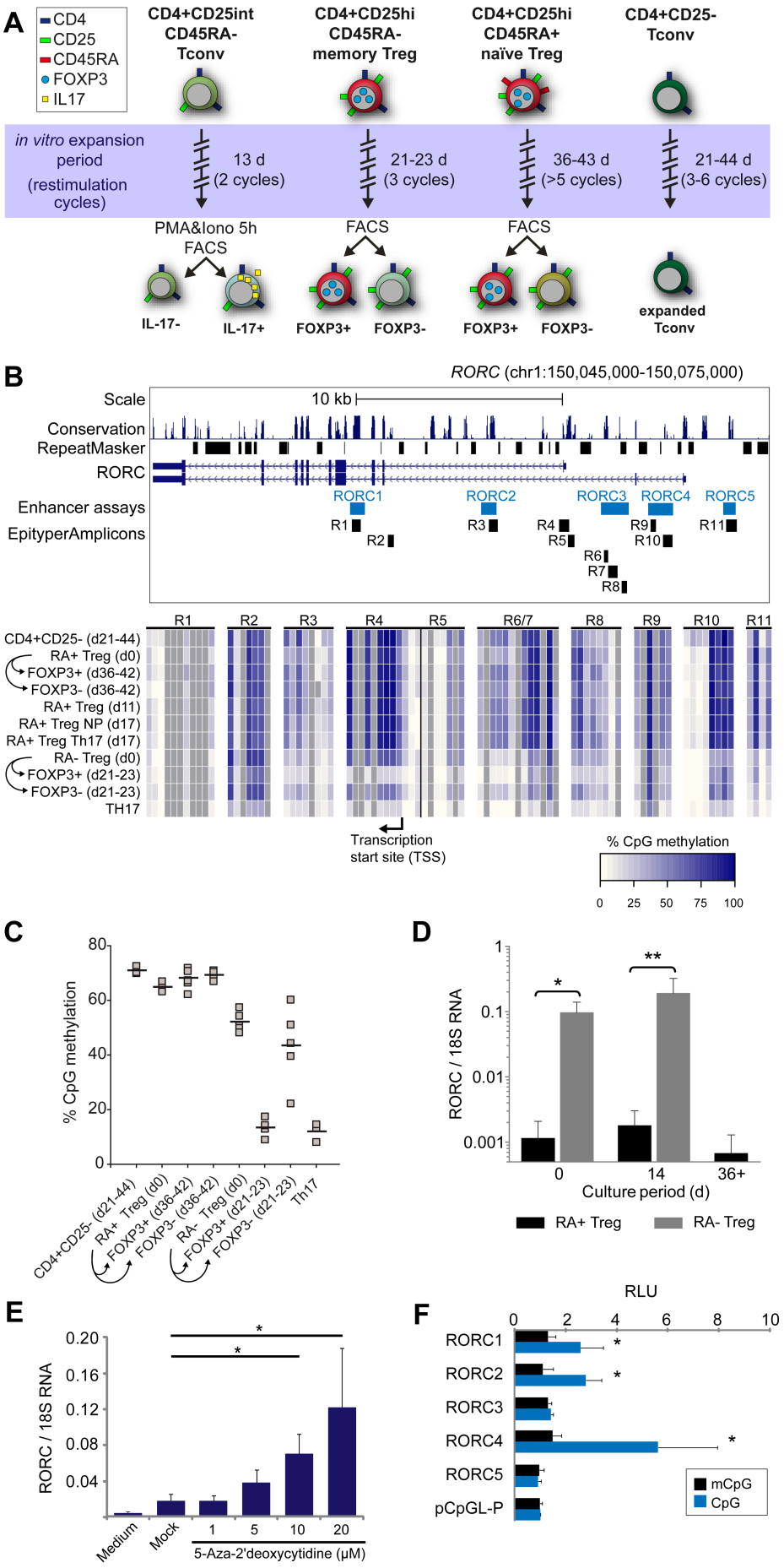
A
CD4
CD25
CD45RA
FOXP3
IL17
CD4+CD25int CD45RA- Tconv
CD4+CD25hi CD45RA- memory Treg
CD4+CD25hi CD45RA+ naïve Treg
CD4+CD25- Tconv
in vitro expansion period (restimulation cycles)
13 d (2 cycles)
21-23 d (3 cycles)
36-43 d (>5 cycles)
21-44 d (3-6 cycles)
PMA&Iono 5h FACS
FACS
FACS
IL-17-
IL-17+
FOXP3+
FOXP3-
FOXP3+
FOXP3-
expanded Tconv
B
RORC (chr1:150,045,000-150,075,000)
Scale
10 kb
Conservation
RepeatMasker
RORC
Enhancer assays
EpityperAmplicons
RORC1
RORC2
RORC3
RORC4
RORC5
R1
R2
R3
R4
R5
R6
R7
R8
R9
R10
R11
R6/7
CD4+CD25- (d21-44)
RA+ Treg (d0)
FOXP3+ (d36-42)
FOXP3- (d36-42)
RA+ Treg (d11)
RA+ Treg NP (d17)
RA+ Treg Th17 (d17)
RA- Treg (d0)
FOXP3+ (d21-23)
FOXP3- (d21-23)
TH17
Transcription start site (TSS)
% CpG methylation
0
25
50
75
100
C
% CpG methylation
80
60
40
20
0
CD4+CD25- (d21-44)
RA+ Treg (d0)
FOXP3+ (d36-42)
FOXP3- (d36-42)
RA- Treg (d0)
FOXP3+ (d21-23)
FOXP3- (d21-23)
Th17
D
RORC / 18S RNA
1
0.1
0.01
0.001
*
**
0
14
36+
Culture period (d)
RA+ Treg
RA- Treg
E
RORC / 18S RNA
0.20
0.16
0.12
0.08
0.04
*
*
Medium
Mock
1
5
10
20
5-Aza-2'deoxycytidine (μM)
F
RLU
0
2
4
6
8
10
RORC1
RORC2
RORC3
RORC4
RORC5
pCpGL-P
*
*
*
mCpG
CpG

Figure 1:

DNA methylation status of the human *RORC* locus of Treg subpopulations. (**A**) Schematic presentation of analyzed cell types. For the generation of Th17 cells FACS-purified $CD4^+CD25^{int}CD45RA^-$ Tconv cells were polyclonally expanded, restimulated with PMA/ionomycin, intracellularly stained for IL-17 and the cytokine-positive fraction was isolated by FACS. Memory $CD4^+CD25^{high}CD45RA^-$ (RA-) and naïve $CD4^+CD25^{high}CD45RA^+$ (RA+) Treg cells from healthy donors were *in vitro* expanded as detailed in the 'Material and Methods' section before intracellular staining and FACS-based fractionation into $FOXP3^+$ and $FOXP3^-$ cells. Intact genomic DNA isolated from these cell populations was used for methylation analysis. (**B**) Schematic map of the human *RORC* locus (from the UCSC browser, http://genome.ucsc.edu/) with the following features from top to bottom: scale, conservation over 17 mammalian species, repeats, *RORC* gene structure and isoforms, regions cloned for enhancer reporter assays shown in (**F**) (blue boxes) and amplicons generated for methylation analysis by MALDI-TOF MS (black boxes). The methylation status of individual CpGs is shown in a heat map for the indicated cell types. In addition to the subpopulations detailed in (A), $CD45RA^+$ Treg were also analyzed after an *in vitro* expansion for 11d under non-polarizing culture conditions followed by an additional 6d culture period either under identical, non-polarizing conditions (RA+ Treg NP) or under Th17-polarizing conditions (RA+ Treg Th17). Each CpG is represented by a small square with methylation levels ranging from 0% (white) to 100% (dark blue) or not analyzed (grey). Data represent means of at least three independent experiments. (**C**) Overall CpG methylation status of the promoter region at the transcription start site (TSS) (R4 in Fig. 1B) of individual samples. Each box represents one donor and the black line displays the respective average. Significant differences exist between the following T cell populations: RA+ and RA- Treg/d0 ($P<0.001$), RA- Treg/d0 and $FOXP3^+$ RA- Treg/d21-23 ($P<0.001$), $FOXP3^+$ and $FOXP3^-$ RA- Treg/d21-23 ($P<0.001$), Th17 cells and all other populations except $FOXP3^+$ RA- Treg/d21-23 (all $P<0.005$; n=3-7; Student's *t*-test). (**D**) *RORC* mRNA expression of RA+ and RA- Treg directly after isolation (d0) and after *in vitro* expansion for the indicated time periods.. mRNA expression was measured by qRT-PCR and normalized to 18S rRNA expression. Data represent means + SD from n=4 (d0), n=8 (d14) and n=3 (d36+) independent cultures set up with cells from up to 8 different donors. Asterisks indicate significant differences between subpopulations (*$p<0.05$, **$p<0.01$, paired two-tailed Student's *t*-test). (**E**) *RORC* expression of $CD4^+CD25^-CD45RA^+$ T cells polyclonally activated for 5d in the presence of 0, 1, 5, 10 or 20 µM 5-Aza-2'deoxy-cytidine. *RORC* expression was measured via qRT-PCR and normalized to 18S RNA expression. Asterisks indicate significant differences between treatment groups (n=3; $p<0.05$, Student's *t*-test). (**F**) Several conserved regions of *RORC* (blue boxes in B) were cloned upstream of a basic EF1-promoter into the CpG-free luciferase vector pCpGL. The indicated plasmids were *in vitro Sss*I methylated or left unmethylated and subsequently transfected transiently into Jurkat T cells which were stimulated with TGFβ after transfection. Luciferase activity was normalized to a cotransfected *Renilla* construct and to the unmethylated "empty" control vector which harbors only the EF1-promoter (pCpGL-P). Asterisks indicate significant differences between methylated and unmethylated plasmids ($P < 0.05$, Student's *t*-test).

Several DMR in the RORC locus harbour newly identified methylation-dependent enhancer activity

To investigate whether the differential DNA methylation patterns found at the *RORC* locus of expanded RA+ and RA- Treg cells are functionally relevant, we initially treated $CD4^+CD25^-CD45RA^+$ naïve Tconv cells with 5-aza-2'deoxycytidine, a potent DNA methyl-transferase inhibitor. Treatment with the demethylating agent for five days led to a dose-dependent induction of *RORC* mRNA expression (Fig. 1E), indicating that *RORC* expression is regulated at least in part by DNA methylation. Next, we designed reporter constructs to test the DNA methylation-dependent ability of promoter-distal conserved regions (RORC1-5, positions are indicated in Fig. 1B as light blue boxes) to enhance the activity of a heterologous promoter and performed luciferase reporter assays in Jurkat T cells. As shown in Fig. 1F, three out of five promoter-distal regions significantly enhanced the activity of the basal (CpG-free) EF1 promoter (Klug and Rehli 2006). All regions lost enhancer activity when DNA was methylated, suggesting that their activity is critically dependent on their CpG methylation status, as previously observed for Treg and Tconv specific DMR at *FOXP3* and other loci (Schmidl et al. 2009).

IL-17 producers emerge predominantly among the subpopulation of RA- Treg cells with stable FOXP3 expression

The observed DNA methylation patterns suggested increased transcription of *RORC* especially in *in vitro* expanded FOXP3+ memory-type RA- Treg cells. Since it is difficult to obtain intact mRNA from intracellularly stained and sorted cells, we analyzed the impact of *ex vivo* expansion on the capacity of the various Treg populations to secrete IL-17, an important consequence of RORC expression and key characteristic of Th17 cells (Fig. 2). Fig. 2A provides a particularly distinctive example and Fig. 2C combined data regarding the proportion of IL-17 producers among the respective Treg cell populations as determined by simultaneous intracellular staining for FOXP3 and IL-17 after 5h PMA/ionomycin stimulation. The results demonstrate that the ability to produce IL-17 was most pronounced in the $FOXP3^+$ subpopulation of *in vitro* expanded RA- Treg cells (Fig. 2A & C), which correlates with the extensive DNA demethylation seen at the promoter region as well as in several other DMRs across the *RORC* locus in these cells. In contrast, RA+ Treg cells maintained FOXP3 expression to a large extent (Fig. 2B) and showed no or only a marginal tendency to secrete IL-17, even after repetitive *in vitro* stimulation (Fig. 2C). Similar differences were observed between freshly isolated as well as *in vitro* expanded naive and memory-type Tconv cells (Suppl. Fig. S2D).

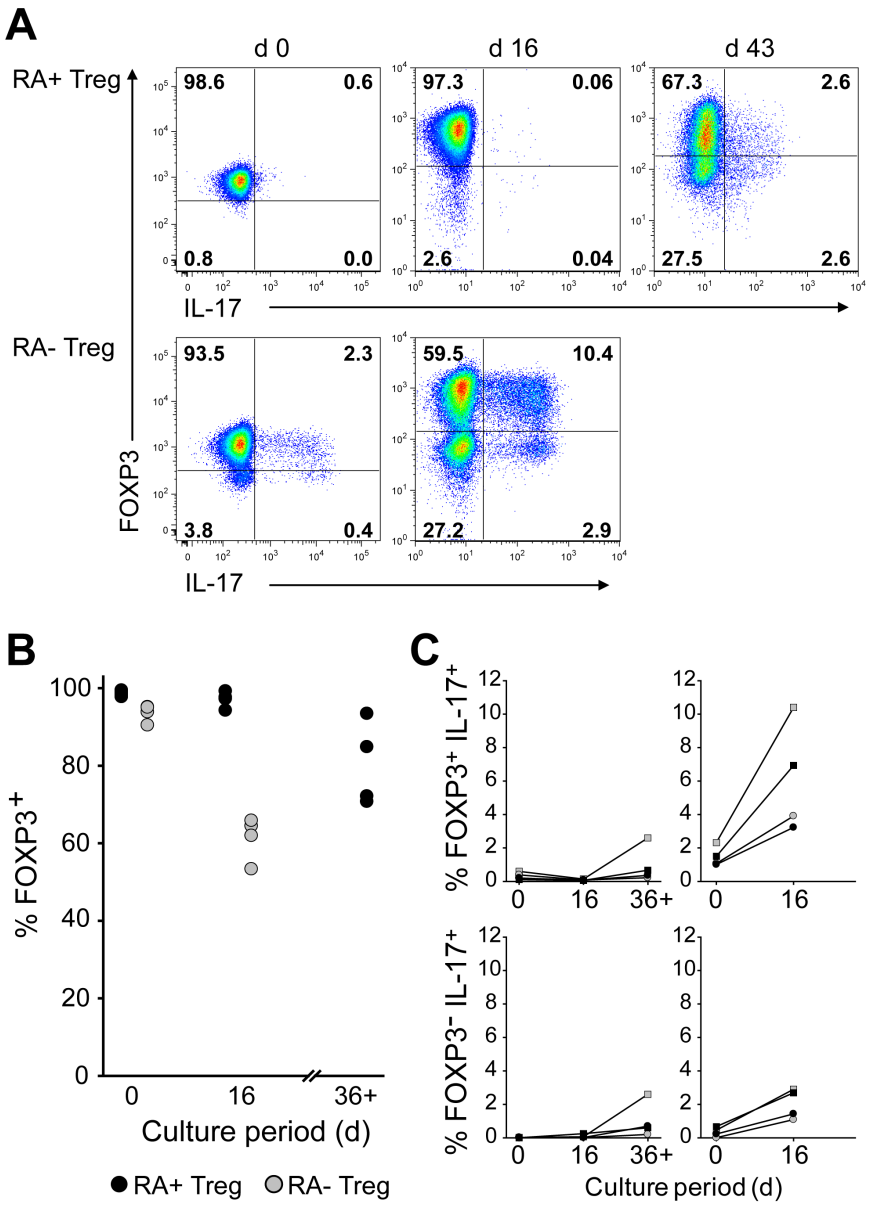

Figure 2:

Emergence of FOXP3⁺ and FOXP3⁻ IL17-producers in naïve and memory Treg cell cultures. CD45RA⁺ (naïve) and CD45RA⁻ (memory) Treg cells were sorted from PBMC and cultured as detailed in the 'Material and Methods' section. Freshly sorted or *in vitro* expanded cells were stimulated with PMA/ionomycin for 5h followed by simultaneous intracellular staining for FOXP3 and IL-17. A particularly distinctive example (**A**) and combined data of FOXP3 expression (**B**) and proportion of FOXP3⁺IL-17⁺ and FOXP3⁻IL-17⁺ cells (**C**) in 4 different naïve (RA⁺) or memory (RA⁻) Treg cultures from 4 different donors. RA+ Treg cells had to be kept in culture for at least 36d and restimulated at least 5 times before downregulating FOXP3. RA- Treg were kept for a maximum of 16 d.

CONCLUDING REMARKS

In conclusion, we show that *ex vivo* expansion of natural CD45RA$^-$ memory-type Treg cells even under neutral, non-Th17-polarizing culture conditions results in the epigenetic reprogramming of their *RORC* locus and the development of Th17-like cells. In sharp contrast, naïve Treg cells do not show this tendency during *in vitro* culture. It is unknown to date to which extent conversion of Treg cells can occur after adoptive transfer in patients, especially under inflammatory conditions. However, their well-documented molecular and functional stability during *in vitro* culture clearly favours the use of CD45RA$^+$ naïve Treg cells for future clinical applications.

MATERIALS AND METHODS

Cell purification and culture

PBMCs were isolated from leukapheresis products of healthy volunteers (approved by the local Ethics committee and with their informed consent) by density gradient centrifugation. $CD4^+CD25^{high}CD45RA^+$ naïve Treg cells, $CD4^+CD25^{high}CD45RA^-$ memory Treg cells and $CD4^+CD25^-$ Tconv cells were isolated by FACS (BD FACSAria, BD Biosciences, Heidelberg, Germany) and expanded *in vitro* as described previously (Hoffmann et al. 2004; Hoffmann et al. 2006b). In brief, T cells were cultured on irradiated, huCD32-expressing L929 cells with anti-CD3 (OKT3; Orthoclone®, Ortho Biotech (Neuss, Germany)) and anti-CD28 antibodies (CD28.2, BD Biosciences; 100 ng/mL each) in the presence of high-dose IL-2 (Proleukin®, Chiron, Amsterdam, Netherlands; 300 U/mL) and restimulated weekly. Cultures were continued until a $FOXP3^-$ subpopulation became detectable, rested for 4d in medium with IL-2, stained for FOXP3 and sorted into $FOXP3^+$ and $FOXP3^-$ cells by FACS. A representative example of the gating strategy for sorting is provided in Supplementary Fig. S1. For the generation of highly purified Th17 cells, FACS-purified $CD4^+CD25^{int}CD45RA^-$ ($FOXP3^-$) T cells were cultured for 11d as detailed above, rested for 2d and re-stimulated for 5h with 20 ng/ml PMA/1 µM ionomycin in the presence of GolgiStop (BD Biosciences). Cells were intracellularly stained with AF488-conjugated anti-human-IL-17A (64DEC17; eBioscience) and $IL\text{-}17A^+$ cells were purified by FACS.

Th17 polarization of in vitro *expanded T cells*

Th17 polarization was carried out according to Manel et al. (Manel et al. 2008) with minor modifications. T cell populations were harvested on d11 of *in vitro* expansion under non-polarizing conditions and further cultured for additional 6 days either under the same conditions (as described above) or in the presence of recombinant human IL-1β (10 ng/ml), recombinant human IL-23 (10 ng/ml; both R&D Systems, Wiesbaden-Nordenstadt, Germany), anti-human IL-4 antibodies (functional grade purified, 1 µg/ml), anti-human IFN-γ antibodies (functional grade purified, 1 µg/ml; both eBioscience) and recombinant human TGF-β1 (10 ng/ml; PeproTech, Hamburg, Germany) for Th17 polarization.

Simultaneous FOXP3 and cytokine detection

Treg cells were harvested from cultures and rested for 4d in medium with IL-2 (300 U/mL) before stimulation with PMA/ionomycin in the presence of GolgiStop for 5h as detailed above.

Simultaneous intracellular staining for FOXP3 and IL-17 was performed according to the manufacturers' instructions using the FOXP3 staining buffer set (eBioscience, San Diego, CA), PE-, APC- or Pacific Blue-labelled anti-human-FOXP3 (PCH101) and AF488- or APC-labelled anti-human-IL-17A (eBio64DEC17) (all from eBioscience).

DNA demethylation with 5-Aza-2'deoxycytidine

Sorted CD4+CD25-CD45RA+ T cells were stimulated with anti CD3/CD28-coated beads (T cell expander Dynabeads®, Invitrogen, Darmstadt, Germany) for 5d in the presence of varying concentrations of 5-Aza-2'deoxycytidin (Sigma Aldrich, Munich, Germany).

Preparation of RNA and DNA and quantitative RT-PCR

Genomic DNA for DNA methylation analysis from fixed and FACS™-purified cells was extracted and quality-controlled as described recently (Hansmann et al. 2010) and outlined in the Supplementary Material. Genomic DNA from unfixed cells was isolated using the DNeasy blood and tissue kit (Qiagen, Hilden, Germany). Total cellular RNA was isolated using the RNeasy Kit (Qiagen) including DNase digestion and qRT-PCR for RORC expression was performed using primer sequences listed in Supplementary Table S1.

Mass spectrometry analysis of bisulfite-converted DNA

MALDI-TOF MS analysis and sodium bisulfite conversion were performed as previously published (Ehrich et al. 2005; Schmidl et al. 2009) (for details see the Supplementary Material). Methylation ratios were determined from mass spectra using the Epityper software v1.0 (Sequenom®). Methylation values indicated in the heatmap in this manuscript are average values of at least three independent experiments. PCR primers were designed using the Methprimer (Li and Dahiya 2002) web tool (http://www.urogene.org/methprimer/).

Reporter assays.

Putative enhancer regions were cloned directly into the CpG-free pCpGL-CMV/EF1 vector (Klug and Rehli 2006) replacing the CMV enhancer with the PCR-amplified region (Primer sequences see Supplementary Table S1), *SssI* methylated *in vitro* or left unmethylated, and DEAE-transfected in Jurkat cells as previously described (Schmidl et al. 2009). Following transfection,

cells were either left untreated or stimulated with TGFβ (PeproTech EC, London, 10 ng/ml over night plus 10 ng/ml added the next morning for additional 5h). Cell lysates were assayed for firefly and *Renilla* luciferase activities using the Dual-Luciferase Reporter Assay System (Promega, Mannheim, Germany) on a Lumat LB9501 (Berthold Detection Systems GmbH, Pforzheim, Germany). Firefly luciferase activity of individual transfections was normalized against *Renilla* luciferase activity.

Statistical analysis

Differences in DNA methylation and mRNA expression between the various T cell populations as well as in the number of IL-17 producing cells per culture or subpopulation and in enhancer activity of selected putative enhancer regions were analyzed using the two-tailed Student's *t*-test. Where applicable, a paired two-tailed Student's *t*-test was performed. *P*-values of less than 0.05 were considered significant.

ACKNOWLEDGMENTS

We thank Rüdiger Eder, Jasmin Stahl and Irene Ritter for excellent cell sorting and technical support. This study was supported by research funding from the German Research Society (KFO 146) to ME, MR and PH, from the Bavarian Immunotherapy Network to ME and from the José Carreras Foundation (FACS facility).

CONFLICTS OF INTEREST

The authors declare no financial conflicts of interest.

Copyright

Figures and Text from chapter 3.3 are taken from: Christian Schmidl, Leo Hansmann, Reinhard Andreesen, Matthias Edinger, Petra Hoffmann, Michael Rehli. "Epigenetic reprogramming of the RORC locus during in vitro expansion is a distinctive feature of human memory but not naïve Treg cells". 2010. European Journal of Immunology 40(5): 1510-1512. (pre-peer reviewed version)

The final version of this article was published at:

http://onlinelibrary.wiley.com/doi/10.1002/eji.201041067/abstract

Copyright Wiley-VCH Verlag GmbH & Co. KGaA. Reproduced with permission.

Supplementary Information

Supplementary Methods:

Preparation of RNA and DNA and quantitative RT-PCR

Genomic DNA for DNA methylation analysis from fixed and FACS™-purified cells was extracted and quality-controlled as described recently (Hansmann et al. 2010). In brief up to 2.5 x 10^6 FACS-sorted cells were resuspended in 300 µl lysis-buffer containing 100 mM NaCl (C. Roth GmbH, Karlsruhe, Germany), 10 mM Tris HCl (Roth), 50 mM EDTA (Merck KGaA, Darmstadt, Germany), 0.5% SDS (Roth), 0.1 mg/ml proteinase K (Roche Diagnostics GmbH, Mannheim, Germany), 20 µg/ml RNase A (Qiagen GmbH, Hilden, Germany) and the pH was adjusted to 8.0 with NaOH (Roth). The lysate was incubated on a thermoshaker at 60°C for approximately 24 h. Then, 300 µl phenol were added and mixed rapidly. After centrifugation at 3,400 x g for 5 min at 4°C, the aqueous (upper) phase was transferred into a new tube and 900 µl of 95% ethanol (Mallinckrodt Baker, Deventer, The Netherlands), 0.12 M sodium acetate (Merck) were added. After vigorous mixing, DNA precipitated and became visible. After incubation for at least 20 min at -20°C, DNA was pelleted for 15 min at 13,700 x g at 4°C and washed with 600 µl 70% Ethanol for 5 min at RT. After centrifugation for 15 min at 13,700 x g at 4°C the supernatant was completely removed and DNA was dried for 10 min at RT or at 60°C to remove residual ethanol. Finally, DNA was dissolved in 100 µl TE-buffer (Qiagen) for approximately 24 h on a shaker at 60°C and another 24 h at 4°C. DNA content and purity were measured using the NanoDrop 1000 spectrometer (NanoDrop Technologies, Wilmington, USA). Fragment length of the obtained DNA was determined by 0.5 % Agarose gel-electrophoresis and ethidiumbromide stained gels were scanned on a Typhoon 9200.

Mass spectrometry analysis of bisulfite-converted DNA

MALDI-TOF MS analysis and sodium bisulfite conversion were performed as previously published (Ehrich et al. 2005; Schmidl et al. 2009). Sodium bisulfite conversion was performed using the EZ DNA methylation kit (Zymo Research, Orange, CA) using 1 µg of genomic DNA and an alternative conversion protocol. The incubation parameters where changed as follows: 95°C for 30 sec, 50°C for 15 min (repeated for 20 cycles). PCR amplification of target regions was followed by SAP treatment, reverse transcription and subsequent RNA base-specific cleavage

(MassCLEAVE™, Sequenom®, San Diego, CA) as previously described. Cleavage products were loaded onto spectroCHIPs (Sequenom®) and analysed by MALDI-TOF mass spectrometry (MassARRAY™ Compact MALDI-TOF, Sequenom®). Methylation ratios were determined from mass spectra using the Epityper software v1.0 (Sequenom®). Methylation values indicated in the heatmap in this manuscript are average values of at least three independent experiments. PCR primers were designed using the Methprimer (Li and Dahiya 2002) web tool (http://www.urogene.org/methprimer/).

Supplementary Figures

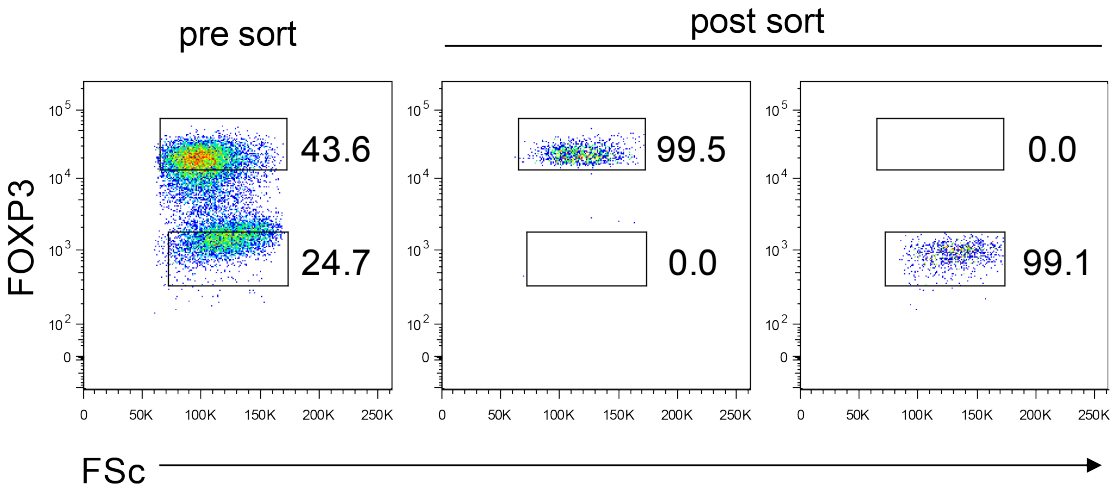

Supplementary Figure S1

Representative example of the gating strategy used to sort *in vitro* expanded RA$^-$ Treg cells into a FOXP3$^+$ and a FOXP3$^-$ cell fraction before isolation of genomic DNA for methylation analysis. Purity of the sorted cells was reproducibly >95%

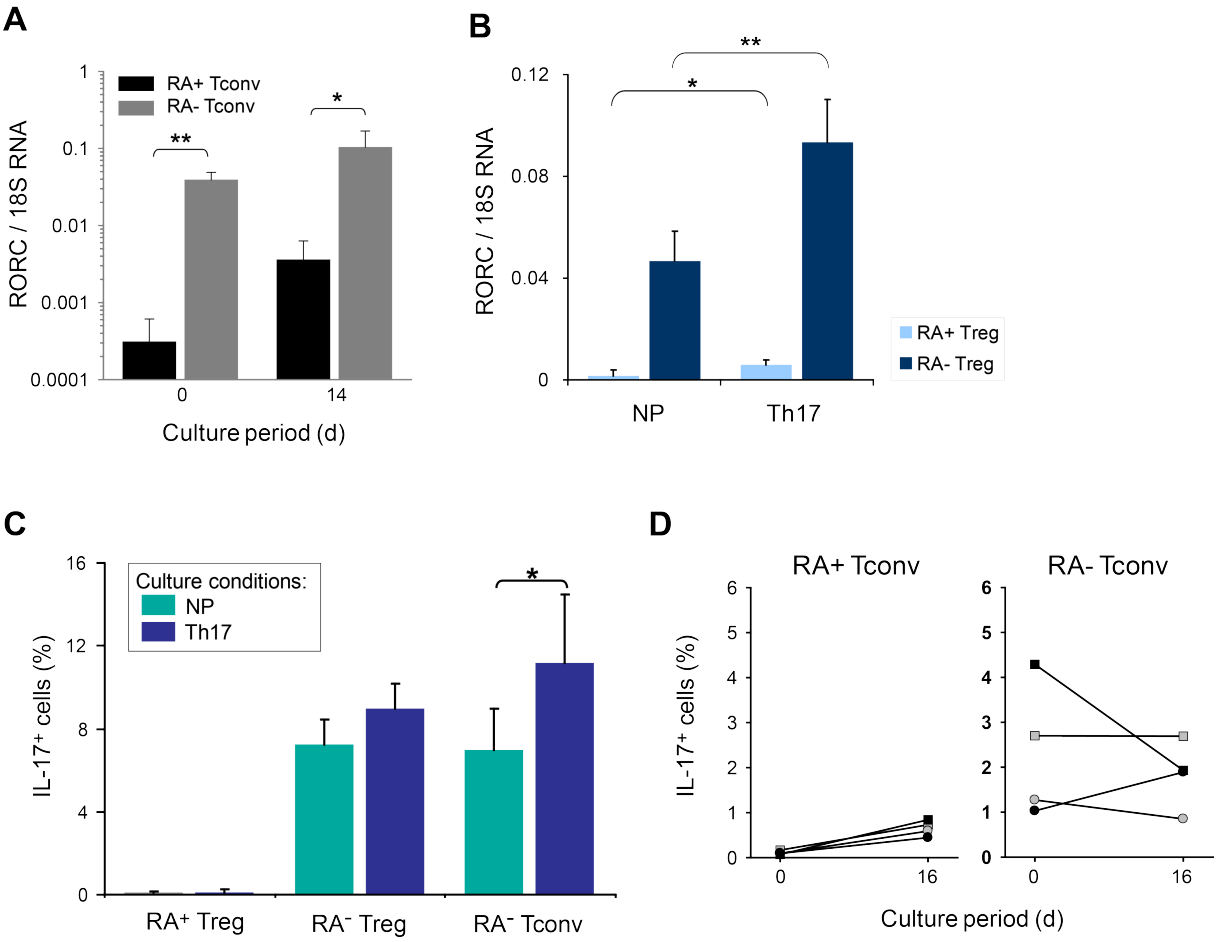

Supplementary Figure S2: RA+ Treg do not convert into Th17 cells under Th17-polarizing culture conditions. (A) CD45RA$^+$ (naïve) and CD45RA$^-$ (memory) CD4$^+$CD25$^-$ Tconv cells were sorted from PBMC and cultured for 14d under non-polarizing conditions as detailed in the 'Material and Methods' section. *RORC* mRNA expression of freshly sorted (d0) or *in vitro* expanded and rested cells (d14) was analyzed by qRT-PCR and normalized to 18S rRNA expression. Data represent means + SD of n=4 independent cultures set up with cells from 4 different donors. Asterisks indicate significant differences between subpopulations (*p<0.05, **p<0.01, paired two-tailed Student's t-test). (B) *RORC* mRNA expression in CD45RA$^+$ and CD45RA$^-$ Treg after *in vitro* expansion for 11d under non-polarizing culture conditions followed by an additional 6d culture period either under identical, non-polarizing conditions (NP) or under Th17-polarizing conditions (Th17). *RORC* mRNA expression was measured by qRT-PCR and normalized to 18S rRNA expression. (C) IL-17-producing cells among CD45RA$^+$ and CD45RA$^-$ Treg cultured as detailed in (B) and stimulated with PMA/ionomycin in the presence of GolgiStop for an additional 5 h. IL-17-producing cells were determined by intracellular staining. CD4$^+$CD25$^-$CD45RA$^-$ Tconv cells (RA$^-$ Tconv) were cultured in parallel as internal control. Data in (B) and (C) represent means + SD of n=4 independent cultures established with cells from 4 different donors. Asterisks indicate significant differences between treatment groups (* p<0,05; **p<0.01; paired two-sided Student's t-test).

3.4 Dominant Th2 differentiation of human regulatory T cells upon loss of FOXP3 expression

Published in: Journal of Immunology. 2012 Feb 1;188(3):1275-82. Epub 2011 Dec 30.

PMID: 22210907

Christian Schmidl performed gene expression and western blot experiments, analyzed data and contributed to manuscript writing

Dominant Th2 differentiation of human regulatory T cells upon loss of FOXP3 expression

Short title: Dominant Th2 differentiation of human Treg

Leo Hansmann, Christian Schmidl, Janina Kett, Lena Steger, Reinhard Andreesen, Petra Hoffmann, Michael Rehli*, Matthias Edinger*

Department of Hematology & Oncology, University Hospital Regensburg, 93053 Regensburg, Germany

*Corresponding Authors:

Matthias Edinger, MD
Department of Hematology & Oncology
University Hospital Regensburg
Franz-Josef-Strauss-Allee 11
D-93053 Regensburg
Germany
phone: +49 (0)941-944 5580
FAX: +49 (0)941-944 5581
matthias.edinger@klinik.uni-regensburg.de

Michael Rehli, PhD
Department of Hematology & Oncology
University Hospital Regensburg
Franz-Josef-Strauss-Allee 11
D-93053 Regensburg
Germany
phone: +49 (0)941-944 5587
FAX: +49 (0)941-944 5593
michael.rehli@klinik.uni-regensburg.de

ABSTRACT

$CD4^+CD25^+FOXP3^+$ regulatory T cells (Treg) are pivotal for peripheral self-tolerance. They prevent immune responses to auto- and alloantigens and are thus under close scrutiny as cellular therapeutics for autoimmune diseases and the prevention or treatment of alloresponses after organ or stem cell transplantation. We previously showed that human Treg cells with a memory cell phenotype, but not those with a naïve phenotype, rapidly down-regulate expression of the lineage-defining transcription factor forkhead box P3 (FOXP3) upon in vitro expansion. We now compared the transcriptomes of stable $FOXP3^+$ Treg and converted $FOXP3^-$ 'ex-Treg' cells by applying a newly developed intranuclear staining protocol that permits the isolation of intact mRNA from fixed, permeabilized and FACS-purified cell populations. Whole genome microarray analysis revealed strong and selective upregulation of Th2 signature genes, including GATA-3, IL-4, IL-5 and IL-13, upon downregulation of FOXP3. Th2 differentiation of converted, $FOXP3^-$ ex-Treg cells occurred even under non-polarizing conditions and could not be prevented by IL-4 signaling blockade. Thus, our studies identify Th2 differentiation as the default developmental program of human Treg cells after downregulation of FOXP3.

INTRODUCTION

Natural regulatory T cells (Treg) are indispensable for the maintenance of dominant self-tolerance and can suppress the activation, proliferation and effector function of a wide range of immune cells, including $CD4^+$ and $CD8^+$ T cells, natural killer and natural killer T cells, B cells and antigen presenting cells. They are thymus-derived and characterized by the expression of CD4, CD25 and the transcription factor forkhead box P3 (FOXP3) (Sakaguchi et al. 2008). FOXP3 is pivotal for the development and function of Treg and loss of function mutations of *FOXP3* cause lethal autoimmune syndromes in mice and man (Brunkow et al. 2001; Wildin et al. 2001). During Treg development and in mature peripheral Treg, FOXP3 represses many inflammation-associated genes but also positively induces a gene expression profile that supports Treg function (Hill et al. 2007; Zheng et al. 2007). This Treg profile seems to depend on the strength and stability of FOXP3 expression, as Treg function is partially lost in genetically modified mice that express only low Foxp3 levels (Wan and Flavell 2007). The stability of FOXP3 expression is in parts regulated by epigenetic mechanisms, as shown by the differential DNA methylation pattern of the *FOXP3* locus and differential histone modifications in Treg and conventional $CD4^+$ T cells (Baron et al. 2007; Kim and Leonard 2007; Miyara et al. 2009; Schmidl et al. 2009; Wei et al. 2009). Recent studies employing conditional *Foxp3* knock-out mice revealed that peripherally induced suppressor cell populations do not compensate for the lack of Treg (Kim et al. 2007; Kim et al. 2009). Thus, thymus-derived Treg are crucial for the preservation of peripheral tolerance and their adoptive transfer is a promising strategy for the treatment of inflammatory bowel disease (Mottet et al. 2003), autoimmunity (Brusko et al. 2008; Miyara et al. 2009) and the prevention of alloresponses after solid organ (Nadig et al. 2010) or stem cell transplantation (Hoffmann et al. 2002a; Edinger et al. 2003; Di Ianni et al. 2011b). For such applications, we previously described culture methods that permit the 100- to 1000-fold expansion of human Treg *in vitro* within two to three weeks (Hoffmann et al. 2004; Hoffmann et al. 2006b). Yet, we and others reported that Treg selected on the basis of a $CD4^+CD25^{high}CD127^{low/neg}$ phenotype were heterogeneous with respect to the frequency of $FOXP3^+$ cells after *in vitro* expansion and we confirmed the down-regulation of FOXP3 in Treg clones (Hoffmann et al. 2009). The loss of FOXP3 was almost exclusively confined to $CD45RA^-$ memory-type Treg, while $CD45RA^+$ naive Treg homogeneously maintained FOXP3 expression even after three weeks in culture (Hoffmann et al. 2006b; Miyara et al. 2009). Based on these findings, we suggested selecting $CD45RA^+$ Treg for the generation of Treg products for clinical trials, while the fate of $CD45RA^-$ Treg after *in vitro* stimulation required further clarification. For this purpose, we now developed new methods that permit the isolation of intact mRNA from fixed, permeabilized and FOXP3-stained, FACS-

sorted cells to compare the differential gene expression profiles in converted vs. stable Treg using whole genome microarrays. We found that Treg rapidly and strongly upregulate Th2 genes upon loss of FOXP3 expression. These findings were confirmed on protein level as converted Treg secrete high amounts of IL-4, IL-5 and IL-13, but hardly any Th1 or Th17 cytokines. Thus, using new technologies that permit the examination of human Treg with the same accuracy as in murine Foxp3-reporter models, we now demonstrate the dominant conversion of human Treg into Th2 cells upon *in vitro* stimulation. These findings are highly relevant for researchers planning adoptive cell therapies with *in vitro* expanded Treg.

MATERIAL AND METHODS

Isolation and cultivation of human Treg

PBMC were isolated from leukapheresis products of healthy volunteers (approved by the Ethics committee and after their informed consent) by density gradient centrifugation. $CD4^+CD25^{high}CD45RA^+$ "naïve" and $CD4^+CD25^{high}CD45RA^-$ "memory" Treg were purified by FACS (BD FACSAria, BD Biosciences, Heidelberg, Germany) from MACS (Miltenyi Biotec, Bergisch Gladbach, Germany) pre-enriched $CD25^+$ cells. Treg were cultured for 11d on $huFcgR^+$ murine feeder cells (L929 cells) with anti-CD3 and anti-CD28 antibodies in the presence of IL-2 (300 U/ml) and rested for additional 3-4 d in medium with IL-2, as described before (Hoffmann et al. 2006b; Hoffmann et al. 2011). For inhibition of IL-4 signaling, anti-IL-4- (clone MP4-25D2, 1 µg/ml; eBioscience, San Diego, CA;), anti IL-4R- (clone 25463, 500 ng/ml; R&D Systems, Minneapolis, MN) or both antibodies were added during expansion and resting.

Intranuclear FOXP3 staining for subsequent RNA extraction ('ethanol/tryptone method')

Surface staining of CD4 (FITC-conjugate; BD Biosciences) was carried out in PBS/2 % FCS. For FOXP3 staining and subsequent RNA extraction, PBS with 2 % tryptone (Roth, Karlsruhe, Germany) and 0.1 % DEPC (Roth) was used. The buffer was autoclaved, cooled to 4°C and used for all washing and incubation steps throughout the procedure except otherwise stated. Following surface staining, cells were washed once, resuspended on a vortex in ice-cold 70 % ethanol (up to 7 x 10^7 cells in 2 ml) and fixed for 15 min at -20°C, then washed twice and resuspended in 1 ml tryptone/DEPC buffer containing 20 µl rat serum (eBioscience) and 20 µl recombinant RNasin® ribonuclease inhibitor (20-40 U/µl; Promega, Madison, WI, USA). After 5 min incubation at 4°C, 50 µl anti-human FOXP3 (APC-conjugate, clone PCH101, eBioscience) were added and cells were incubated for another 25 min at 4°C in the dark. Cells were washed, resuspended at 1 x 10^7 cells/ml and FACS-sorted into tryptone/DEPC buffer. RNA was extracted immediately and its integrity checked with the RNA 6000 Nano Kit on an Agilent Bioanlayzer (Agilent, Böblingen, Germany).

Transcription factor and intracellular cytokine staining

Cells were stimulated for 5h with PMA (20 ng/ml)/ionomycin (1 µM) in the presence of GolgiStop (BD Biosciences) and stained using the FOXP3 staining buffer set (eBioscience, Frankfurt, Germany) and the following anti-human antibodies: FOXP3 (PE-, eFluor450- or APC-conjugated, clone PCH101), IL-4 (APC- or AF488-conjugated, clone 8D4-8), IL-5 (PE-conjugated, clone TRFK5), IL-13 (FITC-conjugated, clone PVM13-1), IL-17A (FITC- or APC-conjugated, clone

eBio64DEC17), all from eBioscience, IFN-γ (FITC-, PE- or APC-conjugated, clone B27, BD Biosciences), IL-10 (AF488- or APC-conjugated, clone JES3-9D7, eBioscience or clone JES3-19F1, BD Biosciences), anti-mouse/human GATA-3 (PE-conjugated, clone TWAJ) and anti-mouse/human T-bet (AF647-conjugated, clone eBio4B10), both from eBioscience. Data were acquired on a BD LSRII or FACSCalibur (BD Biosciences) and analyzed with FlowJo software (Treestar Inc, Ashland, OR, USA).

RNA extraction

RNA was isolated from FACS sorted cells using the RNeasy Micro Kit (Qiagen, Hilden, Germany) or TRizol® Reagent (Invitrogen, Darmstadt, Germany). When RNA was extracted from less than 1 x 10^6 cells, glycogen (Roche GmbH, Mannheim, Germany) was added during the TRizol® procedure.

Microarray analysis of gene expression

RNA preparations from FOXP3-sorted $CD4^+CD25^{high}CD45RA^-$ Treg from five donors were analyzed using Whole Human Genome Oligo Microarrays (Agilent). Labeling and hybridization were performed using the Agilent Gene Expression system according to the manufacturer's instructions. In brief, 50 to 200 ng of high-quality RNA were amplified and Cyanine 3-CTP labeled with the One Color Low Input Quick Amp Labeling Kit (Agilent). Sixhundred ng labeled cRNA were fragmented and hybridized on the Whole Human Genome Expression Array G4851A (8x60K, Agilent). Images were scanned using a DNA microarray scanner, processed using Feature Extraction Software and further analyzed using GeneSpring GX (all from Agilent). Fluorescence signals were normalized to the 75^{th} percentile and baseline transformed to the median of all samples. Features were discarded which did not have a minimum raw expression-value of 40 in at least 3 out of 10 samples. Different microarray probes covering the same gene were combined using the gene-level technology of the GeneSpring GX software. Expression data for the donor-matched comparisons of variance (Supplemental Fig. 2) were percentile normalized as above, but not baseline transformed. Microarray data are available from the NCBI/GEO repository (GSE26190;
http://www.ncbi.nlm.nih.gov/geo/query/acc.cgi?token=zfsphaacqwosqds&acc=GSE26190).

Quantitative RT-PCR

RNA was transcribed into cDNA with Reverse Transcriptase (Promega) and analyzed on an Eppendorf Realplex4 S Cycler. Messenger RNA expression levels were normalized to *Beta-2-Microglobulin* (*B2M*) or 18S RNA. Primer sequences are listed in Supplemental Table 1.

Western blot analysis

For preparation of whole cell extracts 1-5 x 10^6 cells were washed with PBS, pelleted, dissolved in 100 µl of 2x SDS sample buffer with complete protease- and phosphatase inhibitors (Roche) per 5 x 10^6 cells , heated at 95°C for 10 min and vortexed for 1 min. For western blots, equivalents of 0.5-0.75 x 10^6 cells were separated by SDS-PAGE and blotted on PVDF membranes, followed by blocking (1 h at RT withTris-buffered saline/5 % milk powder/0.1 % Tween 20) and probing with polyclonal rabbit anti-human STAT6 (#9362; Cell Signaling Technology, Frankfurt, Germany) or anti-human phospho-STAT6 antibodies (Tyr641, #9361, Cell Signaling Technology) at 4°C overnight. Blots were washed and incubated with alkaline phosphatase-conjugated goat anti-rabbit antibody (Dako Cytomation, Hamburg, Germany). Bands were visualized with ECL solution on Hyperfilm, scanned using a Molecular Dynamics personal densitometer SI and quantified with ImageQuant 5.2 (all from GE Healthcare).

Cytokine detection in culture supernatants

Supernatants were collected on d 11 of Treg cultures. Concentrations of IL-4, IL-5, IL-13, IL-10, IL-17 and IFN-γ were determined using Cytokine Bead Array Flex-Sets (BD Bioscience) according to the manufacturer's instructions.

Statistical analysis

Statistical significance was determined by paired or unpaired two-tailed Student's *t*-test, as indicated in figure legends. A p-value ≤ 0.05 was considered significant.

RESULTS

Isolation of intact RNA from FACS-sorted cells after intranuclear FOXP3 staining

There is increasing evidence for plasticity within the Treg lineage, which includes the loss of FOXP3 and the conversion of Treg into potentially pro-inflammatory T helper cell subsets (Xu et al. 2007; Komatsu et al. 2009; Zhou et al. 2009c; Schmidl et al. 2011). The study of gene expression patterns in FOXP3-losing Treg could extend our understanding of this plasticity and reveal the underlying molecular mechanisms. However, paraformaldehyde (PFA) contained in commercially available FOXP3 staining kits induces conformational changes and covalent as well as non-covalent cross-links in nucleic acids and proteins and thus impedes the subsequent extraction of intact RNA. We therefore established an alternative FOXP3 staining method using 70 % ethanol for fixation and permeabilization that does not induce such cross-links and thus allows the extraction of intact high-quality RNA. Staining for FOXP3 and subsequent flow cytometric sorting was carried out in tryptone- and RNase inhibitor-containing PBS. Both additives were essential for maintaining RNA integrity during the staining and sorting procedure. The frequencies of $FOXP3^+$ cells among *in vitro* expanded $CD45RA^-$ Treg detected with this protocol were comparable to those obtained with a commercial FOXP3 staining kit (Fig. 1A; divergence ranged from -10.6 % to + 5.7 %; n=4). FACS-separated populations routinely showed > 95 % purity upon re-analysis (96.9 ± 1.2 % for $FOXP3^+$ and 98.1 ± 0.9 % for $FOXP3^-$ cells, respectively, n=5; see also Supplemental Fig. 1). RNA extracted from sorted cells displayed little or no signs of degradation (Fig. 1B) and mean RNA integrity numbers (RIN) (Schroeder et al. 2006) were 7.9 (range: 7.3-9.0; n=14) in fixed samples and 9.4 (range:9.2-9.5; n=5) in unfixed controls. RNA yield and quality depended on the time span between fixation and cell lysis for RNA extraction: best results were obtained by keeping preparation times short and samples cold and RNase-free. Thus, this PFA-free FOXP3 staining protocol (referred to as "ethanol/tryptone method") allowed the reliable extraction of largely intact RNA from intranuclearly stained and FACS-sorted cells.

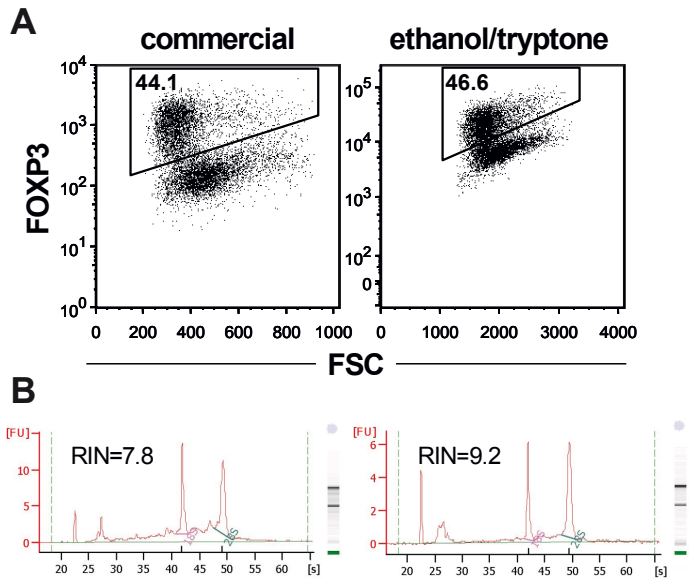

Figure 1

Isolation of intact RNA from human T cells after intranuclear staining for FOXP3

(A) *In vitro* expanded CD45RA$^-$ Treg were stained for FOXP3 using either a commercially available FOXP3 staining kit (left) or the ethanol-tryptone method (right). Plots are representative of n=4 independent experiments. Numbers indicate percentages of cells. **(B)** Electropherograms of RNA extracted from expanded human CD45RA$^-$ Treg. Cells were either stained for FOXP3 using the ethanol/tryptone method and separated by FACS (left; FOXP3$^-$ population; representative of n=14 independent RNA preparations) or remained unfixed before RNA extraction (right; representative of n=5 independent preparations). RIN: RNA Integrity Number.

In vitro expanded CD45RA$^-$ Treg show a Th2 gene expression signature upon loss of FOXP3 expression

We previously showed that FOXP3 expression is primarily lost in CD45RA$^-$ "memory" Treg after *in vitro* stimulation (Hoffmann et al. 2006b; Hoffmann et al. 2009). To analyze the fate of FOXP3-losing memory Treg on the level of gene expression, FACS-sorted CD4$^+$CD25^{high}CD45RA$^-$ Treg were *in vitro* expanded and subsequently sorted into FOXP3$^+$ and FOXP3$^-$ populations applying the ethanol/tryptone method. RNA was extracted and analyzed using whole genome expression microarrays. Combined results of five independent experiments are presented as heatmaps for selected gene classes in Fig. 2A. Detailed mRNA expression levels of individual cell cultures can be found in Supplemental Fig. 2.

As expected, we observed significantly higher mRNA levels of Treg signature genes (e.g. *FOXP3, CTLA4, IL2RA*) in the FOXP3$^+$ as compared to the corresponding FOXP3$^-$population. Yet surprisingly, a dramatic increase of Th2 cytokine mRNA (*IL4, IL5, IL13*) was detected in FOXP3$^-$ cells, but no significant difference between the two subpopulations with respect to other Th cell lineage- and inflammation-associated cytokine genes (*IFNG, IL6, IL9, IL10, IL12, IL17, IL21, IL23, IL24*). Likewise, key transcription factors for Th2 differentiation, namely *GATA3 and GFI1*, showed a significantly higher expression in FOXP3$^-$ cells, whereas the genes *RORC* and *STAT1,* responsible for Th17 and Th1 lineage commitment, respectively, were suppressed. In addition, FOXP3$^-$ cells highly expressed *GPR44*, also known as *CRTH2*, which encodes the Th2 cell-specific G protein-coupled receptor CD294 (Cosmi et al. 2000) (Fig. 2A). Thus, the FOXP3$^-$ population showed a gene signature dominated by Th2 lineage-associated genes including cytokines, transcription factors, signaling molecules and cell surface receptors.

Since STAT6 is critically involved in IL-4-induced Th2 development (Kaplan et al. 1996), we also asked whether the expression of typical STAT6 target genes (including *LTB, SOCS1, IRF8*) would be altered during Treg conversion. Interestingly, their expression levels were not significantly different between FOXP3$^+$ and FOXP3$^-$ populations, neither was that of *MAF* encoding a trans-activator of the IL-4 gene (Lin et al. 2010a).

Microarray data were validated at the single gene level using qRT-PCR (Fig. 2B). As controls, RNA isolated from *in vitro* expanded, FOXP3-stained and sorted CD45RA$^+$ Treg as well as from expanded bulk CD45RA$^-$ Treg without prior fixation were analyzed (Fig. 2B). As expected, FOXP3$^+$ cells from cultures of CD45RA$^-$ and CD45RA$^+$ Treg showed comparably high *FOXP3* and low *GATA3* mRNA expression. When total CD45RA$^-$ unfixed cells were compared to ethanol/tryptone-fixed subpopulations, they mainly showed intermediate mRNA expression, confirming the reliability of the RNA preparation procedure (Fig. 2B). Taken together, the gene expression profile of FOXP3$^-$ cells developing from initially FOXP3$^+$ CD45RA$^-$ Treg upon *in vitro* stimulation indicated Th2 differentiation.

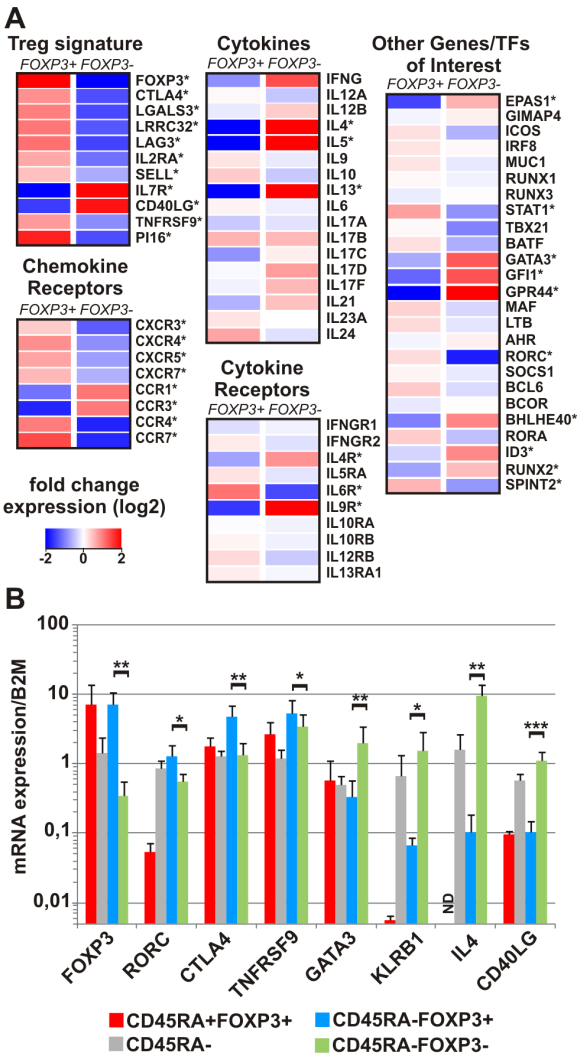

Figure 2: Transcriptome analysis of human FOXP3-sorted CD45RA⁻ Treg (**A**) Relative gene expression levels of selected gene classes of FOXP3-sorted CD45RA⁻ Treg of five independent donors (microarray data normalized to the median of all samples) are presented in heatmaps by a pseudo-color scale as indicated. Data were filtered as described in the methods section. Genes that showed significant expression differences between FOXP3⁺ and FOXP3⁻ subpopulations (paired Student's *t*-test, asymptotic p-value computation, cut-off p≤0.05) with a fold-change of ≥2 are marked by an asterisk. For detailed gene expression levels of selected genes in individual Treg cultures see Supplemental Fig. 2. (**B**) Microarray results were validated by qRT-PCR for the indicated genes in FOXP3⁺ (blue bars) and FOXP3⁻ cells (green bars) derived from CD45RA⁻ Treg cultures. FOXP3⁺ cells sorted from expanded CD45RA⁺ Treg (red bars) and unsorted CD45RA⁻ Treg (gray bars) served as controls. Values represent means +SD (n≥3). Significant differences in gene expression between FOXP3⁺ and FOXP3⁻ cells derived from the CD45RA⁻ Treg population are indicated above bars (*p≤0.05, **p≤0.01, ***p≤0.001, paired two-tailed Student's *t*-test). ND: not detected.

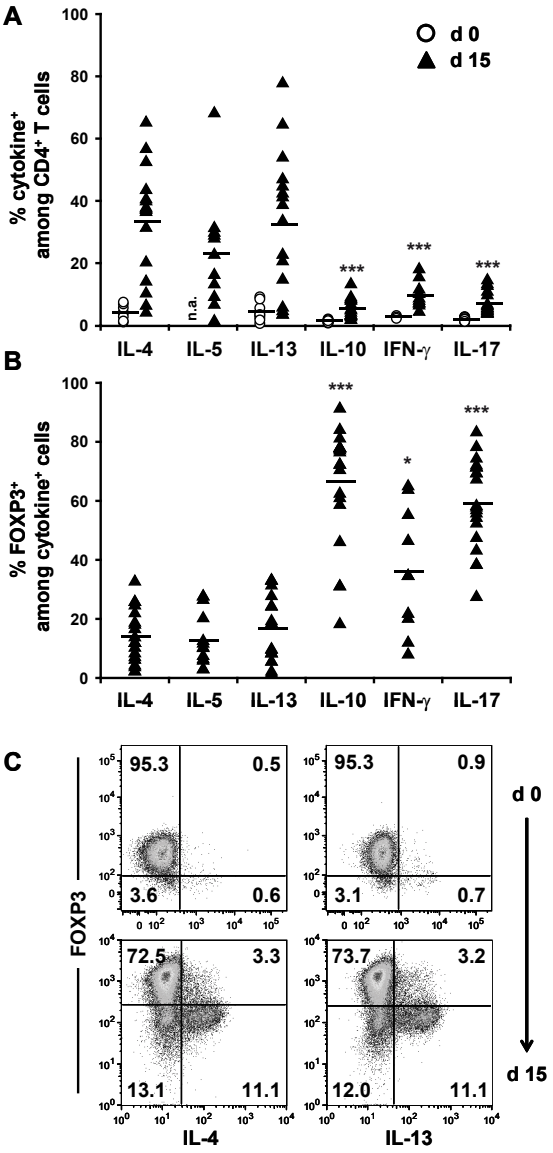

Figure 3: CD45RA$^-$ Treg predominantly produce Th2 cytokines upon loss of FOXP3 expression. CD45RA$^-$ Treg, either *ex vivo* (d 0) or after *in vitro* expansion (d 15), were stimulated for 5h with PMA/ionomycin and stained for FOXP3 and various cytokines. **(A)** Percentages of CD45RA$^-$ Treg producing the indicated cytokines. IL-5 was not determined *ex vivo*. Horizontal bars represent means of n=3-17 independent analyses with cells from different donors. *** p≤0.001 as compared to the number of IL-4 producers; two-tailed unpaired Student's *t*-test. **(B)** Proportion of FOXP3-expressing cells among indicated cytokine producers after *in vitro* expansion. Horizontal bars represent means of n=9-17 independent analyses. * p≤0.05, *** p≤0.001 as compared to the number of FOXP3$^+$ cells among IL-4 producers; two-tailed unpaired Student's *t*-test. **(C)** Representative example of IL-4- and IL13-producing cells among CD45RA$^-$ Treg *ex vivo* (d 0) and after *in vitro* expansion (d 15).

FOXP3- cells from CD45RA- Treg cultures predominantly produce Th2 cytokines

To correlate the mRNA expression data with cytokine production, freshly isolated as well as *in vitro* expanded CD45RA$^-$ and CD45RA$^+$ Treg were stained for FOXP3 and Th cell lineage-defining cytokines (Fig. 3). In freshly isolated cells the expression frequency for one or more Th cell lineage signature cytokines (IL-4, IL-10, IL-13, IFN-γ, IL-17) never exceeded 5 %. In contrast, after *in vitro* expansion approximately 30 % of the cells within CD45RA$^-$ Treg cultures started to produce one or more of the Th2 cytokines IL-4, IL-5 and IL-13 (Fig. 3A). Although we also detected IFN-γ$^+$ and/or IL-17$^+$ cells in these cultures (as previously described by us and others (Ayyoub et al. 2009; Hoffmann et al. 2009; McClymont et al. 2011; Schmidl et al. 2011)), their frequencies were significantly lower than those of the Th2 cytokine producers (Fig. 3A). Th2 cytokine production was largely confined to the FOXP3$^-$ subpopulation, whereas IFN-γ, IL-10 and IL-17 producers were almost equally distributed between FOXP3$^+$ and FOXP3$^-$ cells (Fig. 3B). Confirming our previous findings, CD45RA$^+$ Treg remained uniformly FOXP3$^+$ and comprised hardly any cytokine producing cells before and after *in vitro* expansion ((Hoffmann et al. 2006b; Hoffmann et al. 2009) and data not shown).

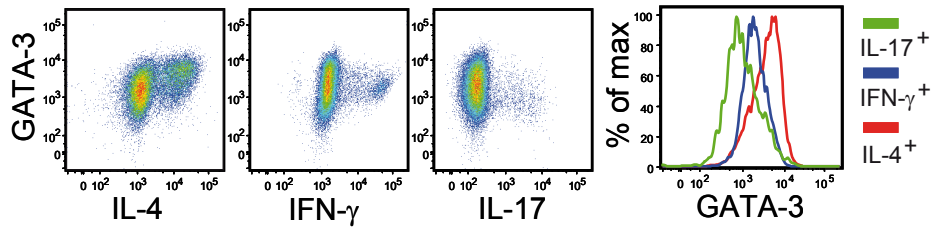

Figure 4

Th2 cytokine production in *in vitro* expanded CD45RA$^-$ Treg is associated with high GATA-3 expression. *In vitro* expanded CD45RA$^-$ Treg were stimulated for 5h with PMA/ionomycin, then stained for GATA-3 and indicated cytokines. The histogram shows GATA-3 expression of IL-4$^+$, IL-17$^+$ or IFN-γ$^+$ cells, respectively. MFI for GATA-3 was significantly different between IL-4$^+$ and IFN-γ$^+$ cells (p=0.046; n=6; two-tailed unpaired Student's *t*-test) as well as IL-4$^+$ and IL-17$^+$ cells (p=0.009; n=5; two-tailed unpaired Student's *t*-test).

Th2 cytokine production in expanded CD45RA$^-$ Treg is associated with high GATA-3 expression

GATA3, the lineage-defining transcription factor for Th2 cells, was highly expressed in CD45RA$^-$ Treg that had downregulated FOXP3 upon *in vitro* stimulation (Fig. 2). To analyze whether *GATA3* expression was restricted to Th2 cytokine producers, *in vitro* expanded CD45RA$^-$ Treg were simultaneously stained for cytokine production and the presence of GATA-3. GATA-3

expression was significantly higher in IL-4 producing cells when compared to IL-17 and IFN-γ producers (Fig. 4).

Inhibition of IL-4 signaling does not block Th2 differentiation in CD45RA$^-$ Treg

Th2 differentiation from naive conventional T cells is mainly driven by IL-4 (Kaplan et al. 1996). Since CD45RA$^-$ Treg secreted IL-4 and other Th2 cytokines under the non-polarizing culture conditions applied in this study, we next asked to which extent endogenous IL-4 supported the conversion of initially FOXP3$^+$ Treg into cells of the Th2 lineage. To block IL-4 signaling, CD45RA$^-$ Treg were cultured in the presence of anti-IL-4-antibodies, anti-IL-4R-antibodies or both during the entire expansion period. The treatment effectively prevented phosphorylation of the transcription factor signal transducer and activator of transcription 6 (STAT6), a crucial step in IL-4 signaling and Th2 induction (Fig. 5A & B). However, despite profound inhibition of STAT6 activation, the frequencies of cytokine secreting cells in CD45RA$^-$ Treg cultures were only marginally altered, with a slight but not statistically significant reduction of Th2 cytokine producers and a minor, statistically insignificant increase in IFN-γ- or IL-17-secreting cells (Fig. 5C & D). In line with these findings, cytokine concentrations in supernatants of blocked and unblocked cultures showed no significant differences, except for IL-4, because IL-4 neutralization by anti-IL-4-antibodies expectedly reduced IL-4 levels, while blockade of the IL-4R increased IL-4 concentrations, proving that IL-4 is consumed in such cultures (Fig. 5E). Overall, these data indicate that Th2 differentiation of CD45RA$^-$ Treg cells does not require endogenous IL-4 but seems to represent the default developmental pathway upon loss of FOXP3.

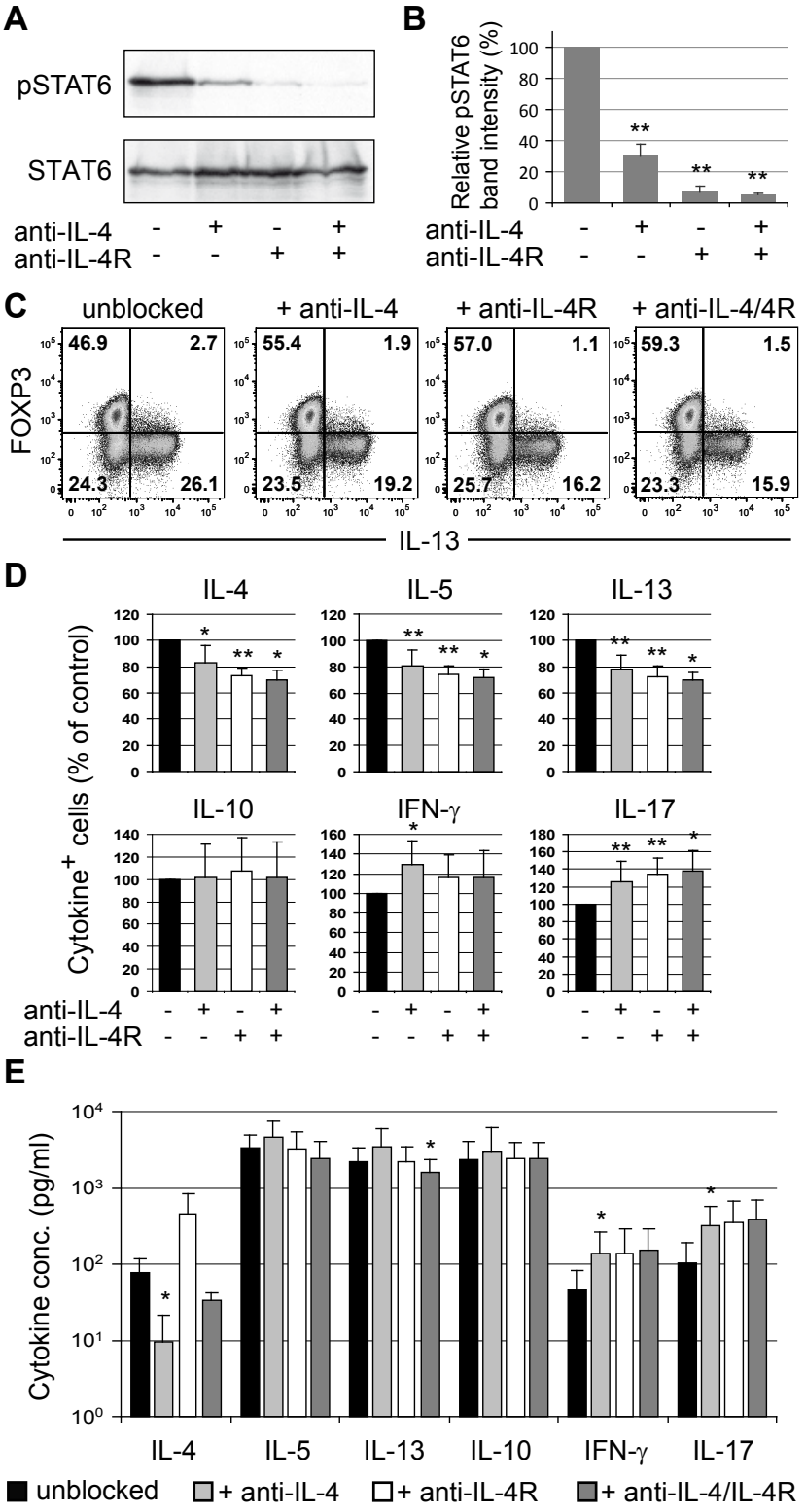
A
pSTAT6
STAT6
anti-IL-4 - + - +
anti-IL-4R - - + +
B
Relative pSTAT6 band intensity (%)
anti-IL-4 - + - +
anti-IL-4R - - + +
C
unblocked
+ anti-IL-4
+ anti-IL-4R
+ anti-IL-4/4R
FOXP3
46.9 2.7 24.3 26.1
55.4 1.9 23.5 19.2
57.0 1.1 25.7 16.2
59.3 1.5 23.3 15.9
IL-13
D
IL-4
IL-5
IL-13
IL-10
IFN-γ
IL-17
Cytokine+ cells (% of control)
anti-IL-4 - + - +
anti-IL-4R - - + +
E
Cytokine conc. (pg/ml)
IL-4 IL-5 IL-13 IL-10 IFN-γ IL-17
unblocked
+ anti-IL-4
+ anti-IL-4R
+ anti-IL-4/IL-4R

Figure 5

Figure 5

Inhibition of IL-4 signaling does not block Th2 differentiation of CD45RA$^-$ Treg during *in vitro* expansion. CD45RA$^-$ Treg were expanded in the presence or absence of anti-IL-4, anti-IL-4R or both antibodies. (**A**) Phosphorylated STAT6 (pSTAT6) in whole cell extracts was analyzed by western blot. Total STAT6 was analyzed as a loading control. Shown is one representative immunostaining (n=3). (**B**) Western blot band intensities were quantified with a densitometer. Phospho-STAT6 band intensities of unblocked cultures were set to 100%. Values represent means + SD (*** $p \leq 0.001$; n=3; two-tailed unpaired Student's *t*-test performed with absolute values). (**C**) and (**D**) Cells were stimulated for 5 h with PMA/ionomycin, then stained for FOXP3 and indicated cytokines. Dot plots in (**C**) show one representative experiment. Bars in (**D**) represent mean percentages + SD of cytokine producers among expanded CD45RA$^-$ Treg. For better comparison of n=5-9 individual cultures, the numbers of cytokine-producing cells in unblocked cultures were scaled to 100%. Unblocked cultures contained on average 29.1%, 15.5% and 26.4% IL-4, IL-5 and IL-13 producers, respectively, and 9.3%, 9.9% and 7.1% IL-10, IFN-γ and IL-17 producers, respectively. **(E)** Supernatants from treated or untreated CD45RA$^-$ Treg cultures were analyzed for cytokine content on d11 of *in vitro* expansion. Bars represent means + SD of n=5-9 independent cultures. * $p \leq 0.05$, ** $p \leq 0.01$ as compared to unblocked cultures; two-tailed unpaired Student's *t*-test

DISCUSSION

There is increasing evidence that Treg lineage commitment may not be irreversible, as down-regulation of FOXP3 and consecutive expression of Th1 and Th2 cytokines by Treg cells has been observed by several groups. (Ayyoub et al. 2009; Beriou et al. 2009; Zhou et al. 2009a; Zhou et al. 2009c; Zhu and Paul 2010; Schmidl et al. 2011). We showed that in particular human CD45RA$^-$ memory-type Treg lose FOXP3 expression upon *in vitro* stimulation, while CD45RA$^+$ naïve Treg maintain high FOXP3 levels even after extended culture periods. Importantly, both FACS-purified starting populations contained equivalent frequencies of FOXP3$^+$ cells before *in vitro* stimulation (>93%) and both showed equally homogeneous demethylation at the Treg-specific demethylated region (TSDR), a sensitive epigenetic mark for the identification of Treg and currently the most reliable marker for the exclusion of contaminations by induced- or non-Treg (Baron et al. 2007; Schmidl et al. 2009; Hansmann et al. 2010). Furthermore, we ultimately proved loss of FOXP3 expression by the serial examination of human Treg clones in our previous studies (Hoffmann et al. 2009). Since Treg instability may be detrimental for future adoptive cell therapies (or those already underway at some centers (Brunstein et al. 2011a; Di Ianni et al. 2011b)), we now examined the fate of Treg that lose FOXP3 upon *in vitro* stimulation. For this purpose, we developed a cell fixation and permeabilization protocol that allowed the isolation of intact mRNA from FOXP3-stained and FACS-sorted cells. In contrast to previously described methods (Boniface et al. 2010), the isolated RNA was not degraded but of high quality and suited for sensitive downstream assays, such as qRT-PCR and microarray based whole genome expression analyses. The use of ethanol for fixation prevented the cross-linking of nucleic acids and proteins (Fowler et al. 2008) that is caused by PFA contained in commercial staining kits. Furthermore, our method improves previously described RNA isolation protocols developed by Esser and colleagues (Esser et al. 1995), because it permits the simultaneous detection of fluorescently labelled surface markers. Since this technology is applicable to a wide variety of transcription factors and cell types, it may advance many areas in cellular biology.

Classical differentiation of naive CD4$^+$ T cells into Th1 or Th2 cells is mainly induced by the local cytokine milieu as well as the type of antigen and antigen presenting cell. IFN-γ and IL-12 polarize toward Th1 differentiation via the transcription factors STAT4, STAT1 and T-bet (Lighvani et al. 2001; Thieu et al. 2008). Th2 cells are induced by IL-4 that induces GATA-3, usually in a STAT6-dependent fashion and the hallmark of Th2 cells is their secretion of IL-4, IL-5 and IL-13 (Shimoda et al. 1996; Takeda et al. 1996; Zheng and Flavell 1997; Zhu et al. 2004). T-bet and GATA-3 reciprocally repress each other (Szabo et al. 1997; Kurata et al. 1999; Djuretic et al. 2007b) and FOXP3 in Treg is supposed to prohibit expression of both these lineage defining transcription factors (Zheng and Rudensky 2007). Nevertheless, co-expression of Foxp3 and T-bet has been observed in activated murine Treg under type 1 inflammatory conditions, which

permits their migration to inflammatory sites, but does not induce Th1 cytokine secretion (Koch et al. 2009). Our comparative analysis of human CD45RA$^-$ memory Treg-derived FOXP3$^+$ and FOXP3$^-$ subpopulations now revealed that typical marker genes of Treg, such as *CTLA4*, *LAG3*, *IL2RA*, *LGALS3* and *LRRC32* are down-regulated upon loss of FOXP3 expression, while *IL7R* and *CD40LG*, usually not expressed by Treg, are up-regulated. More strikingly, the cells losing FOXP3 upon *in vitro* stimulation under non-polarizing conditions converted into Th2-like cells as they started to overexpress a number of Th2-specific genes, such as the signature cytokines *IL4*, *IL5* and *IL13*, the transcription factors *GATA3* and *GFI1* and the surface receptor *GPR44*. In contrast, expression of Th1 or Th17 signature genes, such as *TBX21* and *RORC*, was even lower in FOXP3$^-$ as compared to FOXP3$^+$ cells isolated from the same cultures (Fig. 2). The conversion into Th2 cells upon loss of FOXP3 expression dramatically exceeded the previously described differentiation into Th1 or Th17 cells (Ayyoub et al. 2009; Hoffmann et al. 2009; McClymont et al. 2011; Schmidl et al. 2011). Both, the high frequency of Th2 cytokine producers among FOXP3$^-$ CD45RA$^-$ Treg and the substantial concentrations of Th2 cytokines in CD45RA$^-$ Treg culture supernatants corroborated these results. In murine studies, induction of cytokine secretion in 'former' Treg cells has also been observed, either upon foxp3 deletion (Williams and Rudensky 2007), or upon expression of a non-functional Foxp3 protein (Lin et al. 2007). While Rudensky and coworkers found only Th1 cytokines in C57BL/6 animals (Williams and Rudensky 2007), Chatila's group also observed a dramatic increase in IL-4 secretion after Foxp3 downregulation in BALB/c mice (Lin et al. 2007). Thus, a genetic predisposition may influence the conversion of Treg. Interestingly, however, artificial attenuation of Foxp3 expression has been described to induce predominantly a Th2 phenotype in Foxp3^{low}-expressing cells even in C57BL/6 mice (Wan and Flavell 2007) and this conversion seems to be an intrinsic developmental program that occurs independently of IL4/STAT6 signaling, yet still requires GATA-3 expression (Wang et al. 2010). In Th2 differentiation of naive conventional T cells, IL-4 causes STAT6 phosphorylation by JAK1 and JAK3 kinases leading to STAT6 dimerization and nuclear translocation that in turn supports *IL4* and *IL4R* as well as *GATA3* transcription (Kaplan et al. 1996). Blocking IL-4/STAT6 signaling in human Treg by the addition of anti-IL-4 antibodies, anti-IL-4R antibodies or both during culture resulted in a dramatic reduction of STAT6 phosphorylation, as expected. Yet, the frequencies of IL-4, IL-5 and IL-13 producing cells and the amount of secreted Th2 cytokines were only marginally diminished, suggesting that auto- or paracrine IL-4/STAT6 signaling is not the main cause of Th2 conversion. To which extent IL-4 independent signaling cascades are involved in Th2 conversion of human Treg requires further clarification. For murine T cells it has previously been shown that IL-2 combined with CD28 co-stimulation can induce Th2 differentiation in an IL-4/STAT6-independent, but STAT5-dependent manner (Zhu et al. 2003; Cote-Sierra et al. 2004). Since our stimulation conditions provide all required components (CD3, CD28 and high-dose IL-2 stimulation), this pathway may be involved in Treg conversion.

However, we rather reason that Th2 conversion of CD45RA$^-$ Treg represents a developmental program that is imprinted on the cells by repeated contact to (self-) antigen *in vivo*, as CD45RA$^+$ naïve Tregs do not convert although exposed to the same *in vitro* conditions. In support of this hypothesis, an increased GATA-3 expression in CD45RA$^-$ Treg (as compared to CD45RA$^+$ Treg and Tconv cells) was detectable already before *in vitro* expansion (Supplemental Fig. 3). In mice, Th2 conversion of wild-type Tregs *in vivo* has been described (Wang et al. 2010) as well as conversion into IL-4 secreting follicular B helper T cells (Tsuji et al. 2009) and it remains to be determined whether this is also a frequent event in humans, where diminished FOXP3 expression of Treg has been observed in patients with atopic diseases (Provoost et al. 2009).

In summary, by performing the first comparative transcriptome analyses of human Treg and their converted progeny identified and separated on the basis of their FOXP3 expression level, we show that differentiation towards a Th2 phenotype represents the dominant pathway of human Treg upon loss of FOXP3 expression. These findings further elucidate the developmental plasticity of Treg in humans (Zhou et al. 2009b) and are thus of high relevance for current as well as future adoptive Treg therapies.

ACKNOWLEDGMENTS

We thank R. Eder, J. Stahl and I. Ritter for excellent cell sorting and technical support, and N. Ahrens, Institute of Transfusion Medicine, University Hospital Regensburg, for provision of leukapheresis products.

Supplementary Information

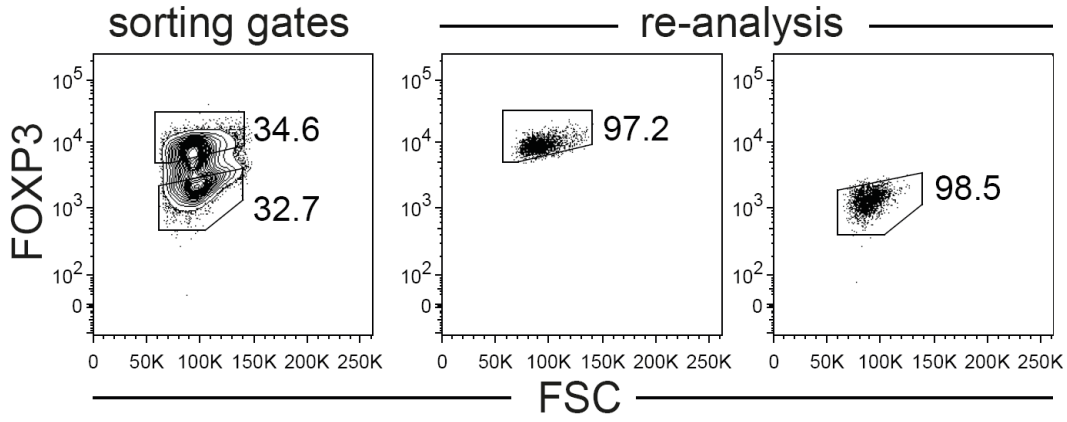

Supplemental Figure 1

The 'ethanol/tryptone method' allows high purity sorting of FOXP3$^+$ and FOXP3$^-$ populations from expanded CD45RA$^-$ Treg. CD45RA$^-$ Treg were *in vitro* expanded and stained for CD4 and FOXP3 using the 'ethanol/tryptone method'. Numbers within the gates indicate percentages of gated cells. Plots are representative of n=5 independent experiments.

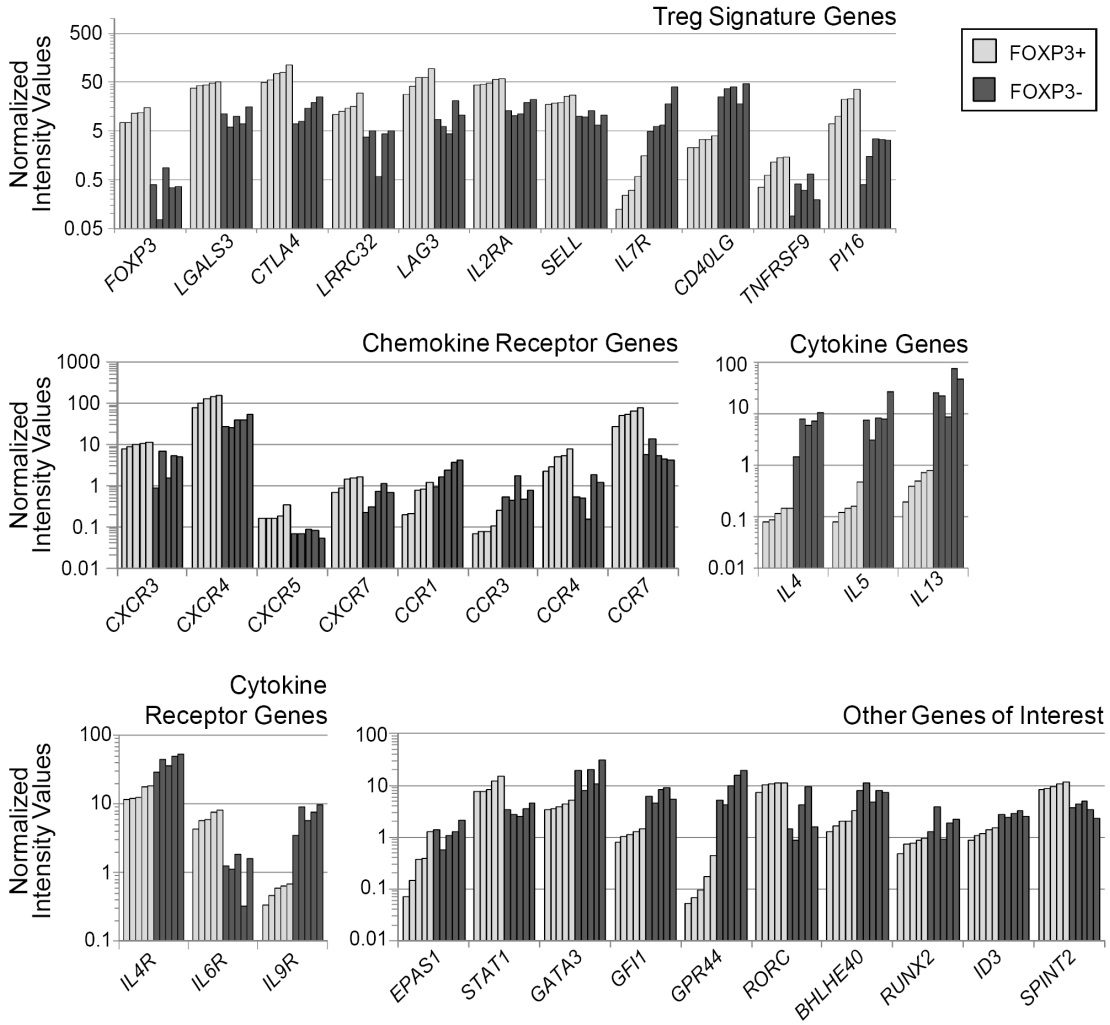

Supplemental Figure 2

Reproducibility of microarray results. Bar charts present normalized microarray probe intensities for genes from Fig. 2A showing significant expression differences for FOXP3^{+} and FOXP3^{-} CD45RA^{-} Treg cell populations after expansion of n=5 different donors. Expression values for FOXP3^{+} samples (light gray bars) and matched FOXP3^{-} samples (dark gray bars) are shown in ascending intensity value order of FOXP3^{+} samples.

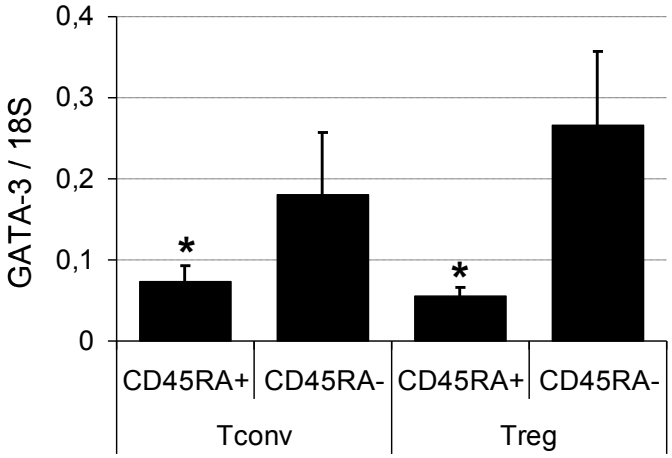

Supplemental Figure 3

Increased GATA-3 expression in freshly isolated CD45RA$^-$ Treg cells. GATA-3 mRNA expression levels were analyzed in freshly isolated and FACS-sorted CD4$^+$CD25$^-$CD45RA$^+$ and CD4$^+$CD25$^-$CD45RA$^-$ Tconv and CD4$^+$CD25^{high}CD45RA$^+$ and CD4$^+$CD25^{high}CD45RA$^-$ Treg cells. Data are shown normalized to 18S RNA. *p≤0.05 as compared to CD45RA$^-$ Treg; n=4; unpaired two-tailed Student's *t*-test.

Supplemental Table 1: Primer Sequences used in real-time qPCR 5'-3'

FOXP3_S	GAAACAGCACATTCCCAGAGTTC
FOXP3_AS	ATGGCCCAGCGGATGAG
RORC_S	GCAGCGCTCCAACATCTTCTC
RORC_AS	GCACACCGTTCCCACATCTC
CTLA4_S	CACGGGACTCTACATCTGCAAGG
CTLA4_AS	GAAGTCAGAATCTGGGCACGG
TNFRSF9_S	GTTGCTTTGGGACATTTAACGATCAG
TNFRSF9_AS	TTCACAAGCACAGACTTTCCATCC
GATA3_S	GACCCTGTCTGCAATGCCTG
GATA3_AS	TCTGGATGCCTTCCTTCTTCATAGTC
KLRB1_S	CTGTGCTGGGATTATTCTCCTTGTC
KLRB1_AS	TTCCTGCTCTGTTGAATGTCCAC
IL4_S	CACAGCAGTTCCACAGGCAC
IL4_AS	CGTACTCTGGTTGGCTTCCTTCAC
CD40L_S	CATGTCATAAGTGAGGCCAGCAG
CD40L_AS	TTTCCAGGGTTACCAAGTTGTTGCTC
B2M_S	TGAGTATGCCTGCCGTGTGA
B2M_AS	TGATGCTGCTTACATGTCTCGAT
18S_S	ACCGATTGGATGGTTTAGTGAG
18S_AS	CCTACGGAAACCTTGTTACGAC

Footnotes

Support:
This work was supported by research funds from the German Research Society (KFO 146) to ME, MR and PH, the Bavarian Immunotherapy Network and the Wilhelm Sander Foundation to ME and the José Carreras Foundation (FACS facility).

Abbreviations:
Treg, regulatory T cells; FOXP3, forkhead box P3;

Copyright

Figures and Text from chapter 3.4 are taken from: Leo Hansmann, Christian Schmidl, Janina Kett, Lena Steger, Reinhard Andreesen, Petra Hoffmann, Michael Rehli, Matthias Edinger, "Dominant Th2 differentiation of human regulatory T cells upon loss of FOXP3 expression" The Journal of Immunology, v. 188, pp. 1275-1282, 2012.

Copyright 2012. The American Association of Immunologists, Inc.

3.5 The enhancer and promoter landscape of human regulatory and conventional T cell subpopulations

Manuscript in preparation

Christian Schmidl performed all experiments except cell isolation and HeliscopeCAGE sequencing, performed computational analyses and wrote the manuscript

The enhancer and promoter landscape of human regulatory and conventional T cell subpopulations

Christian Schmidl[1], Petra Hoffmann[1], Reinhard Andreesen[1], Alistair R. Forrest[2], Timo Lassman[2], Hideya Kawaji[2], Piero Carninci[2], Yoshihide Hayashizaki[2], Matthias Edinger[1], Michael Rehli[1,†]

[1]Department of Hematology, University Hospital Regensburg, D-93042 Regensburg, Germany; [2] RIKEN Omics Science Center, RIKEN Yokohama Institute, 1-7-22 Suehiro-cho Tsurumi-ku Yokohama, Kanagawa, 230-0045 Japan.

[†]Corresponding Author

Michael Rehli, Department of Hematology, University Hospital Regensburg, D-93042 Regensburg, Germany; phone: +49 941 944 5587; fax: +49 941 944 5593; E-mail: michael.rehli@ukr.de

Abstract

CD4+CD25+FOXP3+ human regulatory T cells (Treg) are essential for self-tolerance and immune homeostasis. Here, we describe the promoterome of $CD4^{+}CD25^{high}CD45RA^{+}$ naïve and $CD4^{+}CD25^{high}CD45RA^{-}$ memory Treg and their $CD25^{-}$ conventional T cell (Tconv) counterparts both before and after *in vitro* expansion by cap analysis of gene expression adapted to single molecule sequencing (HeliscopeCAGE). We performed comprehensive comparative digital gene expression analyses and revealed new orphan transcription start sites, of which several were validated as alternative promoters of known genes including *FOXP3* and *CTLA4*. For all *in vitro* expanded subsets, we additionally generated genome-wide maps of poised and active enhancer elements marked by histone H3 lysine 4 monomethylation and histone H3 lysine 27 acetylation. Analysis of cell type-specific regulatory elements revealed a specific enrichment of several transcription factor binding motifs. We validated promising candidates by chromatin immunoprecipitation coupled to next generation sequencing and identified STAT5 and FOXP3 as well as RUNX1 and ETS1 as global regulators of Treg- and Tconv-specific enhancers, respectively. In summary we provide a highly detailed and easily accessible resource of gene expression and -regulation in Treg and Tconv subpopulations.

Introduction

Naturally occurring thymus derived $CD4^+CD25^+$ regulatory T cells (Treg) in humans are crucial to control self-tolerance and immune homeostasis by suppressing a wide variety of immune responses (Sakaguchi 2004). They express the transcription factor FOXP3, which is indispensable for Treg function as FOXP3 mutations cause lethal autoimmune diseases in mice and humans (Bennett et al. 2001; Brunkow et al. 2001). Their suppressive abilities make Tregs interesting for clinical applications as their adoptive transfer can avert unwanted immune reactions in allogeneic hematopoietic stem cell transplantation as well as autoimmune diseases or organ transplantation (Hoffmann et al. 2002a; Edinger et al. 2003; Brusko et al. 2008; Nadig et al. 2010; Edinger and Hoffmann 2011a).

In perspective of their therapeutic application we developed expansion protocols for human Treg cells (Hoffmann et al. 2004) and demonstrated that CD45RA+ naïve Treg cells stably express FOXP3 during *in vitro* culture in contrast to the CD45RA- memory population (Hoffmann et al. 2006b). CD45RA- Treg showed not only a heterogeneous FOXP3 expression profile but also diminished suppressive function and the potential to differentiate into proinflammatory T helper phenotypes after *in vitro* expansion (Hoffmann et al. 2006b; Schmidl et al. 2011; Hansmann et al. 2012). This data raises questions about Treg cell stability, plasticity and inherited subset properties and – in view of clinical applications – demand an in-depth molecular characterization. Recent technical advances in high throughput sequencing technologies such as the adaption of cap analysis of gene expression (CAGE) to Heliscope single molecule sequencing (Heliscope CAGE) increase the accuracy and information content of gene expression analysis (Kanamori-Katayama et al. 2011). Heliscope CAGE quantifies full-length 5'-capped transcripts and maps genuine transcription start sites (TSS) at base pair resolution, which allows studying the proximal regulatory inputs driving gene expression and uncovering novel promoters. FANTOM (functional annotation of the mammalian genome) is an international consortium that determined and quantified the TSS in several hundred cell types and tissues to create a reference database of gene expression and the location of promoters in mice and humans (the FANTOM5 consortium, unpublished observations). Here, as part of the 5^{th} phase of the FANTOM project (FANTOM5) we applied Heliscope CAGE to $CD4^+CD25^{high}CD45RA^+$ naïve and $CD4^+CD25^{high}CD45RA^-$ memory Treg and their $CD25^-$ conventional T cell (Tconv) counterparts both before and after *in vitro* expansion for a detailed delineation of subset-specific TSS locations, gene expression profiles and potentially novel promoters.

In addition to gene promoters, the genome comprises numerous noncoding elements such as enhancers, silencers and boundary elements to regulate gene expression (Ong and Corces 2011). Compelling evidence from global studies identified the enrichment of histone 3 lysine 4

monomethylation (H3K4me1) and histone 3 lysine 27 acetylation (H3K27ac) at "poised" and "active" enhancers, respectively (Heintzman et al. 2007; Creyghton et al. 2010; Rada-Iglesias et al. 2011). Enhancers are distributed throughout the genome in a cell type-specific manner (Heintzman et al. 2009) and are also characterized by local DNA hypomethylation (Schmidl et al. 2009; Sérandour et al. 2011; Stadler et al. 2011) and the binding of general as well as cell type-specific transcription factors (TFs) that translate environmental and inherited cues in cooperation with the chromatin environment into distinct gene expression programs (Lupien et al. 2008; Heinz et al. 2010; Ernst et al. 2011; Sérandour et al. 2011; Pham et al. 2012). In Treg, the stable expression of FOXP3 itself is controlled by both DNA methylation and chromatin state, which both influence the binding of various TFs to its intronic enhancer (Huehn et al. 2009; Lal and Bromberg 2009). We previously extended those initial observations by describing more than 130 differentially methylated regions (DMR) between Treg and Tconv cells (Schmidl et al. 2009). Interestingly, many DMRs were located at key Treg and Tconv gene loci, overlapped with an active chromatin environment and showed methylation sensitive enhancer function (Schmidl et al. 2009). First next generation sequencing studies on human Treg and Tconv described differential FOXP3 binding in activated Treg and Tconv cells and its impact on gene expression (Birzele et al. 2011). However, most of the analyses of TFs regulating Treg function were only performed in rodents or restricted to single loci in human cells.

To better understand the global regulatory networks in human CD4+ T cell subpopulations we herein describe the promoterome of freshly isolated as well as *in vitro* expanded naïve (CD45RA+) and memory (CD45RA-) Treg and Tconv by Heliscope CAGE. In *in vitro* expanded cells we extended the promoter data by the mapping of poised and active enhancers throughout the genome. Enhancers show cell type-specific enrichment of TF binding motifs and we highlight the global role of FOXP3, RUNX1, ETS1 and STAT5 in cell type-specific enhancer architecture and gene regulation by chromatin immunopreciptiation followed by next generation sequencing (ChIP-seq). The integrated analysis of promoters and enhancers identifies subset-specific properties of gene regulation and yields a valuable resource on gene expression and regulation in Treg and Tconv subsets for the scientific community.

Methods

***Cells*–**$CD4^+CD25^-CD45RA^+$, $CD4^+CD25^-CD45RA^-$, $CD4^+CD25^{high}CD45RA^+$ and $CD4^+CD25^{high}CD45RA^-$ T cells were isolated as described elsewhere (Hoffmann et al. 2006b). All T cell populations were *in vitro* expanded as previously described (Hoffmann et al. 2004). Jurkat cells (human T cell leukemia) where cultured as previously described (Schmidl et al. 2009).

***RNA preparation*–**RNA for CAGE sequencing and RACE-PCR was isolated using the miRNeasy RNA isolation kit (Qiagen, Hilden, Germany).

***HeliscopeCAGE-sequencing and data analysis*–**Heliscope CAGE sequencing and sequence alignment was performed as part of the FANTOM5 project (the FANTOM consortium, unpublished information). Normalization of individual tag libraries was done using the common power-law distribution approach (Balwierz et al. 2009). Expression data for annotated coding or noncoding genes (according to Gencode release 10 data) was extracted by collecting normalized tag counts in regions -500 to +200 relative to all annotated transcription start sites associated with a single geneID. Digital gene expression analysis of normalized data was performed using edgeR (Robinson et al. 2010).

***3' and 5'RACE-PCR*–**CDNA from RNA of T cell subpopulations was generated with the SMARTer™ *RACE*cDNA Amplification Kit (Clontech, Saint-Germain-en-Laye, France) according to the manufacturers' instructions. Rapid Amplification of cDNA Ends (RACE) was performed with the Advantage 2 Polymerase System (Clontech) and a gene specific primer (gsp). When no distinct fragment sizes were observed, the PCR product was diluted and amplified with a nested gene specific primer (ngsp). Single bands were gel purified with the Qiagen gel extraction kit (Qiagen), cloned with the StrataClone PCR Cloning Kit (Agilent) according to the manufacturers' instructions and sequenced (Life Technologies, Regensburg, Germany). Primer sequences are listed in Supplemental Table S1.

***ChIP-sequencing and data analysis*–**ChIP of two healthy donors and library construction were done essentially as described (Pham et al. 2012) using antibodies against H3K4me1 (Abcam), H3K27ac (Abcam), STAT5 (Santa Cruz Biotechnology), ETS1 (Santa Cruz Biotechnology), RUNX1 (Abcam) and FOXP3 (Novus Biologicals). Sequence tags were mapped to the current human reference genome (GRCh37/hg19) using Bowtie (Langmead 2010). Downstream analysis of uniquely mapped tags including quality control, peak calling, and motif analysis were done as described using HOMER (Heinz et al. 2010). A UCSC Genome Browser track hub of the entire data set is found at http://www.ag-rehli.de.

De novo *motif analyses*–Enriched sequence motifs were *de novo* extracted from regions surrounding differentially expressed CAGE clusters determined by edgeR ($P \leq 0.01$ for pairwise

comparisons; -300 to +50 bp from cluster center) using HOMER. For ChIP-seq data sets, enhancers (distal H3K4me1 and H3K27ac regions, defined as being located at least 1000 bp away from GencodeV10 annotated TSS) were extracted using a fixed region size of 1kb for replicate samples (and with a tag enrichment in one sample in comparison with the other in case of cell type-specific enhancers). Motifs were extracted from 1kb regions using HOMER.

***Reporter plasmid construction and purification*–**The native as well as new CTLA4 and FOXP3 TSS were amplified from genomic DNA using PCR primers listed in Supplemental Table S1. The PCR fragments were cloned in the pGL4.10 vector (Promega) and sequenced for validation. For transient transfections, plasmids were isolated and purified using the EndoFree Plasmid Kit (Qiagen).

***Transient DNA transfection*–**Jurkat cells were stimulated and transfected using DEAE-dextran essentially as described (Schmidl et al. 2009). The transfected cells were cultivated for 48 h, harvested, and cell lysates were assayed for firefly and renilla luciferase activity in duplicates using the Dual Luciferase Reporter Assay System (Promega) on a Lumat LB9501 (Berthold, Bad Wildbach, Germany) in three independent experiments. Firefly luciferase activity was normalized against Renilla luciferase activity and an empty vector control.

Results

To analyze gene expression as well as the exact promoter locations of T cell subpopulations, we subjected three biological replicates of highly purified primary (labeled with prefixed "p") $CD4^+CD25^{high}CD45RA^+$ naïve Treg (pRA+Treg), $CD4^+CD25^{high}CD45RA^-$ memory Treg (pRA-Treg), $CD4^+CD25^-CD45RA^+$ naïve Tconv (pRA+Tconv) and $CD4^+CD25^-CD45RA^-$ memory Tconv (pRA-Tconv) to HeliscopeCAGE. Additionally, we *in vitro* expanded all subpopulations as previously described (Hoffmann et al. 2006b) and subjected them to HeliscopeCAGE sequencing as well (labeled with prefixed "e"). The sorting strategy with representative FACS plots is charted in Figure 1.

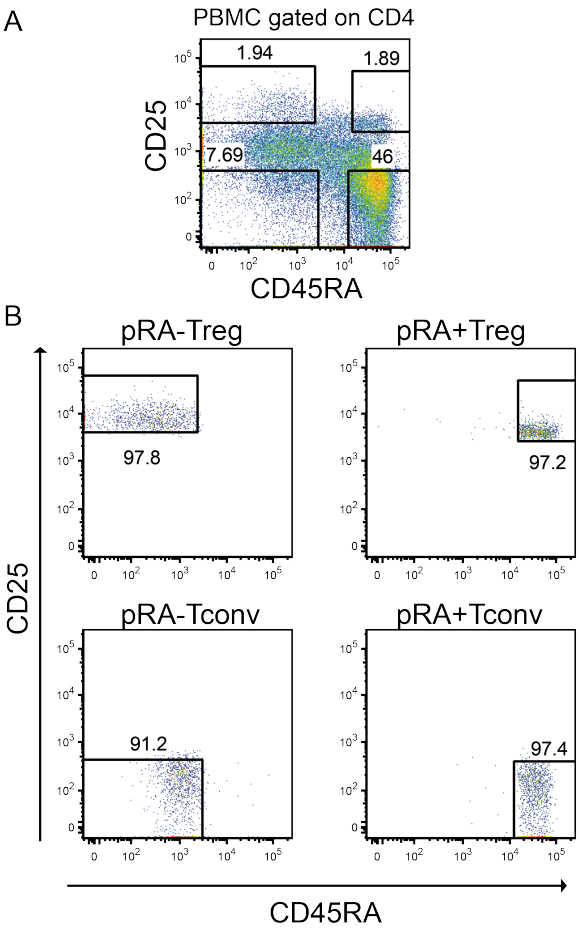

Figure 1:

T cell isolation and expansion. (A.) Sorting strategy for $CD4^+CD25^{high}CD45RA^+$ (pRA+Treg), $CD4^+CD25^{high}CD45RA^-$ (pRA-Treg), $CD4^+CD25^-CD45RA^+$ (pRA+Tconv) and $CD4^+CD25^-CD45RA^-$ (pRA-Tconv) from human PBMCs as described in Methods. (B.) Cells were reanalyzed after sorting on a separate cytometer (FACSCalibur).

To quantify gene expression we collected normalized digital CAGE tag counts for gene promoters associated with known genes (according to GencodeV10 annotation). Overall 11022

protein-coding and 1168 non-coding genes were expressed with at least 1 TPM (tags per million) in one subpopulation. We next performed digital gene expression (DGE) analysis of protein-coding genes using the edgeR software package (Robinson et al. 2010) for pairwise comparisons between subpopulations. A multidimensional scaling plot (MDS) clustered replicates together and clearly separated Treg from Tconv in one dimension and *in vitro* expanded from primary cells in the other dimension (Figure 2A). Figure 2B shows a representative DGE analysis with the top 50 differentially expressed protein-coding genes (ranked by q-value) between pRA+Treg and pRA+Tconv. As expected, well-characterized signature genes appeared in the top ranked list, for example *FOXP3*, *IL2RA*, *CTLA4*, *IKZF2* and *CD40LG*. Plots of top 50 differentially regulated genes of additional pairwise comparisons are displayed in Supplementary Figure S1. We next defined a "core" pTreg gene signature by identifying a set of genes that was differentially expressed in both pRA+Treg vs. pRA+Tconv as well as in pRA-Treg vs. pRA-Tconv comparisons. In addition, we compared the expression levels of these 61 "core" genes in pTreg to those in eTreg (Figure 2C). This Treg core signature comprises intensively studied Treg marker and, additionally, only recently discovered genes found to be essential to foster or restrict Treg function such as *THEMIS* and *SATB1* (Beyer et al. 2011; Chabod et al. 2012). However, we could also include several genes less well described in the Treg context such as *LAIR2*, *METTL7A*, and *RTKN2* as being upregulated as well as *TCF7* (*TCF-1*), *ANK3*, *NELL2* and *ANXA1* as being downregulated in pTreg and eTreg. Interestingly, a transcript isoform of RTKN2, a gene that was previously reported to be expressed in lymphocytes (Collier et al. 2004), showed exclusive expression in Treg when compared to the roughly 3000 samples sequenced in the FANTOM5 project (the FANTON5 consortium, unpublished observations).

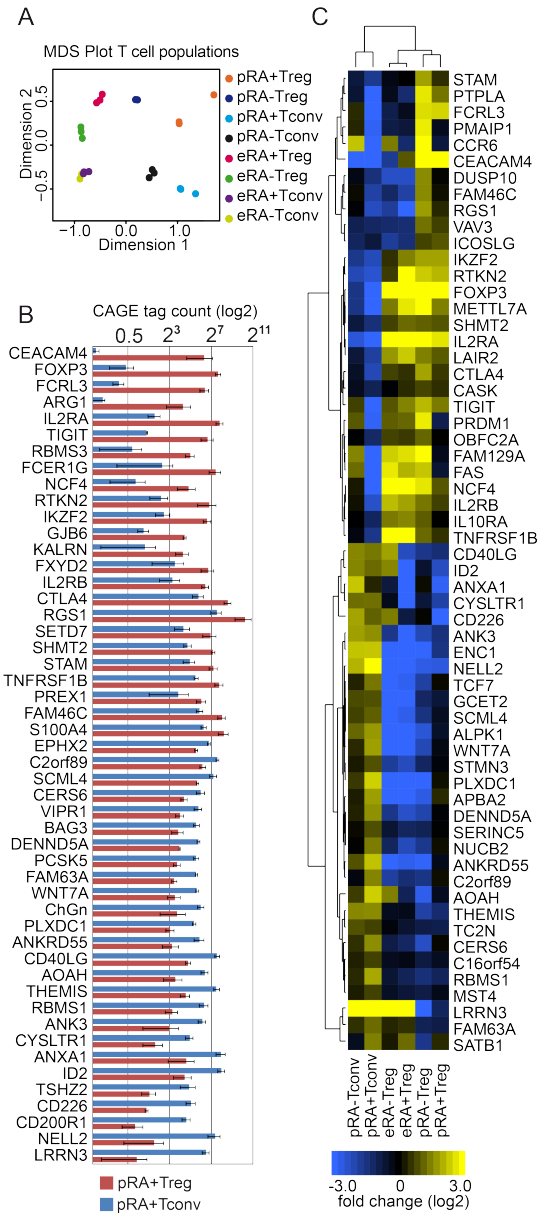

Figure 2:

HeliscopeCAGE-based digital expression analysis. For digital gene expression analysis, tag counts were collected within -500 to +200 bp of GencodeV10 annotated coding gene promoters as outlined in the Methods section. (A.) A multidimensional scaling (MDS) plot for replicate HeliscopeCAGE-based digital expression data shows distance of samples based on tag distribution in expressed genes. (B.) Digital gene expression data for the top 50 differentially expressed genes in a pairwise comparison of pRA+Treg vs. pRA+Tconv. (C.) A Treg "core" signature displaying unsupervised hierarchical clustering of genes differing highly significant in expression between pTreg vs. pTconv in both CD45RA+ naïve and CD45RA- memory subpopulations. eTreg were included in the clustering to visualize expression changes of core Treg genes after *in vitro* expansion. Values were $\log_2$ transformed and normalized to the geometric mean of tag counts in pTreg and pTconv subpopulations for every gene.

Since Treg are intensively studied for future clinical applications, we were particularly interested in the differential expression of Treg-specific effector molecules in the Treg subsets. The genes CTLA4, IL2RA (CD25), TGFB1, TIGIT and TNFRSF10B were highly expressed in all Treg populations (Figure 3A). In contrast, several genes were not expressed in pRA+Treg but upregulated in pRA-Treg, namely TNFRSF18 (GITR), LAG3, GZMA, IL-10, FGL2 and ENTPD1 (CD39). Interestingly, eRA+Treg resembled pRA+Treg with respect to their effector molecule repertoire with the exceptions that they express higher amounts of GITR, LGAS1 and IL2RA than their primary counterparts. Only few molecules were expressed exclusively in eRA-Treg, namely TNFSF11, NRP1, EBI3 (IL-35 subunit) and GZMB. However, since this population shows heterogeneity (Schmidl et al. 2011; Hansmann et al. 2012), unequivocal identification of the cells expressing these effector genes is excluded. Another crucial factor in adoptive T cell therapy is the potential ability of the cells to home to specific locations in the host (Campbell and Koch 2011). The homing receptors that mediate migration to inflamed tissues CCR2, CCR5 and CCR8 as well as the skin/mucosa-, liver- and intestine homing receptors CCR10, CXCR6 and CCR9 were not expressed in pRA+Treg, but were present in pRA-Treg (Figure 3B). Notably, eRA+Treg resembled pRA-Treg cells more than pRA+Treg with regard to their CCR expression with the exception of CCR6, CCR9 as well as CCR10. Interestingly, in contrast to pTreg populations, eTreg do not express CXCR5, a receptor described for homing to B cell follicles and germinal centers. Recent publications suggest that Treg express other lineage specific transcription factors that drive specialized gene expression programs in order to suppress the corresponding T helper cell-associated inflammation (Chaudhry et al. 2009; Koch et al. 2009; Zheng et al. 2009). We therefore investigated if TFs of other lineages are already expressed in our pTreg and if the expression pattern changes upon *in vitro* expansion, as this could influence their suppressive properties. pRA-Treg –in contrast to pRA+Treg- expressed an array of TFs (albeit at low levels) of other T cell lineages as shown in Figure 3C exemplarily for MAF,TBX21 and RORC. The Th2 transcription factors AHR, PRDM1 and GATA3 were expressed in both Treg populations but to a higher degree in pRA-Treg. Of note, upon *in vitro* expansion, eRA+Treg upregulate the Th1 and Th2 transcription factors TBX21 and MAF, respectively. However, the highest expression of Th2-associated TFs was observed in eRA-Treg.

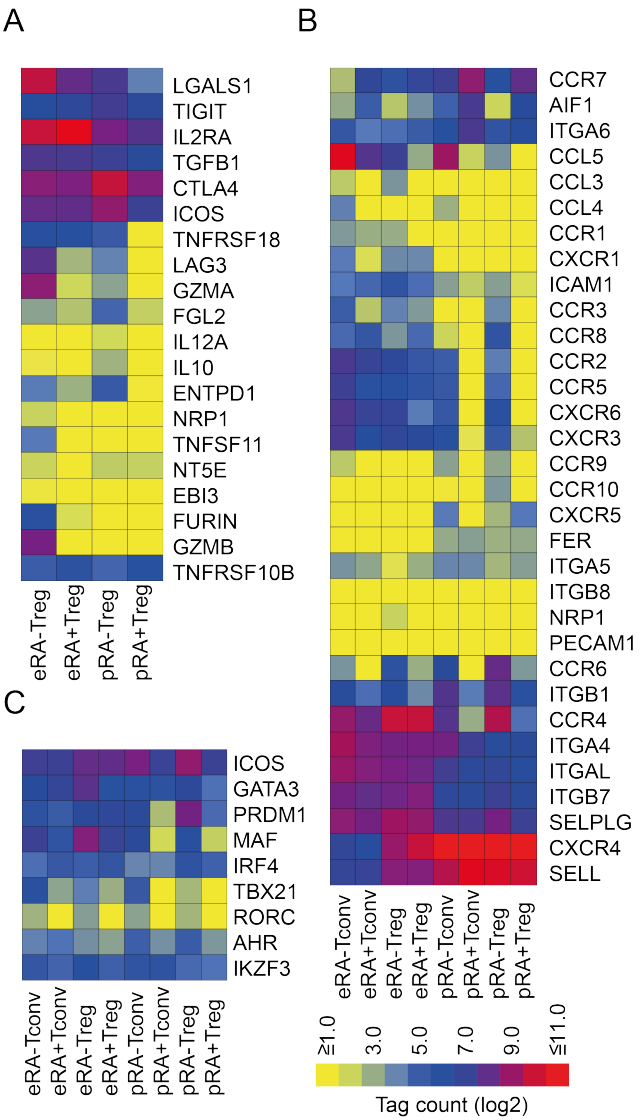

Figure 3

Effector molecule-, homing receptor-, and transcription factor expression in T cell subpopulations. Absolute tag counts (log_2 transformed) of (A.) Treg effector molecules, (B.) genes involved in homing and (C.) transcription factors. Data are presented as a heatmap with yellow, blue and red representing low, intermediate and high expression, respectively.

Finally, DGE was also performed for noncoding genes. Among the most significant transcripts upregulated in RA+Treg compared to RA+Tconv populations is CTC-231011.1, the host transcript for mir146a, a miRNA that is involved in Treg-mediated control of Th1 responses in the murine system (Lu et al. 2010a) (Suppplementary Figure S2). In addition, we identified several uncharacterized noncoding genes that are differentially expressed between subsets and might be involved in subset-specific function. Taken together, our detailed DGE analysis of coding and noncoding genes in T cell subpopulations highlights cell type-specific properties and

presents a foundation to investigate previously uncharacterized but potentially important molecules for the function of Treg and Tconv subsets.

CAGE clusters not annotated to a known promoter could represent promoters of new genes, alternative promoters of known genes or TSS of enhancer RNAs (Kanamori-Katayama et al. 2011; Djebali et al. 2012). As expected, we found that CAGE clusters in close vicinity to known T cell-expressed promoters are surrounded by high levels of H3K27ac and intermediate levels of H3K4me1 (Figure 4A), two histone modifications that demarcate open chromatin around promoters and enhancers. Interestingly, "non-annotated" clusters (distal to GencodeV10 promoter) displayed a similar epigenetic signature (albeit at a lower level), which strongly indicates functionality for a large fraction of genomic elements associated with such CAGE peaks (Figure 4A). To highlight the potency of Heliscope CAGE to detect novel promoters in T cells, we performed 5'RACE PCR for several examples where annotated promoter and CAGE TSS differed. At several selected loci, transcripts of known genes emerging from CAGE TSS were identified (Figure 4B, Supplementary Figure S3A). In addition to the Treg-specific TSS for RTKN2 mentioned above, a second Treg-exclusive non-annotated upstream TSS was found that produced a spliced RNA (Supplementary Figure S3B). Interestingly, novel CAGE TSS were also found at the well-studied Treg signature genes *CTLA4* and *FOXP3* (Figure 4C). The Treg-specific TSS upstream of *CTLA4* yielded *inter alia* transcripts that extended into the annotated *CTLA4* gene and potentially encode for a novel CTLA4 isoform. All sequenced clones derived from 3'- and 5'-RACE PCR of the *CTLA4* upstream TSS are displayed in Supplementary Figure S3C. At the *FOXP3* locus, a conserved cluster of additional Treg-specific TSS was found approximately 1kb upstream of the annotated *FOXP3* promoter. 5'-RACE from the native promoter/5'-untranslated region confirmed spliced transcripts extending to this novel upstream TSS cluster. Reporter assays using upstream sequences of the alternative *FOXP3* TSS but not the novel *CTLA4* TSS showed high luciferase activity when transfected in Jurkat cells, suggesting general activity of the newly discovered *FOXP3* TSS with the capacity to increase transcription after stimulation (Figure 4D). In summary, these results demonstrate that non-annotated CAGE clusters in T cells can indeed represent functional promoters. Intriguingly, we also identified TSS with Treg-exclusive expression as well as new TSS in proximity of well-studied key Treg genes. The biological significance of these novel transcripts will be subject of further research.

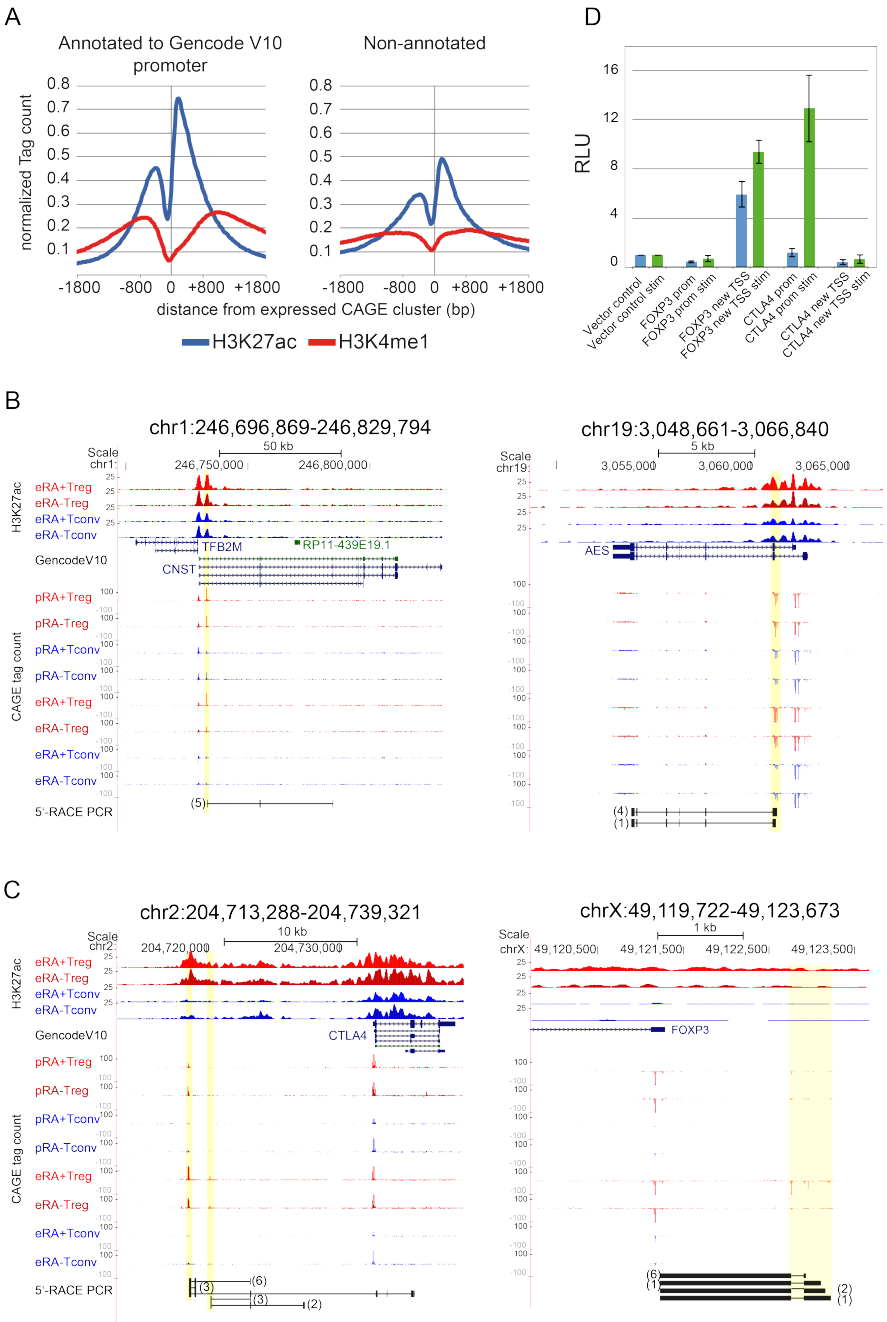

Figure 4: Novel CAGE clusters. (A.) Histogram of histone modifications in the vicinity of CAGE clusters. Expressed clusters (expression >1 tag per million) of all *in vitro* expanded subpopulations were merged and then separated in annotated and non-annotated to a GencodeV10 promoter. H3K4me1 and H3K27ac ChIP-seq tag counts of *in vitro* expanded subpopulations were combined and then annotated to expressed gene promoter-associated or non-annotated CAGE clusters. (B.)-(C.) 5'-RACE confirms the presence of spliced transcripts from novel CAGE TSS. UCSC browser graphics are shown for the indicated genomic positions including H3K27ac signal of expanded populations, GencodeV10 gene annotation, CAGE signals for all eight T cell subpopulations and aligned results from 5'-RACE-PCR. Numbers of sequenced clones are indicated in brackets. (D.) Relative luciferase activity of the new *FOXP3* and *CTLA4* TSS.

Recent studies demonstrated the possibility to identify key regulators in transcriptional regulation by epigenetic "fingerprinting" of cell type-specific enhancers (Pham et al. 2012). Hence, we initially analyzed active enhancers characterized by promoter-distal enrichment of H3K27ac in eRA+Treg and expanded $CD4^+CD25^-$ Tconv ("eTconv"; not separated by CD45RA). This identified 6822 and 7112 putative enhancer regions, respectively. *De novo* motif analysis of enhancers yielded a broad panel of highly enriched DNA sequences with frequent similarities to known TF consensus motifs (Supplementary Figure S4). In addition to analyzing complete enhancer sets we also determined motif fingerprints in eRA+Treg and eTconv-specific enhancers (three-fold difference in H3K27ac signal). eTconv enhancers (a total of 2387 regions) were clearly dominated by an ETS, RUNX and IRF motif-signature whereas eRA+Treg enhancers (1963 regions) lacked a significant RUNX motif but showed a JUN/AP1, KLF, STAT5 and Forkhead signature (Figure 5A). Many TFs corresponding to the extracted *de novo* motifs were shown to play crucial roles in Treg development and function, but the global impact of these factors on enhancer architecture in human Treg has not been shown before. To confirm the *in silico*-derived motif signatures we generated TF-binding data using ChIP-seq for the possible regulators ETS1, RUNX1, STAT5 and FOXP3 in eRA+Treg and eTconv. We then evaluated the ChIP-seq signal strengths of the corresponding TF in the cell type-specific enhancers. First, we merged both eRA+Treg- as well as eTconv-derived peaks of the corresponding TF and overlapped the merged set with the respective cell type-specific enhancer regions. We then counted the transcription factor ChIP-seq signals in the overlapping regions. In line with the observed overrepresentation of motifs in specific enhancers, we indeed observed an enrichment of STAT5 ChIP-seq signal in eRA+Treg-specific enhancers (Figure 5B). In contrast, ETS1 and RUNX1 ChIP-seq tags were both highly enriched in eTconv enhancers, which parallels their motif distribution. Interestingly, FOXP3 ChIP-seq signals were equally enriched in FOXP3 binding sites overlapping with eRA+Treg- as well as with eTconv-specific enhancers. Taken together, we identified enhancers in eRA+Treg and eTconv and could identify the participation of the key regulators ETS1, STAT5, RUNX1 and FOXP3 in cell type-specific enhancer architecture based on their *de novo* motif signatures.

A

eRA+Treg-specific H3K27ac peaks (1963 regions)

Motiv	P-value	Factor (similarity)
	1e-77	ETS (0.98)
	1e-36	KLF (0.93)
	1e-36	JUN/AP1 (0.96)
	1e-33	FOX (0.85)
	1e-31	STAT (0.97)
	1e-29	IRF (0.89)

eTconv-specific H3K27ac peaks (2387 regions)

Motiv	P-value	Factor (similarity)
	1e-159	ETS (0.96)
	1e-85	RUNX (0.97)
	1e-40	ETS (0.89)
	1e-31	IRF (0.94)
	1e-25	RUNX (0.86)

B

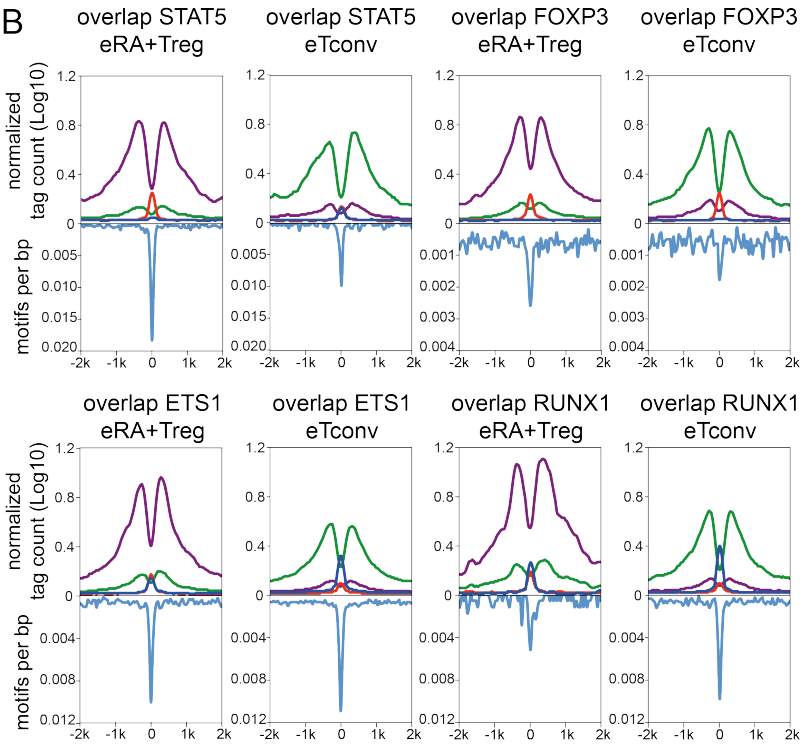

Figure 5

Cell type-specific enhancers. (A.) Motif composition of cell type-specific active enhancers in eRA+Treg compared to eTconv. Shown are extracted *de novo* motifs, their hypergeometric *P*-value and the best matching known motif families (with the similarity score to the best matching known motif in brackets). (B.) ChIP-seq signal strength and corresponding motif enrichment of STAT5, FOXP3, ETS1 and RUNX1 in eRA+Treg- and eTconv-specific active enhancers.

Next, we extended the histone profiling to characterize enhancer elements in all subpopulations. We generated additional maps of H3K4me1 and H3K27ac for eRA+Treg, eRA-Treg, eRA+Tconv and eRA-Tconv from two independent donors that were also used for CAGE profiling. We then isolated distal cell type-specific regions for H3K4me1 and H3K27ac in pairwise comparisons (two-fold difference in enrichment between the two populations to be compared). Enhancers can act over large distances, which makes it difficult to assign distal regulatory regions to the actual target genes. With the matching CAGE expression data now available for every subset we collected all CAGE clusters surrounding specific enhancer regions as well as their expression level (represented by CAGE tag counts). As shown in the bubble plot representations in Figure 6A, subset-specific enhancers defined by H3K4me1 or H3K27ac were significantly associated with higher tag counts in neighboring CAGE clusters of the same cell type ($p<0.001$, Wilcoxon signed rank test), suggesting that these regions indeed represent subset-specific enhancers. Even in highly similar populations (e.g. eRA+Treg vs. eRA-Treg) many enhancers specific for either subpopulation could be identified that were positively associated with neighboring CAGE cluster expression in the same cell type ($p<0.001$, Wilcoxon signed rank test for all comparisons) (Supplementary Figure S5). In summary, we provide the so far most comprehensive enhancer maps of human T cell subpopulations and confirmed their positive correlation to gene expression.

Having determined subset-specific *cis*-regulatory regions from CAGE clusters as well as from H3K4me1/H3K27ac enhancers we systematically determined their motif composition to deduce possible regulators. Different classes of *cis*-regulatory elements (promoters, poised enhancers, active enhancers) varied in their motif composition (Supplementary Figure S6). We then created a non-redundant combined atlas of enriched motifs of *cis*-regulatory regions for eRA+Treg versus eRA+Tconv subpopulations and analyzed which TFs are differentially expressed (adjusted p-value<0.05, Figure 6B). We observed cell type-specific overrepresentation of JUN, PAX, NFE, KLF and forkhead motifs in eTregRA+ and E2F, CREB, TCF, GTF and Helix-loop-Helix motifs in eRA+Tconv. Notably, many specific signature motifs had a corresponding regulated TF candidate- JUNB/FOSL2 (JUN motif), BATF (PAX motif), BACH1 (NFE motif), KLF2/3/7/19 (KLF motif), MAF (MAF motif), FOXP3 (FOX and FOXP motif) in the eRA+Treg set and E2F1/7/8 (E2F motif), CREB2L (CREB motif), TCF7/19 (TCF motif) and ARNTL/AHR/MXD3/ID2 (potentially binding bHLH motif) for the eRA+Tconv set of motifs. Still, we are aware that not all motifs can be explained by differential expression of a TF as expression and activity of some TF classes is regulated by mRNA stability, protein degradation or posttranslational modifications like acetylation or phosphorylation. However, with respect to ChIP-seq confirmation of motif

signatures described before, these results provide a new and comprehensive framework to systematically identify key regulators of gene expression in human T cell subpopulations.

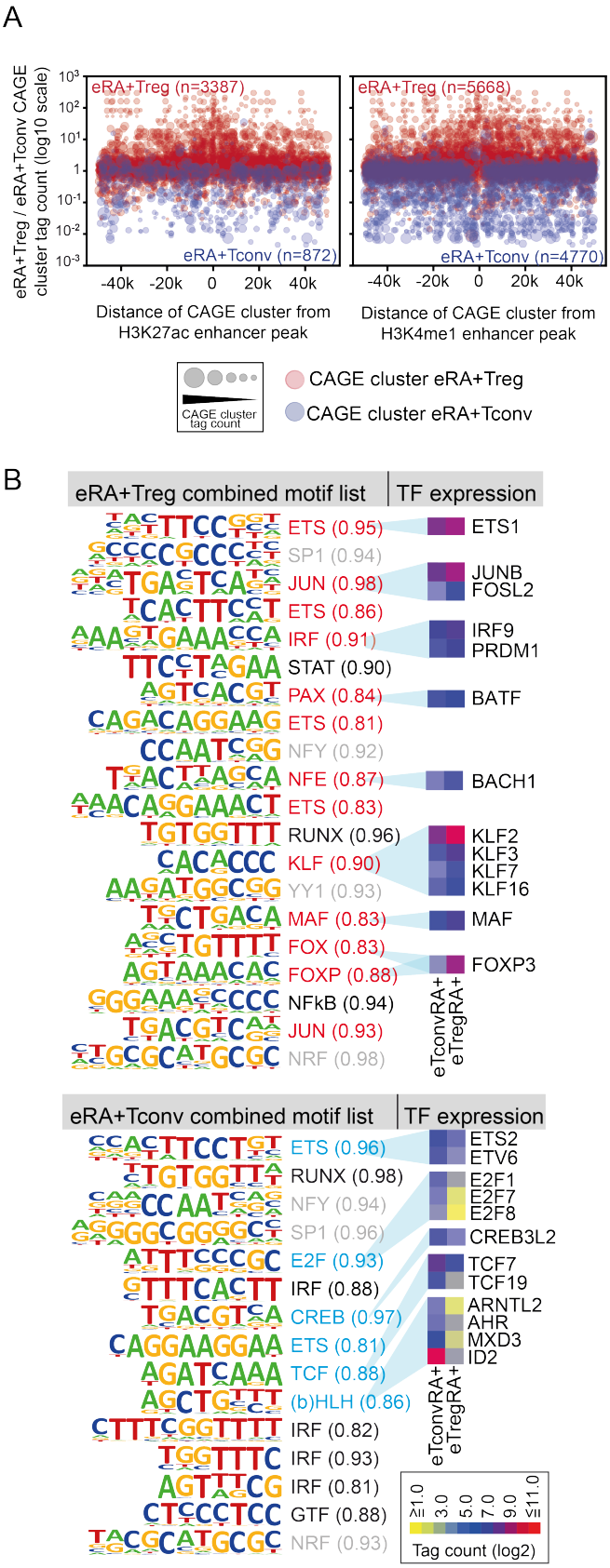

Figure 6

Figure 6:Correlation of cell type-specific enhancers to gene expression and their potential regulators. (A.) Bubble plot representation of CAGE-TSS activity around eRA+Treg vs eRA+Tconv enhancer candidate regions showing at least two-fold different H3K27ac or H3K4me1 signals. The bubble plots encode three quantitative parameters per CAGE cluster: distance from the putative enhancer, log10 of fold change in CAGE cluster tag count between eRA+Treg and eRA+Tconv (Y-axis) and the absolute CAGE cluster tag count of the T cell subset with the highest expression level (bubble diameter). There is a clear bias for the putative enhancer elements to associate with CAGE clusters upregulated in the corresponding cell type ($P<0.001$, Wilcoxon signed rank test). (B.) A non-redundant combined set of *de novo* motifs from CAGE clusters and enhancers in eRA+Treg vs. eRA+Tconv. Shown are motifs with a highly similar match to a known TF motif. Absolute tag counts (log2 transformed) of differentially expressed TFs matching a *de novo* motif are presented as colored boxes with yellow, blue and red representing low, intermediate and high expression, respectively.

Discussion

By using powerful genome-wide approaches we were able to analyze the gene-regulatory landscape of human T cell subpopulations in an unprecedented depth. Recently, human $CD4^+CD25^{high}$ Treg were described as heterogeneous, with $CD45RA^-$ memory Treg expressing TFs and cytokines of other proinflammatory lineages in contrast to $CD45RA^+$ naïve Treg (Hoffmann et al. 2006b; Ayyoub et al. 2009; Miyara et al. 2009; Schmidl et al. 2011; Hansmann et al. 2012). In addition, several murine *ex vivo* Treg populations showed specific gene expression characteristics in dependence of their tissue origin and homing receptor repertoire (Feuerer et al. 2010; Duhen et al. 2012). In line with these observations, we delineated differences in the expression of effector molecules, homing receptors and transcription factors of other T cell lineages between naïve and memory Treg subpopulations. Interestingly, upon *in vitro* expansion, eRA+Treg do not dramatically change their Treg-specific effector molecule repertoire but alter the expression of several homing receptors despite the observation that this population retains a stable Treg phenotype even after extensive *in vitro* expansion (Hoffmann et al. 2006b). These observations should be carefully considered upon adoptive transfer of T cells and are valuable for future analysis of cell fate, plasticity as well as migratory potential of eTreg in clinical applications. Apart from differences we also defined shared expression patterns in pRA+Treg and pRA-Treg. In addition to well-known key Treg genes we also identified unanticipated candidate genes that share the unique Treg-signature expression pattern. Among these genes were transcription factors, enzymes and surface proteins, but further work is required to determine their role in Treg biology.

Using modern molecular methods becomes indispensable to understand the complexity of our genome. Recently, intensive CAGE and RNA sequencing studies in human cells revealed tens of thousands undiscovered TSSs that represent promoters of functional protein coding and

noncoding transcripts (FANTOM5 main paper(Djebali et al. 2012). Strikingly, most gene loci produce several transcript isoforms simultaneously. Isoform transcription can be driven by different regulatory inputs and potentially be translated into alternative peptides, which can have significant impact on the phenotype of a cell. Here, we validated so far undescribed TSSs as new alternative promoters of known genes and could even identify new transcripts at the intensively studied *CTLA4* and *FOXP3* loci. Although their biological significance has to be evaluated, the CTLA4 and FOXP3 TSS were Treg-specific, and the FOXP3 TSS region showed general activity in transient transfections. So how is cell type-specific expression of these TSS achieved? Despite the lack of STAT5, ETS1, RUNX1 or FOXP3 binding in the vicinity of the new CTLA4 or FOXP3 TSSs, *de novo* motif signatures suggest auxiliary TFs of the IRF, NFE, JUN, KLF, MAF, PAX and NFkB family that could drive TSS expression. Interestingly, previous comparative DNA methylation studies in Treg and Tconv cells demonstrated hypermethylation of these two TSS-regions in all analyzed hematopoietic cells except Treg (Schmidl et al. 2009). This suggests epigenetic silencing of these elements in other cell types but their activation in Treg upon DNA demethylation.

Enhancers display an even greater diversity than promoters. They are distributed in a cell type-specific manner throughout the genome and designated by the deposition of H3K4me1 and H3K27ac (Heintzman et al. 2009; Creyghton et al. 2010; Rada-Iglesias et al. 2011). By comparative analysis of H3K27ac and H3K4me1 patterns, we were able to identify several thousand specific enhancers in eTreg and eTconv. Computational analysis of enhancers allowed us to extract sequences that matched consensus-binding motifs of TFs known to be essential for Treg and Tconv function. In comparisons between eRA+Treg and eTconv these included forkhead, ETS, STAT, IRF, JUN/AP1, KLF as well as RUNX motifs. STAT5 was shown to bind and directly regulate expression of the *Foxp3* gene in mice, a finding that was also suggested for human Treg by indirect evidence (Zorn et al. 2006; Yao et al. 2007). In addition, ETS1 and RUNX proteins were also described to regulate Treg gene expression in mice and humans (Bruno et al. 2009; Kitoh et al. 2009; Mouly et al. 2010; Polansky et al. 2010). We therefore generated the first genome-wide maps of ETS1-, RUNX1- and STAT5-binding in human eRA+Treg and eTconv and confirmed increased binding of the particular TF to whether eRA+Treg or eTconv specific enhancers in correspondence to their motif distribution. At least for *in vitro* expanded cells, this brings forth the observation that RUNX1 and ETS1 were more associated with eTconv enhancers than eRA+Treg enhancers on a global scale in contrast to their established significance in Treg development and function. Further, by combining H3K27ac and FOXP3 ChIP-seq, we observed FOXP3 occupancy at eTregRA+-specific enhancers, but also at sites that are potential enhancers in eTconv. This raises the possibility that FOXP3 controls the expression of Tconv-associated genes by the occupation of their distal enhancers. In summary, we generated the so far most

comprehensive dataset on TSS location, gene expression, TF binding, and enhancer profiling in human T cell subpopulations. Moreover, we could show that it is possible to extract key regulators based on their motif "fingerprints" in enhancers as described recently for a monocyte differentiation model (Pham et al. 2012).

Finally, we hope that our dataset ameliorates the clinical application of human Treg. In addition to gene expression studies, genome-wide TF binding and histone modification data will be useful to evaluate mechanisms as well as effects of drugs that modulate signaling pathways or the epigenetic status of T cells. As an example, different classes of HDAC inhibitors (HDACi) were described to have varying effects on immune cells including Treg as well as Tconv (Akimova et al. 2012). Histone deacetylase (HDAC) complexes modify gene expression by controlling the acetylation of histones or other regulatory proteins including STAT5 or FOXP3. Hence, with global maps of histone acetylation as presented here, the impact of different HDACis on the acetylation status of immunologically relevant genes in Treg and Tconv could be studied. This could help to improve *in vitro* expansion strategies and, hence, to improve the potential of therapeutic cell products.

Acknowledgement

We thank Ireen Ritter, Johanna Raithel, Dagmar Glatz, Lucia Schwarzfischer-Pfeilschifter, Monique Germerodt and Rüdiger Eder for excellent technical assistance. The project was funded by grants from the Deutsche Forschungsgemeinschaft to MR and PH)

Authorship Contributions

CS performed experiments, computational analyses and wrote the manuscript, PH, RA, and ME contributed to planning, supervision and manuscript writing, AF, TL, HK, PC and YH organized and performed HeliscopeCAGE sequencing and provided aligned data; MR initiated, planned and supervised the study and contributed to manuscript writing.

Disclosure of Conflict of Interest

The authors declare no competing financial interests.

Correspondence: Michael Rehli, Department of Hematology, University Hospital Regensburg, D-93042 Regensburg, Germany; phone: +49 941 944 5587; E-mail: michael.rehli@ukr.de

Supplementary data

Supplementary Figures

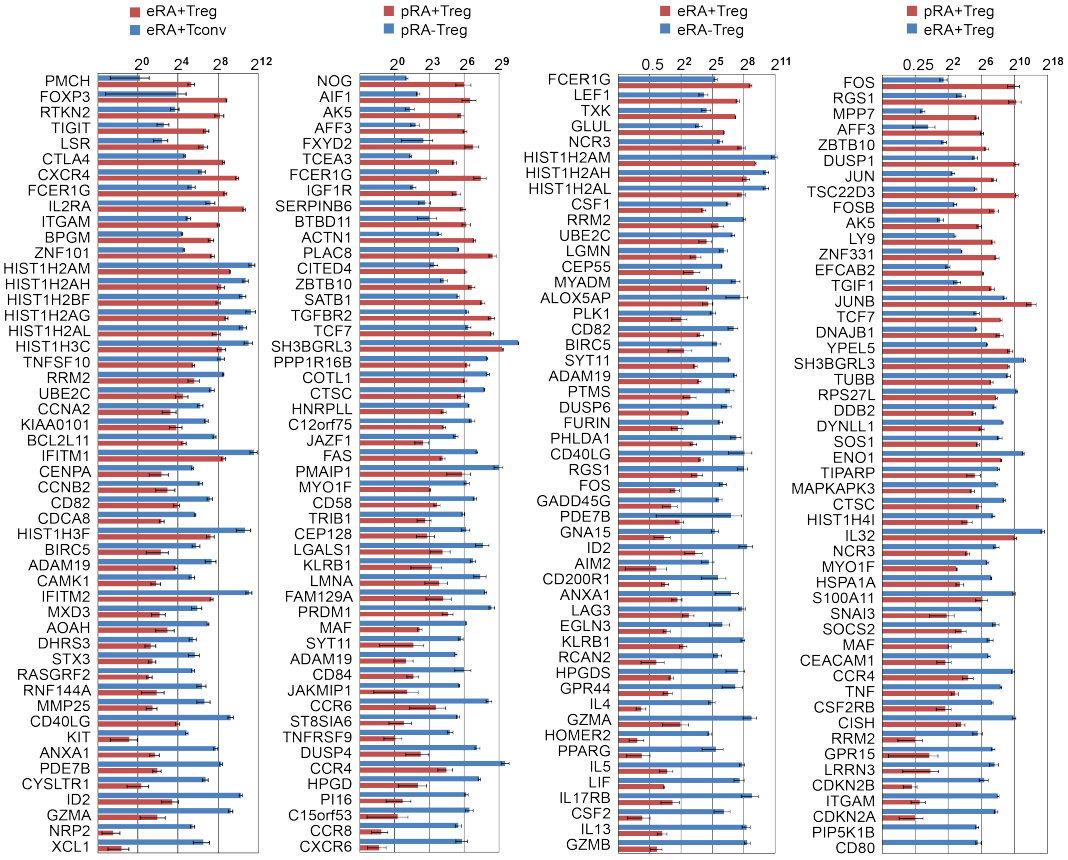

Supplementary Figure S1: Heliscope CAGE-based digital expression analysis of T cell populations. For digital gene expression analysis, tag counts were collected within -500 to +200 bp of GencodeV10 annotated coding gene promoters as outlined in Methods. Digital gene expression data for the top 50 differentially expressed genes of the indicated pairwise comparisons are shown (log2 transformed tag counts).

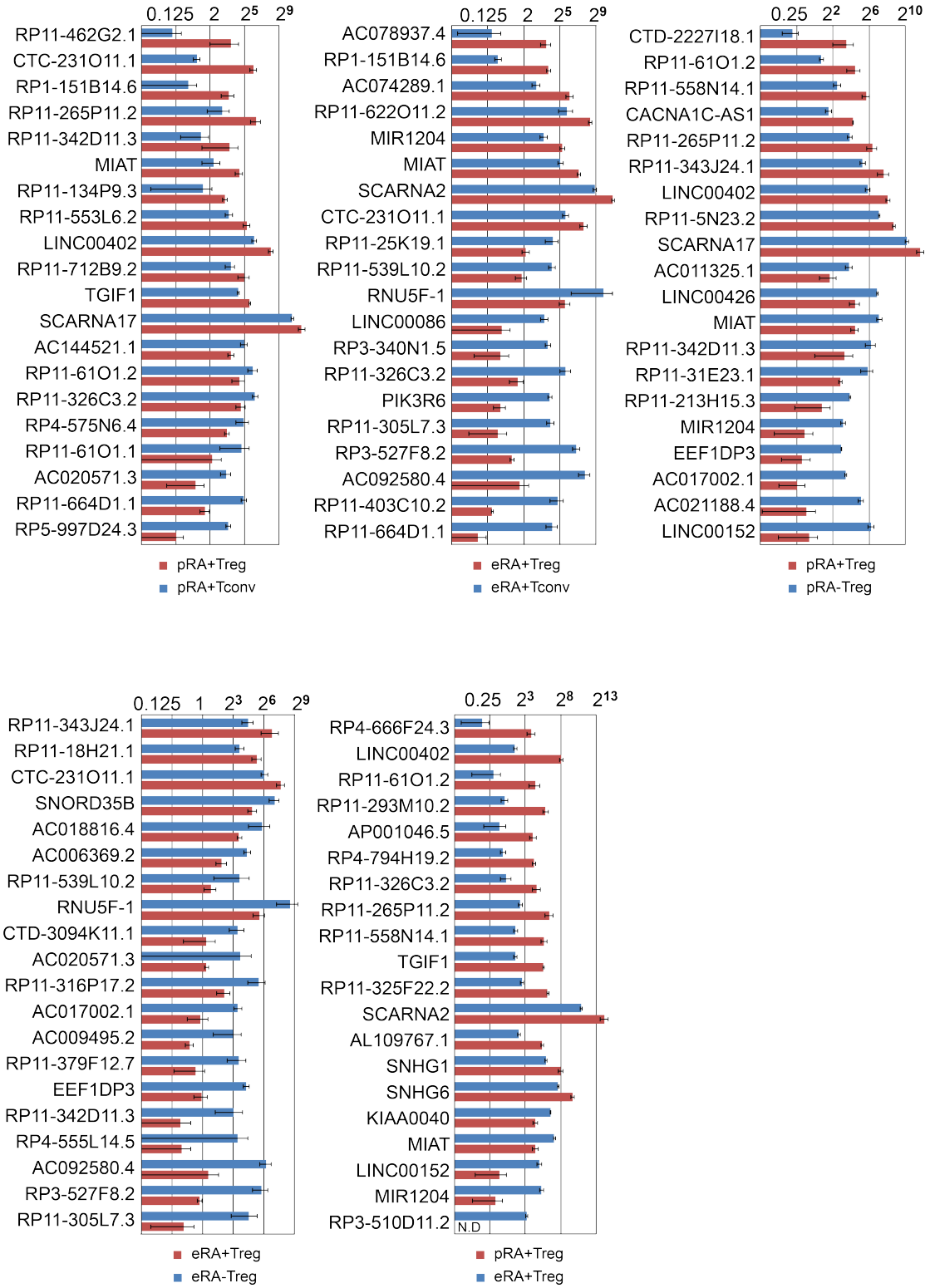

Supplementary Figure S2: Gene expression analysis of noncoding genes. For digital gene expression analysis, CAGE tag counts were collected within -500 to +200 bp of GencodeV10 annotated noncoding gene promoters as outlined in Methods. Digital gene expression data for the top 20 differentially expressed genes of the indicated pairwise comparisons are shown (log2 transformed tag counts).

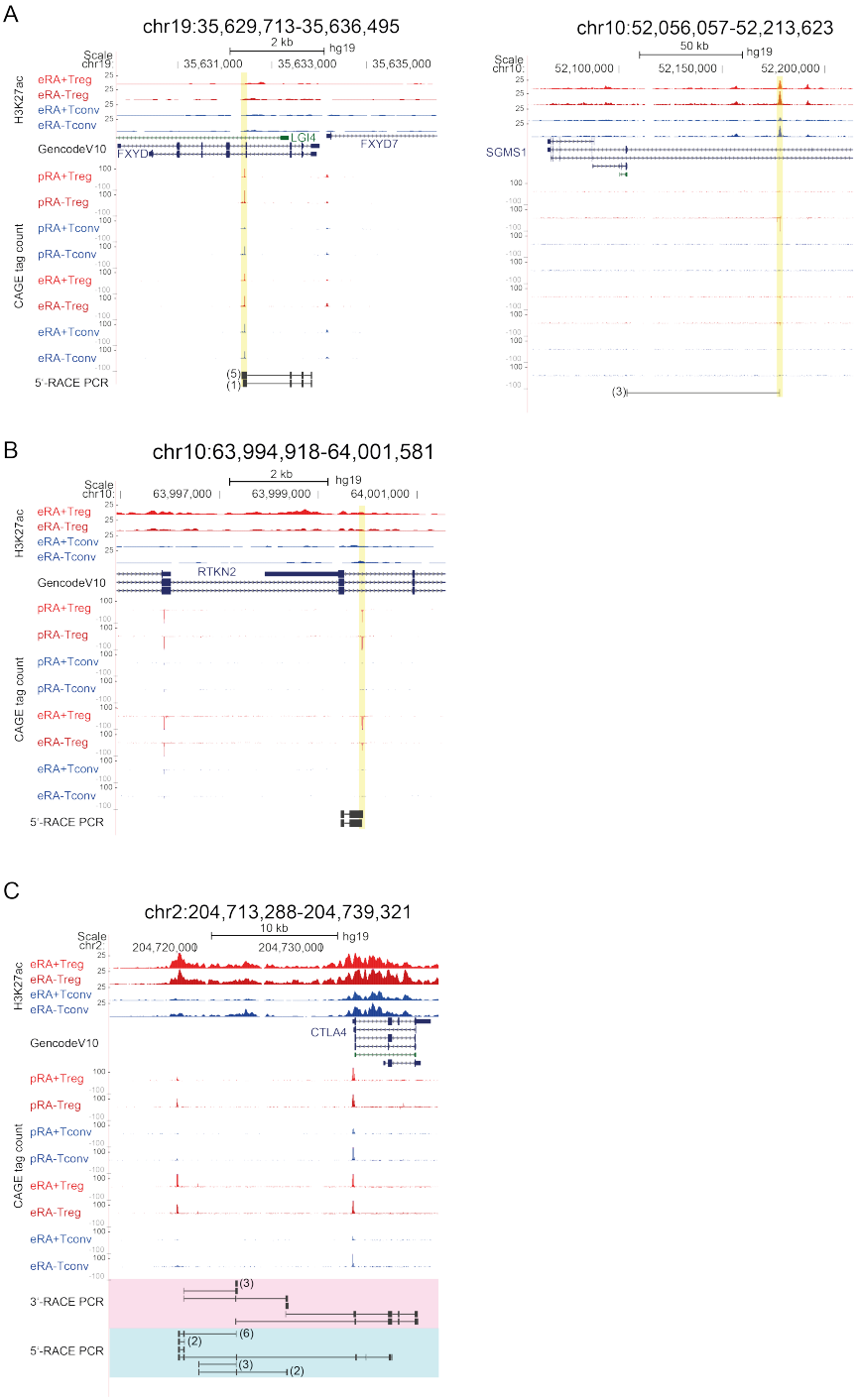

Supplementary Figure S3: RACE-PCR of novel CAGE TSS. (A.)-(C.) 5'RACE-PCR confirms spliced transcript from novel CAGE TSS. UCSC browser graphics are shown for the indicated genomic positions including H3K27ac signal of expanded populations, GencodeV10 gene annotation, CAGE signals for all eight T cell subpopulations and aligned results from 5'-RACE-PCR. Numbers of sequenced clones are indicated in brackets. (C.) Additional 3'-RACE PCR was performed to determine 3'-ends of the transcript emerging from the new CTLA4 upstream TSS.

All distal H3K27ac peaks in eRA+Treg (6822 regions)

Motiv	P-value	Factor (similarity)
	1e-326	ETS (0.97)
	1e-115	IRF (0.95)
	1e-81	RUNX (0.97)
	1e-78	JUN (0.98)
	1e-66	SPI1 (0.79)
	1e-65	IRF (0.88)
	1e-64	IRF (0.87)
	1e-61	FOX (0.84)
	1e-58	ETS (0.77)
	1e-55	ETS (0.72)
	1e-45	FOX (0.78)
	1e-42	STAT (0.92)
	1e-41	KLF (0.96)
	1e-40	ATF (0.79)
	1e-38	? (<0.70 to known)

All distal H3K27ac peaks in eTconv (7112 regions)

Motiv	P-value	Factor (similarity)
	1e-402	ETS (0.98)
	1e-205	ELK (0.91)
	1e-154	RUNX (0.99)
	1e-147	IRF (0.96)
	1e-54	JUN (0.98)
	1e-54	SPI1 (0.78)
	1e-52	IRF (0.92)
	1e-48	FOX (0.83)
	1e-48	? (<0.70 to known)
	1e-45	FOX (0.81)
	1e-41	FOX (0.82)
	1e-35	Dof (0.75)
	1e-35	ct (0.71)
	1e-34	Dof (0.71)
	1e-33	IRF (0.82)

Supplementary Figure S4: Enhancer motif signatures of H3K27ac enhancers. Motif composition of all active enhancers in eRA+Treg and eRA+Tconv defined by H3K27ac. Shown are extracted *de novo* motifs, their hypergeometric *P*-value and the best matching known motif families (with the similarity score to the best matching known motif in brackets).

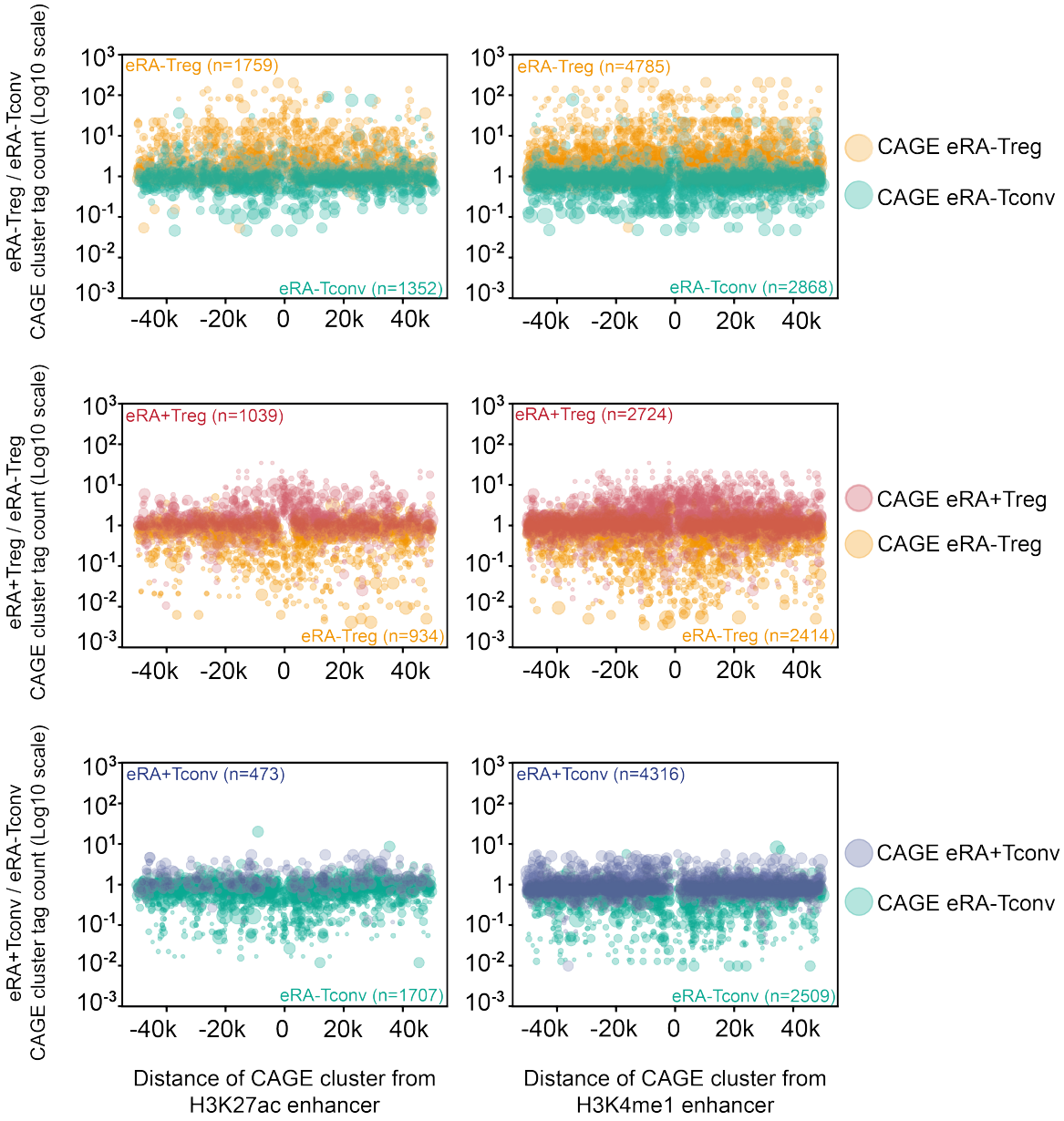

Supplementary Figure S5: Correlation of cell type-specific enhancers to cell type-specific gene expression. Bubble plot representation of CAGE-TSS activity around enhancer candidate regions showing at least two-fold different H3K27ac or H3K4me1 signals. The bubble plots encode three quantitative parameters per CAGE cluster: distance from the putative enhancer, log10 of fold change in CAGE cluster tag count between pairwise compared cell types (Y-axis) and the absolute CAGE cluster tag count of the T cell subset with the highest expression level (bubble diameter). There is a clear bias for the putative enhancer elements to associate with CAGE clusters upregulated in the corresponding cell type (P<0.001, Wilcoxon signed rank test).

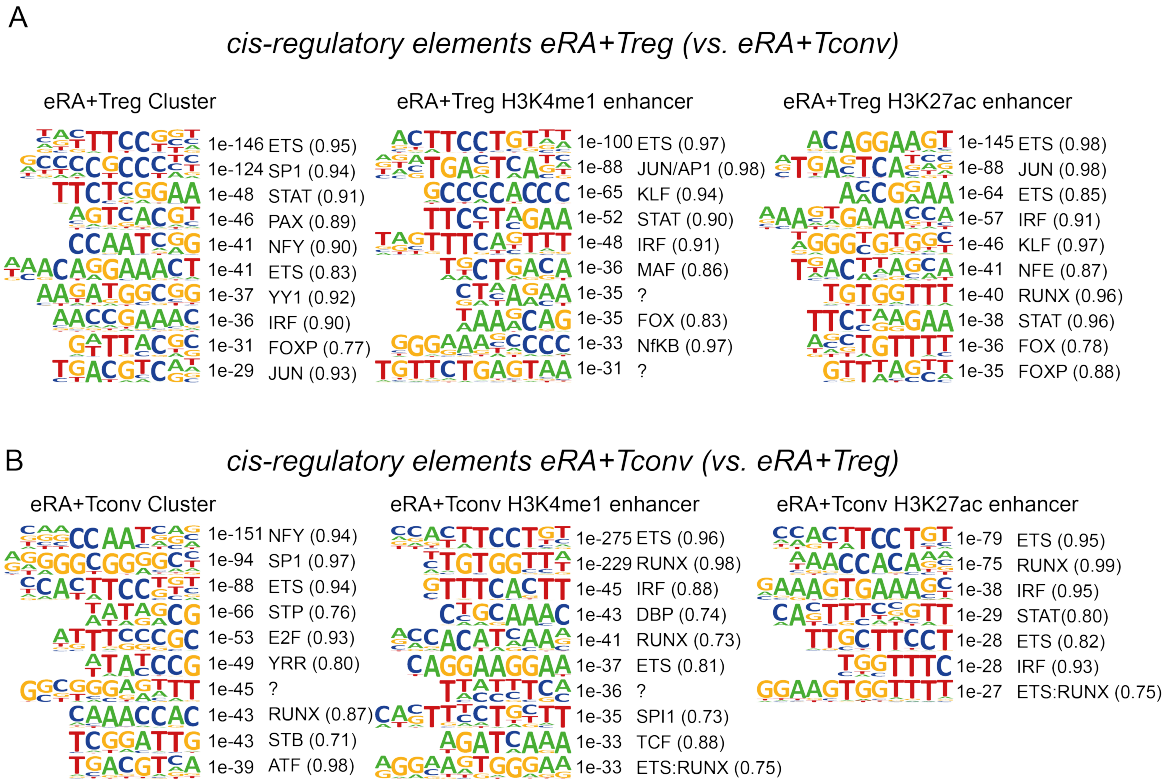

Supplementary Figure S6: Motif signatures in different classes of *cis*-regulatory elements. Motif composition of *cis*-regulatory elements in (A.) eRA+Treg (vs. eRA+Tconv) and (B.) eRA+Tconv(vs. eRA+Treg). Motifs were *de novo* extracted from CAGE clusters, H3K4me1 and H3K27ac enhancers. Shown are extracted *de novo* motifs, their hypergeometric *P*-value and the best matching known motif families (with the similarity score to the best matching known motif in brackets).

Supplemental Tables

Supplemental Table S1

Experiment/Primer name	Sequence 5'-3'
5'RACE-PCR	
CNST_gsp	ACAGAGACTGCAGAACAAGCTTTGGCGC
AES_gsp	GTCACCATCGTGCCCGTTCTTGTCTTCC
FOXP3_gsp	GGTGTGGAAGCCGCAGACCTCTCTCTTC
FXYD1_gsp	AGGTGGAGCGTGGGAGATGTCAGGT
SGMS1_gsp	ACCGATACAGGTACAGCGTGCCAACTATGC
SGMS1_ngsp	GGATGTCTACGCCAATGTTGAGGTGCCC
RTKN2_gsp	CACCACATCAGTATCAAACACATTAGCTCCC
CTLA4_gsp1	TCTGGCCAAATCTGAATCCACGTTCCAC
CTLA4_gsp2	GCAGATGTAGAGTCCCGTGTCC
CTLA4_ngsp1	CAGGACTGCAGCCGAGTATCAG
CTLA4_ngsp2	TCCAAGTGTCAAAAGAATGAACTGG
CTLA4_ngsp3	GCAGCTTCTGGATATGTGATCTTGG
3'RACE-PCR	
CTLA4_gsp	AAAGTTTGTCATCACACCTGCTCTG
CTLA4_ngsp1	ATCACACCTGCTCTGATCCC
CTLA4_ngsp2	ACCAGTTCATTCTTTTGACACTTGG
CTLA4_ngsp3	GCCAATAATACTATGAGGAAGCTGAGGA
cloning of TSS regions	
Promoter_FOXP3_BglII	ACGTCAagatctCTGGCTTGTGGGAAACTGTC
Promoter_FOXP3_NheI	TCGTCAgctagcCCTCAAATATCCTCTCACTCACAG
newTSS_FOXP3_BglII	ACGTCAagatctGTTCTAGTCGTCCAACAACCA
newTSS_FOXP3_NheI	TCGTCAgctagcATCATTAACCTTAGGACCATCACTG
Promoter_Ctla4_NheI	TCGTCAgctagcCCAAGTCTCCACTTAGTTATCCAG
Promoter_Ctla4_BglII	ACGTCAagatctCAGGTCTTCAGGAAGTAGAGCA
newTSS_Ctla4_NheI	TCGTCAgctagcACTCAGAAAGGAAAGGAAACATGG
newTSS_Ctla4_BglII	ACGTCAagatctCGATGTGAAATGCACTGAATCC

4 Discussion

As outlined in the introduction, gene regulation is controlled by the interaction of transcription factors with *cis*-regulatory modules encoded in the DNA sequence. These interactions are governed by epigenetic mechanisms that help to establish and maintain gene expression programs. Basic mechanisms of gene regulation are best studied in model systems that comprise cells emerging from a common progenitor and developing into different functional entities. Ideally, the model system closely resembles the *in vivo* situation to reduce artifacts resulting from experimental conditions or artificial cell systems. Hematopoietic cells emerge from a common progenitor, differentiate into a wide array of specialized cell types and can often be obtained easily from volunteers by leukapheresis and FACS. This makes them a suitable system to analyze differential development and gene expression as well the contribution of epigenetic mechanisms to these processes. With the possibility to obtain highly pure human regulatory and conventional T cells (Treg and Tconv, respectively) and the technologies to expand them *in vitro* (Hoffmann et al. 2004; Hoffmann et al. 2006b), we used Treg and Tconv to obtain insights into basic mechanisms of differential gene expression (chapters 3.1; 3.2; 3.3; 3.4; 3.5). This included the application of high-throughput analysis of DNA methylation, genome-wide *in vivo* DNA-protein interactions and gene expression. Our findings shed light into the role of DNA methylation at distal regulatory regions and helped to identify molecular characteristics, plasticity, stability as well as heterogeneity of T cell populations (chapters 3.1; 3.3; 3.4; 3.5). Moreover, integrated analysis of regulatory features allowed the prediction of key factors involved in global regulation of gene expression in Treg and Tconv (chapter 3.5). These insights are of immediate interest to understand Treg biology in the perspective of regulatory T cells' non-redundant role in maintaining the integrity of the immune system and their prospective application in clinical settings.

4.1 General insights into cell type-specific gene regulation in Treg and Tconv

4.1.1 Distribution of differential DNA methylation in regulatory and conventional T cells

At the beginning of this thesis, most studies on DNA methylation investigated the methylation status of CpG islands (CGIs) in malignant cells (Singal and Ginder 1999; Issa 2004). Aberrant DNA methylation in cancer can occur tumor-specific at many CGIs and is involved in silencing of tumor suppressor genes (Singal and Ginder 1999; Toyota et al. 2001). Hence, analysis of DNA

methylation in cancerous cells is intensively studied to classify cancer types, develop markers for early diagnosis, predict cancer progression and analyze the molecular mechanisms of the disease (Singal and Ginder 1999; Issa 2004; Stumpel et al. 2009; Yan et al. 2012). Until few years ago technical issues restricted DNA methylation analyses to CpG-rich regions, as CpG-content independent genome-wide DNA methylation analysis techniques were only recently established and affinity based methods captured only CpG-dense regions effectively (Suzuki and Bird 2008).

Because of the very limited knowledge about the role of DNA methylation patterns at non-promoter regions in normal cell development, we investigated locus-wide DNA methylation differences between Treg and Tconv (chapter 3.1). To this end, we adapted our methyl-CpG-immunoprecipitation (MCIp) assay to recover both the methylated (mCpG) and unmethylated (CpG) DNA fractions from Treg and Tconv (Gebhard et al. 2006; Schilling and Rehli 2007; Schilling et al. 2009). Comparative hybridization of the precipitated DNA pools from these two cell types on custom microarrays allowed the identification of more than 130 differentially methylated regions (DMRs) at 69 loci representing regions of differentially expressed genes between Treg and Tconv (chapter 3.1). We then validated target regions with mass spectrometry based DNA methylation analysis (MassARRAY) and also evaluated the methylation status of the identified DMRs in various hematopoietic cells including CD8+ T cells, CD56+ natural killer cells, CD14+ monocytes, CD19+ B cells and CD34+ hematopoietic progenitor cells. The DMRs we discovered were mostly well defined and covered several hundreds of base pairs. However, in case of the *FOXP3* locus hypomethylation in Treg stretched over the whole locus, which might reflect the exclusive expression of this transcription factor in Treg (chapter 3.1). Interestingly, most DMRs were not highly conserved, did not overlap with an annotated promoter and had a low to intermediate CpG content. These observations suggest that most promoter and CpG island-centered experiments miss the majority of sites that are differentially methylated. In fact, *in vitro* models of neural progenitors differentiating into neurons showed that DNA methylation changes at promoters are rare events in late differentiation steps and might not be the prevalent mechanisms to control gene expression (Mohn et al. 2008). In line with this, recent genome-wide DNA methylation studies support the finding that DNA methylation is most dynamic at promoter-distal sites of lower CpG-content (Meissner et al. 2008; Stadler et al. 2011).

4.1.2 DMRs are associated with histone marks, novel promoters and enhancer function

Histone modification profiling can be used to classify the function of DNA elements (Ernst et al. 2011). Histone 3 Lysine 4 trimethylation (H3K4me3) marks actively transcribed regions and virtually all CGIs, whereas enhancers are characterized by the presence of Histone 3 Lysine 4

monomethylation, Histone 3 Lysine 4 dimethylation and Histone 3 Lysine 27 acetylation (H3K4me1, H3K4me2 and H3K27ac, respectively) (Barski et al. 2007; Heintzman et al. 2007; Lupien et al. 2008; Heintzman et al. 2009; Ernst et al. 2011; Rada-Iglesias et al. 2011). We performed chromatin immunopreciptiation (ChIP) coupled to microarray hybridization (ChIP-on-chip) to identify H3K4me1, -me2, and -me3 at the same loci we investigated for differential DNA methylation in Treg and Tconv. Interestingly, we found a significant overlap of "active" H3K4 methylation at DMRs, suggesting the presence of regulatory elements at DMRs. When tested in luciferase reporter assays, many DMRs showed enhancer function that was abrogated by *in vitro* methylation of the reporter construct (chapter 3.1). The observed dynamics in DNA methylation at distal regions, the associated "active" chromatin marks and methylation-sensitive enhancer function suggest a close association of DMRs and lineage-specific gene regulation. In fact, our results illustrated for the first time such a close relation of differential DNA methylation and enhancer function in non-malignant cells.

In support of these findings, Sérandour and colleagues reported that upon FOXA1 activation and its cell type-specific recruitment to enhancers in MCF7 or LNCaP cells these enhancers were associated with an increase of H3K4 methylation and a decrease of DNA methylation (Sérandour et al. 2011). Similar reports described cell type-specific DMRs as active regulatory regions in *in vitro* differentiation models of neuronal progenitors (Stadler et al. 2011) and glucocorticoid-responsive cell lines (Wiench et al. 2011). On a genome-wide level, DNA methylation is inversely correlated with the binding of transcription factors, further supporting the view that DMRs often represent regulatory regions (Lister et al. 2009; Stadler et al. 2011). It is still not completely understood how and to what extent DNA methylation controls regulatory regions and how differential DNA methylation patterns are established. However, *in silico* analysis of Treg DMRs revealed an overrepresentation of specific transcription factor (TF) consensus sites including CREB/ATF and STAT5 (chapter 3.1). These factors are essential for FOXP3 expression in Treg and might contribute to the establishment of DMRs (Fontenot et al. 2005a; Kim and Leonard 2007). DNA hypomethylation at enhancers could result from the blocking of DNA methyltransferases (DNMTs) by bound transcription factors (TFs), leading to passive demethylation during DNA replication. In fact, many TFs do not have a CpG in their consensus site and might even bind to their recognition sequence in the close vicinity of methylated DNA, which could promote passive demethylation. In contrast to this consideration, the discovery of 5-hydroxymethylcytosine as an intermediate in active DNA demethylation linked this mark to *cis*-regulatory regions (Stroud et al. 2011; Szulwach et al. 2011; Sérandour et al. 2012). This implies active removal of DNA methylation at enhancers. Moreover, DNA demethylation at distal regions was observed in proliferation-free differentiation systems, which supports active DMR establishment (Klug et al. 2010). In case of the differentially methylated *Foxp3* enhancer (also

known as conserved noncoding sequence 2 [CNS2] or Treg-specific demethylated region [TSDR]), DNA methylation blocks the binding of Runx, ETS-1 and CREB/ATF proteins *in vitro* (Floess et al. 2007; Kim and Leonard 2007; Polansky et al. 2010; Zheng et al. 2010). It is unknown if another DNA methylation-insensitive TF is needed to "open" the enhancer, or if the *in vivo* situation allows binding of these TFs alone or in cooperation with other TFs as discussed in the introduction.

Consistent with our *in silico* analysis is the notion that DNA elements can autonomously determine their DNA methylation status depending on the binding of transcription factors (Lienert et al. 2011). The establishment of DNA hypomethylation was not a function of CpG density, but was based on the presence of TF consensus motifs (Lienert et al. 2011). More mechanistic studies and temporal investigations of changes in DNA methylation will be needed to resolve these complex processes that establish DNA methylation patterns. It would be of great interest if differential DNA methylation was a general hallmark of important cell type-specific enhancers. Genome-wide DNA methylation profiles could then be used to identify specific regulatory regions in any cell type. DNA methylation as a tool for enhancer detection would be advantageous compared to histone modification analysis, because DNA is more stable and, in addition, easier to isolate than chromatin for histone ChIPs. DNA for sensitive downstream applications such as mass spectrometry-based DNA methylation analysis can even be obtained from fixed cells as we demonstrated for FOXP3-stained cells (chapter 3.3).

Obviously the custom microarray for DMR analysis was designed to include differentially expressed genes between Treg and Tconv and is therefore biased towards functionally important regions. Still, it is noteworthy that we found several DMRs at virtually all Treg signature genes including *FOXP3*, *IL2RA*, *CTLA4*, *IKZF2* and *LGAS3* and several Tconv-specific genes including *IFNG* and *CD40LG*. Some of the DMRs covered known enhancers at the *IFNG* and *FOXP3* locus (Floess et al. 2007; Schoenborn et al. 2007a). In addition, by using transient reporter gene assays, we confirmed new potential enhancers at the *IL2RA*, *LRRC32*, *LGALS3*, *TP53INP1*, *PPP1R3F* (the gene upstream of *FOXP3*), *CD40LG*, *IL-26*, *ID2* and *SEPT9* genes. Some DMR-enhancer assays were inactive when transfected into Jurkat cells. This may be caused by the absence of factors in Jurkat cells that would be required for Treg-specific regulatory regions to be active. Thus, transfection of primary cells would be a promising strategy to clarify whether these regions are potential enhancers or not. Another challenge is to link an enhancer to its target promoter, since enhancers can act over long distances and do not necessarily interact with the closest promoter (Lettice et al. 2003; Spilianakis and Flavell 2004; Lomvardas et al. 2006). This is certainly of interest for the putative enhancer located upstream of the FOXP3 gene in the *PPP1R3F* locus. PPP1R3F is not differentially expressed between Treg and Tconv (chapter 3.1). We could demonstrate that in Treg the PPP1R3F enhancer shows H3K27ac, H3K4me1 and

the binding of STAT5 in a Treg-specific manner (chapter 3.5). This suggests that this enhancer contributes to the regulation of another gene than *PPP1R3F*, e.g. *FOXP3*. This hypothesis could be tested with the 3C technique to confirm the physical interaction of the FOXP3 promoter with this upstream DMR (Dekker et al. 2002). However, preliminary 3C experiments on primary cell populations are technically challenging and did not yield evaluable results (data not shown).

We also noted an association of DMRs with H3K4me3 at several loci including *CTLA4* and *RTKN2*. This histone modification is normally associated with active transcription or CGIs, but was rarely connected with enhancers so far (Heintzman et al. 2007; Deaton and Bird 2011; Pekowska et al. 2011). Although few DMRs cover an annotated promoter, there is still the possibility that some harbor transcription start sites (TSSs) of previously unrecognized cell type-specific transcripts because especially Treg were underrepresented in expressed sequence tag/mRNA sequencing and annotation projects due to their scarcity in blood. As part of the FANTOM5 project we could generate global single base pair resolution maps of TSSs in Treg and Tconv by the application of cap analysis of gene expression (CAGE) adapted to single molecule sequencing (Kanamori-Katayama et al. 2011) (chapter 3.5). This detected in fact TSSs signals at one *CTLA4*- and one *RTKN2*- located DMRs in Treg populations (chapter 3.5). 5'-RACE experiments confirmed *inter alia* spliced transcripts emerging from the TSS located upstream of the native *CTLA4* promoter into the annotated *CTLA4* gene. In case of RTKN2, 5'-RACE PCR confirmed a spliced transcript emerging from the intergenic DMR into the downstream exon. Of note, when compared to more than 1900 FANTOM samples, these TSSs are very specific for Treg cells (the FANTOM consortium, unpublished observations). Epigenetic features mirror the Treg-specific expression of the *CTLA4* upstream TSS: MassARRAY analysis revealed exclusive demethylation in regulatory T cells and was not observed in the panel of other hematopoietic lineages (chapter 3.1). Noteworthy, MassARRAY analysis highlighted striking similarities in the DNA methylation profiles at enhancers between *in vitro* expanded and primary T cell populations, which supports earlier experimental evidence that ascribed phenotypic stability to *in vitro* expanded CD45RA+ naïve Treg that were used in these experiments (Hoffmann et al. 2004; Hoffmann et al. 2006b).

Taken together, we identified more than 130 DMRs at immunologically relevant genes in Treg and Tconv. In line with recent publications, we could show that the majority of DMRs were located inter- or intragenic and had a low CpG content (chapter 3.1). Of capital importance was the finding that DMRs were associated with active chromatin marks and showed DNA methylation-sensitive enhancer activity. In two confirmed cases DMRs harbored previously unrecognized cell type-specific TSSs. MassARRAY generated DNA methylation profiles demonstrated similarities between expanded and primary Treg and further showed that DMRs demethylated in Treg or Tconv were normally hypermethylated in progenitor cells and other

hematopoietic lineages. Our results suggest that differential DNA methylation marks enhancers and regulates lineage-specific gene expression. Moreover, we established a methylation "fingerprint" that identifies regulatory T cells on a molecular basis.

4.1.3 Enhancer profiling identifies key regulators in T cell subpopulations

With their rapid improvement and decreasing costs, next generation sequencing technologies became the method of choice for systematic analysis of gene regulation. Global analysis of chromatin states, transcription start sites and transcription factor binding have increased our understanding of the organization and regulation of our genome and is crucial to understand basic principles of biology and disease (Bernstein et al. 2012). As outlined in the introduction, enhancers contribute substantially to gene regulation in complex multicellular organisms. They are more diverse than promoters, activated in a cell type-specific manner and can be dissected by biochemical properties including DNase hypersensitivity as well as the deposition of certain histone modifications (Heintzman et al. 2009; Bernstein et al. 2010; Bernstein et al. 2012; Thurman et al. 2012). "Poised" enhancers are associated with the distal deposition of H3K4me1, whereas "active" enhancers were described to be associated with H3K27ac among other histone modifications (Barski et al. 2007; Heintzman et al. 2007; Creyghton et al. 2010; Rada-Iglesias et al. 2011). To extend our restricted ChIP-on-chip based approach to profile histone modifications in Treg and Tconv, we generated genome-wide maps of H3K4me1 and H3K27ac in *in vitro* expanded CD4+CD25highCD45RA+ naïve Treg (eRA+Treg), CD4+CD25highCD45RA– memory Treg (eRA-Treg), CD4+CD25–CD45RA+ naïve Tconv (eRA+Tconv) and CD4+CD25–CD45RA– memory Tconv (eRA-Tconv) (chapter 3.5). Thereby we were able to identify thousands of putative enhancers in every cell type. By pairwise comparisons we could also identify several thousand putative enhancers that were cell type-specific for even closely related subpopulations (e.g. eRA+Treg and eRA-Treg). A recent report also described H3K4me1 in Treg and Tconv, and claimed to find many specific putative regulatory regions (Tian et al. 2011). However, uncertainty about experimental conditions in cell purification and ChIP experiments prevented us from integrating these available datasets in our analysis. With enhancers binding general- and cell type-specific transcription factors, they are characterized by an overrepresentation of TF consensus binding sequences (Lupien et al. 2008; Heinz et al. 2010; Hardison and Taylor 2012b; Neph et al. 2012). Hence, by analyzing the sequence composition in *in vitro* expanded Treg- and Tconv-specific enhancers we identified the enrichment of motifs that matched known TF consensus sites including STAT, ETS, RUNX, forkhead, KLF and IRF motifs (chapter 3.5). Factors of these families were already described to be essential for Treg development including STAT5, ETS1, RUNX1 and FOXP3. However, with the exception of FOXP3, the contribution of these factors to global gene regulation was only explored in the murine system or on a very

limited basis in humans (chapter 3.5). Hence, we identified the binding of STAT5, ETS1, RUNX1 and FOXP3 by chromatin immunoprecipitation coupled to next generation sequencing (ChIP-seq) in *in vitro* expanded Treg and Tconv. The binding of the corresponding TF followed their motif distribution in cell type-specific enhancers. This demonstrated, in line with a recent report, that *de novo* motif analyses of regulatory regions can identify key regulators of cellular states (Pham et al. 2012). These analyses revealed also that RUNX1 and ETS1 mainly contributed to eTconv-specific enhancer architecture in contrast to their established function in Treg development and function (chapter 3.5; (Kitoh et al. 2009; Mouly et al. 2010), which highlights the importance of global analysis to understand the contribution to gene regulation of a certain TF. In summary we provide the so far most comprehensive resource concerning TF binding and histone profiling on human T cell populations. This data will improve studies on gene regulation of single genes and allows comparative epigenomic analyses in the context of a growing pool of datasets.

4.2 Plasticity, stability and heterogeneity of human T cell populations

4.2.1 Methodology advancements

In contrast to the murine system where genetically engineered mice allow the easy purification of viable fluorescence-labeled Foxp3+ cells (Fontenot et al. 2005b), FOXP3 staining of human cells requires cell permeabilization and fixation with paraformaldehyde. So far, this procedure hindered any purification of nucleic acids for downstream analysis and prohibited functional cellular essays (Hoffmann et al. 2006a). For such purposes, human Treg cells can be FACS-purified only by the use of surrogate markers, namely by high expression of CD4 and CD25 as well as low or absent expression of CD127 (Hoffmann et al. 2006a; Liu et al. 2006; Seddiki et al. 2006).

However, CD4+CD25+CD127lo cells are not a homogeneous cell population but contain, for example, CD45RA- “memory” and CD45RA+ “naive” subpopulations (Hoffmann et al. 2006b). Interestingly, fractions of human CD45RA- memory Treg can produce proinflammatory cytokines and express the T helper (Th)17 determining transcription factor RORC (Koenen et al. 2008; Ayyoub et al. 2009; Beriou et al. 2009; Miyara et al. 2009; Voo et al. 2009). Also, in the murine system, instability or loss of Foxp3 expression led to increased proinflammatory cytokine production in “ex-Treg” (Xu et al. 2007; Duarte et al. 2009; Komatsu et al. 2009; Zhou et al. 2009c). After *in vitro* expansion of human Treg, CD45RA- cells partially lost FOXP3 expression in contrast to their CD45RA+ naïve counterparts that maintained a stable Treg phenotype

(Hoffmann et al. 2006b; Hoffmann et al. 2009). These observations challenge the paradigm of a stable Treg lineage and raise questions about the stability and proinflammatory potential of Treg subpopulations, especially in view of planned and ongoing clinical trials using Treg cell products for the treatment of patients with autoimmune diseases or for the induction of tolerance after stem cell or organ transplantation. Molecular markers prove to be useful to distinguish stable from unstable Foxp3+ cells. As an example, only the complete demethylation of the *Foxp3* TSDR enhancer is associated with stable Foxp3 expression (Floess et al. 2007; Polansky et al. 2008; Hoffmann et al. 2009; Miyao et al. 2012), and therefore we established DNA methylation "fingerprints" that permit conclusions about the stability and identity of T cell populations (chapters 3.2; 3.3).

To analyze molecular characteristics of human expanded T cell subpopulations we first improved molecular methods to isolate DNA and RNA from human FOXP3-stained FACS-sorted cells (chapters 3.2; 3.4). To revert paraformaldehyde-introduced crosslinks of nucleic acids resulting from commercial FOXP3 staining protocols, the sorted cells were incubated at 60°C in the presence of sodium dodecyl sulfate and salt following the "reverse-crosslinking" procedures in ChIP protocols (Kuo and Allis 1999). Subsequent phenol-based DNA purification yielded DNA of high quality and molecular weight that was suitable for sensitive downstream applications such as DNA methylation analysis with the MassARRAY (chapter 3.2). For RNA isolation of FOXP3-sorted cells the staining procedure had to be adapted. Paraformaldehyde was substituted by ethanol for fixation of the cells, which permitted similar cell purities after FACS-sorting as established commercial staining protocols, but allowed the purification of RNA suitable for qPCR as well as microarray hybridizations (chapter 3.4). We then used these technologies to analyze DNA methylation in FOXP3-maintaining and FOXP3-losing expanded CD4+CD25+CD45RA+ and CD4+CD25+CD45RA- expansion cultures (chapter 3.3) as well as gene expression in CD4+CD25+CD45RA-FOXP3+ and CD4+CD25+CD45RA-FOXP3- subpopulations (chapter 3.4).

4.2.2 DNA methylation analysis and gene expression profiling of T cell subpopulations

We found that DNA demethylation at the *RORC* locus occurred mainly in CD45RA- memory but not CD45RA+ naïve Treg after *in vitro* expansion (chapter 3.3). Demethylation was most prominent at the *RORC* promoter, but occurred also at distal sites. In support of our previous findings (chapter 3.1), some distal DMRs harbored methylation sensitive enhancers. Interestingly, DNA hypomethylation was most pronounced in CD45RA- memory Treg that retained FOXP3 expression. In line with this, most Interleukin (IL)-17-producing cells emerged from this population and showed a DNA methylation pattern almost identical to that of *in vitro* generated IL-17-producing cells (chapter 3.3). Microarray-based gene expression analysis of

expanded memory Treg subpopulations revealed that mainly the CD4+CD25+CD45RA-FOXP3- fraction transcribed large amounts of the Th2 cytokines IL-4, IL-5 and IL-13, but few Th1 and Th17 cytokines (chapter 3.4). We confirmed these findings also on protein levels. Expression of Th2-associated genes including GATA3, MAF, GFI1 and GPR44 as well as the Tconv markers CD127 and CD40LG were upregulated in FOXP3- memory Treg whereas the FOXP3+ fraction expressed much higher amounts of Treg signature genes as well as RORC. Taken together, CD45RA+ Treg retain a stable Treg phenotype even after 3-4 weeks of *in vitro* culture. In contrast, some CD45RA- memory Treg cells can develop into potentially harmful Th-like subsets. Moreover, in our culture conditions, the default pathway of Treg development is a Th2 phenotype upon loss of FOXP3 expression. Experiments in mice with unstable Foxp3 expression or *Foxp3* deletion in Treg show increased Th2 cytokine production, which parallels our findings in the human system (Lin et al. 2007; Wan and Flavell 2007). This conversion was dependent on Gata3 (Wang et al. 2010), although we excluded the contribution of IL-4/STAT6 (a pathway for Gata3 activation (Kaplan et al. 1996; Takeda et al. 1996; Zheng and Flavell 1997)) to Th2 development in our system (chapter 3.4). Nevertheless, GATA3 can be activated through alternative signaling pathways mediated by notch (Amsen et al. 2007). Another possibility is the promotion of Th2 conversion by our culture conditions. Treg expansion cultures receive repetitive TCR stimulation and high doses of IL-2, which activate STAT5 signaling that plays a critical role in Th2 differentiation (Kagami et al. 2001; Zhu et al. 2003; Cote-Sierra et al. 2004). The observed prevalence of IL-17 production and *RORC* hypomethylation in expanded FOXP3+ memory Treg is in line with recent publications. Several research groups ascribed RORC/IL-17 expression to FOXP3+ memory cells *in vitro* and *in vivo* (Ayyoub et al. 2009; Beriou et al. 2009; Miyara et al. 2009; Voo et al. 2009). In contrast, even after extended *in vitro* expansion, CD45RA+ Treg did not show increased RORC expression or IL-17 production (chapter 3.3). Importantly, no demethylation of the *RORC* locus was observed in CD45RA+ Treg, arguing for continuous *RORC* silencing in these cells and for a development of IL-17 producing cells preferentially from memory Treg (chapter 3.3). Yet, a recent publication that suggests the emergence of RORC+ cells from CD45RA+ naïve FOXP3+ Treg (Valmori et al. 2010). These discrepancies may be due to differences in cell isolation strategies or caused by varying extracellular stimuli in the respective experimental setups. However, the high cell purity in our experiments and the observed epigenetic stability of the *RORC* locus in CD45RA+ cells strongly argues against their differentiation into IL-17 producing cells. Yet, the *ex vivo* situation does not resemble the actual situation in humans, and it will be a challenge to address the fate of Treg subpopulations *in vivo*.

4.2.3 Cap analysis of gene expression extends the information content of gene expression analysis

In addition to microarray-based gene expression analysis, participation in the FANTOM (functional annotation of the mammalian genome; http://fantom.gsc.riken.jp) project enabled us to use the HeliscopeCAGE technology. Heliscope CAGE (cap analysis of gene expression adapted to single molecule sequencing) maps genuine transcription start sites (TSSs) at base pair resolution and measures gene expression in a PCR unbiased manner (Kanamori-Katayama et al. 2011). Hence, we subjected three biological replicates of highly purified primary (labeled with prefixed "p") CD4+CD25highCD45RA+ naïve Treg (pRA+Treg), CD4+CD25highCD45RA– memory Treg (pRA-Treg), CD4+CD25–CD45RA+ naïve Tconv (pRA+Tconv) and CD4+CD25–CD45RA– memory Tconv (pRA-Tconv) as well as *in vitro* expansion cultures of every subpopulation to HeliscopeCAGE sequencing (chapter 3.5). In addition to known promoters we found many additional TSSs that were not annotated to a transcript. These TSSs could represent alternative promoters, promoters of undiscovered genes, TSSs of enhancer RNAs or re-capping events (Kim et al. 2010; Kanamori-Katayama et al. 2011; Melgar et al. 2011; Djebali et al. 2012). As already addressed above, we could validate several new TSSs as alternative promoters of known genes by 5'-PCR (chapter 3.5). Of great interest was the discovery of new TSSs at immunologically important genes. In addition to the new *CTLA4* TSS, we were even able to identify novel TSSs at a conserved region upstream of the intensively studied *FOXP3* locus. This TSS produced a spliced transcript that extends into the native FOXP3 mRNA. In addition, reporter gene assays demonstrated strong general activity of this TSS cluster in Jurkat T cells, which was further increased after stimulation. The biological significance of these finding is still unclear and demands further research. However, DNA at this new FOXP3 TSS cluster was demethylated in Treg but hypermethylated in all other tested hematopoietic cells (chapter 3.1), which implies epigenetic regulation and can explain Treg-exclusive expression of this element.

In addition, epigenetic profiles around these new TSSs were similar to the profiles at promoters of known genes expressed in the analyzed T cell populations. Hence, these results imply that a significant fraction of the newly discovered TSSs is indeed functional. This is in line with growing evidence that the transcriptional landscape in mammals is much more complex than anticipated, and that a large fraction of non-annotated transcripts is not "noise" or "junk", but highly regulated and functionally important output (Djebali et al. 2012). It will be essential to explore to what extend alternative promoters produce alternative proteins that might have a completely different function or cellular localization due to additional or lacking domains.

In addition to uncovering new TSSs, CAGE also represents a measure of gene expression in general. We therefore could retrieve differences and similarities in the expression of Treg effector molecules, homing receptors as well as TFs in primary and *in vitro* expanded T cell

subpopulations (chapter 3.5). In line with work of Myara and colleagues we find that pRA-Treg show more Treg-specific effector molecules including GZMA and LAG3 as compared to pRA+Treg (Miyara et al. 2009). This observation supports the suggestion that pRA-Treg contain Treg that are in "active suppression mode". *In vitro* expanded eRA+Treg show similar expression of effector molecules as pRA+Treg. Interestingly, *in vitro* expansion clearly changes the expression of the homing receptor repertoire of eRA+Treg that resemble more pRA-Treg in this aspect (chapter 3.5).

The coexpression of homing receptors and TFs of other T helper cell lineages is thought to drive gene expression programs that allows specialized Treg to localize and suppress immune responses of a certain type (Campbell and Koch 2011). As an example, the Th1-associated transcription factor T-bet was shown to be essential for Treg-mediated suppression of Th1 inflammation in mice (Koch et al. 2009). Expression of T-bet in Treg also induced the expression of the chemokine receptor Cxcr3 that enabled T-bet+ Treg to migrate to sites of Th1 infections. These specialized Th-like Treg subpopulations can be distinguished by homing receptor expression and, although still suppressive *in vitro*, by the expression of TFs and cytokines similar to their Th-counterparts (Duhen et al. 2012). We observed the expression of many Th-associated homing receptors in pRA-Treg including CXCR3, CCR4, CCR6, CCR8 as well as CCR10, which are likely expressed only on different fractions of the pRA-Treg pool and represent in parts the aforementioned specialized pRA-Treg subpopulations. In line with chapter 3.3, we observed higher expression of the Th17-determining transcription factor RORC in memory T cell populations. Moreover, we also detected the Treg-Th2 differentiation phenotype (characterized by the expression profile of Th2-related TFs and cytokines including GATA3, MAF, IL-4, IL-5 and IL-13) ascribed to FOXP3- eRA- "ex"Treg in the TSSs expression of the complete eRA-Treg population (not separated in FOXP3+ and FOXP3- cells), which supports our earlier observations (chapter 3.4).

4.3 Treg in the clinic and future perspectives

In summary, our findings strongly support the use of pRA+Treg cells to generate cell products for clinical applications. Primary RA+Treg can be expanded *in vitro* to sufficient numbers and maintain stable FOXP3 expression and suppressive function in contrast to pRA-Treg that have proinflammatory potential (chapters 3.3; 3.4; 3.5). The adoptive transfer of Treg to cure autoimmune diseases or to prevent transplantation-related diseases such as graft versus host disease (GvHD) is well established in model systems (Cohen et al. 2002; Hoffmann et al. 2002a; Mottet et al. 2003; Nguyen et al. 2007) and is explored in first clinical trials. Ambitious pioneer experiments demonstrated longevity of administered *in vitro* expanded Treg in recipients, and no Treg product-related toxicities were observed (Brunstein et al. 2011a; Edinger and Hoffmann

2011a). In another study, administered Treg were used to prevent GvHD in the absence of pharmacologic GvHD prophylaxis, encouraging further clinical trials (Di Ianni et al. 2011b). However, many of the transplanted T cell pools contained high percentages of FOXP3- cells. Our results suggest that these cells could result from CD45RA- populations that might not be suppressive anymore when transplanted and can cause harm to the recipient by conversion to a proinflammatory Th-like phenotype. Hence, we suggest using CD45RA+ Treg as a starting population for *in vitro* expansion. Another strategy to obtain pure Treg products is the expansion of Treg with mTOR (mammalian target of rapamycin) inhibitors, which favors the expansion of Treg while inhibiting Tconv function and proliferation (Tresoldi et al. 2011). However, mTOR inhibitors also induce FOXP3 in Tconv and a contamination of proinflammatory Th cells in theses expansion cultures cannot be excluded (Edinger and Hoffmann 2011a). Nevertheless, one has to take into account that RA+Treg significantly change the expression of many homing receptors upon *in vitro* expansion, which alters their migratory potential after transplantation and may influence therapy outcomes (chapter 3.5).

In future perspectives, our established DNA methylation markers at key Treg genes could be used to characterize the purity and proinflammatory potential of Treg products before administering them to patients. The requirements for this analysis are solely low amounts of high quality genomic DNA that can be obtained easily from the product (chapter 3.2). DNA methylation fingerprints at lineage-specific TFs as demonstrated for the *RORC* locus (chapter 3.3) might be suitable to estimate the risk of converion to another phenotype. Of course, even small populations of Th cells could expand to large numbers *in vivo*, which may not be predictable with the actual level of knowledge. Nonetheless, possibilities and limitations of molecular fingerprinting in predicting cell identity and stability should be further elucidated. The newly developed methods to extract DNA and RNA from sorted human cells could shed more light into the important topic of cell stability, plasticity and heterogeneity (chapters 3.2; 3.4). For example, the TF Helios was suggested to be only expressed in thymus derived but not in induced Treg (Thornton et al. 2010). By separating Helios+ and Helios- human Treg, one could analyze epigenetic fingerprint and gene expression to specify the differential molecular properties of these two populations. In addition, these techniques could be applied to Treg subpopulations that express transcription factors of other lineages to explore their molecular properties.

Our mapping of DNA methylation, genome-wide transcription factor binding as well as histone modifications (chapter 3.5) open the possibility to explore the effect of drugs that alter signaling pathways or the epigenetic status of a cell. As an example, IL-2 pathway inhibitors that ultimately reduce or abrogate STAT5 binding to its target genes were used in clinical settings to dampen effector T cell responses while retaining Treg function (Sewgobind et al. 2010). With

STAT5 binding sites known in eTreg and eTconv (chapter 3.5) it is possible to address changes in STAT5 binding patterns upon IL-2 pathway blockade and explore for example the differences in sensitivity of Treg and Tconv to the respective treatments. Furthermore, histone deacetylase inhibitors (HDACi) inhibit the action of histone deacetylases (HDAC). The latter control the acetylation status of histone and non-histone proteins including several transcription factors, which has impact on chromatin accessibility or protein stability, dimerization as well as DNA binding, respectively (Akimova et al. 2012). Pan-HDACi can inhibit a broad range of HDACs, but there are also substances that allow the targeted inhibition of specific HDACs. The use of HDACi has varying effects on different immune cells including Treg. In mice, trichostatin A (TSA) increased the number as well as suppressive abilities of Treg *in vivo* and, in conjunction with a short course of low-dose rapamycin, induced permanent, Treg-dependent cardiac and islet allograft survival and donor-specific allograft tolerance (Tao et al. 2007). Different classes of HDACi also increased the suppressive potency of primary and *in vitro* expanded human Treg (Akimova et al. 2010). It is suggested that administration of the epigenetic drugs stabilizes Treg transcription factors including FOXP3 as well as STAT5 and induces the heat-shock response to boost Treg function or survival, respectively (van Loosdregt et al. 2010; Beier et al. 2011). In addition, the expression of key Treg-factors are, at least in part, correlated to the gene's acetylation status as demonstrated for the FOXP3 promoter (Mantel et al. 2006). However, the molecular effects of HDACi application on immunologically important genes were not elucidated yet. With the genome-wide distribution of H3K27ac available now (chapter 3.5), one could study global and local changes in acetylation patterns caused by different HDACi to understand molecular mechanisms that underlie phenotypic changes in treated cell populations.

Taken together, the molecular characterization of Treg and Tconv subpopulations presented here provides insights into basic principles of gene regulation and elucidates the impact of DNA methylation, histone modifications and transcription factor binding on cell type-specific gen expression. Moreover, technical refinements of standard methodologies allowed the detailed analysis of the stability, heterogeneity as well as plasticity of T cell subsets and will be valuable to improve the therapeutic potential of T cell products for clinical applications.

5 References

Akimova T, Beier UH, Liu Y, Wang L, Hancock WW. 2012. Histone/protein deacetylases and T-cell immune responses. *Blood* **119**(11): 2443-2451.

Akimova T, Ge G, Golovina T, Mikheeva T, Wang L, Riley JL, Hancock WW. 2010. Histone/protein deacetylase inhibitors increase suppressive functions of human FOXP3+ Tregs. *Clinical Immunology* **136**(3): 348-363.

Allan SE, Crome SQ, Crellin NK, Passerini L, Steiner TS, Bacchetta R, Roncarolo MG, Levings MK. 2007. Activation-induced FOXP3 in human T effector cells does not suppress proliferation or cytokine production. *Int Immunol* **19**(4): 345-354.

Amano T, Sagai T, Tanabe H, Mizushina Y, Nakazawa H, Shiroishi T. 2009. Chromosomal dynamics at the Shh locus: limb bud-specific differential regulation of competence and active transcription. *Developmental cell* **16**(1): 47-57.

Amsen D, Antov A, Jankovic D, Sher A, Radtke F, Souabni A, Busslinger M, McCright B, Gridley T, Flavell RA. 2007. Direct regulation of Gata3 expression determines the T helper differentiation potential of Notch. *Immunity* **27**(1): 89-99.

Annunziato F, Cosmi L, Santarlasci V, Maggi L, Liotta F, Mazzinghi B, Parente E, Fili L, Ferri S, Frosali F et al. 2007. Phenotypic and functional features of human Th17 cells. *The Journal of experimental medicine* **204**(8): 1849-1861.

Annunziato F, Romagnani S. 2011. Mouse T helper 17 phenotype: not so different than in man after all. *Cytokine* **56**(1): 112-115.

Ansel KM, Djuretic I, Tanasa B, Rao A. 2006. Regulation of Th2 differentiation and Il4 locus accessibility. *Annual review of immunology* **24**: 607-656.

Antov A, Yang L, Vig M, Baltimore D, Van Parijs L. 2003. Essential role for STAT5 signaling in CD25(+)CD4(+) regulatory T cell homeostasis and the maintenance of self-tolerance. *Journal of Immunology* **171**(7): 3435-3441.

Aravin AA, Sachidanandam R, Bourc'his D, Schaefer C, Pezic D, Toth KF, Bestor T, Hannon GJ. 2008. A piRNA pathway primed by individual transposons is linked to de novo DNA methylation in mice. *Molecular cell* **31**(6): 785-799.

Asano M, Toda M, Sakaguchi N, Sakaguchi S. 1996. Autoimmune disease as a consequence of developmental abnormality of a T cell subpopulation. *Journal of Experimental Medicine* **184**(2): 387-396.

Attanasio C, Reymond A, Humbert R, Lyle R, Kuehn MS, Neph S, Sabo PJ, Goldy J, Weaver M, Haydock A et al. 2008. Assaying the regulatory potential of mammalian conserved non-coding sequences in human cells. *Genome Biology* **9**(12).

Avni O, Lee D, Macian F, Szabo SJ, Glimcher LH, Rao A. 2002. T(H) cell differentiation is accompanied by dynamic changes in histone acetylation of cytokine genes. *Nature Immunology* **3**(7): 643-651.

Ayyoub M, Deknuydt F, Raimbaud I, Dousset C, Leveque L, Bioley G, Valmori D. 2009. Human memory FOXP3(+) Tregs secrete IL-17 ex vivo and constitutively express the T(H)17 lineage-specific transcription factor ROR gamma t. *Proceedings of the National Academy of Sciences of the United States of America* **106**(21): 8635-8640.

Ball MP, Li JB, Gao Y, Lee J-H, LeProust EM, Park I-H, Xie B, Daley GQ, Church GM. 2009. Targeted and genome-scale strategies reveal gene-body methylation signatures in human cells. *Nature biotechnology* **27**(4): 361-368.

Ballas ZK. 1984. The use of 5-azacytidine to establish constitutive interleukin 2-producing clones of the EL4 thymoma. *Journal of Immunology* **133**(1): 7-9.

Balwierz PJ, Carninci P, Daub CO, Kawai J, Hayashizaki Y, Van Belle W, Beisel C, van Nimwegen E. 2009. Methods for analyzing deep sequencing expression data: constructing the human and mouse promoterome with deepCAGE data. *Genome Biology* **10**(7): R79.

Banerji J, Rusconi S, Schaffner W. 1981. Expression of a beta-globin gene is enhanced by remote SV40 DNA sequences. *Cell* **27**(2 Pt 1): 299-308.

Bannister AJ, Kouzarides T. 2011. Regulation of chromatin by histone modifications. *Cell research* **21**(3): 381-395.

Bannister AJ, Zegerman P, Partridge JF, Miska EA, Thomas JO, Allshire RC, Kouzarides T. 2001. Selective recognition of methylated lysine 9 on histone H3 by the HP1 chromo domain. *Nature* **410**(6824): 120-124.

Barnes MJ, Powrie F. 2009. Regulatory T cells reinforce intestinal homeostasis. *Immunity* **31**(3): 401-411.

Baron U, Floess S, Wieczorek G, Baumann K, Gruetzkau A, Dong J, Thiel A, Boeld TJ, Hoffmann P, Edinger M et al. 2007. DNA demethylation in the human FOXP3 locus discriminates regulatory T cells from activated FOXP3(+) conventional T cells. *European Journal of Immunology* **37**(9): 2378-2389.

Barski A, Cuddapah S, Cui K, Roh T-Y, Schones DE, Wang Z, Wei G, Chepelev I, Zhao K. 2007. High-resolution profiling of histone methylations in the human genome. *Cell* **129**(4): 823-837.

Beier UH, Akimova T, Liu Y, Wang L, Hancock WW. 2011. Histone/protein deacetylases control Foxp3 expression and the heat shock response of T-regulatory cells. *Current Opinion in Immunology* **23**(5): 670-678.

Beisel C, Paro R. 2011. Silencing chromatin: comparing modes and mechanisms. *Nature reviews Genetics* **12**(2): 123-135.

Bell AC, Felsenfeld G. 2000. Methylation of a CTCF-dependent boundary controls imprinted expression of the Igf2 gene. *Nature* **405**(6785): 482-485.

Bell O, Tiwari VK, Thomä NH, Schübeler D. 2011. Determinants and dynamics of genome accessibility. *Nature reviews Genetics* **12**(8): 554-564.

Bennett CL, Christie J, Ramsdell F, Brunkow ME, Ferguson PJ, Whitesell L, Kelly TE, Saulsbury FT, Chance PF, Ochs HD. 2001. The immune dysregulation, polyendocrinopathy, enteropathy, X-linked syndrome (IPEX) is caused by mutations of FOXP3. *Nature genetics* **27**(1): 20-21.

Beriou G, Costantino CM, Ashley CW, Yang L, Kuchroo VK, Baecher-Allan C, Hafler DA. 2009. IL-17-producing human peripheral regulatory T cells retain suppressive function. *Blood* **113**(18): 4240-4249.

Bernstein BE, Birney E, Dunham I, Green ED, Gunter C, Snyder M. 2012. An integrated encyclopedia of DNA elements in the human genome. *Nature* **489**(7414): 57-74.

Bernstein BE, Kamal M, Lindblad-Toh K, Bekiranov S, Bailey DK, Huebert DJ, McMahon S, Karlsson EK, Kulbokas EJ, Gingeras TR et al. 2005. Genomic maps and comparative analysis of histone modifications in human and mouse. *Cell* **120**(2): 169-181.

Bernstein BE, Mikkelsen TS, Xie X, Kamal M, Huebert DJ, Cuff J, Fry B, Meissner A, Wernig M, Plath K et al. 2006. A bivalent chromatin structure marks key developmental genes in embryonic stem cells. *Cell* **125**(2): 315-326.

Bernstein BE, Stamatoyannopoulos JA, Costello JF, Ren B, Milosavljevic A, Meissner A, Kellis M, Marra MA, Beaudet AL, Ecker JR et al. 2010. The NIH Roadmap Epigenomics Mapping Consortium. *Nature biotechnology* **28**(10): 1045-1048.

Bettelli E, Dastrange M, Oukka M. 2005. Foxp3 interacts with nuclear factor of activated T cells and NF-kappa B to repress cytokine gene expression and effector functions of T helper cells. *Proceedings of the National Academy of Sciences of the United States of America* **102**(14): 5138-5143.

Beyer M, Thabet Y, Müller R-U, Sadlon T, Classen S, Lahl K, Basu S, Zhou X, Bailey-Bucktrout SL, Krebs W et al. 2011. Repression of the genome organizer SATB1 in regulatory T cells is required for suppressive function and inhibition of effector differentiation. *Nature immunology* **12**(9): 898-907.

Bird A. 2002. DNA methylation patterns and epigenetic memory. *Genes Dev* **16**(1): 6-21.

Birzele F, Fauti T, Stahl H, Lenter MC, Simon E, Knebel D, Weith A, Hildebrandt T, Mennerich D. 2011. Next-generation insights into regulatory T cells: expression profiling and FoxP3 occupancy in Human. *Nucleic acids research* **39**(18): 7946-7960.

Blow MJ, McCulley DJ, Li Z, Zhang T, Akiyama JA, Holt A, Plajzer-Frick I, Shoukry M, Wright C, Chen F et al. 2010. ChIP-Seq identification of weakly conserved heart enhancers. *Nature Genetics* **42**(9): 806-810.

Boniface K, Blumenschein WM, Brovont-Porth K, McGeachy MJ, Basham B, Desai B, Pierce R, McClanahan TK, Sadekova S, Malefyt RdW. 2010. Human Th17 Cells Comprise Heterogeneous Subsets Including IFN-gamma-Producing Cells with Distinct Properties from the Th1 Lineage. *Journal of Immunology* **185**(1): 679-687.

Boyle AP, Davis S, Shulha HP, Meltzer P, Margulies EH, Weng Z, Furey TS, Crawford GE. 2008. High-resolution mapping and characterization of open chromatin across the genome. *Cell* **132**(2): 311-322.

Brandeis M, Frank D, Keshet I, Siegfried Z, Mendelsohn M, Nemes A, Temper V, Razin A, Cedar H. 1994. SP1 ELEMENTS PROTECT A CPG ISLAND FROM DE-NOVO METHYLATION. *Nature* **371**(6496): 435-438.

Brunkow ME, Jeffery EW, Hjerrild KA, Paeper B, Clark LB, Yasayko SA, Wilkinson JE, Galas D, Ziegler SF, Ramsdell F. 2001. Disruption of a new forkhead/winged-helix protein, scurfin, results in the fatal lymphoproliferative disorder of the scurfy mouse. *Nature Genetics* **27**(1): 68-73.

Bruno L, Mazzarella L, Hoogenkamp M, Hertweck A, Cobb BS, Sauer S, Hadjur S, Leleu M, Naoe Y, Telfer JC et al. 2009. Runx proteins regulate Foxp3 expression. *The Journal of ….*

Brunstein CG, Miller JS, Cao Q, McKenna DH, Hippen KL, Curtsinger J, DeFor T, Levine BL, June CH, Rubinstein P et al. 2011a. Infusion of ex vivo expanded T regulatory cells in adults transplanted with umbilical cord blood: safety profile and detection kinetics. *Blood* **117**(3): 1061-1070.

Brunstein CG, Miller JS, Cao Q, McKenna DH, Hippen KL, Curtsinger J, Defor T, Levine BL, June CH, Rubinstein P et al. 2011b. Infusion of ex vivo expanded T regulatory cells in adults transplanted with umbilical cord blood: safety profile and detection kinetics. *Blood* **117**(3): 1061-1070.

Brusko TM, Putnam AL, Bluestone JA. 2008. Human regulatory T cells: role in autoimmune disease and therapeutic opportunities. *Immunological Reviews* **223**: 371-390.

Bühler M, Verdel A, Moazed D. 2006. Tethering RITS to a nascent transcript initiates RNAi- and heterochromatin-dependent gene silencing. *Cell* **125**(5): 873-886.

Burchill MA, Yang J, Vang KB, Farrar MA. 2007. Interleukin-2 receptor signaling in regulatory T cell development and homeostasis. *Immunol Lett* **114**(1): 1-8.

Campbell DJ, Koch MA. 2011. Phenotypical and functional specialization of FOXP3+ regulatory T cells. *Nature reviews Immunology* **11**(2): 119-130.

Chabod M, Pedros C, Lamouroux L, Colacios C, Bernard I, Lagrange D, Balz-Hara D, Mosnier JF, Laboisse C, Vergnolle N et al. 2012. A spontaneous mutation of the rat Themis gene leads to impaired function of regulatory T cells linked to inflammatory bowel disease. *PLoS Genetics* **8**(1): e1002461.

Chaudhry A, Rudra D, Treuting P, Samstein RM, Liang Y, Kas A, Rudensky AY. 2009. CD4+ regulatory T cells control TH17 responses in a Stat3-dependent manner. *Science* **326**(5955): 986-991.

Chen WJ, Jin WW, Hardegen N, Lei KJ, Li L, Marinos N, McGrady G, Wahl SM. 2003. Conversion of peripheral CD4(+)CD25(-) naive T cells to CD4(+)CD25(+) regulatory T cells by TGF-beta induction of transcription factor Foxp3. *Journal of Experimental Medicine* **198**(12): 1875-1886.

Chong MMW, Rasmussen JP, Rudensky AY, Littman DR. 2008. The RNAseIII enzyme Drosha is critical in T cells for preventing lethal inflammatory disease. *The Journal of experimental medicine* **205**(9): 2005-2017.

Cipolletta D, Feuerer M, Li A, Kamei N, Lee J, Shoelson SE, Benoist C, Mathis D. 2012. PPAR-gamma is a major driver of the accumulation and phenotype of adipose tissue Treg cells. *Nature* **486**(7404): 549-553.

Clapier CR, Cairns BR. 2009. The biology of chromatin remodeling complexes. *Annual review of biochemistry* **78**: 273-304.

Cohen JL, Trenado A, Vasey D, Klatzmann D, Salomon BL. 2002. CD4(+)CD25(+) immunoregulatory T Cells: new therapeutics for graft-versus-host disease. *The Journal of experimental medicine* **196**(3): 401-406.

Collier FM, Gregorio-King CC, Gough TJ, Talbot CD, Walder K, Kirkland MA. 2004. Identification and characterization of a lymphocytic Rho-GTPase effector: rhotekin-2. *Biochemical and biophysical research communications* **324**(4): 1360-1369.

Cosmi L, Annunziato F, Iwasaki M, Galli G, Manetti R, Maggi E, Nagata K, Romagnani S. 2000. CRTH2 is the most reliable marker for the detection of circulating human type 2 Th and type 2 T cytotoxic cells in health and disease. *European Journal of Immunology* **30**(10): 2972-2979.

Cote-Sierra J, Foucras G, Guo LY, Chiodetti L, Young HA, Hu-Li J, Zhu JF, Paul WE. 2004. Interleukin 2 plays a central role in Th2 differentiation. *Proceedings of the National Academy of Sciences of the United States of America* **101**(11): 3880-3885.

Creyghton MP, Cheng AW, Welstead GG, Kooistra T, Carey BW, Steine EJ, Hanna J, Lodato MA, Frampton GM, Sharp PA et al. 2010. Histone H3K27ac separates active from poised enhancers and predicts developmental state. *Proceedings of the National Academy of Sciences of the United States of America* **107**(50): 21931-21936.

Davis MM, Bjorkman PJ. 1988. T-cell antigen receptor genes and T-cell recognition. *Nature* **334**(6181): 395-402.

de Vries IJ, Castelli C, Huygens C, Jacobs JF, Stockis J, Schuler-Thurner B, Adema GJ, Punt CJ, Rivoltini L, Schuler G et al. 2011. Frequency of circulating Tregs with demethylated FOXP3 intron 1 in melanoma patients receiving tumor vaccines and potentially Treg-depleting agents. *Clin Cancer Res* **17**(4): 841-848.

Deaglio S, Dwyer KM, Gao W, Friedman D, Usheva A, Erat A, Chen J-F, Enjyoji K, Linden J, Oukka M et al. 2007. Adenosine generation catalyzed by CD39 and CD73 expressed on regulatory T cells mediates immune suppression. *The Journal of experimental medicine* **204**(6): 1257-1265.

Deaton AM, Bird A. 2011. CpG islands and the regulation of transcription. *Genes & development* **25**(10): 1010-1022.

Dekker J, Rippe K, Dekker M, Kleckner N. 2002. Capturing chromosome conformation. *Science (New York, NY)* **295**(5558): 1306-1311.

Deknuydt F, Bioley G, Valmori D, Ayyoub M. 2009. IL-1 beta and IL-2 convert human Treg into T(H)17 cells. *Clinical Immunology* **131**(2): 298-307.
Delves PJ, Roitt IM. 2000. The immune system. First of two parts. *N Engl J Med* **343**(1): 37-49.
Dhalluin C, Carlson JE, Zeng L, He C, Aggarwal AK, Zhou MM. 1999. Structure and ligand of a histone acetyltransferase bromodomain. *Nature* **399**(6735): 491-496.
Di Ianni M, Falzetti F, Carotti A, Terenzi A, Castellino F, Bonifacio E, Del Papa B, Zei T, Ostini RI, Cecchini D et al. 2011a. Tregs prevent GVHD and promote immune reconstitution in HLA-haploidentical transplantation. *Blood* **117**(14): 3921-3928.
Di Ianni M, Falzetti F, Carotti A, Terenzi A, Castellino F, Bonifacio E, Del Papa B, Zei T, Ostini RI, Cecchini D et al. 2011b. Tregs prevent GVHD and promote immune reconstitution in HLA-haploidentical transplantation. *Blood* **117**(14): 3921-3928.
Djebali S, Davis CA, Merkel A, Dobin A, Lassmann T, Mortazavi A, Tanzer A, Lagarde J, Lin W, Schlesinger F et al. 2012. Landscape of transcription in human cells. *Nature* **489**(7414): 101-108.
Djuretic IM, Levanon D, Negreanu V, Groner Y, Rao A, Ansel KM. 2007a. Transcription factors T-bet and Runx3 cooperate to activate Ifng and silence Il4 in T helper type 1 cells. *Nature Immunology* **8**(2): 145-153.
Djuretic IM, Levanon D, Negreanu V, Groner Y, Rao A, Ansel KM. 2007b. Transcription factors T-bet and Runx3 cooperate to activate lfng and silence ll4 in T helper type 1 cells. *Nature Immunology* **8**(2): 145-153.
Dovat S, Montecino-Rodriguez E, Schuman V, Teitell MA, Dorshkind K, Smale ST. 2005. Transgenic expression of helios in B lineage cells alters B cell properties and promotes lymphomagenesis. *Journal of Immunology* **175**(6): 3508-3515.
Duarte JH, Zelenay S, Bergman M-L, Martins AC, Demengeot J. 2009. Natural Treg cells spontaneously differentiate into pathogenic helper cells in lymphopenic conditions. *European journal of immunology* **39**(4): 948-955.
Duhen T, Duhen R, Lanzavecchia A, Sallusto F, Campbell DJ. 2012. Functionally distinct subsets of human FOXP3+ Treg cells that phenotypically mirror effector Th cells. *Blood* **119**(19): 4430-4440.
Edinger M, Hoffmann P. 2011a. Regulatory T cells in stem cell transplantation: strategies and first clinical experiences. *Current Opinion in Immunology* **23**(5): 679-684.
Edinger M, Hoffmann P. 2011b. Regulatory T cells in stem cell transplantation: strategies and first clinical experiences. *Current opinion in immunology*.
Edinger M, Hoffmann P, Ermann J, Drago K, Fathman CG, Strober S, Negrin RS. 2003. CD4(+)CD25(+) regulatory T cells preserve graft-versus-tumor activity while inhibiting graft-versus-host disease after bone marrow transplantation. *Nature Medicine* **9**(9): 1144-1150.
Ehrich M, Nelson MR, Stanssens P, Zabeau M, Liloglou T, Xinarianos G, Cantor CR, Field JK, van den Boom D. 2005. Quantitative high-throughput analysis of DNA methylation patterns by base-specific cleavage and mass spectrometry. *Proceedings of the National Academy of Sciences of the United States of America* **102**(44): 15785-15790.
ENCODE-consortium. 2011. A user's guide to the encyclopedia of DNA elements (ENCODE). *Plos Biology* **9**(4): e1001046.
Ernst J, Kheradpour P, Mikkelsen TS, Shoresh N, Ward LD, Epstein CB, Zhang X, Wang L, Issner R, Coyne M et al. 2011. Mapping and analysis of chromatin state dynamics in nine human cell types. *Nature*.
Esser C, Gottlinger C, Kremer J, Hundeiker C, Radbruch A. 1995. ISOLATION OF FULL-SIZE MESSENGER-RNA FROM ETHANOL-FIXED CELLS AFTER CELLULAR IMMUNOFLUORESCENCE STAINING AND FLUORESCENCE-ACTIVATED CELL SORTING (FACS). *Cytometry* **21**(4): 382-386.
Evans HG, Suddason T, Jackson I, Taams LS, Lord GM. 2007. Optimal induction of T helper 17 cells in humans requires T cell receptor ligation in the context of Toll-like receptor-activated monocytes. *Proceedings of the National Academy of Sciences of the United States of America* **104**(43): 17034-17039.
Farthing CR, Ficz G, Ng RK, Chan C-F, Andrews S, Dean W, Hemberger M, Reik W. 2008. Global mapping of DNA methylation in mouse promoters reveals epigenetic reprogramming of pluripotency genes. *PLoS Genetics* **4**(6): e1000116.
Felsenfeld G, Groudine M. 2003. Controlling the double helix. *Nature* **421**(6921): 448-453.
Feuerer M, Hill JA, Kretschmer K, von Boehmer H, Mathis D, Benoist C. 2010. Genomic definition of multiple ex vivo regulatory T cell subphenotypes. *Proceedings of the National Academy of Sciences of the United States of America* **107**(13): 5919-5924.
Floess S, Freyer J, Siewert C, Baron U, Olek S, Polansky J, Schlawe K, Chang H-D, Bopp T, Schmitt E et al. 2007. Epigenetic control of the foxp3 locus in regulatory T cells. *Plos Biology* **5**(2): 169-178.
Fontenot JD, Gavin MA, Rudensky AY. 2003. Foxp3 programs the development and function of CD4(+)CD25(+) regulatory T cells. *Nature Immunology* **4**(4): 330-336.

Fontenot JD, Rasmussen JP, Gavin MA, Rudensky AY. 2005a. A function for interleukin 2 in Foxp3-expressing regulatory T cells. *Nature immunology* **6**(11): 1142-1151.

Fontenot JD, Rasmussen JP, Williams LM, Dooley JL, Farr AG, Rudensky AY. 2005b. Regulatory T cell lineage specification by the forkhead transcription factor FoxP3. *Immunity* **22**(3): 329-341.

Fowler CB, O'Leary TJ, Mason JT. 2008. Modeling formalin fixation and histological processing with ribonuclease A: effects of ethanol dehydration on reversal of formaldehyde cross-links. *Laboratory Investigation* **88**(7): 785-791.

Fujita N, Shimotake N, Ohki I, Chiba T, Saya H, Shirakawa M, Nakao M. 2000. Mechanism of transcriptional regulation by methyl-CpG binding protein MBD1. *Molecular and Cellular Biology* **20**(14): 5107-5118.

Garín MI, Chu C-C, Golshayan D, Cernuda-Morollón E, Wait R, Lechler RI. 2007. Galectin-1: a key effector of regulation mediated by CD4+CD25+ T cells. *Blood* **109**(5): 2058-2065.

Gavin MA, Torgerson TR, Houston E, deRoos P, Ho WY, Stray-Pedersen A, Ocheltree EL, Greenberg PD, Ochs HD, Rudensky AY. 2006. Single-cell analysis of normal and FOXP3-mutant human T cells: FOXP3 expression without regulatory T cell development. *Proceedings of the National Academy of Sciences of the United States of America* **103**(17): 6659-6664.

Gebhard C, Benner C, Ehrich M, Schwarzfischer L, Schilling E, Klug M, Dietmaier W, Thiede C, Holler E, Andreesen R et al. 2010. General transcription factor binding at CpG islands in normal cells correlates with resistance to de novo DNA methylation in cancer cells. *Cancer Research* **70**(4): 1398-1407.

Gebhard C, Schwarzfischer L, Pham TH, Schilling E, Klug M, Andreesen R, Rehli M. 2006. Genome-wide profiling of CpG methylation identifies novel targets of aberrant hypermethylation in myeloid leukemia. *Cancer Research* **66**(12): 6118-6128.

Ghisletti S, Barozzi I, Mietton F, Polletti S, De Santa F, Venturini E, Gregory L, Lonie L, Chew A, Wei C-L et al. 2010. Identification and Characterization of Enhancers Controlling the Inflammatory Gene Expression Program in Macrophages. *Immunity* **32**(3): 317-328.

Ghoreschi K, Laurence A, Yang XP, Tato CM, McGeachy MJ, Konkel JE, Ramos HL, Wei L, Davidson TS, Bouladoux N et al. 2010. Generation of pathogenic T(H)17 cells in the absence of TGF-beta signalling. *Nature* **467**(7318): 967-971.

Gondek DC, Lu L-F, Quezada SA, Sakaguchi S, Noelle RJ. 2005. Cutting edge: contact-mediated suppression by CD4+CD25+ regulatory cells involves a granzyme B-dependent, perforin-independent mechanism. *Journal of immunology (Baltimore, Md : 1950)* **174**(4): 1783-1786.

Goto T, Monk M. 1998. Regulation of X-chromosome inactivation in development in mice and humans. *Microbiology and Molecular Biology Reviews* **62**(2): 362-+.

Grafstrom RH, Yuan R, Hamilton DL. 1985. The characteristics of DNA methytation in an in vitroDNA synthesizing system from mouse fibroblasts. *Nucleic acids research* **13**(8): 2827-2842.

Grossman WJ, Verbsky JW, Tollefsen BL, Kemper C, Atkinson JP, Ley TJ. 2004. Differential expression of granzymes A and B in human cytotoxic lymphocyte subsets and T regulatory cells. *Blood* **104**(9): 2840-2848.

Guenther MG, Levine SS, Boyer LA, Jaenisch R, Young RA. 2007. A chromatin landmark and transcription initiation at most promoters in human cells. *Cell* **130**(1): 77-88.

Guermonprez P, Valladeau J, Zitvogel L, Thery C, Amigorena S. 2002. Antigen presentation and T cell stimulation by dendritic cells. *Annual review of immunology* **20**: 621-667.

Hadjur S, Williams LM, Ryan NK, Cobb BS, Sexton T, Fraser P, Fisher AG, Merkenschlager M. 2009. Cohesins form chromosomal cis-interactions at the developmentally regulated IFNG locus. *Nature* **460**(7253): 410-413.

Handoko L, Xu H, Li G, Ngan CY, Chew E, Schnapp M, Lee CWH, Ye C, Ping JLH, Mulawadi F et al. 2011. CTCF-mediated functional chromatin interactome in pluripotent cells. *Nature genetics* **43**(7): 630-638.

Hansmann L, Schmidl C, Boeld TJ, Andreesen R, Hoffmann P, Rehli M, Edinger M. 2010. Isolation of intact genomic DNA from FOXP3-sorted human regulatory T cells for epigenetic analyses. *European Journal of Immunology* **40**(5): 1510-1512.

Hansmann L, Schmidl C, Kett J, Steger L, Andreesen R, Hoffmann P, Rehli M, Edinger M. 2012. Dominant Th2 differentiation of human regulatory T cells upon loss of FOXP3 expression. *Journal of immunology (Baltimore, Md : 1950)* **188**(3): 1275-1282.

Harada Y, Harada Y, Elly C, Ying G, Paik J-h, DePinho RA, Liu Y-C. 2010. Transcription factors Foxo3a and Foxo1 couple the E3 ligase Cbl-b to the induction of Foxp3 expression in induced regulatory T cells. *The Journal of ….*

Hardison RC, Taylor J. 2012a. Genomic approaches towards finding cis-regulatory modules in animals. *Nature reviews Genetics* **13**(7): 469-483.

Hardison RC, Taylor J. 2012b. Genomic approaches towards finding cis-regulatory modules in animals. *Nature reviews Genetics* **13**(7): 469-483.

Hassan AH, Prochasson P, Neely KE, Galasinski SC, Chandy M, Carrozza MJ, Workman JL. 2002. Function and selectivity of bromodomains in anchoring chromatin-modifying complexes to promoter nucleosomes. *Cell* **111**(3): 369-379.

Hatton RD, Harrington LE, Luther RJ, Wakefield T, Janowski KM, Oliver JR, Lallone RL, Murphy KM, Weaver CT. 2006. A distal conserved sequence element controls Ifng gene expression by T cells and NK cells. *Immunity* **25**(5): 717-729.

He Y-F, Li B-Z, Li Z, Liu P, Wang Y, Tang Q, Ding J, Jia Y, Chen Z, Li L et al. 2011. Tet-mediated formation of 5-carboxylcytosine and its excision by TDG in mammalian DNA. *Science (New York, NY)* **333**(6047): 1303-1307.

Heintzman ND, Hon GC, Hawkins RD, Kheradpour P, Stark A, Harp LF, Ye Z, Lee LK, Stuart RK, Ching CW et al. 2009. Histone modifications at human enhancers reflect global cell-type-specific gene expression. *Nature* **459**(7243): 108-112.

Heintzman ND, Ren B. 2009. Finding distal regulatory elements in the human genome. *Current opinion in genetics & development* **19**(6): 541-549.

Heintzman ND, Stuart RK, Hon G, Fu Y, Ching CW, Hawkins RD, Barrera LO, Van Calcar S, Qu C, Ching KA et al. 2007. Distinct and predictive chromatin signatures of transcriptional promoters and enhancers in the human genome. *Nature Genetics* **39**(3): 311-318.

Heinz S, Benner C, Spann N, Bertolino E, Lin YC, Laslo P, Cheng JX, Murre C, Singh H, Glass CK. 2010. Simple combinations of lineage-determining transcription factors prime cis-regulatory elements required for macrophage and B cell identities. *Molecular cell* **38**(4): 576-589.

Heinzel FP, Sadick MD, Holaday BJ, Coffman RL, Locksley RM. 1989. Reciprocal expression of interferon gamma or interleukin 4 during the resolution or progression of murine leishmaniasis. Evidence for expansion of distinct helper T cell subsets. *The Journal of experimental medicine* **169**(1): 59-72.

Herman JG, Baylin SB. 2003. Mechanisms of disease: Gene silencing in cancer in association with promoter hypermethylation. *New England Journal of Medicine* **349**(21): 2042-2054.

Herold M, Bartkuhn M, Renkawitz R. 2012. CTCF: insights into insulator function during development. *Development (Cambridge, England)* **139**(6): 1045-1057.

Hill JA, Feuerer M, Tash K, Haxhinasto S, Perez J, Melamed R, Mathis D, Benoist C. 2007. Foxp3 transcription-factor-dependent and -independent regulation of the regulatory T cell transcriptional signature. *Immunity* **27**(5): 786-800.

Hoffmann P, Boeld TJ, Eder R, Albrecht J, Doser K, Piseshka B, Dada A, Niemand C, Assenmacher M, Orso E et al. 2006a. Isolation of CD4+CD25+ regulatory T cells for clinical trials. *Biol Blood Marrow Transplant* **12**(3): 267-274.

Hoffmann P, Boeld TJ, Eder R, Huehn J, Floess S, Wieczorek G, Olek S, Dietmaier W, Andreesen R, Edinger M. 2009. Loss of FOXP3 expression in natural human CD4+CD25+ regulatory T cells upon repetitive in vitro stimulation. *European Journal of Immunology* **39**(4): 1088-1097.

Hoffmann P, Eder R, Boeld TJ, Doser K, Piseshka B, Andreesen R, Edinger M. 2006b. Only the CD45RA(+) subpopulation of CD4(+)CD25(high) T cells gives rise to homogeneous regulatory T-cell lines upon in vitro expansion. *Blood* **108**(13): 4260-4267.

Hoffmann P, Eder R, Edinger M. 2011. Polyclonal Expansion of Human CD4(+)CD25(+) Regulatory T Cells. In *Suppression and Regulation of Immune Responses: Methods and Protocols*, Vol 677 (ed. MCAI Cuturi), pp. 15-30.

Hoffmann P, Eder R, Kunz-Schughart LA, Andreesen R, Edinger M. 2004. Large-scale in vitro expansion of polyclonal human CD4(+)CD25(high) regulatory T cells. *Blood* **104**(3): 895-903.

Hoffmann P, Ermann J, Edinger M, Fathman CG, Strober S. 2002a. Donor-type CD4(+)CD25(+) regulatory T cells suppress lethal acute graft-versus-host disease after allogeneic bone marrow transplantation. *Journal of Experimental Medicine* **196**(3): 389-399.

-. 2002b. Donor-type CD4(+)CD25(+) regulatory T cells suppress lethal acute graft-versus-host disease after allogeneic bone marrow transplantation. *The Journal of experimental medicine* **196**(3): 389-399.

Holliday R, Pugh JE. 1975. DNA modification mechanisms and gene activity during development. *Science (New York, NY)* **187**(4173): 226-232.

Hoogenkamp M, Krysinska H, Ingram R, Huang G, Barlow R, Clarke D, Ebralidze A, Zhang P, Tagoh H, Cockerill PN et al. 2007. The Pu.1 locus is differentially regulated at the level of chromatin structure and Noncoding transcription by alternate mechanisms at distinct developmental stages of hematopoiesis. *Molecular and Cellular Biology* **27**(21): 7425-7438.

Hori S, Nomura T, Sakaguchi S. 2003. Control of regulatory T cell development by the transcription factor Foxp3. *Science* **299**(5609): 1057-1061.
Hou JZ, Schindler U, Henzel WJ, Wong SC, McKnight SL. 1995. IDENTIFICATION AND PURIFICATION OF HUMAN STAT PROTEINS ACTIVATED IN RESPONSE TO INTERLEUKIN-2. *Immunity* **2**(4): 321-329.
Hsieh C-S, Lee H-M, Lio C-WJ. 2012. Selection of regulatory T cells in the thymus. *Nature reviews Immunology* **12**(3): 157-167.
Hsueh YP, Liang HE, Ng SY, Lai MZ. 1997. CD28-costimulation activates cyclic AMP-responsive element-binding protein in T lymphocytes. *Journal of Immunology* **158**(1): 85-93.
Huehn J, Polansky JK, Hamann A. 2009. Epigenetic control of FOXP3 expression: the key to a stable regulatory T-cell lineage? *Nature Reviews Immunology* **9**(2): 83-89.
Hutchins AS, Mullen AC, Lee HW, Sykes KJ, High FA, Hendrich BD, Bird AP, Reiner SL. 2002. Gene silencing quantitatively controls the function of a developmental trans-activator. *Molecular cell* **10**(1): 81-91.
Hwang ES, Szabo SJ, Schwartzberg PL, Glimcher LH. 2005. T helper cell fate specified by kinase-mediated interaction of T-bet with GATA-3. *Science* **307**(5708): 430-433.
Illingworth R, Kerr A, DeSousa D, Jorgensen H, Ellis P, Stalker J, Jackson D, Clee C, Plumb R, Rogers J et al. 2008. A novel CpG island set identifies tissue-specific methylation at developmental gene loci. *Plos Biology* **6**(1): 37-51.
Infante-Duarte C, Horton HF, Byrne MC, Kamradt T. 2000. Microbial lipopeptides induce the production of IL-17 in Th cells. *Journal of Immunology* **165**(11): 6107-6115.
Issa JP. 2004. CpG island methylator phenotype in cancer. *Nat Rev Cancer* **4**(12): 988-993.
Ito S, D'Alessio AC, Taranova OV, Hong K, Sowers LC, Zhang Y. 2010. Role of Tet proteins in 5mC to 5hmC conversion, ES-cell self-renewal and inner cell mass specification. *Nature* **466**(7310): 1129-1133.
Ito S, Shen L, Dai Q, Wu SC, Collins LB, Swenberg JA, He C, Zhang Y. 2011. Tet proteins can convert 5-methylcytosine to 5-formylcytosine and 5-carboxylcytosine. *Science (New York, NY)* **333**(6047): 1300-1303.
Ivanov II, McKenzie BS, Zhou L, Tadokoro CE, Lepelley A, Lafaille JJ, Cua DJ, Littman DR. 2006. The orphan nuclear receptor ROR gamma t directs the differentiation program of proinflammatory IL-17(+) T helper cells. *Cell* **126**(6): 1121-1133.
Jackson DP, Lewis FA, Taylor GR, Boylston AW, Quirke P. 1990. TISSUE EXTRACTION OF DNA AND RNA AND ANALYSIS BY THE POLYMERASE CHAIN-REACTION. *Journal of Clinical Pathology* **43**(6): 499-504.
Jacobson RH, Ladurner AG, King DS, Tjian R. 2000. Structure and function of a human TAFII250 double bromodomain module. *Science* **288**(5470): 1422-1425.
Janeway CA, Jr., Medzhitov R. 2002. Innate immune recognition. *Annual review of immunology* **20**: 197-216.
Jin C, Zang C, Wei G, Cui K, Peng W, Zhao K. 2009. H3.3/H2A.Z double variant-containing nucleosomes mark 'nucleosome-free regions' of active promoters and other regulatory regions : Article : Nature Genetics. *Nature genetics*.
Jones B, Chen J. 2006. Inhibition of IFN-gamma transcription by site-specific methylation during T helper cell development. *The EMBO Journal* **25**(11): 2443-2452.
Jones PA. 2012. Functions of DNA methylation: islands, start sites, gene bodies and beyond. *Nature reviews Genetics* **13**(7): 484-492.
Jones PA, Liang G. 2009. Rethinking how DNA methylation patterns are maintained. *Nature reviews Genetics* **10**(11): 805-811.
Jones PL, Veenstra GJ, Wade PA, Vermaak D, Kass SU, Landsberger N, Strouboulis J, Wolffe AP. 1998. Methylated DNA and MeCP2 recruit histone deacetylase to repress transcription. *Nature genetics* **19**(2): 187-191.
Jordan MS, Boesteanu A, Reed AJ, Petrone AL, Holenbeck AE, Lerman MA, Naji A, Caton AJ. 2001. Thymic selection of CD4+CD25+ regulatory T cells induced by an agonist self-peptide. *Nature Immunology* **2**(4): 301-306.
Josefowicz SZ, Niec RE, Kim HY, Treuting P, Chinen T, Zheng Y, Umetsu DT, Rudensky AY. 2012. Extrathymically generated regulatory T cells control mucosal TH2 inflammation. *Nature* **482**(7385): 395-399.
Jutras I, Desjardins M. 2005. Phagocytosis: at the crossroads of innate and adaptive immunity. *Annu Rev Cell Dev Biol* **21**: 511-527.

Kagami S, Nakajima H, Suto A, Hirose K, Suzuki K, Morita S, Kato I, Saito Y, Kitamura T, Iwamoto I. 2001. Stat5a regulates T helper cell differentiation by several distinct mechanisms. *Blood* **97**(8): 2358-2365.

Kagey MH, Newman JJ, Bilodeau S, Zhan Y, Orlando DA, van Berkum NL, Ebmeier CC, Goossens J, Rahl PB, Levine SS et al. 2010. Mediator and cohesin connect gene expression and chromatin architecture. *Nature* **467**(7314): 430-435.

Kanamori-Katayama M, Itoh M, Kawaji H, Lassmann T, Katayama S, Kojima M, Bertin N, Kaiho A, Ninomiya N, Daub CO et al. 2011. Unamplified cap analysis of gene expression on a single-molecule sequencer. *Genome research* **21**(7): 1150-1159.

Kaplan MH, Schindler U, Smiley ST, Grusby MJ. 1996. Stat6 is required for mediating responses to IL-4 and for the development of Th2 cells. *Immunity* **4**(3): 313-319.

Kerdiles YM, Stone EL, Beisner DR, Beisner DL, McGargill MA, Ch'en IL, Stockmann C, Katayama CD, Hedrick SM. 2010. Foxo transcription factors control regulatory T cell development and function. *Immunity* **33**(6): 890-904.

Kim H-P, Leonard WJ. 2007. CREB/ATF-dependent T cell receptor-induced FoxP3 gene expression: a role for DNA methylation. *Journal of Experimental Medicine* **204**(7): 1543-1551.

Kim J, Lahl K, Hori S, Loddenkemper C, Chaudhry A, deRoos P, Rudensky A, Sparwasser T. 2009. Cutting Edge: Depletion of Foxp3(+) Cells Leads to Induction of Autoimmunity by Specific Ablation of Regulatory T Cells in Genetically Targeted Mice. *Journal of Immunology* **183**(12): 7631-7634.

Kim JM, Rasmussen JP, Rudensky AY. 2007. Regulatory T cells prevent catastrophic autoimmunity throughout the lifespan of mice. *Nature Immunology* **8**(2): 191-197.

Kim TK, Hemberg M, Gray JM, Costa AM, Bear DM, Wu J, Harmin DA, Laptewicz M, Barbara-Haley K, Kuersten S et al. 2010. Widespread transcription at neuronal activity-regulated enhancers. *Nature* **465**(7295): 182-187.

Kirby KS. 1956. A new method for the isolation of ribonucleic acids for mammalian tissues. *Biochem Jour* **64**((3)): 405-408.

Kitoh A, Ono M, Naoe Y, Ohkura N, Yamaguchi T, Yaguchi H, Kitabayashi I, Tsukada T, Nomura T, Miyachi Y et al. 2009. Indispensable role of the Runx1-Cbfbeta transcription complex for in vivo-suppressive function of FoxP3+ regulatory T cells. *Immunity* **31**(4): 609-620.

Klose RJ, Bird AP. 2006. Genomic DNA methylation: the mark and its mediators. *Trends in biochemical sciences* **31**(2): 89-97.

Klug M, Heinz S, Gebhard C, Schwarzfischer L, Krause SW, Andreesen R, Rehli M. 2010. Active DNA demethylation in human postmitotic cells correlates with activating histone modifications, but not transcription levels. *Genome biology* **11**(6): R63.

Klug M, Rehli M. 2006. Functional Analysis of Promoter CpG Methylation Using a CpG-Free Luciferase Reporter Vector. *Epigenetics* **1**(3): 127-130.

Klunker S, Chong MMW, Mantel P-Y, Palomares O, Bassin C, Ziegler M, Rueckert B, Meiler F, Akdis M, Littman DR et al. 2009. Transcription factors RUNX1 and RUNX3 in the induction and suppressive function of Foxp3(+) inducible regulatory T cells. *Journal of Experimental Medicine* **206**(12): 2701-2715.

Koch MA, Tucker-Heard Gs, Perdue NR, Killebrew JR, Urdahl KB, Campbell DJ. 2009. The transcription factor T-bet controls regulatory T cell homeostasis and function during type 1 inflammation. *Nature Immunology* **10**(6): 595-U557.

Koenen HJPM, Smeets RL, Vink PM, van Rijssen E, Boots AMH, Joosten I. 2008. Human CD25(high)Foxp3(pos) regulatory T cells differentiate into IL-17-producing cells. *Blood* **112**(6): 2340-2352.

Komatsu N, Mariotti-Ferrandiz ME, Wang Y, Malissen B, Waldmann H, Hori S. 2009. Heterogeneity of natural Foxp3(+) T cells: A committed regulatory T-cell lineage and an uncommitted minor population retaining plasticity. *Proceedings of the National Academy of Sciences of the United States of America* **106**(6): 1903-1908.

Kornberg RD. 1977. Structure of chromatin. *Annual review of biochemistry* **46**: 931-954.

Kornberg RD. 2005. Mediator and the mechanism of transcriptional activation. *Trends in biochemical sciences* **30**(5): 235-239.

Kornberg RD, Thomas JO. 1974. Chromatin structure; oligomers of the histones. *Science* **184**(4139): 865-868.

Kuo MH, Allis CD. 1999. In vivo cross-linking and immunoprecipitation for studying dynamic Protein:DNA associations in a chromatin environment. *Methods* **19**(3): 425-433.

Kurata H, Lee HJ, O'Garra A, Arai N. 1999. Ectopic expression of activated Stat6 induces the expression of Th2-specific cytokines and transcription factors in developing Th1 cells. *Immunity* **11**(6): 677-688.

Kyewski B, Peterson P. 2010. Aire, master of many trades. *Cell* **140**(1): 24-26.
Laird PW. 2005. Cancer epigenetics. *Hum Mol Genet* **14 Spec No 1**: R65-76.
Lal G, Bromberg JS. 2009. Epigenetic mechanisms of regulation of Foxp3 expression. *Blood* **114**(18): 3727-3735.
Lal G, Zhang N, van der Touw W, Ding Y, Ju W, Bottinger EP, Reid SP, Levy DE, Bromberg JS. 2009. Epigenetic Regulation of Foxp3 Expression in Regulatory T Cells by DNA Methylation. *Journal of Immunology* **182**(1): 259-273.
Langmead B. 2010. Aligning short sequencing reads with Bowtie. *Curr Protoc Bioinformatics* **Chapter 11**: Unit 11 17.
Lee DU, Agarwal S, Rao A. 2002. Th2 lineage commitment and efficient IL-4 production involves extended demethylation of the IL-4 gene. *Immunity* **16**(5): 649-660.
Lee HJ, Takemoto N, Kurata H, Kamogawa Y, Miyatake S, O'Garra A, Arai N. 2000. GATA-3 induces T helper cell type 2 (Th2) cytokine expression and chromatin remodeling in committed Th1 cells. *The Journal of experimental medicine* **192**(1): 105-115.
Lee J-H, Tate CM, You J-S, Skalnik DG. 2007. Identification and characterization of the human Set1B histone H3-Lys4 methyltransferase complex. *J Biol Chem* **282**(18): 13419-13428.
Lee JT. 2011. Gracefully ageing at 50, X-chromosome inactivation becomes a paradigm for RNA and chromatin control. *Nature Reviews Molecular Cell Biology* **12**(12): 815-826.
Lenhard B, Sandelin A, Carninci P. 2012. Metazoan promoters: emerging characteristics and insights into transcriptional regulation. *Nature reviews Genetics* **13**(4): 233-245.
Lettice LA, Heaney SJH, Purdie LA, Li L, de Beer P, Oostra BA, Goode D, Elgar G, Hill RE, de Graaff E. 2003. A long-range Shh enhancer regulates expression in the developing limb and fin and is associated with preaxial polydactyly. *Hum Mol Genet* **12**(14): 1725-1735.
Li E, Beard C, Jaenisch R. 1993. ROLE FOR DNA METHYLATION IN GENOMIC IMPRINTING. *Nature* **366**(6453): 362-365.
Li E, Bestor TH, Jaenisch R. 1992. Targeted mutation of the DNA methyltransferase gene results in embryonic lethality. *Cell* **69**(6): 915-926.
Li LC, Dahiya R. 2002. MethPrimer: designing primers for methylation PCRs. *Bioinformatics* **18**(11): 1427-1431.
Liang B, Workman C, Lee J, Chew C, Dale BM, Colonna L, Flores M, Li N, Schweighoffer E, Greenberg S et al. 2008. Regulatory T cells inhibit dendritic cells by lymphocyte activation gene-3 engagement of MHC class II. *Journal of immunology (Baltimore, Md : 1950)* **180**(9): 5916-5926.
Lienert F, Wirbelauer C, Som I, Dean A, Mohn F, Schubeler D. 2011. Identification of genetic elements that autonomously determine DNA methylation states. *Nature Genetics* **43**(11): 1091-1097.
Lighvani AA, Frucht DM, Jankovic D, Yamane H, Aliberti J, Hissong BD, Nguyen BV, Gadina M, Sher A, Paul WE et al. 2001. T-bet is rapidly induced by interferon-gamma in lymphoid and myeloid cells. *Proceedings of the National Academy of Sciences of the United States of America* **98**(26): 15137-15142.
Lin B-S, Tsai P-Y, Hsieh W-Y, Tsao H-W, Liu M-W, Grenningloh R, Wang L-F, Ho IC, Miaw S-C. 2010a. SUMOylation attenuates c-Maf-dependent IL-4 expression. *European Journal of Immunology* **40**(4): 1174-1184.
Lin W, Haribhai D, Relland LM, Truong N, Carlson MR, Williams CB, Chatila TA. 2007. Regulatory T cell development in the absence of functional Foxp3. *Nature Immunology* **8**(4): 359-368.
Lin YC, Jhunjhunwala S, Benner C, Heinz S, Welinder E, Mansson R, Sigvardsson M, Hagman J, Espinoza CA, Dutkowski J et al. 2010b. A global network of transcription factors, involving E2A, EBF1 and Foxo1, that orchestrates B cell fate. *Nature immunology* **11**(7): 635-643.
Linterman MA, Pierson W, Lee SK, Kallies A, Kawamoto S, Rayner TF, Srivastava M, Divekar DP, Beaton L, Hogan JJ et al. 2011. Foxp3+ follicular regulatory T cells control the germinal center response. *Nature medicine* **17**(8): 975-982.
Lio CW, Dodson LF, Deppong CM, Hsieh CS, Green JM. 2010. CD28 facilitates the generation of Foxp3(-) cytokine responsive regulatory T cell precursors. *Journal of Immunology* **184**(11): 6007-6013.
Lister R, Pelizzola M, Dowen RH, Hawkins RD, Hon G, Tonti-Filippini J, Nery JR, Lee L, Ye Z, Ngo Q-M et al. 2009. Human DNA methylomes at base resolution show widespread epigenomic differences. *Nature* **462**(7271): 315-322.
Liston A, Lu L-F, O'Carroll D, Tarakhovsky A, Rudensky AY. 2008. Dicer-dependent microRNA pathway safeguards regulatory T cell function. *Journal of Experimental Medicine* **205**(9): 1993-2004.
Liu W, Putnam AL, Xu-Yu Z, Szot GL, Lee MR, Zhu S, Gottlieb PA, Kapranov P, Gingeras TR, Fazekas de St Groth B et al. 2006. CD127 expression inversely correlates with FoxP3 and suppressive function of human CD4+ T reg cells. *The Journal of experimental medicine* **203**(7): 1701-1711.

Lochner M, Peduto L, Cherrier M, Sawa S, Langa F, Varona R, Riethmacher D, Si-Tahar M, Di Santo JP, Eberl G. 2008. In vivo equilibrium of proinflammatory IL-17(+) and regulatory IL-10(+) Foxp3(+) ROR gamma t(+) T cells. *Journal of Experimental Medicine* **205**(6): 1381-1393.

Lohr J, Knoechel B, Kahn EC, Abbas AK. 2004. Role of B7 in T cell tolerance. *Journal of Immunology* **173**(8): 5028-5035.

Lomvardas S, Barnea G, Pisapia DJ, Mendelsohn M, Kirkland J, Axel R. 2006. Interchromosomal interactions and olfactory receptor choice. *Cell* **126**(2): 403-413.

Long M, Park S-G, Strickland I, Hayden MS, Ghosh S. 2009. Nuclear factor-kappaB modulates regulatory T cell development by directly regulating expression of Foxp3 transcription factor. *Immunity* **31**(6): 921-931.

Lorch Y, LaPointe JW, Kornberg RD. 1987. Nucleosomes inhibit the initiation of transcription but allow chain elongation with the displacement of histones. *Cell* **49**(2): 203-210.

Lu LF, Boldin MP, Chaudhry A, Lin LL, Taganov KD, Hanada T, Yoshimura A, Baltimore D, Rudensky AY. 2010b. Function of miR-146a in controlling Treg cell-mediated regulation of Th1 responses. *Cell* **142**(6): 914-929.

Luger K, Mäder AW, Richmond RK, Sargent DF, Richmond TJ. 1997. Crystal structure of the nucleosome core particle at 2.8 A resolution. *Nature* **389**(6648): 251-260.

Lupien M, Eeckhoute J, Meyer CA, Wang Q, Zhang Y, Li W, Carroll JS, Liu XS, Brown M. 2008. FoxA1 translates epigenetic signatures into enhancer-driven lineage-specific transcription. *Cell* **132**(6): 958-970.

Lyon MF. 1961. Gene action in the X-chromosome of the mouse (Mus musculus L.). *Nature* **190**: 372-373.

MacQuarrie KL, Fong AP, Morse RH, Tapscott SJ. 2011. Genome-wide transcription factor binding: beyond direct target regulation. *Trends Genet* **27**(4): 141-148.

Makar KW, Perez-Melgosa M, Shnyreva M, Weaver WM, Fitzpatrick DR, Wilson CB. 2003. Active recruitment of DNA methyltransferases regulates interleukin 4 in thymocytes and T cells. *Nature Immunology* **4**(12): 1183-1190.

Makar KW, Wilson CB. 2004. DNA methylation is a nonredundant repressor of the Th2 effector program. *Journal of Immunology* **173**(7): 4402-4406.

Maloy KJ, Powrie F. 2001. Regulatory T cells in the control of immune pathology. *Nature Immunology* **2**(9): 816-822.

Manel N, Unutmaz D, Littman DR. 2008. The differentiation of human T(H)-17 cells requires transforming growth factor-beta and induction of the nuclear receptor ROR gamma t. *Nature Immunology* **9**(6): 641-649.

Mantel P-Y, Kuipers H, Boyman O, Rhyner C, Ouaked N, Rückert B, Karagiannidis C, Lambrecht BN, Hendriks RW, Crameri R et al. 2007. GATA3-driven Th2 responses inhibit TGF-beta1-induced FOXP3 expression and the formation of regulatory T cells. *PLoS biology* **5**(12): e329.

Mantel PY, Ouaked N, Ruckert B, Karagiannidis C, Welz R, Blaser K, Schmidt-Weber CB. 2006. Molecular mechanisms underlying FOXP3 induction in human T cells. *Journal of Immunology* **176**(6): 3593-3602.

Maston GA, Evans SK, Green MR. 2006. Transcriptional regulatory elements in the human genome. *Annual review of genomics and human genetics* **7**: 29-59.

Mathis D, Benoist C. 2009. Aire. *Annual review of immunology* **27**: 287-312.

McClymont SA, Putnam AL, Lee MR, Esensten JH, Liu W, Hulme MA, Hoffmueller U, Baron U, Olek S, Bluestone JA et al. 2011. Plasticity of Human Regulatory T Cells in Healthy Subjects and Patients with Type 1 Diabetes. *Journal of Immunology* **186**(7): 3918-3926.

Meissner A, Mikkelsen TS, Gu H, Wernig M, Hanna J, Sivachenko A, Zhang X, Bernstein BE, Nusbaum C, Jaffe DB et al. 2008. Genome-scale DNA methylation maps of pluripotent and differentiated cells. *Nature* **454**(7205): 766-U791.

Melgar MF, Collins FS, Sethupathy P. 2011. Discovery of active enhancers through bidirectional expression of short transcripts. *Genome Biology* **12**(11): R113.

Metivier R, Penot G, Hubner MR, Reid G, Brand H, Kos M, Gannon F. 2003. Estrogen receptor-alpha directs ordered, cyclical, and combinatorial recruitment of cofactors on a natural target promoter. *Cell* **115**(6): 751-763.

Mikkelsen TS, Ku M, Jaffe DB, Issac B, Lieberman E, Giannoukos G, Alvarez P, Brockman W, Kim TK, Koche RP et al. 2007. Genome-wide maps of chromatin state in pluripotent and lineage-committed cells. *Nature* **448**(7153): 553-560.

Mikkelsen TS, Xu Z, Zhang X, Wang L, Gimble JM, Lander ES, Rosen ED. 2010. Comparative epigenomic analysis of murine and human adipogenesis. *Cell* **143**(1): 156-169.

Miller SA, Huang AC, Miazgowicz MM, Brassil MM, Weinmann AS. 2008. Coordinated but physically separable interaction with H3K27-demethylase and H3K4-methyltransferase activities are

required for T-box protein-mediated activation of developmental gene expression. *Genes Dev* **22**(21): 2980-2993.
Miyao T, Floess S, Setoguchi R, Luche H, Fehling HJ, Waldmann H, Huehn J, Hori S. 2012. Plasticity of Foxp3(+) T cells reflects promiscuous Foxp3 expression in conventional T cells but not reprogramming of regulatory T cells. *Immunity* **36**(2): 262-275.
Miyara M, Yoshioka Y, Kitoh A, Shima T, Wing K, Niwa A, Parizot C, Taflin C, Heike T, Valeyre D et al. 2009. Functional Delineation and Differentiation Dynamics of Human CD4(+) T Cells Expressing the FoxP3 Transcription Factor. *Immunity* **30**(6): 899-911.
Moarefi AH, Chédin F. 2011. ICF syndrome mutations cause a broad spectrum of biochemical defects in DNMT3B-mediated de novo DNA methylation. *Journal of molecular biology* **409**(5): 758-772.
Mohn F, Weber M, Rebhan M, Roloff TC, Richter J, Stadler MB, Bibel M, Schuebeler D. 2008. Lineage-specific polycomb targets and de novo DNA methylation define restriction and potential of neuronal progenitors. *Molecular Cell* **30**(6): 755-766.
Mosmann TR, Cherwinski H, Bond MW, Giedlin MA, Coffman RL. 1986. Two types of murine helper T cell clone. I. Definition according to profiles of lymphokine activities and secreted proteins. *Journal of Immunology* **136**(7): 2348-2357.
Mottet C, Uhlig HH, Powrie F. 2003. Cutting edge: Cure of colitis by CD4(+) CD25(+) regulatory T cells. *Journal of Immunology* **170**(8): 3939-3943.
Mouly E, Chemin K, Nguyen HV, Chopin M, Mesnard L, Leite-de-Moraes M, Burlen-defranoux O, Bandeira A, Bories J-C. 2010. The Ets-1 transcription factor controls the development and function of natural regulatory T cells. *The Journal of experimental medicine* **207**(10): 2113-2125.
Nadig SN, Wieckiewicz J, Wu DC, Warnecke G, Zhang W, Luo S, Schiopu A, Taggart DP, Wood KJ. 2010. In vivo prevention of transplant arteriosclerosis by ex vivo-expanded human regulatory T cells. *Nature Medicine* **16**(7): 809-U112.
Nan X, Ng HH, Johnson CA, Laherty CD, Turner BM, Eisenman RN, Bird A. 1998. Transcriptional repression by the methyl-CpG-binding protein MeCP2 involves a histone deacetylase complex. *Nature* **393**(6683): 386-389.
Neph S, Vierstra J, Stergachis AB, Reynolds AP, Haugen E, Vernot B, Thurman RE, John S, Sandstrom R, Johnson AK et al. 2012. An expansive human regulatory lexicon encoded in transcription factor footprints. *Nature* **489**(7414): 83-90.
Ng HH, Zhang Y, Hendrich B, Johnson CA, Turner BM, Erdjument-Bromage H, Tempst P, Reinberg D, Bird A. 1999. MBD2 is a transcriptional repressor belonging to the MeCP1 histone deacetylase complex. *Nature Genetics* **23**(1): 58-61.
Nguyen VH, Zeiser R, Dasilva DL, Chang DS, Beilhack A, Contag CH, Negrin RS. 2007. In vivo dynamics of regulatory T-cell trafficking and survival predict effective strategies to control graft-versus-host disease following allogeneic transplantation. *Blood* **109**(6): 2649-2656.
Nishizuka Y, Sakakura T. 1969. Thymus and reproduction: sex-linked dysgenesia of the gonad after neonatal thymectomy in mice. *Science* **166**(3906): 753-755.
Nolting J, Daniel C, Reuter S, Stuelten C, Li P, Sucov H, Kim BG, Letterio JJ, Kretschmer K, Kim HJ et al. 2009. Retinoic acid can enhance conversion of naive into regulatory T cells independently of secreted cytokines. *The Journal of experimental medicine* **206**(10): 2131-2139.
Okano M, Bell DW, Haber DA, Li E. 1999. DNA methyltransferases Dnmt3a and Dnmt3b are essential for de novo methylation and mammalian development. *Cell* **99**(3): 247-257.
Ong C-T, Corces VG. 2011. Enhancer function: new insights into the regulation of tissue-specific gene expression. *Nature reviews Genetics* **12**(4): 283-293.
Onodera A, Yamashita M, Endo Y, Kuwahara M, Tofukuji S, Hosokawa H, Kanai A, Suzuki Y, Nakayama T. 2010. STAT6-mediated displacement of polycomb by trithorax complex establishes long-term maintenance of GATA3 expression in T helper type 2 cells. *The Journal of experimental medicine* **207**(11): 2493-2506.
Ooi SKT, Bestor TH. 2008. The colorful history of active DNA demethylation. *Cell* **133**(7): 1145-1148.
Ouyang W, Beckett O, Ma Q, Paik J-h, DePinho RA, Li MO. 2010. Foxo proteins cooperatively control the differentiation of Foxp3+ regulatory T cells. *Nature immunology* **11**(7): 618-627.
Ouyang W, Kolls JK, Zheng Y. 2008. The biological functions of T helper 17 cell effector cytokines in inflammation. *Immunity* **28**(4): 454-467.
Ozsolak F, Milos PM. 2011. RNA sequencing: advances, challenges and opportunities. *Nature reviews Genetics* **12**(2): 87-98.
Pan Z, Zhou L, Hetherington CJ, Zhang DE. 2000. Hepatocytes contribute to soluble CD14 production, and CD14 expression is differentially regulated in hepatocytes and monocytes. *J Biol Chem* **275**(46): 36430-36435.

Pandiyan P, Zheng L, Ishihara S, Reed J, Lenardo MJ. 2007. CD4+CD25+Foxp3+ regulatory T cells induce cytokine deprivation-mediated apoptosis of effector CD4+ T cells. *Nature immunology* **8**(12): 1353-1362.

Paz MF, Fraga MF, Avila S, Guo M, Pollan M, Herman JG, Esteller M. 2003. A systematic profile of DNA methylation in human cancer cell lines. *Cancer Research* **63**(5): 1114-1121.

Pekowska A, Benoukraf T, Zacarias-Cabeza J, Belhocine M, Koch F, Holota H, Imbert J, Andrau JC, Ferrier P, Spicuglia S. 2011. H3K4 tri-methylation provides an epigenetic signature of active enhancers. *The EMBO Journal* **30**(20): 4198-4210.

Peters AH, O'Carroll D, Scherthan H, Mechtler K, Sauer S, Schöfer C, Weipoltshammer K, Pagani M, Lachner M, Kohlmaier A et al. 2001. Loss of the Suv39h histone methyltransferases impairs mammalian heterochromatin and genome stability. *Cell* **107**(3): 323-337.

Pfoertner S, Jeron A, Probst-Kepper M, Guzman CA, Hansen W, Westendorf AM, Toepfer T, Schrader AJ, Franzke A, Buer J et al. 2006. Signatures of human regulatory T cells: an encounter with old friends and new players. *Genome Biology* **7**(7).

Pham TH, Benner C, Lichtinger M, Schwarzfischer L, Hu Y, Andreesen R, Chen W, Rehli M. 2012. Dynamic epigenetic enhancer signatures reveal key transcription factors associated with monocytic differentiation states. *Blood*.

Plass C, Soloway PD. 2002. DNA methylation, imprinting and cancer. *European Journal of Human Genetics* **10**(1): 6-16.

Polansky JK, Kretschmer K, Freyer J, Floess S, Garbe A, Baron U, Olek S, Hamann A, von Boehmer H, Huehn J. 2008. DNA methylation controls Foxp3 gene expression. *European Journal of Immunology* **38**(6): 1654-1663.

Polansky JK, Schreiber L, Thelemann C, Ludwig L, Krüger M, Baumgrass R, Cording S, Floess S, Hamann A, Huehn J. 2010. Methylation matters: binding of Ets-1 to the demethylated Foxp3 gene contributes to the stabilization of Foxp3 expression in regulatory T cells. *Journal of Molecular Medicine* **88**(10): 1029-1040.

Prokhortchouk A, Hendrich B, Jørgensen H, Ruzov A, Wilm M, Georgiev G, Bird A, Prokhortchouk E. 2001. The p120 catenin partner Kaiso is a DNA methylation-dependent transcriptional repressor. *Genes & development* **15**(13): 1613-1618.

Provoost S, Maes T, van Durme YM, Gevaert P, Bachert C, Schmidt-Weber CB, Brusselle GG, Joos GF, Tournoy KG. 2009. Decreased FOXP3 protein expression in patients with asthma. *Allergy* **64**(10): 1539-1546.

Rada-Iglesias A, Bajpai R, Swigut T, Brugmann SA, Flynn RA, Wysocka J. 2011. A unique chromatin signature uncovers early developmental enhancers in humans. *Nature* **470**(7333): 279-283.

Ramsahoye BH, Biniszkiewicz D, Lyko F, Clark V, Bird AP, Jaenisch R. 2000. Non-CpG methylation is prevalent in embryonic stem cells and may be mediated by DNA methyltransferase 3a. *Proceedings of the National Academy of Sciences of the United States of America* **97**(10): 5237-5242.

Read S, Malmström V, Powrie F. 2000. Cytotoxic T lymphocyte-associated antigen 4 plays an essential role in the function of CD25(+)CD4(+) regulatory cells that control intestinal inflammation. *The Journal of experimental medicine* **192**(2): 295-302.

Ringrose L. 2007. Polycomb comes of age: genome-wide profiling of target sites. *Current opinion in cell biology* **19**(3): 290-297.

Robertson KD. 2000. DNA methylation: past, present and future directions. *Carcinogenesis* **21**(3): 461-467.

Robinson MD, McCarthy DJ, Smyth GK. 2010. edgeR: a Bioconductor package for differential expression analysis of digital gene expression data. *Bioinformatics* **26**(1): 139-140.

Romagnani S. 1994. Lymphokine production by human T cells in disease states. *Annual review of immunology* **12**: 227-257.

Ruan Q, Kameswaran V, Tone Y, Li L, Liou H-C, Greene MI, Tone M, Chen YH. 2009. Development of Foxp3(+) regulatory t cells is driven by the c-Rel enhanceosome. *Immunity* **31**(6): 932-940.

Rudra D, Egawa T, Chong MMW, Treuting P, Littman DR, Rudensky AY. 2009. Runx-CBFβ complexes control expression of the transcription factor Foxp3 in regulatory T cells. *Nature immunology* **10**(11): 1170-1177.

Sadlon TJ, Wilkinson BG, Pederson S, Brown CY, Bresatz S, Gargett T, Melville EL, Peng K, D'Andrea RJ, Glonek GG et al. 2010. Genome-wide identification of human FOXP3 target genes in natural regulatory T cells. *Journal of immunology (Baltimore, Md : 1950)* **185**(2): 1071-1081.

Sakaguchi S. 2004. Naturally arising CD4+ regulatory t cells for immunologic self-tolerance and negative control of immune responses. *Annual review of immunology* **22**: 531-562.

Sakaguchi S. 2005. Naturally arising Foxp3-expressing CD25+CD4+ regulatory T cells in immunological tolerance to self and non-self. *Nature Immunology* **6**(4): 345-352.

Sakaguchi S, Ono M, Setoguchi R, Yagi H, Hori S, Fehervari Z, Shimizu J, Takahashi T, Nomura T. 2006. Foxp3+ CD25+ CD4+ natural regulatory T cells in dominant self-tolerance and autoimmune disease. *Immunological reviews* **212**: 8-27.

Sakaguchi S, Sakaguchi N, Asano M, Itoh M, Toda M. 1995. Immunologic self-tolerance maintained by activated T cells expressing IL-2 receptor alpha-chains (CD25). Breakdown of a single mechanism of self-tolerance causes various autoimmune diseases. *Journal of Immunology* **155**(3): 1151-1164.

Sakaguchi S, Takahashi T, Nishizuka Y. 1982. Study on cellular events in post-thymectomy autoimmune oophoritis in mice. II. Requirement of Lyt-1 cells in normal female mice for the prevention of oophoritis. *The Journal of experimental medicine* **156**(6): 1577-1586.

Sakaguchi S, Yamaguchi T, Nomura T, Ono M. 2008. Regulatory T cells and immune tolerance. *Cell* **133**(5): 775-787.

Salomon B, Lenschow DJ, Rhee L, Ashourian N, Singh B, Sharpe A, Bluestone JA. 2000. B7/CD28 costimulation is essential for the homeostasis of the CD4(+)CD25(+) immunoregulatory T cells that control autoimmune diabetes. *Immunity* **12**(4): 431-440.

Salomon R, Kaye AM. 1970. Methylation of mouse DNA in vivo. *Biochimica et Biophysica Acta (BBA) - Nucleic Acids and Protein Synthesis* **204**(2): 340-351.

Santos-Rosa H, Schneider R, Bernstein BE, Karabetsou N, Morillon A, Weise C, Schreiber SL, Mellor J, Kouzarides T. 2003. Methylation of histone H3 K4 mediates association of the Isw1p ATPase with chromatin. *Molecular cell* **12**(5): 1325-1332.

Schilling E, El Chartouni C, Rehli M. 2009. Allele-specific DNA methylation in mouse strains is mainly determined by cis-acting sequences. *Genome Research* **19**(11): 2028-2035.

Schilling E, Rehli M. 2007. Global, comparative analysis of tissue-specific promoter CpG methylation. *Genomics* **90**(3): 314-323.

Schlesinger Y, Straussman R, Keshet I, Farkash S, Hecht M, Zimmerman J, Eden E, Yakhini Z, Ben-Shushan E, Reubinoff BE et al. 2007. Polycomb-mediated methylation on Lys27 of histone H3 pre-marks genes for de novo methylation in cancer. *Nature genetics* **39**(2): 232-236.

Schmidl C, Hansmann L, Andreesen R, Edinger M, Hoffmann P, Rehli M. 2011. Epigenetic reprogramming of the RORC locus during in vitro expansion is a distinctive feature of human memory but not naive Treg. *European Journal of Immunology* **41**(5): 1491-1498.

Schmidl C, Klug M, Boeld TJ, Andreesen R, Hoffmann P, Edinger M, Rehli M. 2009. Lineage-specific DNA methylation in T cells correlates with histone methylation and enhancer activity. *Genome Research* **19**(7): 1165-1174.

Schoenborn JR, Dorschner MO, Sekimata M, Santer DM, Shnyreva M, Fitzpatrick DR, Stamatoyannopoulos JA, Wilson CB. 2007a. Comprehensive epigenetic profiling identifies multiple distal regulatory elements directing transcription of the gene encoding interferon-gamma. *Nature Immunology* **8**(7): 732-742.

Schoenborn JR, Dorschner MO, Sekimata M, Santer DM, Shnyreva M, Fitzpatrick DR, Stamatoyonnapoulos JA, Wilson CB. 2007b. Comprehensive epigenetic profiling identifies multiple distal regulatory elements directing transcription of the gene encoding interferon-gamma. *Nature Immunology* **8**(7): 732-742.

Schoenborn JR, Wilson CB. 2007. Regulation of interferon-gamma during innate and adaptive immune responses. *Adv Immunol* **96**: 41-101.

Schotta G, Ebert A, Krauss V, Fischer A, Hoffmann J, Rea S, Jenuwein T, Dorn R, Reuter G. 2002. Central role of Drosophila SU(VAR)3-9 in histone H3-K9 methylation and heterochromatic gene silencing. *The EMBO Journal* **21**(5): 1121-1131.

Schroeder A, Mueller O, Stocker S, Salowsky R, Leiber M, Gassmann M, Lightfoot S, Menzel W, Granzow M, Ragg T. 2006. The RIN: an RNA integrity number for assigning integrity values to RNA measurements. *Bmc Molecular Biology* **7**.

Seddiki N, Santner-Nanan B, Martinson J, Zaunders J, Sasson S, Landay A, Solomon M, Selby W, Alexander SI, Nanan R et al. 2006. Expression of interleukin (IL)-2 and IL-7 receptors discriminates between human regulatory and activated T cells. *The Journal of experimental medicine* **203**(7): 1693-1700.

Seddon B, Mason D. 1999. Peripheral autoantigen induces regulatory T cells that prevent autoimmunity. *The Journal of experimental medicine* **189**(5): 877-882.

Sérandour AA, Avner S, Oger F, Bizot M, Percevault F, Lucchetti-Miganeh C, Palierne G, Gheeraert C, Barloy-Hubler F, Péron CL et al. 2012. Dynamic hydroxymethylation of deoxyribonucleic acid marks differentiation-associated enhancers. *Nucleic acids research*.

Sérandour AA, Avner S, Percevault F, Demay F, Bizot M, Lucchetti-Miganeh C, Barloy-Hubler F, Brown M, Lupien M, Métivier R et al. 2011. Epigenetic switch involved in activation of pioneer factor FOXA1-dependent enhancers. *Genome research* **21**(4): 555-565.

Sewgobind VD, Quaedackers ME, van der Laan LJ, Kraaijeveld R, Korevaar SS, Chan G, Weimar W, Baan CC. 2010. The Jak inhibitor CP-690,550 preserves the function of CD4CD25FoxP3 regulatory T cells and inhibits effector T cells. *Am J Transplant* **10**(8): 1785-1795.

Shevach EM. 2009. Mechanisms of foxp3+ T regulatory cell-mediated suppression. *Immunity* **30**(5): 636-645.

Shi Y, Lan F, Matson C, Mulligan P, Whetstine JR, Cole PA, Casero RA. 2004. Histone demethylation mediated by the nuclear amine oxidase homolog LSD1. *Cell* **119**(7): 941-953.

Shilatifard A. 2008. Molecular implementation and physiological roles for histone H3 lysine 4 (H3K4) methylation. *Current opinion in cell biology* **20**(3): 341-348.

Shimoda K, vanDeursen J, Sangster MY, Sarawar SR, Carson RT, Tripp RA, Chu C, Quelle FW, Nosaka T, Vignali DAA et al. 1996. Lack of IL-4-induced Th2 response and IgE class switching in mice with disrupted Stat6 gene. *Nature* **380**(6575): 630-633.

Shukla S, Kavak E, Gregory M, Imashimizu M, Shutinoski B, Kashlev M, Oberdoerffer P, Sandberg R, Oberdoerffer S. 2011. CTCF-promoted RNA polymerase II pausing links DNA methylation to splicing. *Nature* **479**(7371): 74-79.

Singal R, Ginder GD. 1999. DNA Methylation. *Blood*.

Song F, Mahmood S, Ghosh S, Liang P, Smiraglia DJ, Nagase H, Held WA. 2009. Tissue specific differentially methylated regions (TDMR): Changes in DNA methylation during development. *Genomics* **93**(2): 130-139.

Soutto M, Zhou W, Aune TM. 2002. Cutting edge: distal regulatory elements are required to achieve selective expression of IFN-gamma in Th1/Tc1 effector cells. *Journal of immunology (Baltimore, Md : 1950)* **169**(12): 6664-6667.

Spilianakis CG, Flavell RA. 2004. Long-range intrachromosomal interactions in the T helper type 2 cytokine locus. *Nature immunology* **5**(10): 1017-1027.

St Johnston D, Nusslein-Volhard C. 1992. The origin of pattern and polarity in the Drosophila embryo. *Cell* **68**(2): 201-219.

Stadler MB, Murr R, Burger L, Ivanek R, Lienert F, Scholer A, van Nimwegen E, Wirbelauer C, Oakeley EJ, Gaidatzis D et al. 2011. DNA-binding factors shape the mouse methylome at distal regulatory regions. *Nature* **480**(7378): 490-495.

Sterner DE, Berger SL. 2000. Acetylation of histones and transcription-related factors. *Microbiol Mol Biol Rev* **64**(2): 435-459.

Stroud H, Feng S, Morey Kinney S, Pradhan S, Jacobsen SE. 2011. 5-Hydroxymethylcytosine is associated with enhancers and gene bodies in human embryonic stem cells. *Genome Biology* **12**(6): R54.

Stumpel DJ, Schneider P, van Roon EH, Boer JM, de Lorenzo P, Valsecchi MG, de Menezes RX, Pieters R, Stam RW. 2009. Specific promoter methylation identifies different subgroups of MLL-rearranged infant acute lymphoblastic leukemia, influences clinical outcome, and provides therapeutic options. *Blood* **114**(27): 5490-5498.

Sun CM, Hall JA, Blank RB, Bouladoux N, Oukka M, Mora JR, Belkaid Y. 2007. Small intestine lamina propria dendritic cells promote de novo generation of Foxp3 T reg cells via retinoic acid. *The Journal of experimental medicine* **204**(8): 1775-1785.

Suzuki MM, Bird A. 2008. DNA methylation landscapes: provocative insights from epigenomics. *Nature reviews Genetics* **9**(6): 465-476.

Szabo SJ, Dighe AS, Gubler U, Murphy KM. 1997. Regulation of the interleukin (IL)-12R beta 2 subunit expression in developing T helper 1 (Th1) and Th2 cells. *Journal of Experimental Medicine* **185**(5): 817-824.

Szabo SJ, Kim ST, Costa GL, Zhang XK, Fathman CG, Glimcher LH. 2000. A novel transcription factor, T-bet, directs Th1 lineage commitment. *Cell* **100**(6): 655-669.

Szulwach KE, Li X, Li Y, Song CX, Han JW, Kim S, Namburi S, Hermetz K, Kim JJ, Rudd MK et al. 2011. Integrating 5-hydroxymethylcytosine into the epigenomic landscape of human embryonic stem cells. *PLoS Genetics* **7**(6): e1002154.

Takeda K, Tanaka T, Shi W, Matsumoto M, Minami M, Kashiwamura S, Nakanishi K, Yoshida N, Kishimoto T, Akira S. 1996. Essential role of Stat6 in IL-4 signalling. *Nature* **380**(6575): 627-630.

Tao R, de Zoeten EF, Ozkaynak E, Chen C, Wang L, Porrett PM, Li B, Turka LA, Olson EN, Greene MI et al. 2007. Deacetylase inhibition promotes the generation and function of regulatory T cells. *Nature Medicine* **13**(11): 1299-1307.

Tartar DM, VanMorlan AM, Wan X, Guloglu FB, Jain R, Haymaker CL, Ellis JS, Hoeman CM, Cascio JA, Dhakal M et al. 2010. FoxP3(+)ROR gamma t(+) T Helper Intermediates Display Suppressive Function against Autoimmune Diabetes. *Journal of Immunology* **184**(7): 3377-3385.

Tate PH. 1993. ScienceDirect.com - Current Opinion in Genetics & Development - Effects of DNA methylation on DNA-binding proteins and gene expression. *Current opinion in genetics & development*.

Taylor PA, Lees CJ, Blazar BR. 2002. The infusion of ex vivo activated and expanded CD4(+)CD25(+) immune regulatory cells inhibits graft-versus-host disease lethality. *Blood* **99**(10): 3493-3499.

Thieu VT, Yu Q, Chang H-C, Yeh N, Nguyen ET, Sehra S, Kaplan MH. 2008. Signal Transducer and Activator of Transcription 4 Is Required for the Transcription Factor T-bet to Promote T Helper 1 Cell-Fate Determination. *Immunity* **29**(5): 679-690.

Thomson JP, Skene PJ, Selfridge J, Clouaire T, Guy J, Webb S, Kerr ARW, Deaton A, Andrews R, James KD et al. 2010. CpG islands influence chromatin structure via the CpG-binding protein Cfp1. *Nature* **464**(7291): 1082-1086.

Thornton AM, Donovan EE, Piccirillo CA, Shevach EM. 2004. Cutting edge: IL-2 is critically required for the in vitro activation of CD4+CD25+ T cell suppressor function. *Journal of Immunology* **172**(11): 6519-6523.

Thornton AM, Korty PE, Tran DQ, Wohlfert EA, Murray PE, Belkaid Y, Shevach EM. 2010. Expression of Helios, an Ikaros transcription factor family member, differentiates thymic-derived from peripherally induced Foxp3+ T regulatory cells. *Journal of Immunology* **184**(7): 3433-3441.

Thurman RE, Rynes E, Humbert R, Vierstra J, Maurano MT, Haugen E, Sheffield NC, Stergachis AB, Wang H, Vernot B et al. 2012. The accessible chromatin landscape of the human genome. *Nature* **489**(7414): 75-82.

Tian Y, Jia Z, Wang J, Huang Z, Tang J, Zheng Y, Tang Y, Wang Q, Tian Z, Yang D et al. 2011. Global mapping of H3K4me1 and H3K4me3 reveals the chromatin state-based cell type-specific gene regulation in human Treg cells. *PloS one* **6**(11): e27770.

Tone Y, Furuuchi K, Kojima Y, Tykocinski ML, Greene MI, Tone M. 2008. Smad3 and NFAT cooperate to induce Foxp3 expression through its enhancer. *Nature Immunology* **9**(2): 194-202.

Toyota M, Kopecky KJ, Toyota MO, Jair KW, Willman CL, Issa JP. 2001. Methylation profiling in acute myeloid leukemia. *Blood* **97**(9): 2823-2829.

Tresoldi E, Dell'Albani I, Stabilini A, Jofra T, Valle A, Gagliani N, Bondanza A, Roncarolo MG, Battaglia M. 2011. Stability of human rapamycin-expanded CD4+CD25+ T regulatory cells. *Haematologica* **96**(9): 1357-1365.

Tsuji M, Komatsu N, Kawamoto S, Suzuki K, Kanagawa O, Honjo T, Hori S, Fagarasan S. 2009. Preferential Generation of Follicular B Helper T Cells from Foxp3(+) T Cells in Gut Peyer's Patches. *Science* **323**(5920): 1488-1492.

Tuteja G, Jensen ST, White P, Kaestner KH. 2008. Cis-regulatory modules in the mammalian liver: composition depends on strength of Foxa2 consensus site. *Nucleic acids research* **36**(12): 4149-4157.

Underhill DM, Ozinsky A. 2002. Toll-like receptors: key mediators of microbe detection. *Current Opinion in Immunology* **14**(1): 103-110.

Valmori D, Raffin C, Raimbaud I, Ayyoub M. 2010. Human ROR gamma t(+) T(H)17 cells preferentially differentiate from naive FOXP3(+)Treg in the presence of lineage-specific polarizing factors. *Proceedings of the National Academy of Sciences of the United States of America* **107**(45): 19402-19407.

van Loosdregt J, Vercoulen Y, Guichelaar T, Gent YY, Beekman JM, van Beekum O, Brenkman AB, Hijnen DJ, Mutis T, Kalkhoven E et al. 2010. Regulation of Treg functionality by acetylation-mediated Foxp3 protein stabilization. *Blood* **115**(5): 965-974.

Vang KB, Yang J, Mahmud SA, Burchill MA, Vegoe AL, Farrar MA. 2008. IL-2, -7, and -15, but not thymic stromal lymphopoeitin, redundantly govern CD4+Foxp3+ regulatory T cell development. *Journal of Immunology* **181**(5): 3285-3290.

vanKooten C, Banchereau J. 1997. Functions of CD40 on B cells, dendritic cells and other cells. *Current Opinion in Immunology* **9**(3): 330-337.

Vaquerizas JM, Kummerfeld SK, Teichmann SA, Luscombe NM. 2009. A census of human transcription factors: function, expression and evolution. *Nature reviews Genetics* **10**(4): 252-263.

Vermeulen M, Eberl HC, Matarese F, Marks H, Denissov S, Butter F, Lee KK, Olsen JV, Hyman AA, Stunnenberg HG et al. 2010. Quantitative interaction proteomics and genome-wide profiling of epigenetic histone marks and their readers. *Cell* **142**(6): 967-980.

Vermeulen M, Mulder KW, Denissov S, Pijnappel WWMP, van Schaik FMA, Varier RA, Baltissen MPA, Stunnenberg HG, Mann M, Timmers HTM. 2007. Selective anchoring of TFIID to nucleosomes by trimethylation of histone H3 lysine 4. *Cell* **131**(1): 58-69.

Vignali DAA, Collison LW, Workman CJ. 2008. How regulatory T cells work. *Nature Reviews Immunology* **8**(7): 523-532.

Viré E, Brenner C, Deplus R, Blanchon L, Fraga M, Didelot C, Morey L, Van Eynde A, Bernard D, Vanderwinden J-M et al. 2006. The Polycomb group protein EZH2 directly controls DNA methylation. *Nature* **439**(7078): 871-874.

Visel A, Blow MJ, Li Z, Zhang T, Akiyama JA, Holt A, Plajzer-Frick I, Shoukry M, Wright C, Chen F et al. 2009. ChIP-seq accurately predicts tissue-specific activity of enhancers. *Nature* **457**(7231): 854-858.

Volpe E, Servant N, Zollinger R, Bogiatzi SI, Hupe P, Barillot E, Soumelis V. 2008. A critical function for transforming growth factor-beta, interleukin 23 and proinflammatory cytokines in driving and modulating human T(H)-17 responses. *Nature Immunology* **9**(6): 650-657.

Voo KS, Wang Y-H, Santori FR, Boggiano C, Wang Y-H, Arima K, Bover L, Hanabuchi S, Khalili J, Marinova E et al. 2009. Identification of IL-17-producing FOXP3(+) regulatory T cells in humans. *Proceedings of the National Academy of Sciences of the United States of America* **106**(12): 4793-4798.

Walsh CP, Chaillet JR, Bestor TH. 1998. Transcription of IAP endogenous retroviruses is constrained by cytosine methylation. *Nature Genetics* **20**(2): 116-117.

Wan YY, Flavell RA. 2007. Regulatory T-cell functions are subverted and converted owing to attenuated Foxp3 expression. *Nature* **445**(7129): 766-770.

Wang R, Wan Q, Kozhaya L, Fujii H, Unutmaz D. 2008a. Identification of a Regulatory T Cell Specific Cell Surface Molecule that Mediates Suppressive Signals and Induces Foxp3 Expression. *Plos One* **3**(7).

Wang Y, Souabni A, Flavell RA, Wan YY. 2010. An Intrinsic Mechanism Predisposes Foxp3-Expressing Regulatory T Cells to Th2 Conversion In Vivo. *Journal of Immunology* **185**(10): 5983-5992.

Wang Y, Su MA, Wan YY. 2011. An essential role of the transcription factor GATA-3 for the function of regulatory T cells. *Immunity* **35**(3): 337-348.

Wang Z, Zang C, Rosenfeld JA, Schones DE, Barski A, Cuddapah S, Cui K, Roh T-Y, Peng W, Zhang MQ et al. 2008b. Combinatorial patterns of histone acetylations and methylations in the human genome. *Nature Genetics* **40**(7): 897-903.

Weber M, Hellmann I, Stadler MB, Ramos L, Paabo S, Rebhan M, Schubeler D. 2007. Distribution, silencing potential and evolutionary impact of promoter DNA methylation in the human genome. *Nature Genetics* **39**(4): 457-466.

Wei G, Wei L, Zhu J, Zang C, Hu-Li J, Yao Z, Cui K, Kanno Y, Roh T-Y, Watford WT et al. 2009. Global Mapping of H3K4me3 and H3K27me3 Reveals Specificity and Plasticity in Lineage Fate Determination of Differentiating CD4(+) T Cells. *Immunity* **30**(1): 155-167.

Wieczorek G, Asemissen A, Model F, Turbachova I, Floess S, Liebenberg V, Baron U, Stauch D, Kotsch K, Pratschke J et al. 2009. Quantitative DNA methylation analysis of FOXP3 as a new method for counting regulatory T cells in peripheral blood and solid tissue. *Cancer Research* **69**(2): 599-608.

Wiench M, John S, Baek S, Johnson TA, Sung M-H, Escobar T, Simmons CA, Pearce KH, Biddie SC, Sabo PJ et al. 2011. DNA methylation status predicts cell type-specific enhancer activity. *The EMBO Journal* **30**(15): 3028-3039.

Wigler M, Levy D, Perucho M. 1981. The somatic replication of DNA methylation. *Cell* **24**(1): 33-40.

Wildin RS, Ramsdell F, Peake J, Faravelli F, Casanova JL, Buist N, Levy-Lahad E, Mazzella M, Goulet O, Perroni L et al. 2001. X-linked neonatal diabetes mellitus, enteropathy and endocrinopathy syndrome is the human equivalent of mouse scurfy. *Nature Genetics* **27**(1): 18-20.

Williams LM, Rudensky AY. 2007. Maintenance of the Foxp3-dependent developmental program in mature regulatory T cells requires continued expression of Foxp3. *Nature Immunology* **8**(3): 277-284.

Wing K, Onishi Y, Prieto-Martin P, Yamaguchi T, Miyara M, Fehervari Z, Nomura T, Sakaguchi S. 2008. CTLA-4 control over Foxp3(+) regulatory T cell function. *Science* **322**(5899): 271-275.

Wing K, Suri-Payer E, Rudin A. 2005. CD4+CD25+-regulatory T cells from mouse to man. *Scand J Immunol* **62**(1): 1-15.

Wittkopp PJ, Kalay G. 2012. Cis-regulatory elements: molecular mechanisms and evolutionary processes underlying divergence. *Nature reviews Genetics* **13**(1): 59-69.

Wu Y, Borde M, Heissmeyer V, Feuerer M, Lapan AD, Stroud JC, Bates DL, Guo L, Han A, Ziegler SF et al. 2006. FOXP3 controls regulatory T cell function through cooperation with NFAT. *Cell* **126**(2): 375-387.

Wysocka J, Swigut T, Xiao H, Milne TA, Kwon SY, Landry J, Kauer M, Tackett AJ, Chait BT, Badenhorst P et al. 2006. A PHD finger of NURF couples histone H3 lysine 4 trimethylation with chromatin remodelling. *Nature* **442**(7098): 86-90.

Xu GL, Bestor TH, Bourc'his D, Hsieh CL, Tommerup N, Bugge M, Hulten M, Qu X, Russo JJ, Viegas-Pequignot E. 1999. Chromosome instability and immunodeficiency syndrome caused by mutations in a DNA methyltransferase gene. *Nature* **402**(6758): 187-191.

Xu L, Kitani A, Fuss I, Strober W. 2007. Cutting edge: Regulatory T cells induce CD4(+)CD25(-)Foxp3(-) T cells or are self-induced to become Th17 cells in the absence of exogenous TGF-beta. *Journal of Immunology* **178**(11): 6725-6729.

Yagi R, Junttila IS, Wei G, Urban JF, Jr., Zhao K, Paul WE, Zhu J. 2010. The transcription factor GATA3 actively represses RUNX3 protein-regulated production of interferon-gamma. *Immunity* **32**(4): 507-517.

Yamashita M, Ukai-Tadenuma M, Miyamoto T, Sugaya K, Hosokawa H, Hasegawa A, Kimura M, Taniguchi M, DeGregori J, Nakayama T. 2004. Essential role of GATA3 for the maintenance of type 2 helper T (Th2) cytokine production and chromatin remodeling at the Th2 cytokine gene loci. *J Biol Chem* **279**(26): 26983-26990.

Yan P, Frankhouser D, Murphy M, Tam HH, Rodriguez B, Curfman J, Trimarchi M, Geyer S, Wu YZ, Whitman SP et al. 2012. Genome-wide methylation profiling in decitabine-treated patients with acute myeloid leukemia. *Blood*.

Yang XO, Nurieva R, Martinez GJ, Kang HS, Chung Y, Pappu BP, Shah B, Chang SH, Schluns KS, Watowich SS et al. 2008a. Molecular antagonism and plasticity of regulatory and inflammatory T cell programs. *Immunity* **29**(1): 44-56.

Yang XO, Pappu BP, Nurieva R, Akimzhanov A, Kang HS, Chung Y, Ma L, Shah B, Panopoulos AD, Schluns KS et al. 2008b. T helper 17 lineage differentiation is programmed by orphan nuclear receptors ROR alpha and ROR gamma. *Immunity* **28**(1): 29-39.

Yao Z, Kanno Y, Kerenyi M, Stephens G, Durant L, Watford WT, Laurence A, Robinson GW, Shevach EM, Moriggl R et al. 2007. Nonredundant roles for Stat5a/b in directly regulating Foxp3. *Blood* **109**(10): 4368-4375.

Ye P, Rodriguez FH, Kanaly S, Stocking KL, Schurr J, Schwarzenberger P, Oliver P, Huang W, Zhang P, Zhang J et al. 2001. Requirement of interleukin 17 receptor signaling for lung CXC chemokine and granulocyte colony-stimulating factor expression, neutrophil recruitment, and host defense. *The Journal of experimental medicine* **194**(4): 519-527.

Zaret KS, Carroll JS. 2011. Pioneer transcription factors: establishing competence for gene expression. *Genes & development* **25**(21): 2227-2241.

Zhang F, Boothby M. 2006. T helper type 1-specific Brg1 recruitment and remodeling of nucleosomes positioned at the IFN-gamma promoter are Stat4 dependent. *The Journal of experimental medicine* **203**(6): 1493-1505.

Zhang F, Meng G, Strober W. 2008. Interactions among the transcription factors Runx1, ROR gamma t and Foxp3 regulate the differentiation of interleukin 17-producing T cells. *Nature Immunology* **9**(11): 1297-1306.

Zhang Y, Ng HH, Erdjument-Bromage H, Tempst P, Bird A, Reinberg D. 1999. Analysis of the NuRD subunits reveals a histone deacetylase core complex and a connection with DNA methylation. *Genes & development* **13**(15): 1924-1935.

Zheng WP, Flavell RA. 1997. The transcription factor GATA-3 is necessary and sufficient for Th2 cytokine gene expression in CD4 T cells. *Cell* **89**(4): 587-596.

Zheng Y, Chaudhry A, Kas A, deRoos P, Kim JM, Chu T-T, Corcoran L, Treuting P, Klein U, Rudensky AY. 2009. Regulatory T-cell suppressor program co-opts transcription factor IRF4 to control T(H)2 responses. *Nature* **458**(7236): 351-356.

Zheng Y, Josefowicz S, Chaudhry A, Peng XP, Forbush K, Rudensky AY. 2010. Role of conserved non-coding DNA elements in the Foxp3 gene in regulatory T-cell fate. *Nature* **463**(7282): 808-812.

Zheng Y, Josefowicz SZ, Kas A, Chu T-T, Gavin MA, Rudensky AY. 2007. Genome-wide analysis of Foxp3 target genes in developing and mature regulatory T cells. *Nature* **445**(7130): 936-940.

Zheng Y, Rudensky AY. 2007. Foxp3 in control of the regulatory T cell lineage. *Nature Immunology* **8**(5): 457-462.

Zhou L, Chong MMW, Littman DR. 2009a. Plasticity of CD4(+) T Cell Lineage Differentiation. *Immunity* **30**(5): 646-655.

Zhou L, Ivanov, II, Spolski R, Min R, Shenderov K, Egawa T, Levy DE, Leonard WJ, Littman DR. 2007. IL-6 programs T(H)-17 cell differentiation by promoting sequential engagement of the IL-21 and IL-23 pathways. *Nature Immunology* **8**(9): 967-974.

Zhou L, Lopes JE, Chong MM, Ivanov, II, Min R, Victora GD, Shen Y, Du J, Rubtsov YP, Rudensky AY et al. 2008a. TGF-beta-induced Foxp3 inhibits T(H)17 cell differentiation by antagonizing RORgammat function. *Nature* **453**(7192): 236-240.

Zhou VW, Goren A, Bernstein BE. 2011. Charting histone modifications and the functional organization of mammalian genomes. *Nature reviews Genetics* **12**(1): 7-18.

Zhou X, Bailey-Bucktrout S, Jeker LT, Bluestone JA. 2009b. Plasticity of CD4(+) FoxP3(+) T cells. *Current Opinion in Immunology* **21**(3): 281-285.

Zhou X, Bailey-Bucktrout SL, Jeker LT, Penaranda C, Martinez-Llordella M, Ashby M, Nakayama M, Rosenthal W, Bluestone JA. 2009c. Instability of the transcription factor Foxp3 leads to the generation of pathogenic memory T cells in vivo. *Nature Immunology* **10**(9): 1000-U1104.

Zhou X, Jeker LT, Fife BT, Zhu S, Anderson MS, McManus MT, Bluestone JA. 2008b. Selective miRNA disruption in T reg cells leads to uncontrolled autoimmunity. *Journal of Experimental Medicine* **205**(9): 1983-1991.

Zhu J, Paul WE. 2010. Heterogeneity and plasticity of T helper cells. *Cell Research* **20**(1): 4-12.

Zhu JF, Cote-Sierra J, Guo LY, Paul WE. 2003. Stat5 activation plays a critical role in Th2 differentiation. *Immunity* **19**(5): 739-748.

Zhu JF, Min B, Hu-Li J, Watson CJ, Grinberg A, Wang Q, Killeen N, Urban JF, Guo LY, Paul WE. 2004. Conditional deletion of Gata3 shows its essential function in T(H)1-T(H)2 responses. *Nature Immunology* **5**(11): 1157-1165.

Ziegler SF. 2006. FOXP3: of mice and men. *Annual review of immunology* **24**: 209-226.

Zorn E, Nelson EA, Mohseni M, Porcheray F, Kim H, Litsa D, Bellucci R, Raderschall E, Canning C, Soiffer RJ et al. 2006. IL-2 regulates FOXP3 expression in human CD4(+)CD25(+) regulatory T cells through a STAT-dependent mechanism and induces the expansion of these cells in vivo. *Blood* **108**(5): 1571-1579.

6 Publications

Schmidl C, Hoffmann P, Andreesen R, Forrest AR, Lassmann T, Kawaji H, Carninci P, Hayashizaki Y, Edinger M, Rehli M. The enhancer and promoter landscape of regulatory and conventional T cell subpopulations. *Manuscript in preparation*.

Hansmann L, **Schmidl C**, Kett J, Steger L, Andreesen R, Hoffmann P, Rehli M, Edinger M. 2012. Dominant Th2 differentiation of human regulatory T cells upon loss of FOXP3 expression. *Journal of immunology* **188**(3): 1275-1282.

Schmidl C*, Hansmann* L, Andreesen R, Edinger M, Hoffmann P, Rehli M. 2011. Epigenetic reprogramming of the RORC locus during in vitro expansion is a distinctive feature of human memory but not naive Treg. *European Journal of Immunology* **41**(5): 1491-1498.

Hansmann L*, **Schmidl C***, Boeld TJ*, Andreesen R, Hoffmann P, Rehli M, Edinger M. 2010. Isolation of intact genomic DNA from FOXP3-sorted human regulatory T cells for epigenetic analyses. *European Journal of Immunology* **40**(5): 1510-1512.

Schmidl C, Klug M, Boeld TJ, Andreesen R, Hoffmann P, Edinger M, Rehli M. 2009. Lineage-specific DNA methylation in T cells correlates with histone methylation and enhancer activity. *Genome Research* **19**(7): 1165-1174.

* Shared first authorship

7 Danksagung

Auf dieser Seite möchte ich mich herzlich bei allen bedanken, die zum Gelingen dieser Arbeit beigetragen haben.

Herrn Prof. Dr. Reinhard Andreesen danke ich für die Möglichkeit, die Dissertation in seiner Abteilung anfertigen zu dürfen.

Mein ganz besonderer Dank gilt Prof. Dr. Michael Rehli, für die unglaublich gute Betreuung meiner Arbeit und der Förderung des Wissenschaftlers in mir. Vielen herzlichen Dank für die Diskussionen, Dein immer offenes Ohr, Deine mitreißende Begeisterung für Forschung, die tollen Reisen und Retreats, und dafür dass ich auch immer ein paar „cores“ abbekommen habe! Ich habe viel gelernt und hatte eine schöne und spannende Zeit!

Vielen herzlichen Dank an PD. Dr. Petra Hoffmann und Prof. Dr. Matthias Edinger für die tolle Zusammenarbeit! Eure Korrekturen, Begutachtungen, Vorschläge und Diskussionen haben mich immer weiter gebracht. In diesem Zusammenhang möchte ich mich auch bei Leo Hansmann für das fruchtbare Teamwork bedanken. Der Ag-Edihoff danke ich vielmals für die Hilfe- was hätte ich ohne Rüdiger gemacht?!

Ich möchte mich gerne bei Prof. Dr. Gernot Längst für die Mitbetreuung meiner Arbeit und die Gelegenheit, ein Praktikum in Chile zu betreuen, vielmals bedanken.

Ganz besonders bedanken möchte ich mich bei der ganzen Ag-Rehli und den „Ehemaligen“ für das beste Arbeitsumfeld, das es gibt! Ich habe mich von Anfang an sauwohl in unserer Truppe gefühlt, und ich danke für Unterstützung, Spaß in der Arbeit und Freizeit, Freundschaft und super Zusammenarbeit Thu Hang Pham, Lucia Schwarzfischer, Monika Lichtinger, Carol El Chartouni, Claudia Gebhard, Maja Klug, Ireen Ritter, Dagmar Glatz, Johanna Raithel, Sabine Pape, Julia Wimmer, Sandra Schmidhofer, Sandra Pohl, Julia Minderjahn, Saskia Patschorke, Elmar Schilling, Thomas Gross, Tobias Weil und Daniel Heudobler von ganzem Herzen. Ich werde Euch vermissen!

Vielen Dank auch an die Ag-Kreutz für die Zusammenarbeit und unsere schöne „Nachbarschaft“!

Für ihre Unterstützung und unseren Zusammenhalt danke ich unseren Familien. Meinen Eltern danke ich ganz besonders dafür, dass sie immer für mich da sind und mir durch ihre Unterstützung meinen Werdegang erst ermöglichten!

Für ihre Geduld das alles mit zu machen, ihr unendliches Vertrauen und ihre Liebe danke ich meiner Frau.